A Simulation Framework for Electricity Markets



Ioan Alexandru Puiu

Mansfield College

University of Oxford

A thesis submitted for the

Doctor of Philosophy

August 2022

Acknowledgements

First and foremost, this work was only possible thanks to Prof. Chris Breward and Prof. Colin Please, who founded the Industrially Focused Mathematical Modelling (InFoMM) research program, and offered me the opportunity to be a part of it. I am also grateful to the CGM London Power and Gas desk within Macquarie Group for partially funding this research, and providing the opportunity to work on the topic of my interest.

I would like to express my deepest gratitude to my DPhil advisor, Prof. Raphael Hauser, for giving me the opportunity to undertake this very exciting journey and believing in me. I am very grateful for the opportunity to learn from you. Thank you for your technical and non-technical counselling, and guidance.

I am also extremely grateful to Prof. Coralia Cartis, for the guidance provided in the early stages of my DPhil, that helped me transition to the research world. I would also like to further thank you for the invaluable feedback provided in the early stages of my thesis.

I am honored to have met and interacted with Prof. Peter Grindrod CBE during my Master's and DPhil journeys. Thank you for your invaluable feedback during the early stages of my DPhil, and for agreeing to serve as my thesis referee.

My deepest thanks go also to Prof. Kenneth Bruninx, for serving as my thesis referee, providing invaluable feedback and for taking the time to meeting with me for the viva to discuss the contents of my work.

I am extremely grateful to Dr. Kathryn Gillow, who was not only an amazing and inspiring course director during my Masters' program, but also offered me vital support during the end stages of my DPhil journey. I especially thank you for the top quality feedback of my final thesis.

I am also very grateful for my interaction and discussions with Prof. Andrew Wathen, who helped me improve my research and my thinking. Thank you for taking the time to understand my work and sharing your invaluable knowledge and thoughts.

I am also thankful to Prof. Ben Hambly and Prof. Samuel Cohen for reviewing my work and the feedback offered during my Confirmation of Status.

I would also like to thank Vincent Guffens, Graham Allsop, Chris Doyle and Ben Readman for the very insightful discussions, believing in me, and consistent support. I thank to Descartes Labs for extending the account, and Jeremy Malczyk and Chris Moulton for offering technical support with the Descartes Labs platform.

I am deeply indebted to my amazing secondary school physics teacher, Hirean Liliana, who helped me discover my passion for exact sciences and taught me to believe in myself, by always believing in me. I am also extremely grateful to my inspiring high school physics teacher, Jean Marius Rotaru, for the countless hours invested in teaching me and believing in me.

On a more personal level, words cannot express my gratitude to all my family. My deepest gratitude goes to my mother, for her unwavering emotional, financial and any imaginable form of support, and for always believing in me. I am also grateful to my father for his support and believing in me.

I am extremely grateful to have been blessed with my twin brother, from who I always have the opportunity to learn and improve myself. Thank you for always being there and for your unconditional support on my continuous journey to becoming a becoming a better person and researcher. I am also thankful for the opportunity to learn and grow together, the countless discussions on mathematics during my thesis and the invaluable feedback and advice.

I would also like to thank all my close friends for enriching my life and not giving up on me. I am thankful to everyone who taught me something, or said something positive.

Last but not least, I am truly grateful to my fiancée Qian. Thank you for always taking the time to listen and offer invaluable advice, and for your invaluable feedback on my thesis work. I am grateful for your unconditional love and support, for always believing in me and for bearing with me through my continuous journey of becoming a better person and researcher.

Ioan Alexandru Puiu
Oxford, August 2022

Abstract

Electricity Markets are paramount to the economy of any country and therefore lie at the foundation of society. These markets are usually very complex when compared to traditional financial markets due to the physical nature of the asset traded, difficulty of storage and distribution. Supply and demand balancing, network constraints, renewable energy influx, desire of participants to maximise their own profits, their risk aversion, fuel costs required for production, and the market clearing mechanism, do not exhaust the list of factors that influence the market outcome, but are perhaps the most important ones. The market outcome includes the prices and quantities allocated whose understanding is of great importance for market regulators and market participants alike.

This work is focused on improving the fundamental understanding of the Spot Electricity Markets which lie at the core of Electricity Trading and represent the majority of trading volume. In particular we focus on Day Ahead Auctions which represent the vast majority of Spot Electricity trading, due to the difficulty of storing electricity, coupled with uncertainty in demand and production patterns. Every market has its own peculiarities and, we consider as a case study the Central Western European (CWE) Day Ahead Auction (DAA) for the period of $01/01/2019-31/12/2019$. The Central Western European market includes Austria, Belgium, Germany, France and the Netherlands.

Following an introductory chapter, due to the lack of full and complete network constraints historical data, Chapter 2 is focused on the reconstruction of historical network constraints, that are a key input in any fundamental model considering the electricity grid's structure. Further, network constraints may impose price decoupling between countries, which is of great interest to practitioners, academics and regulators. The task is very challenging due to the input data being very large and sparse. We reconstruct the network constraints data, known as the Power Transmission Distribution Factors (PTDFs) and Remaining Available Margins (RAMs), by first recovering the underlying time dependent signals known as the Generation Shift Keys (GSKs) and Phase Angles (PAs), and the electricity grid characteristics, via a mathematical optimisation problem that is solved by exploiting problem structure. The second step maps GSKs and PAs to the network constraints via the electricity grid characteristics. Our reconstruction achieves good in- and out-of- sample relative errors when compared to a naive approach.

With the network constraints available, and by obtaining the cost and capacity characteristics of suppliers, in Chapter 3 we formulate a fundamental model to resolve for the zonal prices and quantities assigned to each participant, based on a simplification of the CWE market clearing mechanism, known as the Social Welfare Maximisation Problem (SWM). We also propose a novel market clearing mechanism which we call the Total Cost Minimisation Problem, because as we show, the prices are generally much lower and the total cost of supplying electricity is guaranteed to be lower by definition. Solving the Cost Minimisation problem is more challenging than solving the SWM, due to zonal prices appearing as explicit variables, but we obtain strong (but partial) analytical results to aid numerical solutions and provide efficient numerical algorithms. For both clearing mechanisms, demand is considered as inflexible, and producers bid marginal prices linear in the quantities produced. Since as expected, the SWM better represents the target data, this is further used as the market clearing mechanism. We consider the case when producers truthfully bid (TB) their cost curves, which is usually assumed by the regulators and many academic papers. However, we also consider the case of players trying to maximise their own profit, tand thus forming a Game Theoretic (GT) framework. For our CWE case study, both GT and TB models generally give an accurate representation of the actual price outcomes. Further, we define a method based on simple hypothesis testing to identify if and when the players are bidding strategically (gaming). We show that in fact, while for a large majority of times we cannot say with high confidence whether the players are bidding strategically or bidding truthfully, the number of times we are confident that players are gaming is much higher than the number of times we are confident that the players are bidding truthfully. Our results show that, in general, strategic bidding appears to be especially pronounced at peak demand hours: between $8am - 1pm$ and $5pm - 9pm$. A different regime, where renewable energy influx appears to dominate the price action is also identified and this effect is generally more pronounced at off-peak morning hours ($0am - 6am$). Our model can thus be used as a fundamental approach for market outcome and price prediction, understanding the impact various fundamental factors on the price, understanding of producers' behaviour, and identifying if and when players are not bidding truthfully. These are all of interest to academics, market participants, and regulators.

Contents

1 Introduction and Overview **1**

1.1 Modelling of Electricity Day Ahead Markets and their Constraints 6

1.1.1 Overview of the DC Grid Model based Network Constraints 7

1.1.2 Overview of Market Clearing and Player Behaviour Modelling 9

1.2 Main Contributions 11

2 Principled Data Completion of Network Constraints for Spot Electricity Markets **17**

2.1 Introduction and Background Information 17

2.2 Background Information 20

2.2.1 The DC model and Line - Nodal Network Constraints 20

2.2.2 Line - Zonal Network Constraints 25

2.2.3 Practical Considerations 28

2.2.4 The Problem and Proposed Solution 31

2.3 Analysis of the Input Data 33

2.3.1 Constraints Data 34

2.3.2 Power Production Data 35

2.3.3 Grid Data 36

2.3.3.1 Transmission Grid 36

2.3.3.2 Adding the Production Grid 38

2.3.4 Other Time Series Data 39

2.4 Mathematical Optimisation Model 39

2.4.1 A Regularisation for the GSKs 40

2.4.2 Expressivity of the Nodal PTDF Map 44

2.4.3 The Optimisation Model 44

2.5 Numerical Optimisation 47

2.5.1 Optimising over $\boldsymbol{\nu}_{s,t}$ 47

2.5.2 Optimising over $\hat{\mathbf{b}}$ 48

2.5.3 Optimising over $\boldsymbol{\chi}$ 48

2.5.4 Optimising for $\mathbf{g}^1_{\theta^g_t}$ 48

2.5.5 Optimising over $\boldsymbol{\alpha}^L_{\theta^\alpha_t}$ . . . 49
2.5.6 Obtaining New Values for $\mathbf{g}^1_{\theta^g_t}$ and $\boldsymbol{\alpha}^L_{\theta^\alpha_t}$ after the Model Fit . . . 49
2.6 Numerical Results . . . 49
2.6.1 PTDFs and RAMs Reconstruction . . . 50
2.6.2 Structure Analysis of the Reconstructed GSKs and PAs . . . 54
2.7 Conclusion . . . 55

3 A Game Theoretic approach for Spot Electricity Markets 57
3.1 Introduction and Motivation . . . 57
3.2 Background Information . . . 64
3.2.1 Inelastic Demand . . . 66
3.2.2 A New Proposed Mechanism for Day Ahead Spot Market . . . 68
3.3 A Cost Minimisation Two-Zone Market Model . . . 74
3.3.1 A Game Theoretic Resolution of the Spot Auction . . . 81
3.3.2 Numerical Implementation . . . 84
3.4 Cost Minimisation Spot Model: Generalisation to any Number of Zones and Network Constraints . . . 86
3.4.1 Introduction of Ellipsoid Network Constraints . . . 86
3.4.2 The Spot Auction Model . . . 87
3.4.3 Game Theoretic Resolution of the N_z Zones Spot Auction . . . 94
3.4.4 A Mean-Variance Framework for Risk Averse Players . . . 97
3.4.5 Solving the Market Problem over the Polytope via Iterative Elliptical Constraints . . . 116
3.5 The general Cost Minimisation model with capacity constraints . . . 118
3.5.1 A Bilinear Formulation for the Market Clearing Problem . . . 119
3.5.2 Market Clearing Solutions . . . 120
3.5.2.1 Iterative Enhanced quasi-LP Solution . . . 120
3.5.2.2 Iterative Ellipsoid Constraints Solution . . . 121
3.5.2.3 Branch and Bound Tree Based Solution . . . 124
3.5.2.4 Iteratively Bounded Convex Quadratic Programming solution (ib-CQP) . . . 129
3.5.3 Coupled and Decoupled Market Outcomes . . . 132
3.5.4 Robust Strategy Selection as a Risk Aversion Model . . . 132
3.5.5 Finding the Feasible Active Player Sets . . . 137
3.5.6 Nash Equilibria Computation . . . 140
3.6 The Social Welfare Maximisation Spot Model . . . 142
3.7 Numerical Results . . . 144
3.7.1 Synthetic Data Experiments (no capacity constraints) . . . 144
3.7.1.1 Risk Neutral Players . . . 144

3.7.1.2 Risk Averse Players . . . 144
3.7.2 Synthetic Data Experiments for Capacity Constrained Model and Algorithms . . . 146
3.7.2.1 Evaluation of Approaches for Solving the Market Clearing . 148
3.7.2.2 Evaluation of Approaches for Computation of Profit Function and Best Responses . . . 154
3.7.2.3 Computation of Nash Equilibria and Evaluation of its Properties . . . 158
3.7.3 Application to Real World Data (CWE Market 2019 – 2020) . . . 161
3.7.3.1 Input Data . . . 162
3.7.3.2 Model Calibration . . . 167
3.7.3.3 Truthful Bidding: Social Welfare Maximisation vs Cost Minimisation . . . 170
3.7.3.4 Social Welfare Maximisation: Truthful Bidding vs Game Theoretic . . . 175

4 Conclusion and Future work **187**
4.1 Summary of Current Work . . . 187
4.1.1 Main Points from the Literature Review . . . 187
4.1.2 Main Results . . . 189
4.1.2.1 An Overview of the Main Results of the Thesis . . . 189
4.1.2.2 Main results for each chapter of the thesis . . . 189
4.2 Future Work . . . 195
4.2.1 Forecasting of the GSKs and PAs . . . 195
4.2.2 General Bids and General Cost Functions . . . 195
4.2.3 Speeding Up the Market Clearing Solution Algorithms . . . 196
4.2.4 Increasing Model Richness . . . 196
4.2.5 Considering both future and spot markets . . . 197
4.2.6 Detection and forecasting of market state . . . 198

Bibliography **199**

List of Figures

1.1 Simplified schematic of the spot market system. Square elements represent decision making entities while round ones represent data items. An arrow from a data item to a decision entities represents an input, while the reverse represents an output. 6

2.1 Running example: an electricity network with two zones represented by different colors. Production and consumption nodes are represented by square and circular shapes respectively. 20
2.2 Running example: assigned nodal power vector for the base case ($\mathbf{p}_N^0$), and the resulting power flows across lines ($\mathbf{F}^{\text{ref}}$), given the susceptances $\hat{\mathbf{b}}$. 27
2.3 Number of recorded data points for the first 45 lines (left) and scenarios (right), sorted in descending order of recorded information amount. 35
2.4 CWE Grid Model. Each country is assigned two colours, with the more frequent one representing consumption nodes, while the other represents power plants. For Austria, the consumption nodes are colored in dark blue. Critical lines and outages (contingencies) are marked in red and cyan respectively. Lines that are both CNEs and Contingencies (for other CNEs) are marked in yellow. 39
2.5 Convergence of GSKs (left) and base case (right). 43
2.6 PTDF values on an Austrian line (left) and a German-Dutch crossing line (right) showing the reconstruction of the PTDF based on the regularisation values of $\hat{\mathbf{b}}^0$ and $\{\hat{g}_t^1\}_{t\in\mathcal{T}}$. 43

2.7 Detailed reconstruction results. Plots (a), (c) and (d) show the PTDF (French entry), RAM, and $\mathbf{F}^{\text{ref}}$ reconstruction results for a representative (French-German) line. The blue lines (and dots) indicate the reconstruction, while the black and red dots indicate the training and test data points respectively. The grey line is an interpolation between available data points for better visualisation only. The heat map in (b) indicates the relative RAM error in the sixth column, and relative PTDF error for the five countries, corresponding to the first five columns. These errors are computed with respect to the mean, since due to data scarcity on many (l, s) with very few observations, the standard deviation is very inaccurate or even zero. 52
2.8 Clustering results for the Generation Shift Keys and Phase Angles. For each subplot, the horisontal axis corresponds to time indices while the vertical axis corresponds to entries in $\mathbf{g}_t^1$ and $\boldsymbol{\alpha}_t^L$ respectively, and the vertical dark bars are delimiters between the clusters. 54

3.1 Example of offer preference issue for Social Welfare objective for discrete bids. The green offers are the ones selected by the social welfare. The market has one zone. 61
3.2 Variations of Cost Minimisation models considered. Richness and mathematical complexity is increased from top to bottom. Models are in blue while algorithms for solving them are in teal. White boxes explain changes between two linked model variations. 69
3.3 Market setup with inflexible demand. 74
3.4 Order books of offers: optimal choices based on SWM and CM. Note that we compute the negative of SWM objective such that the optimal solution is obtained by minimisation, consistent with CM. 75
3.5 Example of market clearing for fill-or-kill orders based on CM and SWM . . 76
3.6 Obtaining the optimal price function: (a) visualisation of player sets identification, and (b) the resulting (optimal) zonal stack curves 129
3.7 Local Nash Equilibria found: colored by numbers for comparison across players. The strategy set for each shown player is plotted in each subfigure, and the colorbar indicates the profit level for each player. 144
3.8 Local Nash Equilibria found: indexed by numbers for comparison across players. The strategy set for each player is plotted in each subfigure, and the colorbar indicates the profit level for each player. 146
3.9 Local Nash Equilibria found satifying the condition that the profit of all players is non-negative. Local Nash Equilibria are indexed by numbers for comparison across players. The strategy set for each player is plotted in each subfigure, and the colorbar indicates the profit level for each player. 147

3.10 Zonal price and zonal quantity estimator $\hat{y}_z$ vs number of iterations for ieq-LP and ieq-LP-ma with $\alpha = 0.5$. 148
3.11 ie-CQP: Zonal price, quantities, and convergence parameters for each iteration. 149
3.12 Constraints value. Each $(\mathbf{b}_I)_l - (\mathbf{A}_I)_l \mathbf{z}^j$ represents a plot line, evaluated at the solution obtained at iteration j, $\mathbf{z}^j$. 149
3.13 ie-CQP-wr: Zonal price, quantities, and convergence parameters for each iteration. 150
3.14 Convergence of the BBTree algorithm. Red nodes represent pruning, while the active nodes with the smallest lower bound and the best feasible solutions are represented by yellow and blue respectively. If the two coincide, they are represented in green. 150
3.15 Total cost (objective function) for the three-zone problem, given optimal $\mathbf{x}$ for every $\mathbf{y}$. Across the lines formed by the red points are the changes in the three player sets (at optimal $\mathbf{x}$ given $\mathbf{y}$): $\mathcal{P}^I$, $\mathcal{P}^M$, $\mathcal{P}^F$, highlighting the boundaries between which the objective function is continuous, quadratic and strictly convex. The golden and cyan stars represent the optimal points found by ib-CQP and BBTree respectively. 151
3.16 Player 1: Zonal price and quantity, time taken for ieq-LP-ma, ie-CQP-wr, BBTree, ib-CQP, fractional change in quantities, total cost and player profit under $(\mathbf{m}^I, \mathbf{a}^I)$. 154
3.17 Player 5: Zonal price and quantity, time taken for ieq-LP-ma, ie-CQP-wr, BBTree, ib-CQP, fractional change in quantities, total cost and player profit under $(\mathbf{m}^I, \mathbf{a}^I)$. 154
3.18 Player 2: Zonal price and quantity, time taken for ieq-LP-ma, ie-CQP-wr, BBTree, ib-CQP, fractional change in quantities, total cost and player profit under $(\mathbf{m}^{II}, \mathbf{a}^{II})$. 155
3.19 Player 3: Zonal price and quantity, time taken for ieq-LP-ma, ie-CQP-wr, BBTree, ib-CQP, fractional change in quantities, total cost and player profit under $(\mathbf{m}^{II}, \mathbf{a}^{II})$. 155
3.20 Change in optimal strategy of player 5 at NE (left) and total and average run times (right) for different discretisation levels. 159
3.21 Profit function for player 5 at NE (at N_{pts}), computed with 512 discretisation points. The red star indicates the exact location of the best response on this plot. 159
3.22 Strategy updates, computational times and optimality gaps for C-JS iterations under CNEP-Q 160
3.23 Capacity per production types per country, and illustration of player choice. Sub-figures (a)-(e) show the largest 10 production types per country. Sub-figure (f) illustrates the thresholding process. 164
3.24 Type of runs considered for the SWM and CM models. 170

3.25 Trends Comparison: electricity, gas and coal price vs SWM-TB model prediction, for the $\mathcal{T}_{train}$ (left of orange line), and $\mathcal{T}_{test}$ (right of orange line). Electricity prices are smoothed by taking an exponentially weighted average over 49 hours centered in the point of interest. Only FR electricity prices are shown for better visualisation. 171
3.26 Training set: SWM-TB and CM-TB model results comparison with target prices, with indicative demand series. 172
3.27 Test set: SWM-TB and CM-TB model results comparison with target prices, with indicative demand series. 173
3.28 Average daily profile for each country: sub-figures (a) - (e) and (f) the ratio of the CM profile to SWM profile, as well as the total cost ratio. 174
3.29 Price time series results (Training set): SWM - Truthful Bids (blue) and SWM - Game Theoretic (black) comparison against observed prices (red). . . 177
3.30 Price time series results (Test set): SWM - Truthful Bids (blue) and SWM - Game Theoretic (black) comparison against observed prices (red). 178
3.31 Classification of time points to their the most representative state. The red bars represent 97.5% CI for each axis respectively. 179
3.32 Comparison of price time series (individual TD-SD): State Detection results vs observed prices. 182
3.33 Comparison of price time series (aggregate TD-SD): State Detection results vs observed prices. 183
3.34 Results for the average day: proportion of each observed state. 184

List of Tables

2.1 Training and test errors for the two data splits $\mathcal{D}_1$ and $\mathcal{D}_2$. 51

3.1 Example problem parameters for numerical experiment on NE isolation. . . . 145
3.2 Objective functions, times taken and convergence indicators for ieq-LP, ie-CQP, BBTree, ib-CQP and their variants. 152
3.3 Time taken to compute profit functions for each player, with $N_{pts} = 20$ discretisation points on $\mathcal{B}_{LB}(.)$ 156
3.4 Results for $\overline{e}_z(\mathcal{T}_{train})$ for each zone and aggregate. 170
3.5 Results for $\overline{e}_z(\mathcal{T}_{test})$ for each zone and aggregate. 170

3.6 Comparison of relative mean errors for the Truthful Bids and Game Theoretic models, on train and test data sets. 176

Glossary

AC	*Alternating Current* is a type of current that periodically reverses direction and continuously changes its magnitude. 1
ATC	*Available Transfer Capacity.* An approach treating all nodes inside a zone as equivalent, and using box constraints on zonal quantities for the market clearing. 18
BBTree	*Branch and Bound Tree* is a branch and bound method in the zonal quantity space that we introduce to solve the Cost Minimisation market clearing problem. This guarantees global convergence and offers a certificate of optimality. 140
CB	*Critical Branch* (older terminology). A network element, usually a transmission line that is monitored by the TSOs to ensure that its power flow is within the safety limits. 29
CBCO	*Critical Branch - Critical Outage* (older terminology). A combination of a considered CB under a specified CO. 29
CM	*Cost Minimisation*, here referring to an objective for the day ahead market clearing optimisation problem, or to the whole optimisation problem. 12
CNE	*Critical Network Element* (newer terminology). A network element, usually a transmission line that is monitored by the TSOs to ensure that its power flow is within the safety limits. 29
CNEC	*Critical Network Element and Contingency* (newer terminology). A combination of a considered CNE under a specified CO (*Contingency*). 29
CO	*Critical Outage* (older terminology). A scenario where one network element, usually a transmission line that is removed from the grid. The grid has to remain operational under this assumption. 29
CWE	*Central Western Europe.* In this case, a whole region containing Austria, Belgium, France, Germany and the Netherlands. For this region, a single market exists. 3

DAA *Day Ahead Auction.* A general type of spot market where participants place bids and offers and the outcome is solved for all at once, and announced one day before the delivery day. 1

DC *Direct Current.* 1

ENTSOE *European Network of Transmission System Operators for Electricity.* Represents 39 electricity transmission system operators from 35 countries across Europe, extending beyond EU borders. 38

FAV *Final Adjustment Values.* A term introduced by the TSOs when computing the RAMs, to account for errors due to model simplifications, by using expert knowledge. 30

FBMC *Flow Based Market Coupling.* A type of market clearing for the DAA in power markets that maximises the SW subject to Network Constraints and possibly other type of constraints. 2

FCG *Final Transmission Grid.* A term introduced here to describe the transmission grid, which contains only the nodes and lines corresponding to transmission and consumption, and not those corresponding to production. 38

FPA *First Price Auction* is a pricing scheme for the market clearing mechanism, finding the unique price such that supply and demand are balanced. All ask offers must have prices below or equal to the unique price, while the reverse is true for the bid offers 58

FRM *Flow Reliability Margins.* A term introduced to correct the RAM values, due to model errors. The correction is based on the statistics of the empirical error distribution over each line. 30

GSK *Generation Shift Key.* A pattern that estimates how one extra unit of production in a zone is distributed amongst nodes in this zone. It is used to make nodes equivalent. Can be a vector if referred to one zone, or a matrix if referred to multiple zones. 3

GT *Game Theory* or Game Theoretic, depending on the context. Game Theory is a branch of mathematics concerned with studying strategic behaviour. 162

GU *Generation Unit*. A power plant connected to the grid. 38

ib-CQP *iteratively bounded Convex Quadratic Programming* is a method based on iteratively solving convex quadratic programs bounded on polytopes that we introduce to solve the Cost Minimisation market clearing problem. This method uses strong (but partial) analytical results and guarantees global convergence on the sub-domain containing the end solution. 140

ie-CQP *iterative ellipsoids CQP* is a method based on iteratively solving trust-region like problems on ellipsoid domains we introduced to solve the Cost Minimisation market clearing problem. This guarantees (slightly stronger than) local convergence. 118

ieq-LP *iterative enhanced quasi Linear Programs* is a method based on iteratively solving LPs we introduced to solve the Cost Minimisation market clearing problem. 118

ISRC *Iterative Sensitivity of Regression Coefficient*. A data driven approach to obtain the Generation Shift Keys iteratively, based on SRC, without knowledge of the base case. 42

LMP *Locational Marginal Prices*. Generally, they are prices obtained as dual variables of energy balance constraints at each node. Can be different for each node. 4

MCM *Market Clearing Mechanism* is any mathematical optimisation problem or set of rules that uses the order book (and possibly an objective and constraints) to determine a price and quantity allocation outcome for the spot market. 9

NEX *Net Exports*. The difference between exports and imports at zonal (country) level. 39

OPF *Optimal Power Flow* is a well studied optimisation problem in power systems. The objective is to find an operating point that minimises the cost of electricity generation while satisfying operating constraints and meeting supply and demand balance. 59

PA *Phase Angles* describe the shift between total voltage and total electric current in AC current. In our case this name is somewhat abused, and we often refer to differences in Phase angles between adjacent nodes as PAs. 4

PaB *Pay-as-Bid*. A pricing mechanism that assigns to every producer or consumer the price asked or offered for each quantity accepted. 58

PTDF *Power Transmission Distribution Factor*. They can be line-nodal or line-zonal, showing how the flow on each line changes for one unit of power change at each node or zone respectively. In the linear set of constraints they form, that can be written as $b_L \leq Ax \leq b_U$, they play the role of A. 18

RAM *Remaining Available Margin*. Shows the maximum change of power flow that can occur on a transmission line before reaching the safety limit. For each line there are two values, defining a lower and upper limit. In the linear set of constraints they form, that can be written as $b_L \leq Ax \leq b_U$, they play the role of b_L and b_U respectively. 18

SRC *Sensitivity of Regression Coefficients*. A data driven model to compute Generation Shift Keys based on regression coefficients of a linear regression model on power plant production levels. 40

SW *Social Welfare*. A common objective used for the Day Ahead Auction market clearing in Power Markets. It is the sum of consumer and producer surpluses. 1

SWM *Social Welfare Maximisation* is a market clearing mechanism focused on maximising the sum of consumer and producer surplus, subject to supply and demand balance and operational constraints. 5

TB *Truthful Bidding* means that each player places their market orders to perfectly reflect their true cost (or benefit) structure. This is often used as an assumption but could also be a result of equilibrium under certain setups. When used as an assumption, it removes the need for consideration of strategic bidding. 5

TSO *Transmission System Operators*. They manage the grid ensuring that the network constraints are not violated. They define the base case and the GSKs, and solve the market clearing optimisation model. 17

Mathematical Notation

L	Number of transmission lines in the grid.	21
N	Number of nodes in the grid.	21
N_c	Number of polytope linear network constraints.	86
N_z	Number of zones in the market.	86
U_i	Utility of player i, here based on mean-variance framework applied to profit.	100
$\Delta P_{z,t}$	Change in zonal production level with respect to the base case value for zone z at time t.	8
η_i	Risk aversion parameter of player i.	100
PSDF	Matrix of Power Shift Distribution Factors, mapping phase angle differences on lines to the corresponding power flows exclusively due o these differences.	8
PTDF_t	Matrix of line-zonal Power Transmission Distribution Factors at each time t. Entry $(\text{PTDF}_t)_{l,z}$ shows the impact of one unit of power change on zone z on line l.	8
$\text{PTDF}_{s,t}$	Matrix of line-zonal Power Transmission Distribution Factors at each time t under outage scenario s. Entry $(\text{PTDF}_{s,t})_{l,z}$ shows the impact of one unit of power change on zone z on line l. Often this represents the *target data* matrix.	30
ρ_z	The market clearing price in zone z.	69
d	The total demand over the grid ($d = \mathbf{1}^T\mathbf{d}$).	88
l	Usually represents a line in the grid, sometimes simply an index.	21
r_s	The radius of the ellipsoid, from the definition of ellipsoid constraints over $\mathbf{y}$, $\|\mathbf{A}_s\mathbf{y} - \mathbf{p}_s\|_2 \leq r_s$.	87
s	Outage scenario s, under which a grid line is removed. This is often used as a subscript to various quantities.	30
t	Time index t, usually representing a one hour interval in this work. This is often used as a subscript to various quantities.	8

z	Represents a zone in the market, which is usually a country, and this is generally used as a subscript or superscript for various quantities to indicate that the quantity is constrained to this zone.	8
Π_i	Profit of player i.	82
$\mathbf{\Omega}(s)$	Projection matrix removing the line corresponding to outage scenario s.	32
$\mathbf{\Omega}_{\text{cne}}$	Projection matrix retaining the set of critical lines from the set of all transmission lines in the grid.	29
$\mathbf{\Omega}_{ref}$	Projection matrix removing reference node.	22
$\mathbf{\Omega}_{s,t}$	Projection matrix retaining data on lines corresponding to the observed data for time t and outage scenario s.	32
$\boldsymbol{\alpha}_t$	Vector of phase angle differences across transmission lines of interest at time t.	8
$\boldsymbol{\chi}$	Concatenation of $\boldsymbol{\chi}^p$ for all power plants p.	44
$\boldsymbol{\chi}^p$	Vector telling us how one unit of power generated by plant p is distributed across (neighbouring) nodes.	44
$\boldsymbol{\delta}_N$	Vector of nodal phase angles.	22
$\hat{\alpha}_z$	The slope for the zonal price ρ_z as a function of total produced quantity y_z, at optimal $\mathbf{x}_z$ given fixed y_z, $\rho_z = \hat{\alpha}_z y_z + \hat{\beta}_z$.	79
$\hat{\beta}_z$	The intercept for the zonal price ρ_z as a function of total produced quantity y_z, at optimal $\mathbf{x}_z$ given fixed y_z, $\rho_z = \hat{\alpha}_z y_z + \hat{\beta}_z$.	79
$\hat{\mathbf{A}}_s$	Line adjacency matrix encoding the graph structure of the electricity grid, when the grid line corresponding to outage scenario s is removed from the graph.	32
$\hat{\mathbf{B}}_s$	Diagonal matrix of line susceptances, with the line corresponding to outage scenario s being removed.	32
λ_i	The asked (marginal) price by player i for generating x_i units of electricity. We here parametrise $\lambda_i(x_i) := m_i x_i + a_i$.	69
$\mathbf{A}$	Line adjacency matrix encoding the graph structure of the electricity grid. If element $\mathbf{A}_{j,i}$ is non-zero then node i is one end of line j.	21
$\mathbf{A}_s$	The matrix from the definition of ellipsoid constraints over $\mathbf{y}$, $\|\mathbf{A}_s\mathbf{y} - \mathbf{p}_s\|_2 \leq r_s$. Note the distinction with $\hat{\mathbf{A}}_s$ which denotes the line-adjacency matrix of the grid under outage scenario s.	87

$\mathbf{B}$	Diagonal matrix of line susceptances. Each element $B_{j,j}$ represents the susceptance of line j of the electricity grid	22
$\mathbf{E}$	A linear map from the accepted quantities to the net energy production in the zone.	120
$\mathbf{F}^{\max}$	Vector of maximum allowed power flows on each line.	8
$\mathbf{F}_t^{\text{ref}}$	Vector of reference flows on transmission lines under the base case, at each time t.	8
$\mathbf{G}_t^1$	Matrix of Generation Shift Keys (GSKs) indexed by time t. Sometimes the temporal dependence is ignored, and this is then denoted as $\mathbf{G}^1$. If temporal dependence matters, then $\mathbf{G}^1$ refers to the collection of all $\mathbf{G}_t^1$.	8
$\mathbf{G}_{s,t}^1$	Matrix of Generation Shift Keys (GSKs) indexed by time t and outage scenario s.	31
$\mathbf{M}_p$	The matrix of polytope linear constraints on $\mathbf{y}$, $\mathbf{M}_p\mathbf{y} \leq \mathbf{b}_p$.	86
$\mathbf{P}(\hat{\mathbf{b}}, \mathbf{A})$	Line-nodal PTDF matrix as a function of line susceptances $\hat{\mathbf{b}}$ and line-adjacency matrix $\mathbf{A}$.	24
$\mathbf{P}_s(\hat{\mathbf{b}}, \mathbf{A})$	Line-nodal PTDF matrix when considering outage scenario s, as a function of line susceptances $\mathbf{b}$, and line-adjacency matrix $\mathbf{A}$. Sometimes written as $\mathbf{P}_s(\mathbf{b})$, where explicit dependency on the line-adjacency matrix is not shown.	30
$\mathbf{Q}$	The vector of production capacities for all players. The entry Q_i represents the production capacity of player i. The vector $\mathbf{Q}_z$ is the collection of production capacities for all players in zone z.	118
$\mathbf{R}_t$	Vector of upper bounds on changes allowed with respect to the base case on transmission lines. Upper Remaining Available Margins.	8
$\hat{\mathbf{b}}$	Vector of line susceptances. Each element $\hat{b}_j$ represents the susceptance of line j of the electricity grid.	8
$\mathbf{a}$	The vector of intercepts for the asked marginal price as a function of quantity. The entry a_i represents the intercept of player's i asked price $\lambda_i(x_i) = m_i x_i + a_i$. The vector $\mathbf{a}_z$ is the collection of intercepts for all players in zone z.	98

$\mathbf{b}$ The vector of intercepts for the marginal cost as a function of quantity. The entry b_i represents the intercept of marginal cost of player i $\frac{\partial C}{\partial x_i}(x_i) = c_i x_i + b_i$. The vector $\mathbf{b}_z$ is the collection of intercepts for marginal costs of all players in zone z. 85

$\mathbf{b}_p$ The vector of polytope linear constraints on $\mathbf{y}$, $\mathbf{M}_p\mathbf{y} \leq \mathbf{b}_p$. 86

$\mathbf{c}$ The vector of slopes for the marginal cost as a function of quantity. The entry c_i represents the slope of marginal cost of player i $\frac{\partial C}{\partial x_i}(x_i) = c_i x_i + b_i$. The vector $\mathbf{c}_z$ is the collection of slopes for marginal costs of all players in zone z. 85

$\mathbf{d}$ The vector of zonal demands, as determined by the market clearing mechanism. Each entry d_z denotes the demand in zone z. 86

$\mathbf{g}_t^0$ Vector of nodal base case production concatenated over all zones z at time t. 8

$\mathbf{g}_t^1$ Vector of generation shift keys concatenated over all zones z at time t. 8

$\mathbf{g}_{z,t}^0$ Vector of nodal base case production for zone z at time t. 8

$\mathbf{g}_{z,t}^1$ Vector of generation shift keys for zone z at time t. 8

$\mathbf{i}_L$ Vector of current across the transmission lines. 21

$\mathbf{i}_N$ Vector of current injected at each node in the grid. 21

$\mathbf{m}$ The vector of slopes for the asked marginal price as a function of quantity. The entry m_i represents the slope of player's i asked price $\lambda_i(x_i) = m_i x_i + a_i$. The vector $\mathbf{m}_z$ is the collection of slopes for all players in zone z. 98

$\mathbf{p}_L$ Vector of line power flows for all transmission lines in the grid. 22

$\mathbf{p}_N$ Vector of nodal power levels for all nodes in the grid. 22

$\mathbf{p}_s$ The vector defining the centre of the ellipsoid, from the definition of ellipsoid constraints over $\mathbf{y}$, $\|\mathbf{A}_s\mathbf{y} - \mathbf{p}_s\|_2 \leq r_s$. 87

$\mathbf{p}_{z,t}^N$ Vector of nodal power levels in zone z at time t. 8

$\mathbf{r}_t$ Vector of lower bounds on changes allowed with respect to the base case on transmission lines. Lower Remaining Available Margins. 8

$\mathbf{v}$ At optimality, the vector of zonal prices, as determined by the market clearing mechanism. Each entry v_z denotes the price variable in zone z. 121

$\mathbf{v}_L$	Vector of voltage drop across the transmission lines.	22
$\mathbf{v}_N$	Vector of voltage at each node in the grid.	22
$\mathbf{x}$	The vector of assigned production quantities based on the market clearing solution. Each entry x_j denotes the quantity assigned for player j and $\mathbf{x}_z$ denotes the vector of assigned quantities for all players in zone z.	64
$\mathbf{y}$	The vector of zonal production levels, as determined by the market clearing mechanism. Each entry y_z denotes the quantity produced zone z.	86
$\mathcal{LST}$	The triple of time index, line index and outage scenario combinations (l, s, t) observed in the data, where $l \in \mathcal{L}$, $s \in \mathcal{S}$, $t \in \mathcal{T}$.	34
$\mathcal{LS}$	The set of line-outage scenario combinations (l, s) observed in the data, where $l \in \mathcal{L}$, $s \in \mathcal{S}$.	35
$\mathcal{L}$	The set of lines in the electricity grid.	21
$\mathcal{L}_{\text{cne}}$	The set of (observed) critical lines in the electricity grid. These are the lines for which the operators consider transmission constraints, or at least the ones we observe.	29
$\mathcal{L}_{s,t}$	The set of (observed) critical lines in under outage scenario s at time t. Can be expressed mathematically as $\mathcal{L}_{s,t} := \{j : (j, s, t) \in \mathcal{LST}\}$.	32
$\mathcal{N}$	The set of nodes in the electricity grid.	17
$\mathcal{ST}$	The double of time index and outage scenario combinations (s, t) observed in the data, $s \in \mathcal{S}$, $t \in \mathcal{T}$. Can be expressed as $\mathcal{ST} := \{(s, t) : (l, s, t) \in \mathcal{LST}\}$	34
$\mathcal{S}$	The outage scenario set considered by the operators. This is restricted in this work to transmission line outages only.	29
$\overline{\mathbf{A}}$	The extension of $\mathbf{A}_s$, $\overline{\mathbf{A}} := (\mathbf{A}_s, \mathbf{0})$.	90
$\tilde{\mathbf{A}}$	Line adjacency matrix encoding the graph structure of the electricity grid, with the reference node i_0 removed.	22

Chapter 1

Introduction and Overview

Electricity Markets play a key role in the economies of contemporary societies, and are frequently organised as Day Ahead Auctions (DAA) due to the difficulty of storing electricity, coupled with uncertainty in demand and production patterns. When compared to traditional financial markets, the complexity of electricity markets is drastically increased, as a consequence of the physical nature of the asset traded, difficulty of storage and distribution. As a result of these complexities, each market generally has its own idiosyncrasies, yielding a plethora of different market clearing approaches corresponding to different economic areas. In particular, European power markets tend to be poorly understood by market participants [83], due to the complexity and occasional ambiguity of methodology, and scarce available data. This thesis aims to contribute to a better understanding of European spot electricity markets in particular, but also contributes to knowledge on spot electricity markets in general.

The market price is perhaps the variable that is given the most importance by market practitioners. The price is determined by maximising what is known as the *Social Welfare* (SW), which is an estimate of the sum of consumer and producer surplus, subject to market clearing constraints (i.e. supply equals demand). This requires the allocation of production and consumption levels at each point in the electricity grid, which completely determine the flow across the electricity grid via Kirchhoff's Laws. However, possible outcomes are constrained by the physical limitations of the transmission grid. In particular, flows on each line need to be kept below a physical limit to avoid burn out. Thus, it is essential for any market clearing mechanism to include a representation of the physical constraints of the grid, and this requires having a grid representation to start with. While AC models are commonly used for grid modelling and tend to be more accurate, they are non-linear and generally too computationally expensive to be applicable to the market clearing mechanism. Instead, a DC model, which is a linearisation of the AC model, is generally used, since they are computationally much cheaper, and offer an acceptable level of accuracy. The DC model provides a set of linear constraints that approximate the physical ones, and the application

of this DC model in conjunction with a market clearing mechanism based on *Social Welfare* maximisation is known as the Flow Based Market Coupling (FBMC) mechanism in European power markets [78], [19]. Further simplifications are generally made in this model, to treat power production or consumption at any node within a zone (e.g. country) as equivalent for the network constraints and pricing.

The complexity of the market clearing procedure means that not all apparently economically viable bids or offers can be accepted, due to the grid constraints, bid related constraints such as *fill or kill* or *parent-child* type of bids, as well as potential inefficiencies introduced by the market mechanism, even at a theoretical level. Indeed, by the Myerson-Satterthwaite impossibility theorem, there exists no mechanism satisfying all of the following, expressed informally as: (i) incentivise players to participate, (ii) self financing auction, (iii) incentivise bidding truthfully at equilibrium, and (iv) economic efficiency [54]. Thus, at least one of these properties is automatically sacrificed by any market clearing mechanism, which may also leave the possibility for strategising. Further, inefficiencies may be introduced at the numerical solution level: the resulting market clearing optimisation problem is generally non-convex and non-linear, and thus obtaining the global, or even a local minimum can be very challenging in practice, especially due to the inherently large data size. We here focus on the network constraints and the understanding and solving of the market clearing mechanism, and ignore the issues related to bid constraints. Nevertheless, even this simplified setup introduces uncertainty for market participants, which are generally interested in maximising some form of risk adjusted reward. We mention the theoretical challenges and properties of various researched market mechanisms only briefly in Chapter 3, since we focus on obtaining and describing the market solution, and not on market design, which is a whole topic in itself, and some recent studies on auction design are [62], [40], and [59]. We use the Central Western European (CWE) wholesale electricity market mechanism as a case study to illustrate our methodology. This is motivated by anecdotal evidence suggesting that this market is not well understood by market participants. Further theoretical analysis of this market is rather limited, since the employed mechanism uses a pricing scheme that is non-standard for the electricity market mechanism design literature, see for example [36], [68], [85]. This is discussed in greater detail in Chapter 3.

It is thus clear that some of the most important questions related to the power market spot auction are: (i) the understanding of constraints, how they are obtained, and if market participants could estimate future constraints, (ii) resulting prices, how they are affected by the definition of the market clearing mechanism, by bids and offers, constraints, and market participants' behaviour, (iii) acceptance of trading orders, how they are affected by the definition of the market clearing mechanism, by bids and offers, constraints, and other participants' behaviour, and (iv) how to quantify risk exposure and devise a trading strategy from the perspective of a market participant. We employ and develop mathematical techniques to facilitate the understanding of some of these points and answering some of the questions, and our work represents a stepping stone for all (i)-(iv).

Market participants may generally prefer fundamental approaches over purely statistical ones because: (i) the market has many complex features that may not be easily captured by statistical methods, and often sufficient data is not available, (ii) the market procedures are generally relatively new, for example starting in May 2015 for the CWE, meaning that the amount of data available is limited, (iii) the market is experiencing constant change, making older data less relevant or even obsolete, but the new features can usually be easily introduced in a fundamental approach, and (iv) perhaps most importantly, even if the price is forecasted perfectly, for market participants this only matters to the extent that they are in or out of the market under the forecasted price. Owing to orders' structure, network and other order-related constraints, offering even all the available quantity below the ideal forecasted price does not guarantee that any fraction of this quantity can be absorbed by the market at the offered price, or even at higher prices, neither in the discrete, not in the continuous orders case. Further, producing a small quantity may be very unprofitable especially if requiring switching on production from zero, as detailed in the work of Troha and Hauser [53]. In other words, market participants are interested in price-quantity pairs, as opposed to just prices, and the quantities allocated are an underlying variable of the fundamental pricing process, strongly depend on other bids and offers, the constraints, and are not observed at participant's level. This makes using statistical methods for estimating the allocation of quantities very difficult, and perhaps even impossible in certain setups.

Thus, this thesis is concerned with exploring a fundamental approach to answer the questions posed before. Chapter 2 then focuses on the understanding of grid constraints and how they are obtained. Grid constraints can be introduced in various forms, but the two most common ones are via the Optimum Power Flow (OPF) model [85], [64] used for most North American markets, and Flow Based Market Coupling (FBMC) constraints, introduced for European markets in 2015. Since we consider European markets, we here focus on the FBMC approach, which constructs a set of linear constraints imposed on the net positions of each country (zone) [19], while nodes within the zone are treated as equivalent. While for a market using the OPF model, constraints are very granular and are always fixed, the FBMC constraints generally yield varying domains across time, due to the need to re-evaluate the approximation of equivalence within zone based on various market factors [19]. Nonetheless, market participants are interested in estimating future domains as part of their risk management strategies. For the Central Western European (CWE) power market, it turns out that the historical data of grid constraints is very sparse, including just a small number of all the constraints used during the market clearing process. However, the sparse data poses a challenge for forecasting future feasible domains, and to exploring the outcome space thoroughly market participants need the full set of constraints. Thus, Chapter 2 focuses on data completion of network constraints, based on the fundamental equations defining the network constraints. The constraints are obtained by mapping lower dimensional, time dependent underlying signals known as Generation Shift Keys (GSKs) and

Phase Angles (PAs) through static maps defined by the grid structure and physical characteristics. Historical data of these underlying signals is unavailable, and the grid structure is also not easily available. The core idea of our solution approach uses an optimisation model to fit the underlying signals and variables representing the graph structure to the available constraints data, starting with some initial estimates. The exact procedure requires more attention to detail and inclusion of multiple features, and is explained in depth in Chapter 2. We obtain results of acceptable accuracy for practical purposes, despite the large data sparsity and challenging optimisation problem. The obtained network constraints can then be used as input for the market clearing mechanism.

It is therefore natural to next aim at theoretical and practical understanding of price formation and quantity allocation. Given the network constraints, this is investigated in Chapter 3, where bids and offers are resolved based on a Market Clearing Mechanism (MCM). Placing orders is studied well via game theory for markets using LMP pricing with OPF network constraints. For this market clearing setup, a strategic gaming model for analysing markets where a single firm has strong market power is analysed in [36]. For the same market clearing setup, an oligopolistic environment is considered from a game-theoretic perspective, and an Equilibrium Problem with Equilibrium Constraints (EPEC) is obtained and solved. A similar game theoretic model using OPF based maximisation of the social welfare was proposed in [38]. Many other studies exist when considering OPF based market clearing and LMP pricing [32], [14], [47]. However, to the best of our knowledge no game theoretic studies of markets based on Zonal Marginal Pricing (ZMP) with Flow Based Market Coupling (FBMC) constraints exist, and the literature on optimisation models modelling the corresponding market clearing is also much scarcer, although some studies exist [5]. Market clearing for ZMP pricing with FBMC constraints is investigated in Chapter 3, where we also consider the possibility of market participants playing a (risk adjusted) profit maximisation game against the other participants. It is difficult for a fundamental model to encapsulate all the relevant key features of the market, and still retain computational tractability. Academic models usually make simplifying assumptions on the constraints, and more importantly on price formation. Most commonly, Locational Marginal Prices (LMP) are used [85], but these define prices at nodal level in the grid, while in practice, many European markets yield a market price that is unique at zonal (country) level, where a zone contains dozens or hundreds of nodes. Even these simplified models are generally very computationally intense to solve and to apply to the full scale real world data [85].

Our goal is to devise a fundamental model that retains as much as possible of the key features, while being computationally tractable, with the end goal of being applicable to the CWE power market. This enables understanding of the price formation and quantity allocation, investigating player behaviour and examining different strategies. We therefore also investigate the possibility of market participants playing a game of profit maximisation, where the price-quantity bids pairs placed need not be defined by their costs. We start with a very simple model of two zones and two participants per zone, and extend it to a model with

any number of zones and participants. Demand is taken as inflexible and we show that in this situation, risk aversion is required to eliminate the possibility of arbitrarily large prices. We present a novel formulation of the market clearing optimisation problem, that retains the main key features of the market, but also propose a Cost Minimisation (CM) based market clearing. We build novel algorithms to solve the CM market clearing problem much more efficiently, and we present a range of algorithms with different *"speed versus accuracy"* trade-offs. We also investigate numerically these algorithms and show their performance. We devise a method for *approximate global Nash Equilibrium* computation under a specific type of risk aversion that we introduce, and numerically evaluate the impact of different factors on the *approximate global NE*. The next step is to apply this model to the real world example of CWE power market, and investigate the performance of our models, confirming their relevance. We finally devise a method to identify if and when players are bidding strategically (instead of truthfully), and while we cannot state with certainty, we find statistical evidence indicating that strategic bidding may be fairly pronounced.

1.1 Modelling of Electricity Day Ahead Markets and their Constraints

In this section, we provide a quick overview of the focus of this work, and the main concepts used, but we leave the in-depth introduction and discussion of the concepts for the beginning of Chapter 2 and Chapter 3, each representing a piece of work with different focus, and different required concepts, although the two are highly inter-connected. We here focus on the *high level overview*, introducing the main concepts and showing how they relate to each other in this thesis. A simplified schematic of the spot market system is shown in Figure 1.1, revealing the main interaction between different data items and decision entities. The reader is encouraged to take some time to familiarise themself with this diagram, as it represents a simplified schematic of the main elements of interest for spot electricity markets, and reveals the focus of our work. However, this should not be taken too literally in the broader sense of

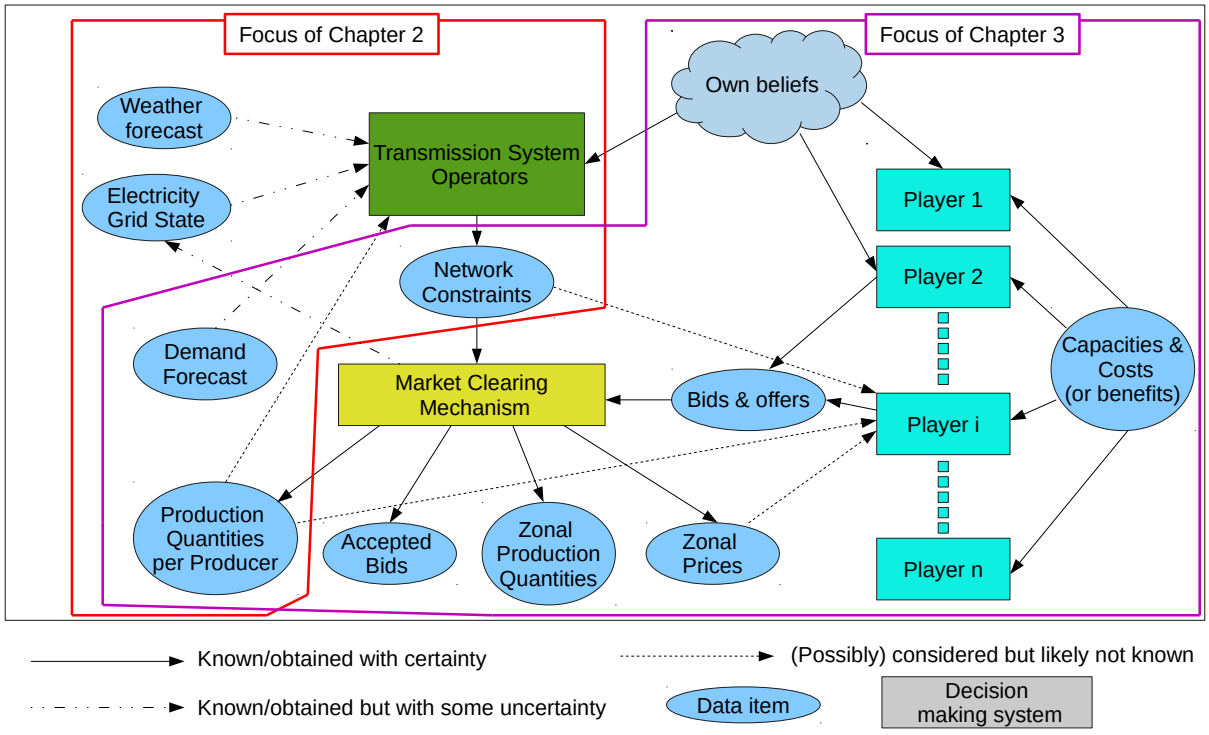


Figure 1.1: Simplified schematic of the spot market system. Square elements represent decision making entities while round ones represent data items. An arrow from a data item to a decision entities represents an input, while the reverse represents an output.

electricity markets or even for this thesis, as expressing all elements and relationships, and how they change with different (implied) assumptions would result in a much more complex diagram. Note that arrows from and to players are used to represent dependencies only sparingly, to avoid congestion on the figure.

The Transmission System Operators (TSO), the Market Clearing Mechanism and the players (producers or consumers) are decision entities because based on a set of inputs they

produce a response, regardless of whether the response is fully automated or not. The combination of a data item with an arrow represents either an input or an output. One can observe that the relations between different types of data are rather complex, even on this simplified diagram, and that different levels of certainty are present.

It can also be observed that given a defined Market Clearing Mechanism, the two main inputs are the network constraints, and the bids and offers. The market clearing mechanism gives the final prices and quantity allocation (acceptance of bids and offers), and thus by having models for the decision entities and the required data, a fundamental model for price formation and quantity allocation is obtained. However, some of the main issues of building a fundamental model for this system are as follows: (i) we can only observe a very sparse version of past historical data of the network constraints, (ii) historical data of bids and offers is generally not available, (iii) the market clearing mechanism may be very difficult to solve and (iv) many of the data items illustrated here (and others not mentioned) are not easily (or at all) available. These issues require separate and in-depth treatment, and for this reason, Chapter 2 focuses on obtaining the full set of network constraints, while Chapter 3 is focused on obtaining the bids and offers (the order book). Note that there is no data available on the order book, and therefore one has to model player behaviour to obtain some form of bids and offers. Two common ways for such modelling are: (i) assuming that the players bid and offer according to their true cost or benefit curves, or (ii) assume that players aim to maximise their own utility (or profit), resulting in a game theoretic framework. Since (ii) is strongly connected to the Market Clearing Mechanism, price formation and quantity allocation, this becomes a central point of interest for Chapter 3. One can observe the overlaps between the work for the two chapters in Figure 1.1, which can be roughly summarised in a single sentence as follows: *The full set of network constraints is the main output of Chapter 2, and is a key input for Chapter 3.* We can also observe that there are arrows pointing from elements of Chapter 3 to elements of Chapter 2, suggesting that the work could not be separated as described. However, in reality the TSO have to use estimates of those quantities *ex-ante*, and this breaks the loop at the cost of increased uncertainty. The demand forecast is of interest for Chapter 3 as well, because once we consider consumers as purely inflexible, their behaviour can be modelled based on demand exclusively.

1.1.1 Overview of the DC Grid Model based Network Constraints

We briefly review the main concepts required for Chapter 2 here, but we derive and discuss the concepts in detail in the introduction of Chapter 2. To obtain a mathematical representation of the grid constraints, one requires a grid model in the first place. On an electricity grid, an edge represents a transmission line, while a node represents a production (power plant) or consumption entity. We are here concerned with the application of the DC-Power flow model [19] to obtain a (linear) representation of the network constraints. Note that the

grid constraints change over time, and thus appropriate quantities are indexed by t, and the assumption is that the quantities remain fixed over intervals of time (usually 1 hour) represented by t [78]. Further, operators are concerned with feasibility of power transfer between different countries and therefore each zone z (usually a country in Europe) is treated as a separate entity. A key equation is the expansion of the vector of nodal power levels, $\mathbf{p}^N_{z,t}$, for each zone z at time t as

$$\mathbf{p}^N_{z,t} = \mathbf{g}^0_{z,t} + \Delta P_{z,t}\mathbf{g}^1_{z,t}, \tag{1.1}$$

where $\mathbf{g}^0_{z,t}$ and $\mathbf{g}^1_{z,t}$ are fixed vectors determined by the TSOs. While $\mathbf{g}^0_{z,t}$ represents an *ex-ante* guess of the nodal power levels at time t, $\mathbf{g}^1_{z,t}$ represents a guess of the way in which the actual nodal power levels may differ from the *ex-ante* guess if the zonal production level changed by $\Delta P_{z,t}$ with respect to the initial guess of zonal production level (which is fully defined by $\mathbf{g}^0_{z,t}$). By using the decomposition in (1.1), one can obtain the vector of flows through each line of the grid as $\mathbf{F}^{\text{ref}}_t = \mathbf{P}(\mathbf{b}, \mathbf{A})\mathbf{g}^0_t + \text{PSDF}(\mathbf{b}, \mathbf{A})\boldsymbol{\alpha}_t$, where $\mathbf{g}^0_t$ is the concatenation of initial guesses for all zones, and $\mathbf{P}(\mathbf{b}, \mathbf{A})$ is a map defined by the graph topology $\mathbf{A}$, and physical characteristics $\hat{\mathbf{b}}$. The second term, $\text{PSDF}(\mathbf{b}, \mathbf{A})\boldsymbol{\alpha}_t$ represents the limited controls that the TSOs have over the flows, which also depend on the grid through the map $\text{PSDF}(\mathbf{b}, \mathbf{A})$ and on the control variables $\boldsymbol{\alpha}_t$. The zonal power level changes can be mapped via the PTDF_t map to line flow changes as

$$\delta\mathbf{F} = \text{PTDF}_t\delta\mathbf{p}_t, \tag{1.2}$$

where $\delta\mathbf{p}_t$ is the concatenation of the $\Delta P_{z,t}$ scalars for all zones, and the map is

$$\text{PTDF}_t = \mathbf{P}(\mathbf{b}, \mathbf{A})\mathbf{G}^1_t, \tag{1.3}$$

where the $\mathbf{G}^1_t = \text{diag}(\mathbf{g}^1_t)$ matrix is given by the diagonal concatenations of $\mathbf{g}^1_{z,t}$ guesses. Knowing the initial guess flows $\mathbf{F}^{\text{ref}}_t$, and the vector of maximum allowed flows (before line burnout occurs) $\mathbf{F}^{\max}$, one can bound the feasible changes of zonal power production as

$$\mathbf{r}_t \leq \text{PTDF}_t\delta\mathbf{p}_t \leq \mathbf{R}_t, \tag{1.4}$$

where $\mathbf{r}_t = -\mathbf{F}^{\max} - \mathbf{F}^{\text{ref}}_t$ and $\mathbf{R}_t = \mathbf{F}^{\max} - \mathbf{F}^{\text{ref}}_t$. Equation (1.4) is crucial because it gives the final constraints used by the market clearing mechanism. One can observe that the TSOs play a key role in the formation of the network constraints represented by (1.4), because they define (or choose) $\mathbf{G}^1_t$, $\mathbf{g}^0_t$ and $\boldsymbol{\alpha}_t$. We refer to these as the *underlying signals* throughout this work, and extensive effort is made to obtain these values, as there is no data available on this. One may also notice that the other key element is the grid structure, which determines the (directional) line-node adjacency matrix $\mathbf{A}$, and the grid's line susceptances $\mathbf{b}$. These

are also not easily available and extensive effort is put into obtaining these quantities. However, assuming the grid characteristics $(\mathbf{b}, \mathbf{A})$ and the underlying signals $\mathbf{G}_t^1$, $\mathbf{g}_t^0$ and $\boldsymbol{\alpha}_t$ are available, one can compute the full set of constraints, which is not available in practice, and can even aim to forecast them into the future, since the underlying signals are much lower dimensional and have much less erratic changes with respect to time and other relevant parameters.

1.1.2 Overview of Market Clearing and Player Behaviour Modelling

With the network constraints now available, one is now ready to analyse player behaviour and market clearing mechanisms not only theoretically but also via numerical experiments on real world data. This is the focus of Chapter 3, and we next briefly discuss Market Clearing, and player behaviour, both of which are discussed in great detail in Chapter 3.

We start by briefly considering the design of Market Clearing Mechanism, which is defined according to a set of objectives and a set of constraints. For example some possible objectives could be: social welfare maximisation, procurement cost minimisation, price stability, etc, while constraints are usually represented by: (i) economic constraints, (ii) physical constraints such as network constraints, capacity constraints, and (iii) order book related constraints such as fill-or-kill. This type of problems naturally translate to a mathematical optimisation problem, and thus throughout this work, when we refer to a Market Clearing Mechanism (MCM), we often actually refer to its corresponding optimisation problem. An MCM must define a way to: (i) accept and reject bids and offers, that is allocate quantities to producers and consumers and (ii) determine the prices of transactions. Commonly (i) is achieved first and often heuristics or another optimisation problem is used for (ii). The inputs to the MCM optimisation problem depend on its definition, but crucially they always require some form of constraints, and the set of bids and offers. A fairly general form of a market clearing mechanism reads

$$\begin{aligned} &\min_{\mathbf{v},\mathbf{x}} F(\mathbf{v}, \mathbf{x}; \omega), \\ &s.t.\ \mathbf{G}(\mathbf{v}, \mathbf{x}; \omega) \geq \mathbf{0}, \\ &\mathbf{H}(\mathbf{v}, \mathbf{x}; \omega) = \mathbf{0}, \end{aligned} \tag{1.5}$$

where $F(\mathbf{v}, \mathbf{x}; \omega)$ is the objective function, $\mathbf{v}$ represents the price vector, $\mathbf{x}$ the quantity vector and ω are the parameters of the optimisation problem which include participants' bids, network constraints, capacity constrains etc. Further, $G(\mathbf{v}, \mathbf{x}; \omega)$ and $H(\mathbf{v}, \mathbf{x}; \omega)$ are (possibly

nonlinear) functions defining the sets of inequality and equality constraints respectively. We can further split $\omega = (\sigma; \theta)$, where σ represents the bid and offers and θ all other parameters.

Solving for both prices and quantities at the same time usually results in a much more complex optimisation problem and often the constraints and objective are adjusted to exclude $\mathbf{v}$, which is then solved for separately, given $\mathbf{x}$, via a pricing rule which can be a heuristic or another optimisation problem. Note that the quantity allocation to each and every participant is given by the MCM as a result of input bids and offers (and other parameters), and is *not* chosen by the participants. This is because bids and offers are effectively limit orders (as opposed to market orders) that are collated and solved for simultaneously via the MCM, instead of on the fly as the reader may be familiar with, from more traditional financial markets (such as equities).

Finally, it is worth making a clear distinction between cost of producers and their offers (or benefits of consumers versus bids). The producers have little or no control over the costs since these are given by the power plant type, fuel costs, and other factors, but they have full control over their submitted offers. This means that the production costs (consumption benefits) and offers (bids) are different in principle, and it is the decision of the producer (consumer) to offer at their marginal cost (benefit) or otherwise. The offers and bids are therefore the decision variables of the producers and consumers respectively, and are not known, while the costs of production and benefits of consumption are much less controllable but estimates of these quantities can in principle be obtained. To obtain the bids and offers, it is often assumed that they are simply the fair values corresponding to the cost and benefits [78], but this does not have to be the case in general. Another way to obtain estimates of bids and offers is via a game-theoretic framework, where players are assumed to be perfectly rational with the objective of maximising their own utility (here strongly related to profit). Each player i then has a strategy σ_i, an objective function $u_i(\sigma_i; \sigma_{-i})$ where σ_{-i} represents the strategies of all other players except i, and a constraints set $C_i(\sigma_i; \sigma_{-i}) \geq 0$. In our case, the strategy σ_i can be price-quantity pairs or the asked (offered) marginal price for each extra unit of power production (consumption).

Note that in our case, since player's utility depends on the Market Clearing solution, it is more instructive to represent the utility as

$$u_i = u_i(\sigma_i; MCM(\sigma_i; \sigma_{-i}; \theta; i)) \tag{1.6}$$

where $MCM(\sigma_i; \sigma_{-i}; \theta; i)$ is the function that returns the market clearing output variables required by player i to compute utility u_i, under the submitted strategies $(\sigma_i; \sigma_{-i})$ and other parameters θ.

It is standard in Game Theory to look for equilibria where no player can improve their utility by changing their strategy, given the strategy of all other players is fixed. This is known as a Nash Equilibrium (NE), and it gives us a way to recover estimates of bids and

offers under the condition of strategic equilibrium. Formally, a set of strategies σ^* is a NE if and only if for all i:

$$u_i(\sigma_i; MCM(\sigma_i^*; \sigma_{-i}^*; i)) \geq u_i(\sigma_i; MCM(\sigma_i; \sigma_{-i}^*; i)), \quad \forall \sigma_i \in \mathcal{S}_i, \tag{1.7}$$

where $\mathcal{S}_i$ is the feasible strategies set of player i. One can now observe that solving the Market Clearing Mechanism requires a set of bids, while finding the set of equilibrium bids requires computing the solution of the MCM. Thus, the two cannot be separated under the Game Theoretic framework, and the importance of the MCM becomes obvious. From a computational perspective, player's utility depends on the MCM outcome, and thus MCM has to be solved for at multiple strategies σ, when finding a NE, whether this is done by iterative improvements or via an exhaustive search. From a theoretical perspective, changing the MCM may change the position and properties of the Nash Equilibria, or even their existence.

1.2 Main Contributions

In the previous sections of this chapter we introduced the reader to the spot electricity markets in general, some questions of interest, some of the main challenges faced by researchers and practitioners, and provided an overview main concepts used, and how they relate to each other in this thesis. In this section, we state the main contributions of the thesis and how they relate to existing literature, for each chapter individually.

Chapter 2

Chapter 2 is focused on the time series of electricity grid constraints, which play a very important role in price (and quantity) allocation during the market clearing. Our main contributions to this are as follows:

1. We obtain the full electricity grid of the Central Western European (CWE) trading region. This requires significant work due to incomplete grid information in certain instances. We then map the network constraints data (PTDFs and RAMs) to the grid. This is far from trivial since the data sets come from different sources, and the mapping has to be done for each line using endpoint names. We obtain the location, capacity constraints and historical production time-series for 436 plants in CWE, as well as their type. This is a challenging task as the location of power plants is not easily available and their names are often encoded.

2. We recognise that the published network constraints data is very sparse, and thus we devise a Mathematical Optimisation model to obtain the full network constraints

set at each time index. This is done by first obtaining the (much lower dimensional) *"underlying signals"*, known as the GSKs and Phase Angles, which give insight into the operator behaviour, but are not publicly available. Thus our work offers, for the first time, a way to extract estimates of key operator behaviour (encoded in GSKs and PAs), only using publicly available data, and by considering the network structure. To our knowledge, previous work on this area generally takes the view of the operator, or assumes a purely reactive operator that defines their response based on simplified metrics. By contrast, we make none of these assumptions, but use a fundamental model to uncover estimates of the GSKs and PAs from the observed data.

3. Due to the large data size, efficient numerical optimisation is required, and thus we devise an alternating minimisation approach to solve our optimisation model. This leverages marginal convexity in certain sub-spaces, and uses stochastic optimisation for the most computationally intense parts. It also uses efficient tensor implementation which is key to reducing computational time. We obtain good representation of the actual constraints, in the rather strict sense of relative error based on euclidean norm, as opposed to domain-based metrics.

4. We finally show that the GSKs may be grouped well in a small subset of clusters, with added noise on top, suggesting that operators have typical response patterns that they choose and adjust based on their knowledge and expertise. The strategies for choosing the GSKs, discussed in the work of Dierstein (2017) [21], are consistent with our findings, suggesting that the recovered underlying signal is representative of the true ones.

Chapter 3

Chapter 3 is focused on the outcome of the spot electricity market, and in particular of the Day Ahead Auction market clearing. This is analysed considering the assumption of truthful bidding of participants, but also under a game-theoretic framework, where players bid strategically. Our main contributions in this chapter may be better understood by splitting them in three parts.

Chapter 3 (Part 1) looks at simpler models with the goal of theoretical and practical understanding, and is comprised by the sections up to and including Section 3.4. The contributions made here are as follows:

1. We consider the case of network constraints, inflexible demand and assuming producers have very large production capacity (unconstrained production limit). For this case we introduce a Cost Minimisation (CM) optimisation model as a market clearing mechanism for the DAA which, unlike the Social Welfare Maximisation known as SWM (used in practice in the CWE), expresses the true cost of electricity procurement when the demand is inflexible, as opposed to the apparent cost implied by the SWM.

This apparent cost implied by the SWM can be viewed under inflexible demand as the pay-as-bid cost, but is inconsistent with the marginal pricing rule used. Following the approach in [38], [68], and [85], we consider ask marginal prices orders submitted to the auction that are linearly increasing in the produced power.

2. Since solving CM is more challenging than solving SWM, we introduce the idea of ellipsoid network constraints and show how market clearing can be solved for efficiently in this case, requiring numerical optimisation of a Trust-Region like quadratic problem only in a very low dimensional space, corresponding to the number of trading zones in the market (which is 5 in the case of CWE). All other variables can be then computed analytically. We then extend this idea to network constraints of polytope form, by solving iteratively over ellipsoids contained in the polytope.

3. Similar to the work of Hu and Ralph (2007) [85], we define a game over the Day-ahead auction, but solve the corresponding numerical problem differently by leveraging partial analytical results to define a system of non-linear equations that completely describes the stationary Nash Points (a weaker version of NE, [85]). These are then solved for efficiently via iterative descent methods (Gradient or Newton based). This approach is fast since it only requires solving one (or more for polytope constraints) 5D Trust-Region like sub-problem for each outer optimisation step when finding the stationary Nash points. However, this comes at the cost of ignoring producers' capacity constraints, which are important for price formation. We address this in the next sections.

4. We discuss the issue of producers' market power, and from a theoretical perspective, we argue that if participants are not risk averse, prices can be arbitrarily large in the case of inflexible demand. By considering a mean-variance framework to represent risk aversion, we show that risk aversion places a ceil on the ask prices, that results in a ceil in market prices, as well as total cost. Further, given that everything else stays the same, increasing the risk aversion of the least risk averse player will reduce the price ceil, and in the limit of infinitely risk averse players, producers will bid to be paid their true costs, even when strategising to maximise their own risk adjusted profit.

5. For the simple case of two zones and two players per zone we also show that if the least risk averse player is sufficiently risk averse, the Nash stationary points (and thus Nash Equilibria) become isolated, although in practice, when considering synthetic data, we observe that they may remain close to each other. Since the theoretical results are not very descriptive and not easily generalisable, this motivates us to introduce a different type of risk aversion in Section 3.5.

Chapter 3 (Part 2) is composed of Section 3.5, and is focused on adding capacity constraints and resolving the issues associated with the mean-variance risk aversion framework.

Since the resulting CM problem (with producer capacity constraints) is much more complex than before, this focuses largely on algorithms to solve the DAA market clearing, and related issues such as risk aversion of participants. This work is key to enable building and solving efficiently for a realistic model that can represent real world markets. The contributions made here are as following:

1. We introduce a more general cost minimisation optimisation model for the DAA market clearing, that includes producers' capacity constraints, and write an equivalent bilinear formulation of this model. We show how the iterative ellipsoid idea can still be applied to solve for this market, but due to the capacity constraints of the producers, the optimisation process has to be lifted to a much higher dimensional space, with dimensionality roughly corresponding to the number of players. This increases the computational cost and the risk of ill-conditioning. Nevertheless, we introduce a way to re-condition the ellipsoids that drastically improves performance, and we call this approach ie-CQP-wr.

2. We also introduce and explore three other methods with different trade-offs between computational cost (convergence speed) and convergence guarantees. The four methods we devise are therefore (i) ieq-LP-ma: a method based on iterateively solving simple LPs, that is generally fast but has no convergence guarantees, (ii) ie-CQP-wr which is an extension of the iterative ellipsoids method described before and offers (slightly stronger than) local convergence guarantees, (iii) a branch and bound method (in the space of zonal quantities) that leverages the structure of the problem, and offers global convergence guarantees and a global optimality certificate, and (iv) ib-CQP that uses strong (but partial) analytical results to iteratively solve polytope-constrained Convex Quadratic Programs over regions that depend on players' bids and capacities. This method offers global convergence guarantees on the (finite size) subdomain corresponding to the last solved CQP, which may be large at times. This convergence guarantee is fairly strong, but slightly weaker than purely global convergence guarantee.

3. The partial analytical results corresponding to ib-CQP allow us to obtain an analytical form of what we call *optimal zonal stack curves* for offers, and the result and concept are new to our knowledge. For the type of bids considered, these curves are piecewise linear, and the price is strictly increasing function of quantity but there may be discontinuities (upward price jumps across y_z for dy_z quantity increase).

4. We evaluate the four methods on synthetic data to provide some intuition of the advantages and disadvantages of each method, and discuss what may be the appropriate method to use based on different requirements and resource available, although due to time limitation, our study and discussion are not exhaustive, and could be greatly extended.

5. A novel type of risk aversion is introduced, in which players first ensure that they maximise their profit in a *worst case scenario*. We refer to this type of risk aversion as Robust Strategy Selection (RSS) and this is explained in detail in Section 3.5.4. It turns out that there is a convex, bounded and one dimensional space of such choices under the offer structure considered in this thesis. The added benefits of this risk aversion model are then: (i) the non-parametric form, (ii) reduced dimensionality for the strategy variables, which allow for faster NE computation, and (iii) boundedness of strategy set, ensuring that the zonal prices are also bounded.

6. Using the fact that the strategy sets under RSS are one dimensional and bounded, we discretise the strategy space for each player, and this allows us to compute *approximate* global Nash Equlibria. Similar to [85], we perform Gauss-Seidel or Jacobi updates of an initial guess of strategies until reaching an equilibrium point. The difference lies in the risk aversion used and the discretisation of strategy space which allows us for faster computation, and finding approximate global Nash Equilibria. Time and computationally efficient algorithms are implemented using multiprocessing and multitasking to compute the Nash Equilibria, via cloud computing services provided by *Descartes Labs* [46].

Chapter 3 (Part 3) is comprised of Section 3.6 and Section 3.7.3 is focused on the application of the methodology to real world case of the CWE Day Ahead Auction. The contributions made here are as following:

1. We introduce a version of the Social Welfare Maximisation (SWM) market clearing mechanism, which can be used directly under the game-theoretic framework and for the corresponding equilibrium-finding algorithms.

2. Using the network constraints data obtained in Chapter 2, and by gathering data about producers, we define players based on their fuel type, similar to the work of Troha (2015) [77]. We obtain producers' cost structure, that are parametrised in a rather simplistic way, but consider fuel price changes over time. We propose an optimisation approach to calibrate the models to the data, under the truthful bidding assumption. The number of parameters fit is very small and only represents the scale of the cost structures for each zone. We also propose a simple scaling approach to improve our guess of the cost scales in the case of game-theoretic models. While our models are fundamental, and require no calibration in principle, if sufficiently granular and accurate data is available, due to time limitations we only obtain the fuel costs and production capacities based on a bottom up approach, but fit the cost scales instead of obtaining them from a bottom-up approach.

3. We run numerical simulations of our CM and SWM market clearing models combined with the Truthful Bidding assumption and Game theoretic framework respectively,

on the real data of CWE, and obtain results that represent the actual price time series well. To the best of our knowledge, detailed results from the application of such models to real world spot electricity markets have not been obtained before, and this confirms the computational efficiency of our models and algorithms from a practical perspective, as well as their ability to represent the market.

4. Our numerical results show that our the SWM model generally replicates the actual prices well. However, we also show on the real data that using CM as a market clearing instead, reduces the market power of producers, as generally it decreases zonal prices by a significant amount, and always decreases the total cost of electricity procurement. This suggests that the CM model introduced by us, could be used to reduce producer's market power if required.

5. We attempted to infer whether players are bidding truthfully or strategically in the CWE market, comparing the results given by the SWM-Truthful bidding model and SWM Game-Theoretic model against the real world price data. We devise a simple method based on hypothesis testing and use the simulation results based on the real data to identify if and when players are bidding strategically. While we cannot identify with high certainty the bidding behaviour of players for a large number of times, we find statistical evidence that strategic bidding (in at least one zone at each time) may be fairly pronounced. In fact, the fraction of times we can conclude with high confidence that players in all zones were bidding truthfully is small by comparison with the number of times we can conclude with high confidence that players are bidding strategically.

Chapter 2

Principled Data Completion of Network Constraints for Spot Electricity Markets

2.1 Introduction and Background Information

The Central Western European (CWE) Power Market is a market in which several countries trade electricity in a day-ahead auction (DA). The power grid consists of a graph $\mathcal{G}$, with a transmission lines set $\mathcal{L}$ ($|\mathcal{L}| = L$), and node set $\mathcal{N}$ ($|\mathcal{N}| = N$), at which electric power can be injected or extracted, the total injection across all nodes equalling the total extraction. Producers and consumers place bids or offers consisting of price-quantity pairs over given time windows. They interact in a market where power is purchased or sold. The price finding mechanism of this market reveals partial information about the decisions of other market participants and guarantees the balance between total injection and extraction.

Each set of decisions about power injections and extractions causes flows across the lines of the network, which are completely determined by Kirchhoff's Law. Transmission system operators (TSO) monitor grid transmission lines (and possibly other grid elements), ensuring that power flows do not exceed the safety limits. The resulting mathematical constraints are given by the combination of Power Transmission Distribution Factors (PTDF) and Remaining Available Margin (RAM), which define how lines are affected by power injection or extraction, and the allowed flow changes respectively.

Power markets are frequently organised as Day Ahead Auctions (DAA) due to the difficulty of storing electricity, coupled with uncertainty in demand and production patterns. European Electricity Markets have been concerned with clearing the market at a unique

zonal price, where zones usually correspond to countries. We consider the Flow Based Market Coupling (FBMC) approach, which enables zonal market clearing, by using physical principles for tracking the flow loads in the grid. This has become increasingly popular for multiple reasons, when compared to the Available Transfer Capacity (ATC) approach [4], which was used prior to May 2015. First, it offers increased trading volume, and the European Commission targets a more efficient use of energy sources, which they believe can be achieved more easily by allowing for higher inter-zonal electricity exchange [70]. Secondly, by allowing for higher inter-zonal trade, market clearing becomes less constrained resulting in larger Social Welfare (SW) on average [4]. Finally, as a result of more accurate grid modelling when compared to ATC, the FBMC approach was observed to offer increased operational safety [4]. FBMC was pioneered in the Central Western European (CWE) Power Market, which we use as a case study for our methodology.

The core of the FBMC approach is a set of linear constraints enforced at each time step on the zonal (country) production levels, which ensure that the electricity grid always operates within the safety limits [17], [30]. This set of constraints governs the feasibility domain of power production and flow patterns, and thus ultimately determines zonal prices and their potential decoupling. However, only a very small subset of these constraints is published *ex-post* [11], which is generally insufficient for domain reconstruction or thorough statistical analysis that accounts for the data complexity. Nevertheless, for risk management reasons, market participants must understand their risk exposure in a wide range of scenarios, some of which are far from the *"expected outcomes"* and closer to tail events. Under such circumstances the active set of constraints can be totally different than the ones published in the past, and thus the full set of constraints is needed. Furthermore, the constraint set is sharp, in the sense that a small change in the dispatch vector can result in totally different active constraints. This, coupled with the fact that small changes in constraints may have large impact on the outcomes of market participants with bids close to the margin, makes it imperative for market participants to understand the full set of constraints as well as possible. To further complicate matters for market participants, these constraints change rather erratically in time and thus naive techniques are inappropriate for sound quantitative decision making. For the DAA participants, this translates to reduced ability to manage risk, and ultimately to increased market price inefficiencies.

To the best of our knowledge, obtaining the full set of constraints was not addressed before in the literature. Thus, we propose a methodology that uses the physical principles of the FBMC approach and publicly available data to reconstruct the full set of linear constraints, known as the combination of Power Transmission Distribution Factors (PTDFs) and Remaining Available Margins (RAMs). To this end, we first recover the electricity grid structure, as well as the underlying time-dependent signals known as the Generation Shift Keys (RAMs) and Phase Angles (PAs). The GSKs and PAs are then transformed to the PTDFs and RAMs using maps determined by the graph structure. We achieve the reconstruction by formulating an optimisation model based on the principles of FBMC,

regularised by the available prior knowledge. We exploit the structure of the optimisation problem by solving via alternating minimisation: stochastic optimisation is used for the non-linear and computationally intensive parts of the objective, and convex quadratic programming for the marginally convex components. We are able to show good results for the reconstruction of PTDFs and RAMs in out-of-sample tests, outperforming the naive approach. Further, we analyse the structure of the recovered grid characteristics, as well as of the GSKs and PAs signals, and we show that we recover specific clustering structure, suggesting good reconstruction quality.

Our approach provides a different view to the ones available in the current literature, which are directly or indirectly focused on the TSOs's point of view: assuming knowledge of certain data, parameters and choices, explain or analyse the FBMC methodology [18], [15]. By contrast, our novel methodology takes the view of the market participant, considering its interests, available information, and unknowns. Participants' position in the electricity market are totally different than the TSOs': market participants have different goals, do not know what the operators know, and they do not know what the operators forecast. Calculations of the GSKs based on fundamental equations require TSOs' prediction of the market outcomes in advance, as explained in [18]. However, these are not known by the market participants, and should not be mistaken for their own predictions of the market, which are likely to be obtained by using different methodologies or even different data. Further, market participants fully replicating TSOs' methodology may require too much computational and labour effort for their end goal: they are not concerned with managing the grid, but rather with optimising their risk-return exposure in the market. While some of these predictions may be available one day ahead, it is insufficient for market participants' planning horizon, which is a much longer period, and the corresponding data is unavailable. Since the market participants do not have the TSOs' prediction of the market outcome, they cannot use a purely model-based TSO approach, motivating the need for our proposed method.

The novel contribution of our approach is fourfold: (i) a graph model containing the quantitative physical characteristics is obtained, which is useful for any fundamental model that relies on the graph structure, (ii) the underlying GSKs and PAs signals are recovered, which give insight into the transmission system operators' behaviour, (iii) full reconstruction of the PTDFs and RAMs, allowing for full feasibility domain analysis by market participants, and (iv) our approach enables simulation and forecasting based on the reconstructed signals. Forecasting based on the available sparse PTDF and RAM data is extremely challenging. However, one can use the GSKs and PAs data recovered by our model, which is much lower dimensional, changes slower in time, and allows for explicitly incorporating impact of changes in the grid structure, or other fundamental factors.

The rest of the chapter is structured as follows: the theory of the DC grid model and resulting network constraints used in the FBMC are presented in Section 2.2 and the extra complexities required in practice are then introduced. A brief discussion of the Market Data

is given in Section 2.3. Sections 2.4 & 2.5 present the main optimisation model and its algorithmic solution. Numerical results are presented in Section 2.6, and conclusions are drawn in Section 2.7.

2.2 Background Information

Since our method is model-based, relying on the fundamentals of Flow-Based Market Coupling approach, in this section we introduce the reader to the main concepts and equations that are necessary for our method. The interested reader is referred to [52] for a brief but complete review, to [19], [18], [69], [30], [81] for detailed reviews and to [78] for the official documentation of the methodology. Basic knowledge of AC and DC electric circuits is assumed.

2.2.1 The DC model and Line - Nodal Network Constraints

Each set of power injections and extractions decisions determines the flows across the lines of the network, via Kirchhoff's Law. As mentioned before, we here consider a DC model, as a linearisation of the AC grid model. The DC linearisation approximation is based on three assumptions: (i) the resistance on transmission lines is much smaller than the reactance, i.e. there are no losses on transmission lines, (ii) the voltage profile is flat, i.e. all nodes have the same voltage, and (iii) the voltage angle differences are small for neighbouring nodes. We introduce a running example in Figure 2.1 to facilitate a better understanding of the concepts. The electricity grid can be represented as a collection of nodes and edges,

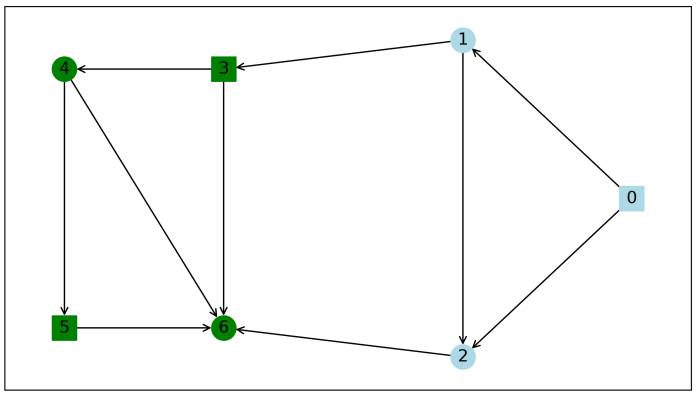


Figure 2.1: Running example: an electricity network with two zones represented by different colors. Production and consumption nodes are represented by square and circular shapes respectively.

where power extraction or production takes place at nodes, and lines transmit electricity between them. The quantities of interest at every node are power injection or extraction, phase angles, and the voltage potential. The quantities important for the transmission lines

are the voltage drop, the current, the power flow, and the phase shift angles. Note that a directionality has to be assigned for each line, to measure the current and the power flow, as well as the voltage drop. In the running example, the directionality is implied by the arrows. This is arbitrary but has to be fixed at the start once and for all.

An important concept is the line-node incidence matrix of the power grid defined as

$$\mathbf{A}_{ji} = \begin{cases} +1 & \text{if line } j \text{ originates in node } i \\ -1 & \text{if line } j \text{ terminates at node } i \\ 0 & \text{otherwise} \end{cases}, \tag{2.1}$$

where $\mathbf{A} \in \mathbb{R}^{L \times N}$, and L is the number of transmission lines, while N is the number of nodes. By ordering the edge set as $\mathcal{L} = \{(0,1),(0,2),(1,2),(2,6),(1,3),(3,4),(4,5),(5,6),(4,6),(3,6)\}$, the line-node incidence matrix corresponding to the running example in Figure 2.1 is

$$\mathbf{A} = \begin{bmatrix} 1 & -1 & 0 & 0 & 0 & 0 & 0 \\ 1 & 0 & -1 & 0 & 0 & 0 & 0 \\ 0 & 1 & -1 & 0 & 0 & 0 & 0 \\ 0 & 0 & 1 & 0 & 0 & 0 & -1 \\ 0 & 1 & 0 & -1 & 0 & 0 & 0 \\ 0 & 0 & 0 & 1 & -1 & 0 & 0 \\ 0 & 0 & 0 & 0 & 1 & -1 & 0 \\ 0 & 0 & 0 & 0 & 0 & 1 & -1 \\ 0 & 0 & 0 & 0 & 1 & 0 & -1 \\ 0 & 0 & 0 & 1 & 0 & 0 & -1 \end{bmatrix}. \tag{2.2}$$

By Kirchhoff's current law, the sum of the currents flowing out, minus the sum of the currents flowing in must be the net flow in at the nodal level. Base on the line-nodal incidence matrix, this can be expressed in vector form as:

$$\mathbf{i}_N = \mathbf{A}^T \mathbf{i}_L, \tag{2.3}$$

where $\mathbf{i}_N \in \mathbb{R}^N$ and $\mathbf{i}_L \in \mathbb{R}^L$ are the vector of nodal and line currents. Since we assumed very small resistence, the admittance is entirely given by the susceptance, and one can write Ohm's law for every line l as $V_l = \hat{b}_l i_l$ where V_l is the voltage drop across the line, i_l is the current and $\hat{b}_l$ is the susceptance of the line. Thus, equation (2.3) can be written in vector

form as

$$\mathbf{i}_N = \mathbf{A}^T \mathbf{B} \mathbf{v}_L, \tag{2.4}$$

where $\mathbf{B}$= diag($\hat{\mathbf{b}}$) $\in \mathbb{R}^{L \times L}$ is the matrix containing the line susceptances on the diagonal and $\mathbf{v}_L$ is the vector of line voltage drops. Finally, one can link line voltages to nodal voltages $\mathbf{v}_N$ as

$$\mathbf{v}_L = \mathbf{A} \mathbf{v}_N, \tag{2.5}$$

and therefore by equation (2.4) we obtain

$$\mathbf{i}_N = \mathbf{A}^T \mathbf{B} \mathbf{A} \mathbf{v}_N, \tag{2.6}$$

where $\boldsymbol{\Upsilon} = \mathbf{A}^T \mathbf{B} \mathbf{A}$ is known as the admittance matrix.

Next, the power across a line l between two nodes q and s can be expressed as

$$P_l = \frac{|V_q||V_s|}{X_l} \sin(\delta_s - \delta_q), \tag{2.7}$$

where $\hat{b}_l = X_l^1$ is the susceptance and δ_s is the phase angle at node s. By using the second assumption of flat voltage profile, i.e. $|V_s| = |V_q| = V_0$, and that the angles are small, we obtain

$$\mathbf{p}_L = V_0^2 \mathbf{B} \mathbf{A} \boldsymbol{\delta}_N, \tag{2.8}$$

where $\mathbf{p}_L$ is the vector of power flows across lines, and $\boldsymbol{\delta}_N$ is the vector of nodal phase angles. Further, by using the flat voltage profile assumption and small angle assumption, the vector of nodal power can be written as

$$\mathbf{p}_N = |\mathbf{i}_N \odot \mathbf{v}_N| = \mathbf{A}^T \mathbf{B} \mathbf{A} \cdot V_0^2 \boldsymbol{\delta}_N, \tag{2.9}$$

where $\odot$ denotes element-wise multiplication and the absolute value is taken for each element separately. Alternatively, one can observe that by conservation of energy at each node we must have that $\mathbf{p}_N$= $\mathbf{A}^T \mathbf{p}_L$. Either way, by using equations (2.8) and (2.9) to eliminate $\boldsymbol{\delta}_N$ we obtain

$$\mathbf{p}_L = \mathbf{B} \mathbf{A} (\mathbf{A}^T \mathbf{B} \mathbf{A})^{-1} \mathbf{p}_N. \tag{2.10}$$

However, the equations in (2.8) are linearly dependent, and as a result $\mathbf{A}^T \mathbf{B} \mathbf{A}$ is not full rank. To remedy this problem, one (arbitrary) node, say i_0, has to be chosen as reference and the corresponding column in A eliminated, obtaining $\tilde{\mathbf{A}}$= $\mathbf{A} \boldsymbol{\Omega}_{ref}^T$, where $\boldsymbol{\Omega}_{ref}$ is a projection matrix obtained by deleting row i_0 of the identity matrix $I_N \in \mathbb{R}^{N \times N}$. The power balance equation, $\mathbf{1}^T \mathbf{p}_N = 0$, needs to be introduced to ensure that the DC model is well defined, but this is guaranteed by the market clearing mechanism. In the running example we eliminate

node 6. We now obtain

$$\mathbf{p}_L = \mathbf{B}\tilde{\mathbf{A}}(\tilde{\mathbf{A}}^T\mathbf{B}\tilde{\mathbf{A}})^{-1}\tilde{\mathbf{p}}_N. \tag{2.11}$$

which describes how the power injection or extraction at each node is distributed across lines. In particular, due to linearity in $\mathbf{p}_N$ the equation also describes how changes in nodal injections and extractions translate to power flow changes on lines. The matrix that maps nodal changes to line changes is known as the line-nodal Power Transmission Distribution Factors (PTDFs), and is defined as

$$\mathbf{P}(\hat{\mathbf{b}}, \mathbf{A}) := \mathbf{B}\tilde{\mathbf{A}}(\tilde{\mathbf{A}}^T\mathbf{B}\tilde{\mathbf{A}})^{-1}, \tag{2.12}$$

which is a function of network structure defined by $\mathbf{A}$, and susceptances $\hat{\mathbf{b}}$, but is fixed for a fixed grid. The choice of the reference node is arbitrary, and does not affect the computed $\mathbf{p}_L$, but it means that the line-nodal PTDF is only unique up to the choice of the reference node. Note that the actual value of entries in $\hat{\mathbf{b}}$ only matters up to scale.

In our running example, by considering the line susceptances to be

$$\hat{\mathbf{b}}^T = \begin{bmatrix} 1.0 & 2.0 & 1.0 & 0.3 & 0.4 & 1.0 & 1.0 & 1.5 & 2.0 & 1.0 \end{bmatrix} \tag{2.13}$$

we obtain the line-nodal PTDF matrix as

$$\mathbf{P}(\hat{\mathbf{b}}, \tilde{\mathbf{A}}) = \begin{bmatrix} 0.402 & -0.176 & 0.19 & -0.033 & -0.009 & -0.004 \\ 0.598 & 0.176 & -0.19 & 0.033 & 0.009 & 0.004 \\ -0.102 & 0.264 & -0.285 & 0.05 & 0.014 & 0.006 \\ 0.496 & 0.439 & 0.525 & 0.083 & 0.023 & 0.009 \\ 0.504 & 0.561 & 0.475 & -0.083 & -0.023 & -0.009 \\ 0.211 & 0.235 & 0.199 & 0.385 & -0.171 & -0.068 \\ 0.049 & 0.054 & 0.046 & 0.089 & 0.191 & -0.323 \\ 0.049 & 0.054 & 0.046 & 0.089 & 0.191 & 0.677 \\ 0.163 & 0.181 & 0.153 & 0.296 & 0.638 & 0.255 \\ 0.293 & 0.326 & 0.276 & 0.533 & 0.148 & 0.059 \end{bmatrix}. \tag{2.14}$$

For example, $\left[\mathbf{P}(\hat{\mathbf{b}}, \tilde{\mathbf{A}})\right]_{5,1} = 0.504$ tells us that for every extra $1MW$ of power production at node 0 (since node zero corresponds to column one), $0.504MW$ of extra power will flow through line $(1, 3)$ from node 1 to node 3 (since the fifth line is $(1, 3)$). Thus, very importantly, the PTDFs give us a way to track flows across lines based on nodal productions

and consumption, which correspond to the quantities allocated to market participants. By tracking these changes and ensuring that the flows across lines remain within the safety limits, the Transmission System Operators (TSOs) can ensure that the allocation of quantities to market participants stays feasible.

As we will see in the next subsection, a more useful alternative formulation of equation (2.11) is

$$\mathbf{p}_L = \mathbf{F}^{\text{ref}} + \Delta\mathbf{p}_L = \mathbf{P}(\hat{\mathbf{b}}, \mathbf{A})\tilde{\mathbf{p}}_N^0 + \mathbf{P}(\hat{\mathbf{b}}, \mathbf{A})\Delta\tilde{\mathbf{p}}_N, \tag{2.15}$$

where $\tilde{\mathbf{p}}_N^0 = \boldsymbol{\Omega}_{ref}\mathbf{p}_N^0$, $\Delta\mathbf{p}_L :=\mathbf{P}(\hat{\mathbf{b}}, \mathbf{A})\Delta\tilde{\mathbf{p}}_N$, and $\mathbf{p}_N^0$ is known as the base case [52], and $\mathbf{F}^{\text{ref}}$ as the reference flow corresponding to the base case, which could be obtained as $\mathbf{F}^{\text{ref}} = \mathbf{P}(\hat{\mathbf{b}}, \mathbf{A})\tilde{\mathbf{p}}_N^0$, but need not be, and other models such as an AC model could be used to compute $\mathbf{F}^{\text{ref}}$ based on $\mathbf{p}_N^0$. While in this example, equation (2.15) does not seem to add any value, this form becomes very important when $\Delta\tilde{\mathbf{p}}_N$ can only be estimated or approximated, as we shall see in the next subsection and later throughout this chapter.

Similarly to mapping changes in node injections to line injections, the change in phase angle differences across lines, $\Delta\boldsymbol{\alpha}^L$ can also be mapped to power flow changes through the Phase Shift Distribution Factor (PSDF) [19], defined as

$$\text{PSDF}(\hat{\mathbf{b}}, \mathbf{A}) := \mathbf{B} - \mathbf{B}\tilde{\mathbf{A}}(\tilde{\mathbf{A}}^T\mathbf{B}\tilde{\mathbf{A}})^{-1}\tilde{\mathbf{A}}^T\mathbf{B}, \tag{2.16}$$

which yields the linear mapping $\Delta^\alpha\mathbf{p}_L = \text{PSDF}(\hat{\mathbf{b}}, \mathbf{A})\Delta\boldsymbol{\alpha}^L$, where $\Delta^\alpha\mathbf{p}_L$ is the line power changes given by $\Delta\boldsymbol{\alpha}^L$. The entry $\Big[\text{PSDF}(\hat{\mathbf{b}}, \mathbf{A})\Big]_{lk}$ then tells us by how much the flow changes on line l given the change in one angle unit (radian) on line k. Note that this linearisation is accurate only for sufficiently small $\Delta\boldsymbol{\alpha}^L$. Since we never deal with absolute values, but only with changes relative to some reference, let us simplify notation and denote $\Delta\boldsymbol{\alpha}^L$ as $\boldsymbol{\alpha}^L$. A further split can then be performed to write

$$\mathbf{F}^{\text{ref}} = \mathbf{P}(\hat{\mathbf{b}}, \mathbf{A})\mathbf{p}_N^0 + \text{PSDF}(\hat{\mathbf{b}}, \mathbf{A})\boldsymbol{\alpha}^L, \tag{2.17}$$

$$\Delta\mathbf{p}_L = \mathbf{P}(\hat{\mathbf{b}}, \mathbf{A})\Delta\mathbf{p}_N. \tag{2.18}$$

One can now write the safety limits for each line as

$$-\mathbf{F}^{\max} \leq \mathbf{F}^{\text{ref}} + \mathbf{P}(\hat{\mathbf{b}}, \mathbf{A})\Delta\mathbf{p}_N \leq \mathbf{F}^{\max}, \tag{2.19}$$

which is more often written as

$$\mathbf{r} := -\mathbf{F}^{\max} - \mathbf{F}^{\text{ref}} \leq \mathbf{P}(\hat{\mathbf{b}}, \mathbf{A})\Delta\mathbf{p}_N \leq \mathbf{F}^{\max} - \mathbf{F}^{\text{ref}} =: \mathbf{R}, \tag{2.20}$$

where $\mathbf{r}$ and $\mathbf{R}$ are known as Remaining Available Margins. This form is more useful

because in practice $\mathbf{F}^{\text{ref}}$ is pre-computed based on some base case $\mathbf{p}_N^0$ that is an estimate of the expected market outcome, at the time of defining the constraints, before the participants submit their bids. The choice of $\mathbf{p}_N^0$ matters to the extent that $\Delta\mathbf{p}_N$ can only be estimated following drastic simplifications. A better understanding of the relevance of splitting of equations (2.24) and (2.18) in this form is facilitated by the next subsection. The simplifying assumptions introduced in this subsection facilitate the simplification of an AC model to a DC one, drastically reducing the computational burden. As explained in [19], the error introduced by the three assumptions is generally small, perhaps with the exception of the flat voltage profile assumption, which is still reasonable but tends to introduce larger errors. However, in the next section, simplifying assumptions to facilitate the reduction of the grid model are made, and these introduce the main source of error for the FBMC constraints.

2.2.2 Line - Zonal Network Constraints

Constraining the Day Ahead Auction by (2.20) is not practical, as a very large number of constraints that are very high dimensional (due to a large number of nodes), need to be tracked. Further, power injection and extraction at each node would have to be treated separately. However, power is not traded or priced on a per node (power-plant) basis. Instead, nodes are collated into zones, and power injection at each node within a zone (usually country) is treated as equivalent and traded at a zonal price. Therefore, a simplification of nodal power injections to their zonal power equivalent is required by the model. However, in practice, unlike in the theory explained in [19], the lines inside a zone are not absorbed in an equivalent *"zonal node"*, since they may still become congested (reach capacity) even in the case when nodes within a zone are treated as equivalent [52]. In fact, nodal equivalence can only be guaranteed if lines inside a zone do not get congested, which happens fairly often in practice. Therefore, the simplification presented next is not a grid reduction in the full sense, but only in the sense that nodes inside a zone can thereafter be treated as equivalent, while transmission lines cannot.

Let us define ΔP_z as the change in zonal power production for each zone. In the running example from 2.1, we have two zones, and thus two values are to be considered. Let us imagine that the operators know or can accurately estimate, for each zone z, the change at every node for each unit of change in zonal power, and denote this by $\mathbf{g}_z^1$. Thus, we must have that $\mathbf{1}^T\mathbf{g}_z^1 = 1$. Let us denote the column-wise concatenation of these vectors by $\mathbf{G}^1$. This matrix is known as the Generation Shift Key (GSK) matrix, and its role will become clear later. In our running example, the two zones could, for example, have a GSK matrix as

$$(\mathbf{G}^1)^T = \begin{bmatrix} 1.3 & -0.2 & -0.1 & 0.0 & 0.0 & 0.0 & 0.0 \\ 0.0 & 0.0 & 0.0 & 0.6 & 0.0 & 0.4 & 0.0 \end{bmatrix}, \tag{2.21}$$

where the first and second column of $\mathbf{G}^1$ (rows of $(\mathbf{G}^1)^T$) correspond to the first and second zone respectively. Rows of $\mathbf{G}^1$ correspond to nodes, and only one column of $\mathbf{G}^1$ for each row can have a nonzero entry, the one that corresponds to the zone in which the considered node lies. The entry $\mathbf{G}^1_{i,z}$ then tell us for every unit of power increase in zone z, how much the production needs to change at node i. Clearly, columns are bound to have zeros for nodes that are outside the considered zone z. Nodes corresponding to power plants will generally have positive entries, as shown in the example. It is always the case that nodes can be sorted in such a way that the matrix has non-zero vectors only on the diagonal.

The GSK matrix can then be used to approximate the nodal power change as

$$\Delta \mathbf{p}_N = \sum_z \mathbf{g}^1_z \Delta P_z, \tag{2.22}$$

where the implicit assumption that $\mathbf{g}^1_z$ stays constant with ΔP_z has been made. Therefore, equation (2.15) can then be approximated by writing

$$\mathbf{p}_L = \mathbf{P}(\hat{\mathbf{b}}, \mathbf{A})\tilde{\mathbf{p}}^0_N + \mathbf{P}(\hat{\mathbf{b}}, \mathbf{A}) \sum_z \mathbf{g}^1_z \Delta P_z = \mathbf{P}(\hat{\mathbf{b}}, \mathbf{A})\tilde{\mathbf{p}}^0_N + \mathbf{P}(\hat{\mathbf{b}}, \mathbf{A})\mathbf{G}^1 \boldsymbol{\delta}\mathbf{p}, \tag{2.23}$$

where $\boldsymbol{\delta}\mathbf{p}$ is the vector of zonal power changes, i.e. $\boldsymbol{\delta}\mathbf{p}_z = \Delta P_z$. The equations describing the constraints then become

$$\mathbf{F}^{\text{ref}} = \mathbf{P}(\hat{\mathbf{b}}, \mathbf{A})\mathbf{p}^0_N + \text{PSDF}(\hat{\mathbf{b}}, \mathbf{A})\boldsymbol{\alpha}^L, \tag{2.24}$$

$$\mathbf{r} := -\mathbf{F}^{\max} - \mathbf{F}^{\text{ref}} \leq \mathbf{P}(\hat{\mathbf{b}}, \mathbf{A})\mathbf{G}^1 \boldsymbol{\delta}\mathbf{p} \leq \mathbf{F}^{\max} - \mathbf{F}^{\text{ref}} =: \mathbf{R}, \tag{2.25}$$

where $\text{PTDF}(\hat{\mathbf{b}}, \mathbf{A}, \mathbf{G}^1) := \mathbf{P}(\hat{\mathbf{b}}, \mathbf{A})\mathbf{G}^1 \in \mathbb{R}^{L \times Z}$ is known as the line-zonal PTDF matrix and gives the final form of the linear constraints, as in (2.25). Note that the equations corresponding to the reference flows were not simplified by treating all nodes within a zone as equivalent. This is because, unlike for the DC model in the previous subsection, the point $\mathbf{p}^0_N$ around which the linearisation and zonal simplification is made now matters, and crucially, accuracy can be extracted by using the nodal data to obtain the reference flow. The way that this is used in practice is as follows: (i) the operators use their expectation of the market clearing outcome, containing $\mathbf{p}^0_N$ and $\boldsymbol{\alpha}^L$ to compute the reference flows, (ii) based on this expectation, the GSKs are defined, representing expected *patterns of power production deviations* based on zonal changes, and (iii) the line-zonal PTDF matrix and the two RAM vectors are computed.

It now becomes clear that the base case, defined by $(\mathbf{p}^0_N, \boldsymbol{\alpha}^L)$, and the GSKs are key elements in the methodology. All these quantities have to be estimated before the fact, which is a challenging task that may introduce large errors. However, the operators are not primarily interested in the accuracy of the constraints, but rather that the resulting

polytope lies strictly inside the actual feasible set, and that the size of the simplified feasible set is large enough to allow for acceptable cross-border trading. By abuse of language, we often refer to $\mathbf{p}_N^0$ as the base case.

To apply this on our running example we need to define a base case as well. In the theory provided by [19], it is mentioned that commonly a self sufficiency scenario is considered, namely $\sum_{i \in \mathcal{N}_z} (\mathbf{p}_N^0)_z = 0$, but in practice this is rarely the case, as we shall see in the next subsection. We thus take

$$(\mathbf{p}_N^0)^T = \begin{bmatrix} 5 & -1 & -2 & 4 & -3 & -5 & 2 \end{bmatrix}, \tag{2.26}$$

and let the maximum flow on grid lines be defined as

$$(\mathbf{F}^{\max})^T = \begin{bmatrix} 3 & 3.5 & 3 & 5 & 4 & 3 & 3 & 3.6 & 3 & 3 \end{bmatrix}. \tag{2.27}$$

Let us define $\mathbf{E} \in \mathbb{R}^{Z \times N}$ as the map that adds all nodal quantities within a zone. We then have that $\mathbf{E}\mathbf{p}_N^0 = (2, -2)^T$ in our example. Thus, zone 1 is a net exporter while the opposite is true of zone 2, under the base case. Let us take $\boldsymbol{\alpha}^L = \mathbf{0}$ for simplicity. The reference flows

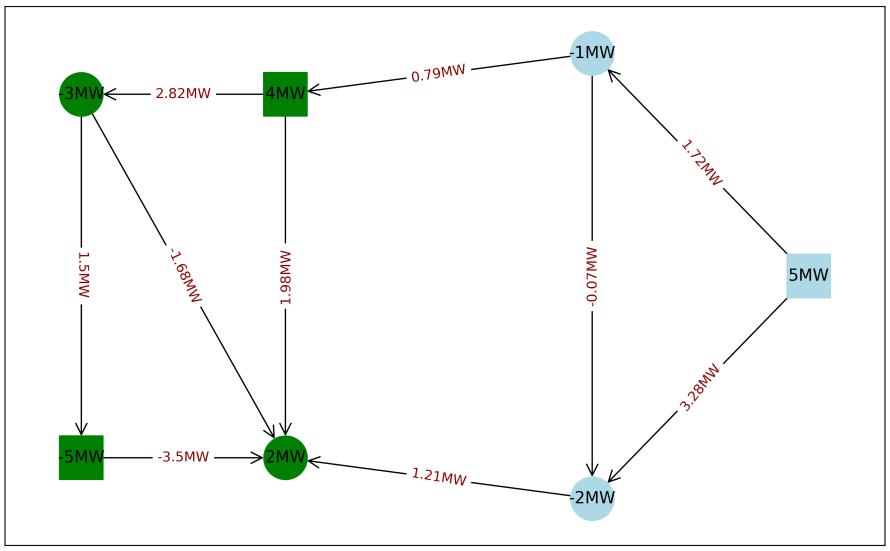


Figure 2.2: Running example: assigned nodal power vector for the base case ($\mathbf{p}_N^0$), and the resulting power flows across lines ($\mathbf{F}^{\text{ref}}$), given the susceptances $\hat{\mathbf{b}}$.

across the lines are then

$$\begin{aligned} \left(\mathbf{F}^{\text{ref}}\right)^T &= (\mathbf{P}(\hat{\mathbf{b}}, \mathbf{A})\mathbf{p}_N^0 + \mathbf{0})^T \\ &= \begin{bmatrix} 1.72 & 3.28 & -0.07 & 1.21 & 0.79 & 2.82 & 1.5 & -3.5 & -1.68 & 1.98 \end{bmatrix}, \end{aligned} \tag{2.28}$$

and the nodal and zonal power quantities can be visualised in Figure 2.2. We can see that

in this case all reference flows are below the maximum flows (in absolute value), but this does not have to be the case. If it ever happens that the absolute value of a reference flow is above the maximum flow, then the network is referred to as pre-congested. The constraints can then be calculated as per equation (2.30), and we obtain

$$\begin{bmatrix} -4.72 \\ -6.78 \\ -2.93 \\ -6.21 \\ -5.79 \\ -5.82 \\ -4.5 \\ -0.1 \\ -1.32 \\ -4.98 \end{bmatrix} \leq \begin{bmatrix} 0.54 & -0.02 \\ 0.76 & 0.02 \\ -0.16 & 0.03 \\ 0.5 & 0.05 \\ 0.5 & -0.05 \\ 0.21 & 0.2 \\ 0.05 & -0.08 \\ 0.05 & 0.32 \\ 0.16 & 0.28 \\ 0.29 & 0.34 \end{bmatrix} \boldsymbol{\delta}\mathbf{p} \leq \begin{bmatrix} 1.28 \\ 0.22 \\ 3.07 \\ 3.79 \\ 4.21 \\ 0.18 \\ 1.5 \\ 7.1 \\ 4.68 \\ 1.02 \end{bmatrix}, \tag{2.29}$$

as the final set of linear constraints. While this is the core of the FBMC approach for obtaining the linear constraints representing the network's physical constraints, there are many practical considerations that need to be taken into account to arrive at the final form of these constraints, as they are applied in the real market clearing mechanism. We explore these considerations in the next subsection.

2.2.3 Practical Considerations

To begin with, in the CWE Power Market, most of the countries consistently import or export rather large amounts of energy, and are almost never in the self sufficiency scenario, as the theory often assumes. This means that the self sufficiency scenario is a poor approximation of what is expected to happen [52]. As a result, the power deviations given by the GSKs would be poor, since they offer a linear approximation that is only accurate in the neighbourhood of the base case. For this reason, in practice, the base case is a forecast of what is expected to happen, rather than a self sufficiency scenario [52]. This has the following implications:

1. energy balance does not have to be achieved for the base case at zonal level, but only at network level,

2. and the TSOs aim to forecast the production and consumption levels. This is determined by the expected price, but they can partially control this via the GSKs and

the base case which give the grid constraints. This is to some extent circular, since the defined constraints depend on the expected price, the expected price is meant to estimate the actual price, and the actual price depends on the constraints.

In addition, the operators have little or no control over the consumption nodes, and thus the GSKs are considered to be nonzero only at production nodes here. As a result, we often use a version of equation (2.24) for production nodes only, and the version of $\mathbf{p}_N^0$ concerned only with production nodes is denoted as $\mathbf{g}^0$.

Futher, even as the number of nodes has been reduced, the number of lines is still very large. For example, for the full CWE electricity grid we record around 1800 lines. To reduce this large number of constraints, the operators only monitor a small subset of lines that are likely to become congested. The definition for selecting these lines is usually that an entry in the corresponding line-zonal PTDF has to be above 0.05 in absolute value. Note that critical lines can also lie strictly inside a zone. The set of monitored lines is known as Critical Network Elements (CNE) or Critical Branches (CB), and we denote this set here as $\mathcal{L}_{\text{cne}}$. We further denote $\mathbf{\Omega}_{\text{cne}} \in \mathbb{R}^{|\mathcal{L}_{\text{cne}}| \times L}$ as the map from all lines to the critical ones. The linear set of constraints then becomes:

$$\mathbf{r} := -\mathbf{\Omega}_{\text{cne}}\mathbf{F}^{\max} - \mathbf{\Omega}_{\text{cne}}\mathbf{F}^{\text{ref}} \leq \mathbf{\Omega}_{\text{cne}}\mathbf{P}(\hat{\mathbf{b}}, \mathbf{A})\mathbf{G}^1\boldsymbol{\delta}\mathbf{p} \leq \mathbf{\Omega}_{\text{cne}}\mathbf{F}^{\max} - \mathbf{\Omega}_{\text{cne}}\mathbf{F}^{\text{ref}} =: \mathbf{R}. \tag{2.30}$$

For compactness, whenever we refer to observed data, we drop the $\mathbf{\Omega}_{\text{cne}}$ term and we refer to the corresponding quantities directly on the critical lines.

Next, the base case and GSKs are in reality time dependent quantities, as the expectations of the TSOs change over time due to changing information and due to seasonality. This means that $\mathbf{G}_t^1$ and $\mathbf{g}_t^0$ are then actually time series, and as a consequence, so are $\mathbf{r}_t$, $\mathbf{R}_t$, PTDF_t, and thus are indexed by time.

Further, the operators have the obligation to ensure what is known as an $N-1$ security criterion [19]. This criterion states that the network shall withstand the unplanned outage of one element of the system and stay in operation without jeopardising the system's operational integrity [19]. This may refer to the unplanned outage of multiple types of network elements but here we restrict our attention to transmission lines. In the CWE, an *umbrella approach* is used, where the critical contingencies are determined *ex-ante* and taken into account in the optimization. As a result there are multiple *scenarios* known as Critical Outages (CO) or *Contingencies*, to be considered at each time step. The combination of Critical Branches with Critical Outages is then known as CBCO or CNEC. Under each scenario, the constraints are computed as usual after the corresponding line was removed from the grid. In principle, the base case and GSKs may be different for different scenarios even if at the same time. Let the scenarios be indexed by $s \in \mathcal{S}$, where $\mathcal{S}$ is the scenario set. From here on, we use s, t as subscripts for each quantity to denote the corresponding

scenario-time pair, and move the previous subscripts as super-scripts where necessary. The line-zonal PTDF, $\text{PTDF}_{s,t}$, is then defined by

$$\text{PTDF}_{s,t} = \mathbf{P}_s(\hat{\mathbf{b}}, \mathbf{A})\mathbf{G}^1_{s,t}, \tag{2.31}$$

where the subscript s denotes explicit scenario dependence, $\mathbf{P}_s(\hat{\mathbf{b}}, \mathbf{A}) := \mathbf{P}(\hat{\mathbf{b}}_s, \mathbf{A}_s)$, and $\mathbf{G}^1_{s,t} = ||^H_{z\in\mathcal{Z}}(\overline{\mathbf{g}}^1_{s,t,z}) \in \mathbb{R}^{N\times Z}$ is the horizontal concatenation of the GSKs for each zone under scenario s at time t. Note that when horizontally concatenating vectors we view them as a matrix with one column, and thus $\mathbf{G}^1_{s,t}$ is a matrix. The constraints can now be written as

$$\mathbf{r}_{s,t} \leq \text{PTDF}_{s,t}\delta\mathbf{p}^Z_t \leq \mathbf{R}_{s,t}, \tag{2.32}$$

where the RAMs are defined as

$$\mathbf{r}_{s,t} = -\mathbf{F}^{\max}_{s,t} - \mathbf{F}^{\text{ref}}_{s,t}, \tag{2.33}$$

$$\mathbf{R}_{s,t} = \mathbf{F}^{\max}_{s,t} - \mathbf{F}^{\text{ref}}_{s,t}, \tag{2.34}$$

and $\delta\mathbf{p}^Z_t := ||^V_{z\in\mathcal{Z}}(\Delta P_{z,t}) \in \mathbb{R}^Z$ is the vector of zonal power changes, with respect to the base case values given by $\mathbf{1}^T\mathbf{g}^0_{z,t}$ [11]. By writing $\text{PSDF}_s(\hat{\mathbf{b}}, \mathbf{A}) := \text{PSDF}(\hat{\mathbf{b}}_s, \mathbf{A}_s)$, the reference flows are expressed as

$$\mathbf{F}^{\text{ref}}_{s,t} = \mathbf{P}_s(\hat{\mathbf{b}}, \mathbf{A})\mathbf{g}^0_{s,t} + {V_0}^2\text{PSDF}_s(\hat{\mathbf{b}}, \mathbf{A})\boldsymbol{\alpha}^L_t, \tag{2.35}$$

where V_0 is the flat voltage profile [19].

Moreover, due to limitations of the model used, the TSOs allow themselves to apply some safety margins to account for errors, in the form of Flow Reliability Margins (FRMs) and final Adjustment Values (FAVs) on the flow constraints bounds, and therefore we have that

$$\mathbf{r_{s,t}} = -\mathbf{F}^{\max}_{s,t} - \mathbf{F}^{\text{ref}}_{s,t} + \text{FRM} - \text{FAV}, \tag{2.36}$$

$$\mathbf{R_{s,t}} = \mathbf{F}^{\max}_{s,t} - \mathbf{F}^{\text{ref}}_{s,t} - \text{FRM} - \text{FAV}. \tag{2.37}$$

The FRMs are introduced to account for TSO's grid modelling errors, which mainly includes the linearisation simplification but also flow measurements uncertainties [11]. They are computed for each line as a multiple of the standard deviation σ_D, of the error series defined as the difference between measured and computed flows, as shown below

$$\sigma^2_D(l) = \frac{1}{|\mathcal{T}|}\sum_{t\in\mathcal{T}}\frac{1}{|\mathcal{S}_t|}\sum_{s\in\mathcal{S}_t}\left((\mathbf{F}^{\text{ref}}_{s,t})_l - (\mathbf{F}^0_t)_l\right)^2 - \left(\frac{1}{|\mathcal{T}|}\sum_{t\in\mathcal{T}}\frac{1}{|\mathcal{S}_t|}\sum_{s\in\mathcal{S}_t}((\mathbf{F}^{\text{ref}}_{s,t})_l - (\mathbf{F}^0_t)_l)\right)^2, \tag{2.38}$$

where $(\mathbf{F}_t^0)_l$ is the actual recorded flow at time t through a line l. The final adjustment values (FAV) incorporate TSO information not accounted for in the DC model [11]. However, this term is often omitted in reality and in the literature [83], and thus we neglect the FAV term for simplicity.

The critical lines constraints version of (2.32) is then used in conjunction with the bids, offers and the Welfare Maximisation Problem (WMP) to obtain the optimal $\delta\mathbf{p}_t^Z$ values which ultimately incorporate the accepted orders and determine the zonal prices [9].

2.2.4 The Problem and Proposed Solution

Due to the changing nature of $\mathbf{g}_{s,t}^0$ and $\mathbf{G}_{s,t}^1$, the RAM vectors $\mathbf{r_{s,t}}, \mathbf{R_{s,t}}$ and the line-zonal PTDF matrix $\mathbf{P}_{s,t}^{LZ}(\hat{\mathbf{b}}) := \mathbf{P}_s(\hat{\mathbf{b}})\mathbf{G}_{s,t}^1$ change every hour. The values of these parameters are computed by the TSOs, on the basis of their best forecasts of $\mathbf{g}^0$ and $\mathbf{G}^1$, for the time windows corresponding to the delivery day that lies two days into the future. Partial historical data of $\mathbf{r}, \mathbf{R}, \mathbf{P}^{LZ}$, corresponding to active constraints in the pricing optimisation problem at that time are published [11]. Further, these values change rather erratically in time. Thus at each time, the full set of constraints corresponding to critical lines is not available, meaning that an exploration of the full outcome space is not possible based on the published constraints alone. A further consequence is that building a forecaster directly on the PTDFs and RAMs is very difficult, and would not allow for any physical interpretation of the model. For these reasons, we aim to infer the line susceptances, the GSKs, PAs by using an initial guess as regularisation and fitting to the observed constraints data, and these inferred quantities can then be used to recompute the full set of constraints for the Flow Based Domain. More precisely, we aim to obtain the *underlying signals* of $(\mathbf{g}^0, \boldsymbol{\alpha}^L)$ and $\mathbf{G}^1$ and use (2.36), (2.37), (2.35) and (2.31) to obtain the PTDFs ($\mathbf{P}_{s,t}^{LZ}$) and the RAMs ($\mathbf{r_{s,t}}$, $\mathbf{R_{s,t}}$). However $\mathbf{g}_{s,t}^0$ and $\mathbf{G}_{s,t}^1$, and the graph model are not easily available. The former are confidential and simply unavailable, while the latter is not readily available, and the exact model used by the TSOs is unknown. Thus, we first attempt to reconstruct the graph structure $(\mathbf{b}, \mathbf{A})$, and $\mathbf{g}_{s,t}^0$ and $\mathbf{G}_{s,t}^1$ time series.

The core idea is to fit $(\mathbf{g}^0, \boldsymbol{\alpha}^L)$ and $\mathbf{G}^1$ and the graph structure to the PTDF and $\mathbf{F}^{\text{ref}}$ time series. Note that directly fitting to the RAMs is not possible, but the $\mathbf{F}^{\text{ref}}$ are also available. Alternatively the reference flows can be obtained using the line capacity and the RAMs (possibly with further assumptions), using equations (2.36), (2.37). The available PTDFs can be expressed as

$$\tilde{\mathbf{P}}_{s,t}^{LZ} = \boldsymbol{\Omega}_{s,t}\mathbf{P}_s^N(\hat{\mathbf{b}})\mathbf{G}_{s,t}^1, \tag{2.39}$$

while the available reference flows can be written as

$$\mathbf{F}_{s,t}^{\text{ref}} = \boldsymbol{\Omega}_{s,t}\left(\mathbf{P}_s(\hat{\mathbf{b}}, \mathbf{A})\mathbf{g}_{s,t}^0 + {V_0}^2\text{PSDF}_s(\hat{\mathbf{b}}, \mathbf{A})\boldsymbol{\alpha}_t^L\right), \tag{2.40}$$

where $\mathbf{\Omega}_{s,t} \in \mathbb{R}^{|\mathcal{L}_{s,t}| \times L}$ is a projection matrix that selects only the rows in a small index set $\mathcal{L}_{s,t}$ of lines that correspond to active constraints in the pricing optimisation problem at time t and under scenario s. We next describe the optimisation problem for recovering $\hat{\mathbf{b}}$ and $\mathbf{G}^1_{s,t}$, given the PTDF data set, and assuming that $\mathbf{A}$ is known. The optimisation problem reads

$$\begin{aligned} \min_{\hat{\mathbf{b}} \in \mathbb{R}^{|\mathcal{L}|}, \mathbf{G}^1_{s,t} \in (N-1) \times Z} & \sum_{s,t \in \mathcal{ST}} \left\| \tilde{\mathbf{P}}^{LZ}_{s,t} - \mathbf{\Omega}_{s,t} \mathbf{P}_s(\hat{\mathbf{b}}) \mathbf{G}^1 \right\|^2_F \\ \text{s.t. } & \mathbf{1}^T \mathbf{G}^1_{s,t} = \mathbf{1}, \\ & \hat{\mathbf{b}} \geq 0, \end{aligned} \tag{2.41}$$

where $\mathcal{ST}$ is the set of all available combinations (s,t). Note that $\mathbf{\Omega}_{s,t}$ is known, since the critical lines and critical outages combinations are specified when published. Furthermore, $\mathbf{P}_s(\hat{\mathbf{b}})$ is defined as the nodal PTDF that results from the choice $\hat{\mathbf{A}}_s = \mathbf{\Omega}(s)\mathbf{A}$ and $\hat{\mathbf{B}}_s = \mathbf{\Omega}(s)\text{diag}(\hat{\mathbf{b}})\mathbf{\Omega}(s)^T$ that is,

$$\mathbf{P}_s(\hat{\mathbf{b}}) = \hat{\mathbf{B}}_s \hat{\mathbf{A}}_s (\hat{\mathbf{A}}_s^T \hat{\mathbf{B}}_s \hat{\mathbf{A}}_s)^{-1}, \tag{2.42}$$

where $\mathbf{\Omega}(s) \in \mathbb{R}^{L-1 \times L}$ has the row corresponding to the line that has an outage under scenario s removed. Our choice of reference node might be mismatched by the TSO, and as a result of the approach described, we can recover $\mathbf{P}^{LZ}_{s,t}$ only up to a rank one matrix. This can be remedied by introducing the following mean centering: for each line j, let $\mathcal{ST}_j = \{(s,t) : j \in \mathcal{L}_{s,t}\}$, and let $\mathbf{Y} \in \mathbb{R}^{L \times |\mathcal{Z}|}$

$$\mathbf{Y}_{j,:} := \begin{cases} \frac{1}{|\mathcal{ST}_j|} \sum_{(s,t) \in \mathcal{ST}_j} (\tilde{\mathbf{P}}_{s,t})_{j,:}, & \text{if } \mathcal{ST}_j \neq \emptyset, \\ \text{NaN} & \text{otherwise.} \end{cases} \tag{2.43}$$

Likewise, we can compute the average impact on line j, $\{\tilde{y}_j(\hat{\mathbf{b}}, t)\}_{j \in L}$, as

$$\tilde{\mathbf{y}}_j(\hat{\mathbf{b}}, t) := \frac{1}{N-1} (\mathbf{P}_s(\hat{\mathbf{b}}))_{j,:} \cdot \mathbf{1}. \tag{2.44}$$

The recentred version of Problem (2.41) is then given by

$$\begin{aligned}\min_{\hat{\mathbf{b}}\in\mathbb{R}^{|\mathcal{L}|},\mathbf{G}^1_{s,t}\in(N-1)\times Z} & \sum_{s,t\in\mathcal{ST}} \left\| \left(\tilde{\mathbf{P}}^{LZ}_{s,t} - \boldsymbol{\Omega}_{s,t}\mathbf{Y}\right) - \boldsymbol{\Omega}_{s,t}\left(\mathbf{P}_s(\hat{\mathbf{b}}) - [\tilde{\mathbf{y}}(\hat{\mathbf{b}},t),\ldots,\tilde{\mathbf{y}}(\hat{\mathbf{b}},t)]\right)\mathbf{G}^1_{s,t}\right\|^2_F \\ \text{s.t. } & \mathbf{1}^T\mathbf{G}^1_{s,t} = \mathbf{1}, \\ & \hat{\mathbf{b}} \geq \mathbf{0}.\end{aligned} \tag{2.45}$$

However, even for known $\mathbf{A}$, full line-zonal PTDF matrix $\mathbf{P}^{LZ}_{s,t}$ and known $\mathbf{G}^1_{s,t}$, the value of $\hat{\mathbf{b}}$ that minimises (2.45) lies in a rather high dimensional space. Nevertheless, given enough data, $\mathbf{P}(\hat{\mathbf{b}})$ can be shown to be unique. The analysis neglects the dependency on scenario, but this could be extended further. In the ideal case of unperturbed complete data, a set of $\mathbf{P}_s(\hat{\mathbf{b}})$ can be uniquely determined, and the solution space of $\hat{\mathbf{b}}$ is the intersection of the solution spaces for all $s \in \mathcal{S}$. This may or may not give a unique $\hat{\mathbf{b}}$. In practice however we expect these sub-spaces to be perturbed and thus their intersection might be empty. In this case we would require $\hat{\mathbf{b}}$ to be closest to all possible sub-spaces given by $s \in \mathcal{S}$. This may be unique or not.

The real PTDF observed data is about 1% of the data on the critical lines and an even smaller fraction when compared to all lines. This means that by simply using PTDF and RAM data, not even $\mathbf{P}(\hat{\mathbf{b}})$ can be recovered uniquely, with no hope of recovering $\hat{\mathbf{b}}$, which is even more challenging due to the nonlinear mapping. Further, the data sparsity also means that even given $\hat{\mathbf{b}}$ (or $\mathbf{P}_s(\hat{\mathbf{b}})$, for all s), $\mathbf{G}^1_{s,t}$ cannot be recovered. Even worse, in our case we do not know $\hat{\mathbf{b}}$ and $\mathbf{G}^1_{s,t}$ meaning that we have to fit these quantities simultaneously. This makes data reconstruction impossible, by pure means of using (2.45) and the PTDF data. For this reason, a large data gathering exercise and further optimisation models that aim to recover $\hat{\mathbf{b}}$ and $\mathbf{G}^1_{s,t}$ separately are required. These can then be used as regularisation terms for (2.45), as well as starting points for the optimisation algorithm applied to (2.45).

2.3 Analysis of the Input Data

While the general framework of our model is applicable to any FBMC DAA market, it is worth noting that every single power market has its unique features [25], and thus any fundamental model needs to be adapted accordingly. Here we use the CWE DAA Power Market as a case study, and for added clarity we describe its data structure before formulating the final version of the model. The CWE Power Market for 2019-2020 period was composed of five zones of interest: Austria, Belgium, Germany, France and the Netherlands. There are four major data sets: (i) the constraints data including the line-zonal PTDF and RAM [12], (ii) the power production data [29], (iii) the grid data [28], [75], and (iv) other time series data, typically recorded per zone, which also include their day-ahead estimates [29]. Unless

otherwise specified, the data is available at [29]. We restrict our attention to the first 210 days of 2019, which gives $|\mathcal{T}| = 5040$ data points for each hourly time series. The reason for this is three-fold:

1. data sparsity is roughly the same at every t, and thus considering more time instances does not increase the density of the data set, and so it does not directly increase the ability to recover the GSKs and the PAs, which are time dependent signals.

2. If the grid structure was fixed in reality, considering more time instances would increase the ability to recover the physical characteristics of the grid. However, in reality the grid is continuously changing, and thus considering windows that are too large might be detrimental when not tracking time dependent changes of the grid. This issue merits much attention on its own, but is outside the scope of this study.

3. Most importantly, the resulting optimisation problem is very computationally intense. As will become clear later, considering a larger data-set can drastically increases the computational time.

We next describe data preprocessing in more detail and analyse the data briefly.

2.3.1 Constraints Data

The data set, which we denote as $\mathcal{D}_{\mathcal{LST}}$, consists of hourly recorded PTDF, RAM, $\mathbf{F}^{\text{ref}}$, $\mathbf{F}^{\text{ref}}$, and FRM values, on transmission lines corresponding to each zone of interest and is available at [12]. A brief description of the data features is given below:

1. at each time, we observe data only of a small subset of the critical lines $\mathcal{L}_{\text{cne}}$, corresponding to presolved Flow-Based constraints in the optimisation algorithm [9].

2. At each fixed time, for each critical branch, $l \in \mathcal{L}_{\text{cne}}$, we potentially observe multiple corresponding *Contingencies* (C), also known as *Critical Outages (CO)*, $s \in \mathcal{S}$. This gives the following data structure for each line-scenario-time combination $\mathcal{D}_{l,s,t} = \{\text{PTDF}, \text{RAM}, \mathbf{F}^{\text{ref}}, \mathbf{F}^{\max}, \text{FRM}, \text{FAV}\}$. Since we do not observe all (l, s, t) pairs for $l \in \mathcal{L}_{\text{cne}}$, $s \in \mathcal{S}$, and $t \in \mathcal{T}$, we denote the available ones as $\mathcal{LST}$, and $\mathcal{ST} := \{(s, t) : (l, s, t) \in \mathcal{LST}\}$.

3. The chosen line orientation is not given in the data, and we account for this in our model,

4. the constraint data is independent of the grid data, and thus we map this to the grid data described in sub-section 2.3.3, by matching the node names specified in the constraints data, with the ones in the grid data.

We observe 106 CNEs and 152 Contingencies in the considered time interval, and successfully map 102 and 133 respectively. This gives a set of line-scenario combinations $\mathcal{LS}$ observed from the data with $|\mathcal{LS}| = 336$, which is much smaller than the total number of possible combinations, $|\mathcal{L}_{\text{cne}}||\mathcal{S}|$. This is because we do not observe every possible line-scenario pair (l, s) in the data.

The distributions of number of recorded data points for each l or (l, s) are not uniform but tends to resemble a power law, as observed in Figure 2.3. We thus observe that most of

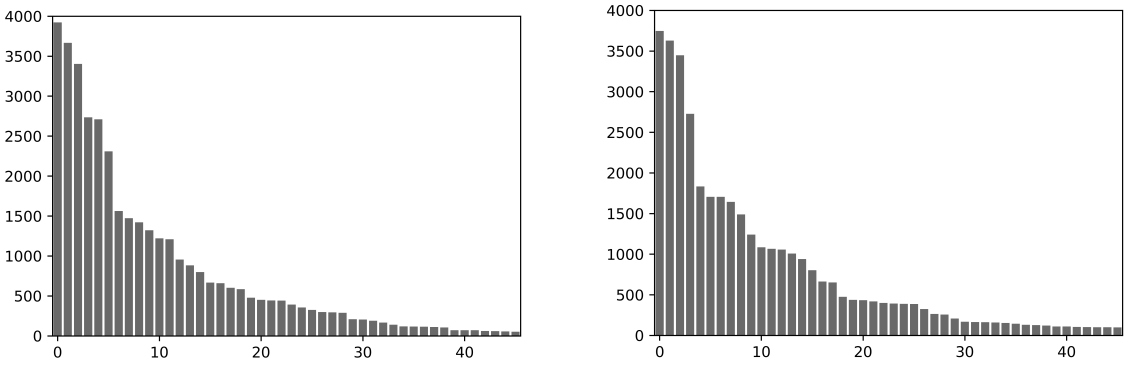


Figure 2.3: Number of recorded data points for the first 45 lines (left) and scenarios (right), sorted in descending order of recorded information amount.

the information is recorded on a small fraction of lines as well as (l, s) combinations. Adding the numbers in Figure 2.3 and dividing by $|\mathcal{LS}||\mathcal{T}|$, we see that the data amounts for only 2.3% of all CNEC (i.e (l, s)) combinations tracked by the TSOs. Clearly, the observed data is very sparse and insufficient for many applications. For example, the data sparsity and rather short available time series means that statistical models for forecasting the flow based domain are expected to perform poorly, especially since new constraints may appear and older ones may vanish as the structure of the grid and other fundamental factors change. Further, the very high dimensionality increases this difficulty. As a result, the effect of these constraints may not be correctly priced in by the market, resulting in sub-optimal economic outcome by making it more expensive (or cheap) for producers and/or consumers to hedge in the futures market.

2.3.2 Power Production Data

The generation units data can be found at [29] and is comprised of hourly production levels for named power plants. We record 35 Austrian, 42 Belgian, 173 German, 142 French and 45 Dutch power plants. A data extraction algorithm was written to download the data. The data accounts for most of the non-renewable production in these countries, but does not include renewables. For each zone, we denote the plant set $\mathcal{GU}_z$, with $|\mathcal{GU}_z| = N_p^z$, the vector of production at each time by $\boldsymbol{\phi}_t^z$ and the concatenation over zones as $\mathcal{GU} = \cup_{z\in\mathcal{Z}}\mathcal{GU}_z$, with $|\mathcal{GU}| = N_p$, and $\boldsymbol{\phi}_t = ||_{z\in\mathcal{Z}}^V(\boldsymbol{\phi}_t^z)$. Further $\boldsymbol{\Omega}_N \in \mathbb{R}^{N_p\times N}$ is the canonical projection from

all nodes to power plant nodes. Note that no geographical coordinates, ID, or any other indication of power plants' connection to the grid is given at [29]. Thus, we locate these mostly by hand since standard algorithms generally give unsatisfactory results. This is clearly a limitation and a source of error, but it is a solution that enables us to use the methodology presented in this chapter. We later compensate for this by allowing some optimisation over the location of the power plants and their connection to the grid, based on observed data, as presented in Section 2.4.2. This is generally the case for any other task performed by hand: while this input data is important and prone to error, during the optimisation process we allow for updating our best guess based on observed data.

2.3.3 Grid Data

We obtain the grid data by first obtaining the transmission grid, after which the production nodes are added.

2.3.3.1 Transmission Grid

Most of the transmission grid nodes and edges are obtained by aggregating information from SciGrid [75], APG [35], Elia [27] and ENSTOE [28], where the latter is used mostly for manual corrections and visualisation purposes. SciGrid contains most of the consumption nodes for Germany and France, a few nodes for the Netherlands, and very incomplete data for Austria and Belgium. They compute resistances R and reactances X based on the following formulas

$$R_l = C_r \frac{N^l_{wires}}{N_{wirestypical}} \frac{N^l_{cables}}{3} \Delta_l, \tag{2.46}$$

$$X_l = C_x \frac{N^l_{wires}}{N_{wirestypical}} \frac{N^l_{cables}}{3} \Delta_l, \tag{2.47}$$

where N^l_{wires} and N^l_{cables} are the number of wires per cable, and number of cables on line l, while Δ_l is the length of the cables. Note that Δ_l does not, in general, coincide with the geodesic distance between the nodes [7]. The value of the constants, and any further information can be found in [7]. The procedure for forming the transmission grid is as follows:

1. The SciGrid data is used as a starting point. The data is comprised of nodes with geographical coordinates (x_k, y_k), and edges l with $\{R, X, \Delta_l, V_l, N_{cables}, N_{wires}\}$ for most of the edges. We use this data for Germany, France and the Netherlands, while Austrian and Belgian nodes and edges are discarded completely due to very large data sparsity. We refer to the remaining grid as the Main Grid, that we keep updating. The required $N_{wirestypical}$ and N^l_{cables} are recorded for each country, based on line voltages.

2. Belgian data is added, by using the edge information available at [27]. For every line, the data has the format $\{$(Node Name 1, Node Name 2), $R_{,l}\, X_l, \Delta_l, V_l\}$, that is, information about nodes, edges with the resistances and reactances, as well as the line's distances. However, the nodes do not have geographical coordinates. One can try to use *geolocator* in *Python* to obtain these locations. However, we observe that this sometimes gives inaccurate results. A much better approach, is to use the PDF map provided by Elia [27]. With this, we obtain the relative positions of the nodes, using a plot digitiser. The absolute positions on the world map can then be used by rescaling every node's position based on the absolute coordinates of two nodes of choice. We pick these far away on both longitude and latitude to minimise the introduced error, and obtain their coordinates with Google maps. This is then added to the Main Grid. The data also contains some inter-zonal lines with one Belgian node.

3. A similar approach to step 2 is performed for Austria, by using the edge information available at [35]. The data is composed of nodes with geographical coordinates (x_k, y_k), and edges l containing $\{R_l, X_l, \Delta_l, V_l, N_{cables}, N_{wires}\}$. We obtain the geographical location as in 2, and add the Austrian network to the Main Grid.

4. The next step is concerned with the Netherlands. The graph structure available from SciGrid is clearly incomplete, and TennetNL does not provide the same information as Elia and APG. Thus, we manually add nodes and lines by comparing the current Main Grid structure with ENTSOE [28] and the map available at [57]. This poses the problem that for any added line, we do not have $\{R_l, X_l, \Delta_l\}$, although V_l can be manually obtained from ENTSOE.

5. By considering the ENTSOE map, we add all the missing inter-zonal lines to the Main Grid. These are all the lines that have the end points in two different countries, and at least one end point in AT, BE, DE, FR or NL. We assign V_l based on ENTSOE, but $\{R_l, X_l, \Delta_l\}$ are still unavailable.

6. The Constraints Data is mapped on the Main Grid as follows. Our mapping algorithm first looks to exact name matches, followed by approximate name matches, and finally assign mapping based on closest node that has no name. Although this procedure is sensible, it does not guarantee perfect matching. Some corrections were performed by hand, where possible. Next, a new line is created for every CB or CO that does not already correspond to a line on the Main Grid. Again, these have unknown $\{R_l, X_l, \Delta_l\}$. If unavailable, we fill in V_l values with the most common ones belonging to those pairs.

7. We fill in the $\{R_l, X_l, \Delta_l\}$ data for the required lines l. For the SciGrid data, the number of cables and wires is highly correlated with the voltages. Thus, using V_l, we assign the most common number of cables and wires corresponding to this voltage.

We compute Δ_l based on the geodesic distance between the nodes. Using (2.46) and (2.47), we compute X_l and R_l for each line, since C_r and C_x are known.

This process gives us an estimate of the transmission grid, which we call the Final Transmission Grid (FCG), based on the available data and a set of assumptions. Note that while the grid is fully connected, we here refer to Transmission and Production grids independently to reflect the fact that the data has to be obtained from different sources. The next step is to add the network elements corresponding to production.

2.3.3.2 Adding the Production Grid

The Generation Units (GU) data described in Section 2.2 contains 436 power plants that can be identified by names, but no geographical location of these is available. We aggregate this data with FCG as follows:

1. We locate some of these nodes with *geopy*, but most of the power plants cannot be located in this way. Manual work is performed to identify the coordinates of these power plants, which was a very time consuming process.

2. We next need to add the links between the power plants and the FCG, but we have no information about this. By visual inspection of few power plants that can be identified on ENTSOE, we observe that these are generally connected only to the closest node available. We thus connect all the power plants to the closest node that is not a power plant, that is, the closest node on the FCG.

3. We assign $V_l = 380kV$ based on ENTSOE power plants observations.

4. We use the approach from Section 2.3.1 item 7 to fill in the rest of the information on the lines.

This gives us the final grid, which we denote as $\mathcal{G}^0$, and all its attributes with the superscript 0. In particular, we now have the line susceptances $\hat{\mathbf{b}}^0$ and graph structure $\mathbf{A}^0$. Note that the line susceptances can easily be computed as $b_l^0 = 1/X_l$. The resulting graph is shown in Figure 2.4. Critical branches and critical outages are displayed in red and teal respectively. If a line is both a CB and a CO then it is represented in red. Each country has two colours for nodes, representing the production and consumption nodes, with the more frequent ones being the consumption. Note that the topology of $\mathcal{G} = (V, E)$ fully defines A, and the only physical characteristic needed are the line susceptances, $\hat{\mathbf{b}}$. To the best of our knowledge, this procedure makes use of the best available public information, but this will still introduce some error. Nevertheless, as we shall see in Section IV, we only use this for initialisation and regularisation in our optimisation model, and thus inaccuracies in the graph structure ($\mathbf{A}$,$\hat{\mathbf{b}}$) can be tolerated.

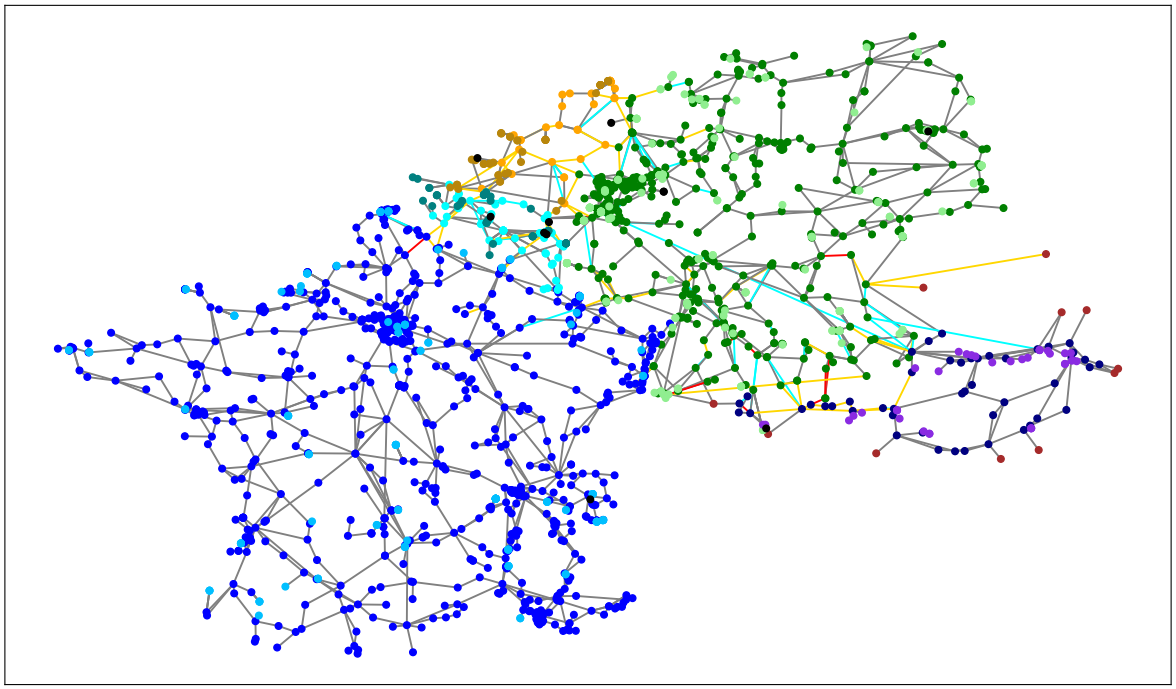


Figure 2.4: CWE Grid Model. Each country is assigned two colours, with the more frequent one representing consumption nodes, while the other represents power plants. For Austria, the consumption nodes are colored in dark blue. Critical lines and outages (contingencies) are marked in red and cyan respectively. Lines that are both CNEs and Contingencies (for other CNEs) are marked in yellow.

2.3.4 Other Time Series Data

The rest of the data used in our model are: (i) zonal time series for the demand $\{D_t^z\}_{t\in\mathcal{T}}$, (ii) import and export giving the Net Export (NEX) series $\{NEX_t^z\}_{t\in\mathcal{T}}$, (iii) solar $\{\boldsymbol{\phi}_t^{s,z}\}_{t\in\mathcal{T}}$ and wind $\{\boldsymbol{\phi}_t^{w,z}\}_{t\in\mathcal{T}}$ renewable energy production, and (iv) the zonal prices $\{S_t^z\}_{t\in\mathcal{T}}$, all of which can be found at [29]. The day-ahead versions of $\{D_t^z\}_{t\in\mathcal{T}}$, $\{\boldsymbol{\phi}_t^{s,z}\}_{t\in\mathcal{T}}$ and $\{\boldsymbol{\phi}_t^{w,z}\}_{t\in\mathcal{T}}$ are also available at [29].

2.4 Mathematical Optimisation Model

The core idea of the model is to fit the GSKs, PAs and grid characteristics to the historical PTDF and $\mathbf{F}^{\text{ref}}$ data described in 2.3.1, via equations (2.31) and (2.35). Once these are obtained data completion can be performed by simply using the fundamental equations described in Section 2.2. Direct fitting to the RAMs is not possible, but note that once $\mathbf{F}^{\text{ref}}$ is recovered, the RAMs can be obtained as per (2.36) and (2.37). When FRM and FAV are unknown, a simple solution is to set them to the mean historical value or zero. We only take FAV $= 0$ and compute the FRMs based on equations (2.36) and (2.37), since we observe $\mathbf{r}$ or $\mathbf{R}$, $\mathbf{F}^{\text{ref}}$ and $\mathbf{F}^{\max}$.

However, due to the sparsity of the data set $\mathcal{D}_{\mathcal{LST}}$, even for fixed $(\hat{\mathbf{b}}, \mathbf{A})$, multiple solutions exist for the GSKs and PAs. To simplify the analysis and increase data density, we assume that the GSK and base case are scenario independent, which is in agreement with literature proposals of defining the GSKs [74], [21], [17]. This means that at every time instant, we only consider a single GSK, instead of one GSK per scenario at every time. Thus we have that $\mathbf{G}^1_{s,t} = \mathbf{G}^1_t$ and $\mathbf{g}^0_{s,t} = \mathbf{g}^0_t$, which immediately implies that the s dependence of the $\{\text{PTDF}_{s,t}\}_{(s,t)\in\mathcal{ST}}$ and $\{\mathbf{F}^{\text{ref}}_{s,t}\}_{(s,t)\in\mathcal{ST}}$ data comes exclusively from A^s and b^s. This reduces the number of time dependent variables and helps preventing over-fitting. However, the corresponding optimisation problem remains under-determined and thus we introduce a regularisation for $\mathbf{g}^1_t$ in Subsection 2.4.1. We then analyse the expressivity of $\mathbf{P}_s(\hat{\mathbf{b}}, \mathbf{A})$ map, which is crucial to reconstruct the PTDFs in Subsection 2.4.2, and we present the main optimisation model in Subsection 2.4.3.

Before we proceed, we mention that the GSKs are only defined on the production nodes, since the TSOs have virtually no control over the demand. Thus, we define $\mathbf{g}^1_{z,t} \in \mathbb{R}^{N^z_p}$, $\overline{g}^1_{z,t} \in \mathbb{R}^{N_p}$ and $\mathbf{G}^1_t \in \mathbb{R}^{N_p \times Z}$ only over the production nodes. We write the expanded form of the nodal production based on the line-zonal simplification, for production nodes only as

$$\boldsymbol{\phi}^z_t = \mathbf{g}^0_{z,t} + \Delta\tilde{P}_{z,t}\mathbf{g}^1_{z,t}, \tag{2.48}$$

where $\mathbf{g}^0_{z,t} \in \mathbb{R}^{N^z_p}$ and $\Delta\tilde{P}_z$ are also re-defined for production nodes only. We will frequently use equation (2.48), instead of an equation that includes consumption nodes as well. However this does not reduce the amount of available information, since no nodal demand data is available. Note that $\Delta\tilde{P}_z$ denotes the total power deviation from the base case production levels.

2.4.1 A Regularisation for the GSKs

To obtain our desired GSKs regularisations, we use the JPW [73] variant of the Sensitivity Coefficients Regression (SRC) model, which was proposed to define the GSKs in Austria [73] and Germany [74]. One could imagine using the fundamental approach for finding the GSKs based on the strategies defined in [21]. However, it is worth noting that this is much more complicated to do from the market participant's perspective, than from the TSOs' perspective. This is because the strategies for defining the GSKs require selecting a subset of power plants, that are then assigned non-zero values based on some rule, that varies between TSOs. The problem is that market participants do not know what subset the operators choose, and thus this would require combinatorial optimisation, which is very computationally intense. For this reason, we use the model proposed in [73]. Note that, consistent with the chapter scope which is data completion and not forecasting, the JPW approach is not used for forecasting here but only to obtain a regularisation for the GSKs for

historical data. For each zone z and time τ, the model solves the linear regression problem denoted as $\mathcal{R}(z, p, \tau)$,

$$\boldsymbol{\phi}^p = \theta + \mathbf{n}\eta + \mathbf{l}\lambda + \mathbf{a}\iota + \mathbf{R}\boldsymbol{\rho} + \mathbf{D}\boldsymbol{\delta} + \mathbf{X}\boldsymbol{\xi} + \epsilon, \tag{2.49}$$

for each plant p in zone z, where ϵ is the error term, $\boldsymbol{\phi}^p \in \mathbb{R}^{T_p^{(\tau)}}$ is the vector of production levels for plant p, with $T_p^{(\tau)} = |\mathcal{T}_p^{(\tau)}|$ and $\mathcal{T}_p^{(\tau)} := \{t : (\boldsymbol{\phi}_t^z)_p \neq 0, t \in [\tau - w_z, \tau]\}$ being the index set of all data points for which plant p has nonzero production and with times shifted backwards at most w_z time units with respect to the time of interest, τ.

The net position vector $\mathbf{n} \in \mathbb{R}^{T_p}$ can be computed based on the import ($I_{z,t}$) and export levels ($E_{z,t}$) for every zone $n_{z,t} = E_{z,t} - I_{z,t}$, while $\mathbf{a}_t := S_t^z$ and $\mathbf{l}_t := D_t^z$ define the vector of zonal energy prices and demands respectively. Wind and solar production levels are considered as exogenous variables and each is assigned a column of $\mathbf{R}^{T_p \times 2}$. The dummy variable matrix $\mathbf{D} \in \mathbb{R}^{T_p \times 3}$ differentiates between peak/offpeak and summer/winter conditions, while $\mathbf{X} \in \mathbb{R}^{T_p \times 3}$ is the interaction matrix of time dummy variables and net position change, such that $\mathbf{X} = \text{diag}(\mathbf{n})\mathbf{D}$. Finally θ, η, λ, $\iota \in \mathbb{R}$ and $\boldsymbol{\rho} \in \mathbb{R}^2$, $\boldsymbol{\delta} \in \mathbb{R}^3$, $\boldsymbol{\xi} \in \mathbb{R}^3$ are the regression coefficients to be determined.

Since for each zone, the GSKs can be expressed as

$$(\mathbf{g}_{z,t}^1)_p = \frac{(\Delta\boldsymbol{\phi}_t)_p}{\Delta n_{z,t}}; \qquad \forall p \in \mathcal{GU}_z, \tag{2.50}$$

where $\Delta\boldsymbol{\phi}_t^z = \boldsymbol{\phi}_t^z - \mathbf{g}_{z,t}^0$ and $\Delta P_{z,t} = \sum_{p \in \mathcal{GU}_z} (\Delta\boldsymbol{\phi}_t^z)_p$, the SRC model sets the GSK entries to be proportional to the infinitesimal version of (2.50) and thus [74]

$$\left(\mathbf{g}_{z,\tau}^1\right)_p \sim \frac{\partial \boldsymbol{\phi}_{p,\tau}}{\partial n_{z,\tau}} = \eta + \mathbf{D}_{\tau,:}\boldsymbol{\xi} =: \upsilon_{z,p,\tau}. \tag{2.51}$$

The SRC then uses the fact that $1^T \mathbf{g}_{z,\tau}^1 = 1$ to obtain the GSK values by normalisation as

$$\left(\mathbf{g}_{z,\tau}^1\right)_p = \frac{\upsilon_{z,p,\tau}}{\sum_{p \in \mathcal{GU}_z} \upsilon_{z,p,\tau}}. \tag{2.52}$$

Since data points for which $(\boldsymbol{\phi}_t^z)_p = 0$ are excluded, the number of data points for some regression problems $\mathcal{R}(z, p, \tau)$ might not be sufficient. In this case, or if $\upsilon_{z,p,\tau}$ is below a (small) threshold value, the corresponding entry in $\upsilon_{z,p,\tau}$ (and thus in $\mathbf{g}_{z,\tau}^1$) is set to zero [74]. This procedure is shown in Heuristic 1.

Heuristic 1 SRC(z, τ) for obtaining the GSKs

input: $\boldsymbol{\phi}^p$, $\mathbf{n}$, $\mathbf{l}$, $\mathbf{a}$, $\mathbf{R}$, $\mathbf{D}$, $\mathbf{X}$ for a zone z and each plant p.
for p in $\mathcal{GU}_z$ **do**
solve the regression problem (2.49) for plant p
set $\nu_{z,p,t} \leftarrow \frac{\partial \phi_{p,t}}{\partial n_{z,t}}$ via (2.51) for each $t \in \mathcal{T}_p$ and 0 otherwise
let $\mu_p = \frac{1}{T_p} \sum_t \nu_{z,p,t}$ be the mean sensitivity
end for
thresholding: set $\nu_{z,p,t} \leftarrow 0$, $\forall p, t$ such that $\nu_{z,p,t} < 0.1 \min_p(\mu_p)$
set the GSK: $(\mathbf{g}_\tau^{1,z})_p = \frac{\nu_{z,p,\tau}}{\sum_{p \in \mathcal{GU}_z} \nu_{z,p,\tau}}$
return $\mathbf{g}_\tau^{1,z}$

One can now apply the procedure for all $\tau \in \mathcal{T}$ to obtain the zonal GSKs which we denote as $\mathbf{G}_z^1(\mathcal{T})$ and we denote this procedure as $SRC(z, \mathcal{T})$, and show how computation is performed in Heuristic 2. It is suggested in [73] that better results are obtained when using

Heuristic 2 SRC(z,$\mathcal{T}$)

choose z
for $\tau = \overline{1, T}$ **do**
$\mathbf{g}_\tau^{1,z} \leftarrow SRC(z, \tau)$
end for
$\mathbf{G}_z^1 = (g_{t_1}^{1,z}, g_{t_2}^{1,z}, ..., g_{t_T}^{1,z}) \in \mathbb{R}^{|\mathcal{GU}_z| \times T}$
return $\mathbf{G}_z^1$

the day-ahead (D-1) version of the regression coefficients. For us, this poses a problem for the left hand side of (2.49), since the D-1 version of $\boldsymbol{\phi}_t^z$ is $\mathbf{g}_{z,t}^0$, which is unknown. However, we propose to achieve this by initialising $\mathbf{g}_{z,t}^0 \leftarrow \boldsymbol{\phi}_t^z$, obtaining $\mathbf{g}_{z,t}^1$ via $SRC(z, \mathcal{T})$, updating $\mathbf{g}_{z,t}^0$ via (2.48) and then iterating again until we reach convergence, which we measure by the norm of the difference of $g_{z.t}^1$ between two consecutive iterations. We call this iterative SRC (ISRC) This is shown in Heuristic 3. We observe that the convergence for Austria

Heuristic 3 iterative SRC(z) (ISRC(z))

set $g_t^0 = \boldsymbol{\phi}_t$ for all t, and choose z and relaxation parameter $f \in (0, 1)$, threshold δ_{conv}
for $\tau = \overline{1, T}$ **do**
k = 0
while $\|\mathbf{g}_\tau^{1,z}(k) - \mathbf{g}_\tau^{1,z}(k-1)\|_2 / \|\mathbf{g}_\tau^{1,z}(k)\|_2 > \delta_{conv}$ **do**
$\mathbf{g}_\tau^{1,z}(k) \leftarrow SRC(z, \tau)$
$\mathbf{g}_t^{0,z}(k) \leftarrow \boldsymbol{\phi}_t^z - \Delta P_{z,t} \mathbf{g}_t^{1,z}$
$k \leftarrow k + 1$
end while
end for
let $\mathbf{G}_z^1 = (\mathbf{g}_{t_1}^{1,z}, \mathbf{g}_{t_2}^{1,z}, ..., \mathbf{g}_{t_T}^{1,z}) \in \mathbb{R}^{|\mathcal{GU}_z| \times T}$
let $\mathbf{G}_z^0 = (\mathbf{g}_{t_1}^{0,z}, \mathbf{g}_{t_2}^{0,z}, ..., \mathbf{g}_{t_T}^{0,z}) \in \mathbb{R}^{|\mathcal{GU}_z| \times T}$
return $\mathbf{G}_z^1$, $\mathbf{G}_z^0$

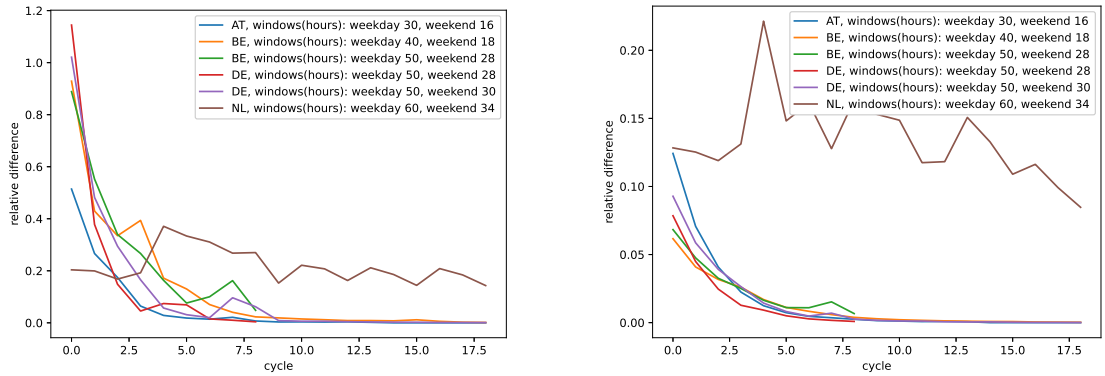


Figure 2.5: Convergence of GSKs (left) and base case (right).

and Germany is really fast, indicating that the TSOs might be using the approach in [74] and [73]. Rather surprisingly, we also obtain fast convergence for Belgium, suggesting that the $ISRC(z)$ is still appropriate. However, for the Netherlands we observe rather slow convergence, and we are not able to reduce the relative change between iterates to zero. This suggests that $SRC(z)$ is not ideal for modelling the dutch GSKs. Nevertheless, due to lacking further insight, we just stop the algorithm when no further progress can be made, as shown in Figure 2.5.

This gives us the GSK regularisation that we denote with a hat from here on, i.e. as $\hat{\mathbf{g}}^1_{z,t}$, $\hat{\mathbf{g}}^1_t$ and $\hat{\mathbf{G}}^1_t$ respectively. By using only the regularisation values b^0 and $\{\hat{g}^1_t\}_{t\in\mathcal{T}}$, we

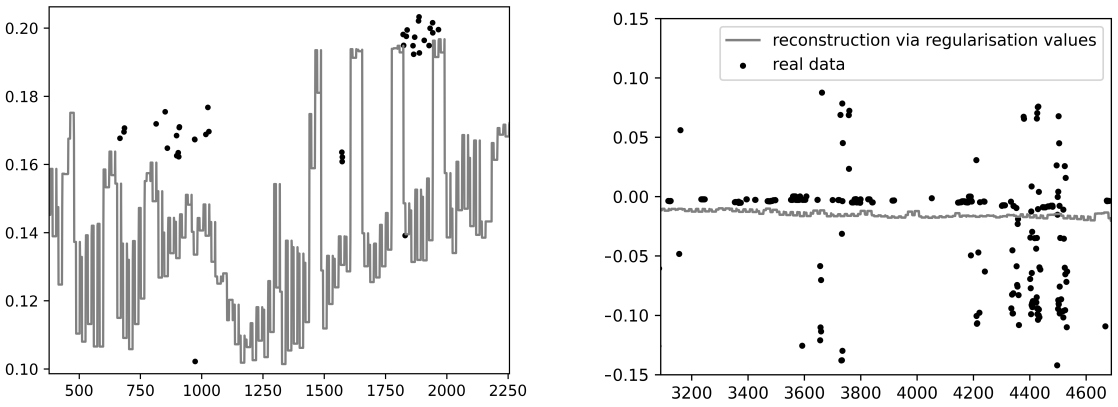


Figure 2.6: PTDF values on an Austrian line (left) and a German-Dutch crossing line (right) showing the reconstruction of the PTDF based on the regularisation values of $\hat{\mathbf{b}}^0$ and $\{\hat{g}^1_t\}_{t\in\mathcal{T}}$.

can already obtain a PTDF reconstruction via (2.31). As seen in Figure 2.6, this generally gives reasonable qualitative reconstruction suggesting that we obtained appropriate regularisations, since the PTDF data was not used up to this point. Nevertheless, the overall reconstruction error is rather large, about 4.5 larger than the mean, and the regularisations' reconstruction performs poorly on many lines, particularly due to the inability to capture large variations, or be centred appropriately, as shown in the right part of Figure 2.6. Further, no reasonable reconstruction of the RAMs is available at this point. This shows the

need for our main optimisation model, introduced in 2.4.3.

2.4.2 Expressivity of the Nodal PTDF Map

When running the main optimisation problem with $\mathbf{\Omega}_N^T$, on many lines, we observe poor ability to reconstruct (expressivity) the PTDFs' large variation, regardless of the chosen GSK. One reason for poor expressivity is that some power plants cannot be differentiated by the grid structure. This is because power plant location was obtained mostly by hand and is thus prone to errors. Further, by artificially connecting the power plants to the closest consumption node, multiple power plants inject power to the same single node, and thus are indistinguishable. To compensate for these errors, one could find the optimal location of each power plant, amongst its k closest neighbours. However, this approach introduces combinatorial complexity, and thus we only consider a convex relaxation of this problem. To this end we replace $\mathbf{\Omega}_N^T$ with the map $\mathbf{M}(\boldsymbol{\chi}) \in \mathbb{R}^{N \times N_p}$ defined as

$$\mathbf{M}(\boldsymbol{\chi})_{:,p} = \sum_{p \in \mathcal{GU}} \mathbf{\Omega}^p \boldsymbol{\chi}^p, \tag{2.53}$$

with $\mathbf{\Omega}^p = [e_{v_1}, e_{v_2}, ...e_{v_k}] \in \mathbb{R}^{N \times k}$, $\forall v_i \in \mathcal{N}_k(p)$, where e_q is the indicator vector for position q, $\mathcal{N}_k(p)$ is the set of k-nearest neighbours of plant p (including itself), and $\boldsymbol{\chi} := ||_{p \in \mathcal{GU}}^V \boldsymbol{\chi}^p$. Thus, $\boldsymbol{\chi}^p$ tells us how the power for plant p is distributed across neighbouring nodes. By optimising over $\boldsymbol{\chi}$, and enforcing that $0 \leq \boldsymbol{\chi}^p \leq 1$ and $\mathbf{1}^T \boldsymbol{\chi} = 1$, we allow finding the most likely power injection pattern of each plant to the k closest neighbours, instead of predefining a single fixed connection to the closest node, and by choosing a sufficiently small $k > 1$ we can avoid over-fitting. Note that each entry of vector $\boldsymbol{\chi}^p$ corresponds to a node and can be seen as the probability that power plant p is located at that node.

2.4.3 The Optimisation Model

We now introduce the main optimisation model, explaining every term individually. The optimisation variables are $\hat{\mathbf{b}}$, $\boldsymbol{\chi}$, the time series $\{\mathbf{g}_t^1\}_{t \in \mathcal{T}}$, $\{\boldsymbol{\alpha}_t^L\}_{t \in \mathcal{T}}$, and the constraints direction, which we model as binary variables $\nu_{l,s,t} \in \{-1, 1\}$ for every $(l, s, t) \in \mathcal{LST}$. We introduce optimisation terms to (i) fit to the PTDF data, (ii) fit to the $\mathbf{F}^{\text{ref}}$ data, (iii) regularise $\hat{\mathbf{b}}$, (iv) regularise g_t^1, and the corresponding physical constraints. We further regularise $\boldsymbol{\alpha}_t^L$ implicitly by taking this to be constant over non-overlapping time windows of length w_α, and $\mathbf{M}(\boldsymbol{\chi})$ by choosing a small value of k. Note that we do not optimise over A since this is NP hard, and because the number of variables would become very large, and thus we write $\mathbf{P}_s(\hat{\mathbf{b}}) := \mathbf{P}_s(\hat{\mathbf{b}}, \mathbf{A})$. This is reasonable since we expect to have a good initial estimate of the graph topology, but it is much less likely that we have accurate physical characteristics of this (such as $\hat{\mathbf{b}}$).

We start by describing the PTDF term. Our choice of reference node might be mismatched by the TSO, and as a result we can recover $\text{PTDF}_{s,t}$ only up to a rank one matrix. This can be remedied by introducing the following mean centering: for each line j, let $\mathcal{ST}_j = \{(s,t) : (j,s,t) \in \mathcal{LST}\}$, $\mathcal{L}_{s,t} := \{j : (j,s,t) \in \mathcal{LST}\}$ and let $\mathbf{Y} \in \mathbb{R}^{L_{\text{cne}} \times Z}$ with

$$\mathbf{Y}_{j,:} := \frac{1}{|\mathcal{ST}_j|} \sum_{(s,t)\in\mathcal{ST}_j} (\text{PTDF}_{s,t})_{j,:}, \tag{2.54}$$

which is well defined since $\mathcal{ST}_j \neq \emptyset$ for all $j \in \mathcal{L}_{\text{cne}}$, and $\text{PTDF}_{s,t} \in \mathbb{R}^{|\mathcal{L}_{s,t}| \times Z}$ is the concatenation of all the available PTDFs at (s,t). Likewise,

$$\tilde{\mathbf{y}}_j(\hat{\mathbf{b}}, s, t) := \frac{1}{N-1}(\mathbf{P}_s(\hat{\mathbf{b}}))_{j,:}\mathbf{1}_N, \tag{2.55}$$

where $\mathbf{1}_N \in \mathbb{R}^N$. The centred PTDF data is then

$$\text{PTDF}^c_{s,t} = \text{diag}(\boldsymbol{\nu}_{s,t})\text{PTDF}_{s,t} - \boldsymbol{\Omega}_{s,t}\mathbf{Y}, \tag{2.56}$$

where $\odot$ denotes the element-wise product, $\boldsymbol{\Omega}_{s,t} \in \mathbb{R}^{|\mathcal{L}_{s,t}| \times L_{\text{cne}}}$ is a projection map from the critical lines to the one observed for (s,t). Similarly, the centred version of the nodal PTDF becomes

$$\mathbf{P}^c_s(\hat{\mathbf{b}}) := \mathbf{P}_s(\hat{\mathbf{b}}) - \tilde{\mathbf{y}}(\hat{\mathbf{b}}, s, t)\mathbf{1}^T_N. \tag{2.57}$$

We further regularise $\mathbf{g}^1_\cdot$ by imposing constant value over a (small) time window w_g via $\theta^g_t = \lfloor t/w_g \rfloor$. The PTDF optimisation term is then

$$f_P(\hat{\mathbf{b}}, \mathbf{g}^1(\mathcal{T}), \boldsymbol{\chi}) = \sum_{s,t\in\mathcal{ST}} \|\text{PTDF}^c_{s,t} - \hat{\boldsymbol{\Omega}}_{s,t}\mathbf{P}^c_s(\hat{\mathbf{b}})\mathbf{M}(\boldsymbol{\chi})\mathbf{G}^1_{\theta^g_t}\|^2_2, \tag{2.58}$$

where $\mathbf{g}^1(\mathcal{T}) = \{\mathbf{g}^1_{\theta^g_t}\}_{t\in\mathcal{T}}$, $\hat{\boldsymbol{\Omega}}_{s,t} = \boldsymbol{\Omega}_{s,t}\boldsymbol{\Omega}_{\text{cne}}$. Note that $PTDF^c_{s,t}$ has to be computed just once, while $\mathbf{P}^c_s(\hat{\mathbf{b}})$ must be updated at every iteration for $\hat{\mathbf{b}}$. The PTDF reconstruction for the CNEs can be then obtained for every (s,t) as

$$\overline{\text{PTDF}}_{s,t} = \mathbf{P}^c_s(\hat{\mathbf{b}})\mathbf{M}(\boldsymbol{\chi})\mathbf{G}^1_{\theta^g_t} + \mathbf{Y}. \tag{2.59}$$

We can obtain the $\mathbf{F}^{\text{ref}}$ optimisation term in a similar way. However, note that since $\boldsymbol{\alpha}^L_\cdot$ are centred around zero, $\text{PSDF}_s(\hat{\mathbf{b}})$ centering is not necessary. Further, since the number of lines is very large, we only allow a small fraction of lines to have nonzero entries in $\boldsymbol{\alpha}^L$. To achieve this we redefine $\boldsymbol{\alpha}^L \in \mathbb{R}^{L_\alpha}$ to be the vector of PAs, and $\boldsymbol{\Omega}_\alpha \in \mathbb{R}^{L\times L_\alpha}$ to be the projection map from the set of nonzero PAs to all lines. We further regularise $\boldsymbol{\alpha}^L$ by

imposing constant value over the time window w_α via $\theta_t^\alpha = \lfloor t/w_\alpha \rfloor$, to obtain

$$f_F(\hat{\mathbf{b}}, \{\boldsymbol{\alpha}^L_{\theta_t^\alpha}\}_{t\in\mathcal{T}}) := \sum_{s,t\in\mathcal{ST}} \|\mathbf{F}^{ref,c}_{s,t} - \hat{\boldsymbol{\Omega}}_{s,t}\mathrm{PSDF}_s(\hat{\mathbf{b}})\boldsymbol{\Omega}_\alpha \boldsymbol{\alpha}^L_{\theta_t^\alpha}\|_2^2, \tag{2.60}$$

where $\mathbf{F}^{ref,c}_{s,t} = \boldsymbol{\nu}_{s,t} \odot \mathbf{F}^{\text{ref}}_{s,t} - \boldsymbol{\Omega}_{s,t}\mu(\mathbf{F}^{\text{ref}})$, with $\mu(\mathbf{F}^{\text{ref}})$ being the mean reference flow values over the critical lines. By comparing (2.60) to (2.35), one can observe that we neglected the term given by g_t^0, which can be written as a function of only $\mathbf{g}_t^1$ via (2.48). In numerical experiments, we found that this term tends to only introduce noise, without improving the quality of fit or generalisation error. We note that this does not mean that the base case g_t^0 does not have an impact for the calculation of the reference flow, but rather that mean centering is the only approach that allowed us to capture a causal relationship. This may be because changes in the PAs may account for most of the flow variability, when compared to changes in the base case, making the task of capturing causal relationship between $\mathbf{g}_t^0$ and $\mathbf{F}^{\text{ref}}$ very challenging. In other words, once the mean production vector is known, it is much more important to know how the TSOs use the grid controls (the PAs), than knowing the exact values of the production vector. Since the PAs can be controlled by the TSOs, and g_t^0 are not, this is a desirable property for safe operation of the grid, as it means that the operators have more control over the critical flows than otherwise. We also enforce that $-\pi/6 \leq \boldsymbol{\alpha}^L_{\theta_t^\alpha} \leq \pi/6$ as per [19], and that there is no pre-congestion, that is, the reference flows do not exceed the maximum allowed flows on the critical lines

$$\overline{lb} \leq \mathbf{P}^{\text{cne}}_{\mathcal{S}}(\hat{\mathbf{b}})\boldsymbol{\alpha}^L_{\theta_t^\alpha} \leq \overline{ub}, \tag{2.61}$$

for every θ_t^α, where $\mathbf{P}^{\text{cne}}_{\mathcal{S}} = ||^V_{s\in\mathcal{S}}\boldsymbol{\Omega}_{\text{cne}}\mathbf{P}_s(\hat{\mathbf{b}})$, the flow bounds are $\overline{ub} = ||^V_{s\in\mathcal{S}}\left(\mathbf{F}^{\max} - \mu(\mathbf{F}^{\text{ref}})\right)$, and $\overline{lb} = ||^V_{s\in\mathcal{S}}\left(-\mathbf{F}^{\max} - \mu(\mathbf{F}^{\text{ref}})\right)$, with $\mathbf{F}^{\max}$ being the vector of maximum recorded $\mathbf{F}^{\max}_{s,t}$ values for each line. Assuming no pre-congestion is reasonable, because case this is very undesirable, and the TSOs choose remedial actions such that pre-congestion is minimised or removed [71].

The regularisation terms can simply be written as

$$f_G(\{\mathbf{g}^1_{\theta_t^g}\}_{t\in\mathcal{T}}) = \sum_{t\in\mathcal{T}} \|\hat{\mathbf{g}}^1_t - \mathbf{g}^1_{\theta_t^g}\|_2^2, \quad f_b(\hat{\mathbf{b}}) = \|\hat{\mathbf{b}}^0 - \hat{\mathbf{b}}\|_2^2. \tag{2.62}$$

By collecting all the terms, the final optimisation problem is:

$$\begin{aligned}
&\min_{\omega} f_P(\hat{\mathbf{b}}, \{\mathbf{g}^1_{\theta^g_t}\}_{t\in\mathcal{T}}, x) + \lambda_F f_F(\hat{\mathbf{b}}, \{\boldsymbol{\alpha}^L_{\theta^\alpha_t}\}_{t\in\mathcal{T}}) + \lambda_G f_G(\{\mathbf{g}^1_{\theta^g_t}\}_{t\in\mathcal{T}}) + \lambda_b f_b(\hat{\mathbf{b}}),\\
&\text{s.t. } \hat{\mathbf{b}} \geq \delta_b \mathbf{1}, \text{ and } \boldsymbol{\nu}_{s,t} \in \{-1,1\}^{|\mathcal{L}_{s,t}|},\\
&\quad \mathbf{1}^T \mathbf{g}^1_{z,\theta^g_t} = 1, \text{ and } -\delta^z_g \mathbf{1} \leq \mathbf{g}^1_{z,\theta^g_t} \leq \delta^z_g \mathbf{1}, \ \forall z \in \mathcal{Z}, t \in \mathcal{T},\\
&\quad \mathbf{1}^T \boldsymbol{\chi}^p = 1, \text{ and } \mathbf{0} \leq \boldsymbol{\chi}^p \leq \mathbf{1}, \ \forall p \in \mathcal{GU},\\
&\quad \overline{lb} \leq \mathbf{P}^{\text{cne}}_{\mathcal{S}}(\hat{\mathbf{b}}) \boldsymbol{\alpha}^L_{\theta^\alpha_t} \leq \overline{ub}, \text{ and } -\frac{\pi}{6} \leq \boldsymbol{\alpha}^L_{\theta^\alpha_t} \leq \frac{\pi}{6}, \forall t \in \mathcal{T},
\end{aligned}$$

where $\delta_b > 0$ is a small number, $0 < \delta^z_g \leq 1$ is the maximum allowed GSK value per entry, $\lambda_\cdot \in \mathbb{R}_+$ are regularisation parameters, and the full set of optimisation variables is denoted as $\omega = (\hat{\mathbf{b}}, \{\mathbf{g}^1_{\theta^g_t}, \boldsymbol{\alpha}^L_{\theta^\alpha_t}\}_{t\in\mathcal{T}}, \boldsymbol{\chi}, \{\boldsymbol{\nu}\}_{s,t\in\mathcal{ST}})$. Note that $\hat{\mathbf{b}}$ is fixed in principle, and once found it can be directly used for future predictions, but $\mathbf{g}^1_{\theta^g_t}$ and $\boldsymbol{\alpha}^L_{\theta^\alpha_t}$ being time dependent can not. However, these can be used for statistical analysis or forecasting.

2.5 Numerical Optimisation

The optimisation problem is highly nonlinear and non-convex over the variable set ω, and very large, with about 4 million variables, but the vast majority of variables are the $\mathbf{g}^1_{\theta^g_t}$, which are decoupled in time. Thus, we propose an alternating minimisation approach, by solving for one variable at a time, while keeping the others fixed, and using the most recent updates. This has the following steps: (i) solve for each $\boldsymbol{\nu}_{s,t}$ independently, (ii) solve for $\hat{\mathbf{b}}$ via stochastic optimisation, (iii) solve for $\boldsymbol{\chi}$ via stochastic optimisation, (iv) solve for $\{\mathbf{g}^1_{\theta^g_t}\}_{t\in\mathcal{T}}$, for each time independently, via Convex Quadratic Programming (CQP), (v) solve for $\{\boldsymbol{\alpha}^L_{\theta_\alpha(t)}\}_{t\in\mathcal{T}}$, for each time independently, via CQP, and (vi) iterate until convergence or time limit is reached. This approach does not guarantee the algorithm reaches a local minimum, since the resulting problems for $\hat{\mathbf{b}}$ and $\boldsymbol{\nu}_{s,t}$ are not marginally convex. However, it makes the problem computationally feasible and leverages the marginally convex structure of the objective function in $\mathbf{g}^1_t$ and $\boldsymbol{\alpha}^L_{\theta_\alpha t}$ as well as time decoupling. Note that we are guaranteed to reduce the objective function value at every optimising step for $\boldsymbol{\nu}_{s,t}$, $\mathbf{g}^1_{\theta^g_t}$, and $\boldsymbol{\alpha}^L_{\theta^\alpha_t}$, but not for $\hat{\mathbf{b}}$ and $\boldsymbol{\chi}$, and thus, great care needs to be taken when optimising over these. We next describe in detail optimising over each set of variables.

2.5.1 Optimising over $\boldsymbol{\nu}_{s,t}$

We optimise over each entry $\boldsymbol{\nu}_{l,s,t} \in \{-1,1\}$ such that $(l,s,t) \in \mathcal{LST}$ independently, by choosing the value that decreases the objective function value most. With all the other

quantities pre-computed, this is fast since we only have to compare two cases for each variable $\boldsymbol{\nu}_{s,t}$. Further, since the data points are independent, this approach gives the global optimal solution when $\hat{\mathbf{b}}$, $\{\mathbf{g}^1_{\theta^g_t}, \boldsymbol{\alpha}^L_{\theta^\alpha_t}\}_{t\in\mathcal{T}}$ and $\boldsymbol{\chi}$ are fixed.

2.5.2 Optimising over $\hat{\mathbf{b}}$

Due to the large number of scenarios $|\mathcal{S}|$, it is extremely expensive to compute all the $\mathbf{P}_s(\hat{\mathbf{b}})$ values, since these require the computation of $(\tilde{\mathbf{A}}_s^T\tilde{\mathbf{B}}_s\tilde{\mathbf{A}}_s)^{-1}$ for every s at every iteration. Further, the number of times $|\mathcal{T}|$ is also very large, making the computation of $f_P(\hat{\mathbf{b}})$, $f_F(\hat{\mathbf{b}})$, $\nabla_b f_F(\hat{\mathbf{b}})$ and $\nabla_b f_P(\hat{\mathbf{b}})$ extremely time and memory intensive, and thus we use tensor implementation in *PyTorch*. Computing the Hessian is impractical, and thus we resort to first order methods. We use stochastic optimisation, at each iteration k, by randomly choosing only a subset $\mathcal{T}_k$ of $\mathcal{T}$ (but all corresponding s), because: (i) this dramatically reduces the energy usage per iteration, due to much fewer inversions and $\mathbf{P}_s(\hat{\mathbf{b}})\mathbf{M}(\boldsymbol{\chi})\mathbf{G}^1_{\theta^g_t}$ products, (ii) it reduces the computational time, and (iii) we observe much larger objective function decrease per iteration when compared to the deterministic optimisation step, since the landscape of $f_P(\hat{\mathbf{b}})$ is noisy, and stochastic methods act as a smoother. To allow step size adjustment, we use ADAM [42] as optimiser, and solve for K_b iterations in every cycle.

2.5.3 Optimising over $\boldsymbol{\chi}$

Although the problem for $\boldsymbol{\chi}$ is convex, and we could solve via CQP, the double sum over s and t makes the problem excessively large, yielding infeasible memory requirements when using *Mosek*. Thus, we perform stochastic optimisation using the ADAM optimiser, similarly to the optimisation over $\hat{\mathbf{b}}$. This makes the computations less memory and energy intensive, but does not guarantee convergence to the optimal solution $\boldsymbol{\chi}^*(\hat{\mathbf{b}}, \mathbf{G}^1)$, even when all the other variables are fixed, since ADAM may not converge even on convex problems [45]. However, we find this to be a good trade-off between computational feasibility and making optimisation progress.

2.5.4 Optimising for $\mathbf{g}^1_{\theta^g_t}$

We solve for each $\mathbf{g}^1_{\theta^g_t}$ independently since the problem is decoupled in time. The resulting optimisation problem reads

$$\min_{\mathbf{g}^1_\tau} \sum_{\mathcal{F}^g_\tau} \|PTDF^c_{s,t} - \hat{\boldsymbol{\Omega}}_{s,t}\mathbf{P}^c_s(\hat{\mathbf{b}})\mathbf{M}(\boldsymbol{\chi})\mathbf{G}^1_{\theta^g_t}\|_2^2 + \lambda_G\|\hat{\mathbf{g}}^1_t - \mathbf{g}^1_{\theta^g_t}\|_2^2$$

$$\text{s.t. } \mathbf{1}^T\mathbf{G}^1_{\theta^g_t} = 1,\ \forall t \in \mathcal{T}, \quad 0 \le (\mathbf{G}^1_{\theta^g_t})_{ij} \le 1,\ \forall t \in \mathcal{T} \qquad ,$$

where $\mathcal{F}^g_\tau := \{(s,t) : s \in \mathcal{S}, \theta^g_t = \tau\}$. The problem is convex, and we solve it using *Mosek*'s API in *Python*, but other convex optimisation solvers could be used. Note that the time spent during this step increases linearly with the size of $\mathcal{T}$. While this is the best one can expect, this step is performed multiple times and thus it can drastically increase the computational time.

2.5.5 Optimising over $\boldsymbol{\alpha}^L_{\theta^\alpha_t}$

Similarly to 2.5.4, the problem is convex, and decoupled in time for every θ^α_t. This reads

$$\begin{aligned}
&\min_{\boldsymbol{\alpha}^L_\tau} \sum_{s\in\mathcal{S},\{t:\theta^\alpha_t=\tau\}} \|\mathbf{F}^{\text{ref},c}_{s,t} - \text{PSDF}_s(\hat{\mathbf{b}})\boldsymbol{\Omega}_\alpha \boldsymbol{\alpha}^L_{\theta^\alpha_t}\|_2^2, \\
&\text{s.t. } \overline{lb} \leq \mathbf{P}^{\text{cne}}_{\mathcal{S}}(\hat{\mathbf{b}})\boldsymbol{\alpha}^L_{\theta^\alpha_t} \leq \overline{ub}; \quad -\frac{\pi}{6} \leq \boldsymbol{\alpha}^L_{\theta^\alpha_t} \leq \frac{\pi}{6},\ \forall t \in \mathcal{T},
\end{aligned}$$

and we solve it using *Mosek*'s API in *Python*.

2.5.6 Obtaining New Values for $\mathbf{g}^1_{\theta^g_t}$ and $\boldsymbol{\alpha}^L_{\theta^\alpha_t}$ after the Model Fit

Once the solution ω of the main optimisation model is available, one can obtain new values for $\mathbf{g}^1_{\theta^g_t}$ and $\boldsymbol{\alpha}^L_{\theta^\alpha_t}$ for $t \notin \mathcal{T}$ ($t > \max_{\tau\in\mathcal{T}} \tau$) by pre-fitting $\boldsymbol{\nu}_{s,t}$ and then solving the corresponding convex optimisation problems 2.5.4 and 2.5.5 once. The number of variables is reduced dramatically and once the $\mathbf{P}_s(\hat{\mathbf{b}})$ maps were pre-computed, this problem can be solved on a usual personal computer in at most few of minutes.

2.6 Numerical Results

We evaluate the model for: (i) in sample quality of fit, (ii) generalisation for $(l,s,t) \notin \mathcal{LST}$, with $l \in \mathcal{L}_{\text{cne}}$, $s \in \mathcal{S}$, $t \in \mathcal{T}$, i.e. for unobserved (l,s,t) containing observed individual elements, and (iii) generalisation for unobserved (l,s,t) with new times $t \notin \mathcal{T}$ and observed $l \in \mathcal{L}_{\text{cne}}$ and $s \in \mathcal{S}$. The first evaluation requires in-sample tests while for the other two we perform out of sample tests. Due to the data sparsity, it is impossible to split the data in a training and test set to perform out-of-sample tests for (ii) and (iii) simultaneously. Thus, we split the data twice, fit the model to each training set, and perform tests on the corresponding test set.

For the first train-test split, we cannot simply remove (say) 20% of the data at random and add it to the test set, because this leaves many (l,s) combinations and t indices with no data. To resolve this, we propose the following heuristic: (i) select an available (l,s,t) point at random, (ii) if the number of points on (l,s) and at time t are above the thresholds

m_{LS} and m_T respectively, remove the point from the training set, and add it to the test set, (iii) otherwise do not remove the point but mark it such that it cannot be chosen again, (iv) repeat until the desired test set size is achieved or no more points can be removed. We choose $m_T = 8$, since this is the average data density with respect to time, and allowing a smaller value would make data rich time indices become data scarce. We choose $m_{LS} = 50$, but generally it is m_T that has a strong impact on maximum fraction of data that can be removed. In this case, the maximum fraction of removed points is about 18%, but this corresponds to is highly inter-dependent choices. Thus, we choose to assign 85% and 15% to the train ($\mathcal{D}_1^{train}$), and test ($\mathcal{D}_1^{test}$) set respectively. We fit the model to the training set and compute the out-of-sample error on the test set.

The second training and test sets are obtained by splitting the time indices at random, such that 20% of the times are assigned to $\mathcal{D}_2^{test-t}$ and the rest to $\mathcal{D}_2^{train}$. Further, $\mathcal{D}_2^{test-t}$ is randomly split in $\mathcal{D}_2^{test-fit}$ and $\mathcal{D}_2^{test-lst}$ which receive 75% and 25% respectively. We fit the model only by using $\mathcal{D}_2^{train}$. However, to test the model we need GSKs, PAs and $\boldsymbol{\nu}_{s,t}$ for each time interval, but these are unavailable. We obtain these by using fixed $\hat{\mathbf{b}}$, $\boldsymbol{\chi}$ (fit based on $\mathcal{D}_2^{train}$), and fit for $\mathbf{g}^1_{\theta_t^g}$, $\boldsymbol{\alpha}^L_{\theta_t^\alpha}$ and $\boldsymbol{\nu}_{s,t}$ only once on $\mathcal{D}_2^{test-fit}$. Out of sample tests are performed on $\mathcal{D}_2^{test-lst}$. This is an indication of generalisation quality to new times, given the time-independent variables $\hat{\mathbf{b}}$ and $\boldsymbol{\chi}$, and thus the corresponding test evaluates if they give a good representation of the real grid.

We run the algorithm on a 72 core machine with 768 GB of memory. We find choosing $k = 5$, $w_\alpha = 8$ and $w_g = 6$ to be a good trade-off between quality of fit and generalisation ability. We stop after running the algorithm for 14 complete cycles, because the objective function value decrease per cycle becomes rather small, and the computational cost is high.

2.6.1 PTDFs and RAMs Reconstruction

We are interested in the performance of the model, but defining summarised statistics for direct comparison of high dimensional polytopes is challenging. Since to our knowledge, our model is the first to reconstruct the PTDFs and RAMs, we can only compare to a benchmark model but due to the limited data available, defining a good benchmark model is also challenging. Thus we consider a benchmark model that assumes all data variation is noise, and thus it reconstructs the data by simply taking the empirical mean value for every line, and assigns this to every single (s, t) combination with $s \in \mathcal{S}$ and $t \in \mathcal{T}$. We define the benchmark model error as $\delta_{null}(.)$ and the corresponding relative error with respect to the benchmark model as $\delta_{rNull}(.) = \delta_{abs}(.)/\delta_{null}(.)$. Since the benchmark may be rather coarse, we evaluate the quality of our reconstruction against we use multiple error measures. We also use the average absolute mean error which we denote as $\delta_{abs}(.)$. To estimate the quality of fit, we compare the error to the variation on the line by taking $\delta_\sigma(.) := \delta_{abs}(.)/\sigma(.)$, where $\sigma(.)$ is the standard deviation of the data set of interest. We use this ratio because if deviations are large, then it is expected that the ability to fit reduces, and thus we should

penalise the model less. Finally, if one is to use these constraints in the optimisation problem for price finding [9], the relative error with respect to the mean value is more relevant, as this measures the fractional error in our constraints. We denote this as $\delta_\mu(.) := \delta_{abs}/\mu(.)$, where $\mu(.)$ takes the mean of the corresponding data set. However, since the PTDFs are mean zero centred we define $\mu(.)$ to be the mean of absolute values in this case.

We show the overall errors obtained across the whole data set in Table 2.1. Considering that only about 2.3% of the existing data is available, and thus used as input in our model, we obtain good reconstruction quality. While the errors are not very small, they are much smaller than the naive approach as indicated by δ_{rNull}, and the average error is significantly lower than the average change in values, as indicated by δ_σ. Finally, the average absolute error δ_{abs} is well below 0.05, which is the threshold for critical branch selection, meaning that a relatively good representation of the PTDFs is obtained. All these metrics indicate that a reasonable estimation of the underlying signals and the flow based constraints was obtained. Since δ_μ is rather small, the reconstructed PTDFs and RAMs can be used to reconstruct the feasibility domain at each time step or for forecasting with reasonable error. Further, we obtain good generalisation for both $\mathcal{D}_1$ and $\mathcal{D}_2$ tests, suggesting that our model is performing well for constraints reconstruction and is likely not over-fitting the parameters to the observed data. The slightly better generalisation for $\mathcal{D}_1$ when compared to $\mathcal{D}_2$ could be because the grid changes, albeit slowly, over time. Grid elements are added, removed

Error measure	δ_{abs}	δ_σ	δ_{rNull}	δ_μ
PTDF on $\mathcal{D}_1^{train}$	0.0122	14.4%	36.1%	22.7%
PTDF on $\mathcal{D}_1^{test}$	0.0119	14.0%	35.2%	22.1%
$\mathbf{F}^{\text{ref}}$ on $\mathcal{D}_1^{train}$	88.1	36.1%	39.6%	11.7%
$\mathbf{F}^{\text{ref}}$ on $\mathcal{D}_1^{test}$	96.6	39.5%	43.4%	12.8%
RAM on $\mathcal{D}_1^{train}$	93.1	42.6%	54.9%	16.0%
RAM on $\mathcal{D}_1^{test}$	94.2	43.1%	55.6%	16.2%
PTDF on $\mathcal{D}_2^{train}$	0.012	14.2%	35.5%	22.3%
PTDF on $\mathcal{D}_2^{test-lst}$	0.014	16.1%	40.5%	25.4%
$\mathbf{F}^{\text{ref}}$ on $\mathcal{D}_2^{train}$	87.5	35.8%	39.3%	11.6%
$\mathbf{F}^{\text{ref}}$ on $\mathcal{D}_2^{test-lst}$	130.4	53.4%	58.5%	17.3%
RAM on $\mathcal{D}_2^{train}$	92.7	42.4%	54.7%	15.9%
RAM on $\mathcal{D}_2^{test-lst}$	105.1	48.2%	62.1%	18.1%

Table 2.1: Training and test errors for the two data splits $\mathcal{D}_1$ and $\mathcal{D}_2$.

or changed, and thus one might consider periodically re-calibrating $\hat{\mathbf{b}}$ to new data, starting with the old $\hat{\mathbf{b}}$ in the optimisation process. By analysing δ_σ, one can see that we obtain a better quality of fit to the PTDFs when compared to the RAMs. This is not contradictory to what one might infer from Figure 2.7, where we perform normalisation with respect to the empirical mean (instead of σ) for every (l, s) combination. This is expected, because the PTDFs are simpler to compute, involving fewer variables and simpler physical equations,

while the target RAM signal is computed by the TSOs based on their base case estimate, which is much more complex [8], [22]. Finally, our model is clearly superior for reconstruction of the PTDFs and significantly better for the reconstruction of $\mathbf{F}^{\text{ref}}$, when compared to the benchmark model, and thus is superior to the naive approach of treating data on every line as purely random. Therefore we capture meaningful structure in the data, and we further illustrate this by showing more detailed results in Figure 2.7.

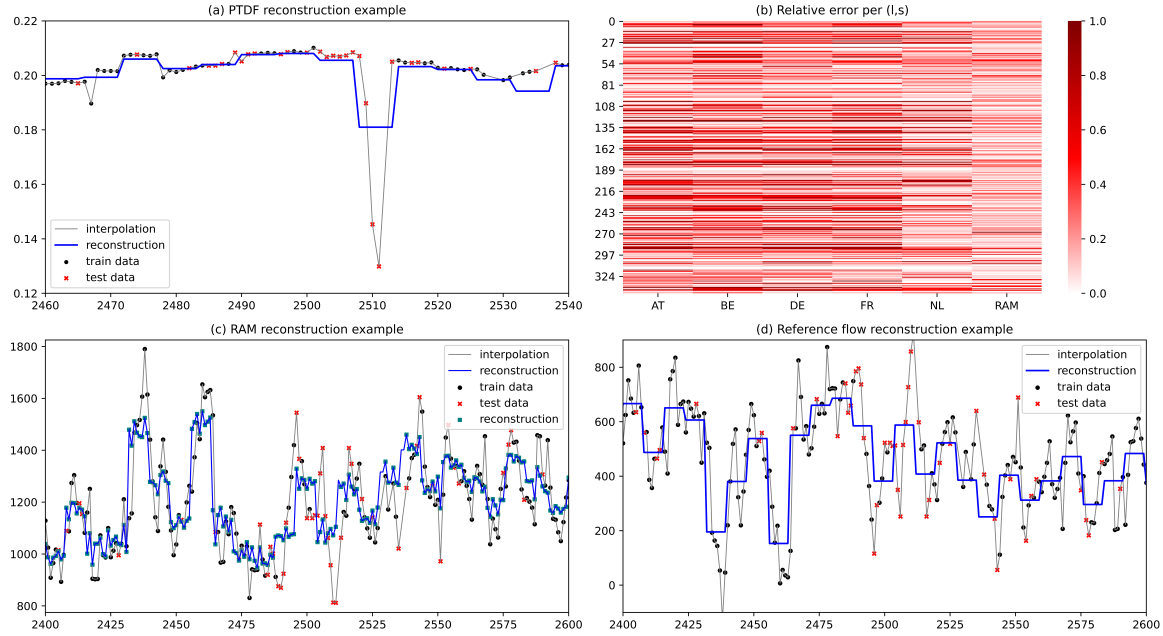


Figure 2.7: Detailed reconstruction results. Plots (a), (c) and (d) show the PTDF (French entry), RAM, and $\mathbf{F}^{\text{ref}}$ reconstruction results for a representative (French-German) line. The blue lines (and dots) indicate the reconstruction, while the black and red dots indicate the training and test data points respectively. The grey line is an interpolation between available data points for better visualisation only. The heat map in (b) indicates the relative RAM error in the sixth column, and relative PTDF error for the five countries, corresponding to the first five columns. These errors are computed with respect to the mean, since due to data scarcity on many (l, s) with very few observations, the standard deviation is very inaccurate or even zero.

We can see that the reconstruction fits the training signal well, and implies reasonable values for time indices where data is unavailable. By analysing Figure 2.7 (a), one can observe that we partially capture the sharp change in the PTDF although these points were not part of the training set. We also obtain good reconstruction for the $\mathbf{F}^{\text{ref}}$ and RAM, although again we cannot fully capture sharp variations. This is because of the introduced time window values chosen for w_α and w_g. We can confirm that much better fit is obtained by letting these to one, but in this case the out of sample generalisation is rather poor. Thus, we found $w_\alpha = 8$ and $w_g = 6$ to be a good trade-off. Note that by (2.33), even with fully available $\mathbf{F}^{\text{ref}}$ values, the RAM cannot be reconstructed without knowing the other terms. To obtain full RAM reconstruction, for each (l, s) pair, we thus always use the last available values at each time index. For this reason, we mark the points where exact $\mathbf{F}^{\max}$

and FRM are used by blue dots in Figure 2.7 (c). Finally, Figure 2.7 (b) shows the δ_μ value, computed for each available line scenario combination, that is each $(l, s) \in \mathcal{LS}$. We can observe that our model generally performs well, although some error entries are rather large. This could be because of small amount of information on some lines, but also because of imperfections in the grid structure, particularly regions where fine grid data is unavailable. While the optimisation model proposed in Section 2.4.3 dramatically improves the quality of fit, due to the problem structure, multiple solutions exist, and finding the global minimum is NP hard. Further, we do not optimise over A, as this is would require solving an integer optimisation problem over variables corresponding to entries in A, where each sub-problem is itself NP hard (the problem we are currently solving). This is clearly computationally infeasible. Nevertheless, our results generally give good reconstruction and generalisation, and outperform the naive approach, and we next show that we recover structure in the GSKs and PAs.

2.6.2 Structure Analysis of the Reconstructed GSKs and PAs

We perform clustering analysis to reveal groups of similar zonal GSKs and PAs respectively. We cluster at zonal level because the TSO in each zone chooses the GSKs independently of the others. We use the k-means algorithm [49], which in this case we found to give better results when compared to the Gaussian Mixture Models [24] solved with via Expectation Maximisation. We run the algorithm 50 times and choose the result that gives the smallest

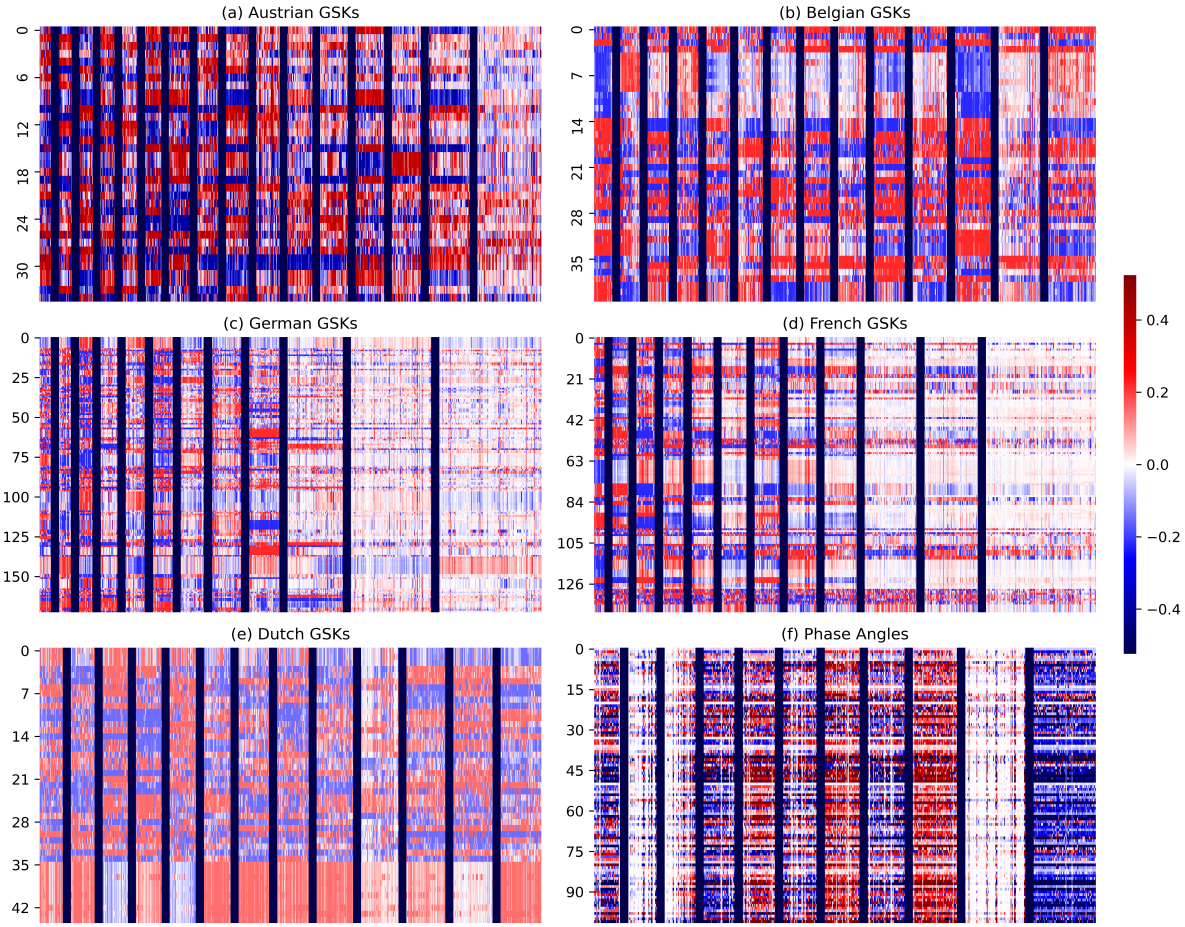


Figure 2.8: Clustering results for the Generation Shift Keys and Phase Angles. For each subplot, the horisontal axis corresponds to time indices while the vertical axis corresponds to entries in $\mathbf{g}_t^1$ and $\boldsymbol{\alpha}_t^L$ respectively, and the vertical dark bars are delimiters between the clusters.

within cluster sum of squares. We choose the number of clusters by using the elbow method, but since there is no clear steep change in the derivative, we err on the parsimonious side. This is because a smaller number of clusters reduces the effect of noise and makes the recovered structure more meaningful. Because of the very high dimension, we show the results via a heat map, where each column corresponds to the values of one $\mathbf{g}_{z,t}^1$ (or $\boldsymbol{\alpha}_t^L$), and we delimit the clusters with dark vertical bars. If within a cluster the entries of all $\mathbf{g}_{z,t}^1$ (or $\boldsymbol{\alpha}_t^L$) are similar, then they are assigned similar colours on the heat map, and the cluster shows relatively uniformly across the horisontal axis.

Figure 2.8 suggests that we recover meaningful clustering structure, with generally well balanced clusters. This suggests that the TSOs choose the GSKs in a rather simplistic and robust way, specifically from a small subset of pre-determined fixed vectors. The variations within the clusters could be explained by expertise-based value adjustment, although a part of this could be due to noisy input data and the limitations of the numerical optimisation process, which does not guarantee reaching the global optimum. Nevertheless, the recovered clusters are meaningful, and the strategies for choosing the GSKs discussed in [21] are consistent with our findings: while the exact strategies differ based on TSO, the operators choose a subset of power plants to have non-zero GSKs and then assign the values based on a simple rule and inputs depending on the physics of the system and expected state of the market. Since the power plants are expected to switch on in order, based on the position in the generation stack, the number of considered possibilities is expected to be rather small. In practice, the physics of the system and the expected state of the market, combined with the simplistic value assignment rules, is expected to result in the formation of clusters of GSKs, where within each cluster, the GSKs could be identical or very similar depending on the value assignment rule. Observing these clusters without imposing such structure indicates that our results are meaningful.

2.7 Conclusion

Day Ahead Auctions in Power Markets that use the Flow Based Market Coupling methodology require linear constraints on all transmission lines to ensure that the auction leads to solutions that do not violate transmission load limits. In reality constraints corresponding to only a very small number of critical lines constraints are published. The missing data reduces market participants' risk management ability and ultimately leads to higher prices.

We propose a methodology that recovers the electricity grid constraints via a mathematical optimisation problem using only publicly available data. The model reconstructs the grid structure and the underlying time dependent signals known as the Generation Shift Keys and Phase Angles, which are then transformed to the Power Transmission Distribution Factors and Remaining Available Margins, via mappings that are determined by the grid structure. Our results show good reconstruction quality and out of sample generalisation, and we recover meaningful clustering structure for the zonal GSKs and PAs, yielding insight into the operator's behaviour and suggesting that the GSKs could be chosen from a (fixed) palette of values up to small adjustments for daily characteristics. Our results lead to increased transparency, which means that the speculators (market makers) would have access to better information and thus reduced uncertainty, which should translate to a better ability to manage risk. In a competitive market this should result in a reduced risk premium that the hedgers (commercials) have to pay to the market makers on futures contracts. It is well known that commercial producers include the a risk premium associated with their

risk exposure in their cost. Since the hedging cost would become lower for the hedgers, then their revenue risk exposure should also be lower, meaning that the risk premium charged on the spot market should also be lower. This results in better (more competitive) prices in the Day Ahead Auction, which ultimately results in increased Social Welfare.

Chapter 3

A Game Theoretic approach for Spot Electricity Markets

3.1 Introduction and Motivation

Electricity markets have undertaken heavy deregulation in the past two decades, and the goal of this liberalisation is to improve economic efficiency and attract new investments [84]. However, for this to be achieved each electricity market requires a market clearing mechanism (MCM) to facilitate the desired outcome. According to [54], there are four main properties that a market outcome needs to satisfy to be desirable:

1. **Individual Rationality (IR)**, which means that the expected utility (or profit) of any participating player i needs to always be at least as large and sometimes greater than when not participating, so that each player has an incentive to participate.

2. **Weakly Balanced Budget (WBB)**, meaning that the total amount paid by consumers must be greater than or equal to the total amount paid to suppliers.

3. **Nash Equilibrium incentive compatible (NEIC)**, namely, there exists an equilibrium where everyone is bidding and offering according to their true benefit or cost structure, and no unilateral change of bids or offers is profitable.

4. **Economic Efficiency (EE)** means that the good is given to the one that values it most.

Clearly, all these properties are desirable for any type of auction, including electricity markets. Unfortunately, by the *Myerson-Satterthwaite impossibility theorem* [54], for the bilateral exchange situation of a single good and two traders, the four properties mentioned above cannot be simultaneously satisfied, meaning that any mechanism must sacrifice *at*

least one. When all information is public, for the general case of m buyers and m sellers it has been shown in [3], that the inefficiency, i.e the amount by which the trader misreports, decreases as $O(1/m)$. However, the same is not true in the case of private information [51], and, like most other markets, electricity markets usually lie somewhere between fully private and fully public information. While this does not rigorously prove that an equivalent result holds in every (peculiar) electricity market, it gives a strong indication that it may, and therefore that any electricity market mechanism is prone to inefficiencies. This means that players may have the possibility to strategize and bid untruthfully, with the end goal of maximising their own profit or utility. Even worse, tacit or direct collusion may also be possible in certain situations. Thus, Game Theoretic Analysis of such systems yields valuable non-trivial insights.

As a consequence of the issues resulting from the *Myerson-Satterthwaite impossibility theorem*, the strong model assumptions unfit for electricity markets, and the undesirable results of the Cournot model, researchers have studied many market mechanisms to be applied to electricity markets, each having different advantages and disadvantages. We here focus on the Day Ahead Auction electricity market which covers the largest part of spot electricity trading. To ensure that market outcomes satisfy a range of feasibility constraints, Day-Ahead electricity markets only allow for placing limit orders once per day, before the market gets cleared for the next day, once and for all. Any market clearing mechanism requires a quantity allocation mechanism and a pricing mechanism, and the two are highly interconnected based on the objective of the central operator that runs the auction.

To better understand the possible range of outcomes when players strategize, it is instructive to review the main results concerning the main type of market mechanisms in electricity markets. To the best of our knowledge, the most well researched market mechanisms are:

- The **Pay-as-Bid (PaB)** mechanism obtains the quantity allocations based on some cost minimisation or welfare maximisation objective [31]. Each producer then receives a payment corresponding to the integral of their submitted cost curve. The submitted cost curve is untruthful (over-stated) in general, since this is the only possibility to ensure positive profit [2]. Thus, the mechanism does not satisfy *incentive compatibility* (NEIC). The mechanism satisfies *IR* and *WBB*, but it also does not necessarily ensure *EE*, and thus has fairly poor properties in general. In electricity markets with no network constraints, [80] obtains that a Nash Equilibrium may not exist for incomplete information, pushing the participants to create cartel agreements to influence prices.

- A **First Price Auction (FPA)** mechanism finds the unique price such that the supply and demand are balanced. When well defined, this mechanism is Nash Equilibrium *incentive compatible*, but not *Dominant Strategy incentive compatible* (DSIC), meaning that a truthfully bidding equilibrium exists, but it is not the only one [2]. The mechanism satisfies *IR* and *WBB* but does not have to satisfy *EE* in general. Even worse, for the case of European electricity markets, which desire a single zonal price,

but allow exchange between zones, the mechanism cannot be directly applied, since at the optimal balance of supply and demand, the highest accepted offered price in one zone may be higher than the lowest accepted bid price in the same zone, due to inter-zonal trade. In this situation zonal price definition becomes unclear, and thus one has to sacrifice either balance of payments or efficiency to enforce feasible and unique zonal prices. The CWE market uses a modified version of this mechanism with unique zonal price [78], that sacrifices *efficiency* by introducing an ad-hoc pricing rule, resulting in removal of initially optimal orders.

- **Locational Marginal Pricing (LMP)** mechanism is widely studied in the literature, and usually applied in North American Electricity Markets [79]. The mechanism relies on a DC model of Optimal Power Flow (OPF) to represent the grid and its constraints. The Locational Marginal Prices (LMP) are defined at each node, and are the Lagrangian Multipliers of the nodal power balance constraint. If the operator's optimisation problem satisfies strong duality, then the optimality gap is zero, and the LMP have economic interpretation. Further, the balance of payments is achieved in this case [50]. The *Dominant Strategy incentive compatible* property holds only under the additional and rather strong assumption of *price taking*, meaning that producers believe they cannot influence the price. This is clearly not true in practice, and thus this mechanism offers producers the possiblity of strategizing individually to maximise their own utilities. If strong duality does not hold, then the balance of payments does not hold and the budget deficit is given by the duality gap [50]. For example, a case when strong duality does not hold is the AC Optimal Power Flow (AC-OPF) model [59]. The CWE market uses elements of these ideas by requiring the ad-hoc determined prices to satisfy the economic relations implied by the shadow prices (dual variables) corresponding to the active line constraints [43].

We can therefore see that all these mechanisms have advantages and limitations. Further, none of these mechanisms can be directly applied without any modifications to the European DAA markets which additionally require the following properties [78]:

1. Power balance across the whole network including multiple zones, while allowing for non-zero exchanges between the zones.

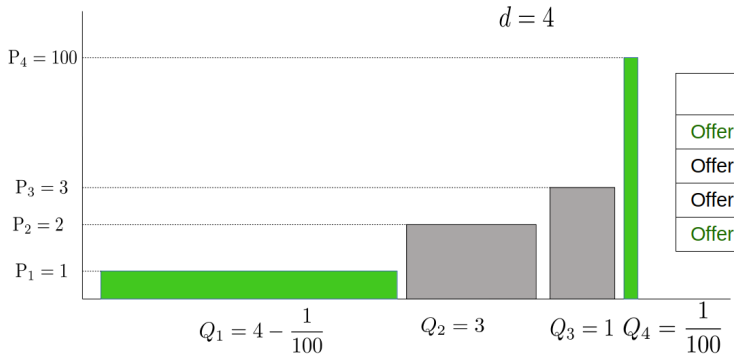
2. Safe operation of the grid has to be guaranteed explicitly via constraints in the market clearing optimisation problem.

3. Uniqueness of price in a zone, where a zone contains multiple nodes and usually corresponds to a country.

4. If the network constraints are inactive, there has to be a single unique price across all zones.

5. The weakly budget-balanced property cannot be sacrificed, meaning that the total payment to the producers cannot exceed the total payment from the consumers.

Clearly, the requirement of unique zonal price is further constraining, reducing the class of mechanisms that can be considered, and thus the possibility of satisfying as many of the four *canonical properties* and ensuring collusion-proofness. This means that the auction mechanism proposed in the CWE may allow producers to strategize. Since market participants are interested in quantity allocations and price formation, the understanding and computation of the market clearing solution is very important, especially under a game theoretic framework that incorporates the possibility of strategizing. A significant amount of work was done by researchers on modelling and solving market clearing mechanisms based on Locational Marginal Prices (LMP) under DC Optimal Power Flow (OPF) grid model. For example in [48], the authors define a mixed integer linear program to model such an auction and propose an algorithm to solve this numerically. In [68] the authors look at a very simple game theoretic approach where only three distinct possible strategies are considered per player, under a simplistic market clearing. Linear marginal prices submitted as bids are considered in the work of [38], where an auction based on LMP with DC-OPF is used, resulting in a bi-level optimisation problem [16]. A similar auction model is considered in [85], and the bi-level problem is transformed into a Mathematical Program with Equilibrium Constraints (MPEC) for each player, the collection of which is denoted as Equilibrium Program with Equilibrium Constraints (EPEC) [85], [33]. Some theory and numerical approaches are provided in this paper. Other similar studies include [82], [72], and [76]. Some of the more recent work for auction modelling and solution includes the work of [55], where the problem of LMP multiplicity is discussed and a solution proposed, as well as [65], where revenue constraints are introduced as part of the auction. In [64], the authors introduce a Consumer Payment Minimisation objective, with Locational Marginal Pricing and OPF network constraints. They remark that under this market setup, when demand is taken as inflexible the Social Welfare Maximisation objective becomes minimising the offer cost. Further, the offer cost is indeed what has to be paid to the producers to clear the market. However, for the case of ZMP pricing with FBMC network constraints, the offer cost is generally strictly less than the total amount paid to the generators, since every generator has to be paid an uniform zonal price rather than its own marginal asked price. This discrepancy raises the question as to what should be the offer cost considered, and as supported by the example in Figure 3.1, for ZMP pricing, we argue that this should not be the one implied by Social Welfare objective, and motivates us to introduce a new objective, of minimising the actual amount paid to the producers which is the true cost incurred by an inflexible demand side.



	Price	Quantity
Offer 1	1	4 - 1/100
Offer 2	2	3
Offer 3	3	1
Offer 4	100	1/100

Figure 3.1: Example of offer preference issue for Social Welfare objective for discrete bids. The green offers are the ones selected by the social welfare. The market has one zone.

$$
\begin{aligned}
O_1 + O_2 &: \; -SW_{1,2} = 10 - \frac{1}{100};\; P_z = 2; \qquad C_{1,2} = 2 \cdot (4 - \frac{1}{100} + 3) = 14 - \frac{1}{50} \\
O_1 + O_3 &: \; -SW_{1,3} = 7 - \frac{1}{100};\; P_z = 3; \qquad C_{1,3} = 3 \cdot (4 - \frac{1}{100} + 1) = 15 - \frac{3}{100} \\
O_1 + O_4 &: \; -SW_{1,4} = 5 - \frac{1}{100};\; P_z = 100; \qquad C_{1,4} = 100 \cdot (4 - \frac{1}{100} + \frac{1}{100}) = 400 \\
O_2 + O_3 &: \; -SW_{3,4} = 9;\; P_z = 3; \qquad C_{2,3} = 3 \cdot (3 + 1) = 12
\end{aligned}
$$

Considering that bids have to be chosen fully or rejected, from the above calculations we can see that the social welfare is maximised when offers 1 and 4 are selected. However, this results in a very large zonal price of 100 when compared to all other options, and by taking a closer look we see that this is due to accepting order 4 which charges a very high price but only offers a very small quantity, but nonetheless has a large impact on the zonal price and on the total cost of procurement $C_{1,4}$. While in a market with many generators, this is not a big issue for Locational Marginal Pricing, where only the generator corresponding to offer 4 would receive a price of 100, for zonal pricing the entire zone has to pay this high price. This issue arises because the Social Welfare objective is inconsistent with the zonal pricing scheme, in the sense the zonal clearing price may increase arbitrarily much while the social welfare can stay the same. Indeed the reader can replace the value 100 by 1000 throughout (or by any other number), and the optimal choice under SWM, as well as the objective value are the same, while the clearing price can change arbitrarily. To address this problem we propose minimising the actual cost paid by the consumer instead, and while cost minimisation is a well studied concept, the variation proposed here is novel to the best of our knowledge, in the context of FBMC constraints and Zonal Marginal Pricing. While it is true that Euphemia has heuristics to deal with this type of issues, for example by first relaxing the integrality constraints [9], this approach purposely avoids picking the optimal solution and creates an inconsistency, and we believe that using an objective that naturally resolves this issue is desirable. Note that by contrast, when using LMP, nodes can always be further split to reduce this problem and in the limit of one node per order, this issue is completely removed. On the other hand, collecting nodes under a single zonal

price amplifies the problem and its impact. This example also illustrates the possibility for bidding strategically. If the generator that submitted offer 1 had an availability of 4 (instead of $4 - \frac{1}{100}$), it would still not be incentivised to offer all 4MW production since it would clear at a much lower price. While in this work we do not address all these complexities, since we do not consider integrality constraints, we lay the foundation for a different objective for European DAA market clearing, and also offer a game theoretic study.

Further differences between ZMP pricing with FBMC network constraints and LMP pricing with OPF are illustrated in [56], where the authors show that a nodal price regime would result in reduced marginal power prices in the majority of European countries, operating cost savings of $1.1\% - 3.6\%$, and an increase in international MW transfers of up to 34%.

Abundant literature on LMP pricing with OPF network constraints exists [86], [1], [20], but this market model is not directly applicable to the CWE methodology of unique zonal prices (as opposed to LMP) and PTDF-RAM constraints (as opposed to DC-OPF). To the best of our knowledge, research on the game theoretic analysis of electricity auctions is also not concerned with a market model directly applicable to the CWE market. In [68] the authors look at a very simple game theoretic approach where only three distinct possible strategies are considered per player, under a simplistic market clearing. Linear marginal prices submitted as bids are considered in the work of [38], where an auction based on LMP with DC-OPF is used, resulting in a bi-level optimisation problem. A similar auction model is considered in [85], and the bi-level problem is transformed into a Mathematical Program with Equilibrium Constraints (MPEC) for each player, the collection of which is denoted as Equilibrium Program with Equilibrium Constraints (EPEC). Some theory and numerical approaches are provided in this paper. However, none of these uses a model directly relevant to the CWE, and the differences in the auction mechanism are crucial: as seen before, different mechanisms may have very different properties and may yield very different market outcomes and optimal behaviours.

The contributions of our work in this chapter are as follows. We introduce the CWE market clearing mechanism along with the payment rule defined by a pricing problem. We prove that when the demand is purely inelastic, this problem is resolved and that consistent pricing can be achieved by a simple max-rule. We introduce a Cost Minimisation objective and we show that this reduces producer's market power, but also facilitates game theoretic analysis through computation of derivatives, for the case of no capacity constraints. We then concentrate on solving the mechanism and on its game theoretic analysis. We introduce the reader via a simple model with two zones only and no capacity constraints. In this case we are able to provide analytical solution to the market clearing mechanism and derive the equations characterising the Nash Equilibria. We then generalise to a model with any number of zones, albeit no capacity constraints, in Section 3.4. Since network constraints are more challenging in this case, and the market clearing problem has bilinear terms, we show how the problem can be solved efficiently if the polytope representing the network

constraints is replaced with ellipsoid constraints. We devise an algorithm that iteratively solves problems over ellipsoid constraints, such that the solution for the polytope constraints case can be approximated arbitrarily well. We leverage the structure of the market clearing problem to compute derivatives of profit for each player and search for stationary points where all derivatives are zero. We find that an abundance of Nash stationary points (weaker form of equilibria) exists. This is because, as we prove, for inflexible demand and in the absence of risk aversion for players, Nash Equilibria with arbitrarily high prices may exist, and under the chosen class of strategies there exists a continuum of such equilibria. c

In Section 3.5 we add capacity constraints, since these are an important consideration for price formation. As a result, the market clearing optimisation problem is much more challenging, and we propose four different algorithms with different trade-offs between speed and convergence guarantees to solve the optimisation problem. What we call ieq-LP has no theoretical guarantees but only relies on solving simple LPs, and is generally very fast, while what we call ie-CQP, uses the iterative ellipsoid approach idea and offers the guarantee of (slightly better than) local minimum at increased computational expense. We also propose a Branch and Bound approach tailored for this specific problem, which we call BBTree. This offers global convergence guarantee within known optimality gap. Finally, we derive strong (but partial) analytical results that enable us to devise an efficient algorithm that iteratively solves Convex Quadratic Programs with polytope constraints, in a very low dimensional space. We call this approach iterative based CQP (ib-CQP), and the method is generally very fast since it leverages partial analytical results, while guaranteeing global convergence on a subdomain of finite size including the found solution. Note that this type of convergence is much stronger than local, but weaker than purely global. The computation of the market solution is critical for the computation of Nash Equilibria. Since the type of risk aversion introduced in the previous section is unsatisfactory, we introduce a *"worst case"* type of risk aversion for each player. Fortunately, this is non-parametric and reduces the strategy space for each player to one dimension, bounded at both ends. This facilitates the exhaustive discretisation of the strategy space and allows for computation of *approximate Global Nash Equilibria*. We provide numerical experiments that compare the four types of market clearing solvers and observe that the Nash Equilibrium point may often be unique in this case. We then introduce a SWM based model and explain how to obtain numerical solutions. We next look at applying our models to the CWE market, and by defining players for each zone, obtaining producers' cost data, and using the network constraints obtained in Chapter 2, we apply the SWM and CM market clearing mechanisms under the game theoretic framework, as well as truthful bidding. We use *Descartes Labs* [46] cloud computing provider to facilitate numerical computations. We obtain results that show that our models are representative of the real world price dynamics in the CWE, and we can confirm that the SWM model is more representative, while the CM model generally gives reduced prices and always gives reduced cost. We finally devise a method based on simple hypothesis testing, and the aforementioned

results, to identify if and when players are bidding strategically and conclude with high confidence that this is more pronounced than generally assumed in literature or practice.

3.2 Background Information

The pricing problem in CWE DAA has integrality constraints corresponding to fill-or-kill orders or blocks of orders. However, we here neglect these constraints for simplicity and focus on the pricing mechanism when any fraction of a bid or offer could be accepted. With the current CWE DAA Market clearing mechanism, the price is determined by:

1. Solving the primal LP problem corresponding to the social welfare maximisation.
2. Solving the dual problem to obtain the dual variables (Lagrangian multipliers) of the power flow constraints (PTDF and RAM).
3. Solving the pricing problem accounting for (i) the marginal transmission costs, (ii) a somewhat arbitrary objective that ensures that the price is *"intuitive"*.

The objective of the primal LP is maximisation of the social welfare expressed as

$$SW(\mathbf{x}_\cdot) = \sum_{z\in\mathcal{Z}} \left(\sum_{b\in\mathcal{B}_z} Q_b^z P_b^z x_b^z - \sum_{o\in\mathcal{O}_z} Q_o^z P_o^z x_o^z \right), \tag{3.1}$$

where $\mathcal{Z}$ is the set of zones and $\mathcal{B}_z$ and $\mathcal{O}_z$ are the sets of bids and offers for zone z, and $\mathbf{x}$ is the vertical concatenation of all the variables $x_\cdot^z \in [0,1]$. The quantities Q_b^z, Q_o^z, P_b^z and P_o^z are non-negative constants and correspond to the quantity and price of the submitted orders.

Let $\mathbf{E} \in \mathbb{R}^{|\mathcal{Z}|\times N_b}$ be a linear map from the bid accepted fractions to the net energy production in the zone. The entries corresponding to offers are assigned $-Q_o^z$ values since positive values are associated with consumption. The PTDF constraints are then:

$$\mathbf{M}_p\mathbf{E}\mathbf{x} \leq \mathbf{b}_p, \tag{3.2}$$

where $\mathbf{M}_p^+ = ||_v \mathbf{P}_s(b)\mathrm{GSK}_t$ is the concatenation of the line-zonal PTDFs corresponding to time t and all considered scenarios s and $\mathbf{M}_p = ||_v(-\mathbf{M}_p^+, \mathbf{M}_p^+)$. A similar concatenation over the RAMs is performed: $\mathbf{b}_p = ||_v(\mathbf{b}_p^{\mathrm{LB}}, \mathbf{b}_p^{\mathrm{UB}})$ where $\mathbf{b}_p^{\mathrm{LB}} = ||_v - R_{s,t}^{\mathrm{LB}}$, $\mathbf{b}_p^{\mathrm{UB}} = ||_v R_{s,t}^{\mathrm{UB}}$. Note that t is fixed here. We also have the element-wise constraints that

$$\mathbf{0} \leq \mathbf{x} \leq \mathbf{1}, \tag{3.3}$$

and the power balance across the zones satisfies

$$\mathbf{e}^T\mathbf{x} = \sum_z \left(\sum_{b\in\mathcal{B}_z} Q_b^z x_b^z - \sum_{o\in\mathcal{O}_z} Q_o^z x_o^z \right) = 0, \tag{3.4}$$

where $\mathbf{e} = \mathbf{1}^T\mathbf{E}$. The primal (market clearing) problem then reads

$$\begin{aligned} \max_{\mathbf{x}} & \sum_{z\in\mathcal{Z}} \left(\sum_{b\in\mathcal{B}_z} Q_b^z P_b^z x_b^z - \sum_{o\in\mathcal{O}_z} Q_o^z P_o^z x_o^z \right) = \mathbf{1}^T\mathbf{E}\mathrm{diag}(P)\mathbf{x} =: \overline{\mathbf{c}}^T\mathbf{x} \\ s.t. \quad & \mathbf{A}_E\mathbf{x} \le \mathbf{b}_p \quad : \quad (\boldsymbol{\gamma}) \\ & \mathbf{e}^T\mathbf{x} = 0 \quad : \quad (y) \\ & \mathbf{x} \le \mathbf{1} \quad : \quad (\mathbf{p}) \\ & \mathbf{x} \ge \mathbf{0}, \quad : \quad (\mathbf{w}) \end{aligned} \tag{MCM-0}$$

where $\mathbf{A}_E = \mathbf{M}_p\mathbf{E}$. This gives us the maximal social welfare, but note that the price is not determined at this point. To achieve this we solve the dual problem

$$\begin{aligned} \min_{y,\boldsymbol{\gamma},\mathbf{p}} & 0\cdot y + \mathbf{b}_p^T\boldsymbol{\gamma} + \mathbf{1}^T\mathbf{p}, \\ s.t. \quad & \mathbf{A}_E^T\boldsymbol{\gamma} + y\mathbf{e} + I(p-w) \ge \overline{\mathbf{c}}, \\ & \boldsymbol{\gamma} \ge \mathbf{0},\ \mathbf{p} \ge \mathbf{0},\ \mathbf{w} \ge \mathbf{0}, \end{aligned} \tag{Dual Problem}$$

and denote $\tilde{\mathbf{p}} = \mathbf{p} - \mathbf{w}$. Once the dual variables $\boldsymbol{\gamma}$ are known, we can impose the marginal transmission costs condition:

$$P_{z_i} - P_{z_j} = \sum_{k\in\mathcal{L}_{\mathrm{cne}}} \gamma_k(\mathrm{PTDF}_{k,z_j} - \mathrm{PTDF}_{k,z_i}), \quad j \ne i \tag{3.5}$$

where $\mathcal{L}_{\mathrm{cne}}$ is the critical branches set. In matrix form, if we let $\boldsymbol{\Omega}_Z \in \mathbb{R}^{|Z|(|Z|-1)/2\times|Z|}$ be the matrix that takes all the pairwise differences between entries in zones we can write

$$\boldsymbol{\Omega}_Z(\boldsymbol{\gamma}^T\mathbf{M}_p)^T = \boldsymbol{\Omega}_Z\boldsymbol{\Pi}, \tag{3.6}$$

where $\boldsymbol{\Pi}$ is the vector of zonal prices. Note that this equation is actually under-determined since many constraints are linear combinations of the others. Thus, to ensure a unique zonal price, the price in each zone is, in practice, required to be close to the average between the

lowest accepted bid and the highest accepted offer [78], such that we solve

$$\min_{\mathbf{\Pi}} \sum_{z} \left(\frac{P_O^z + P_B^z}{2} - \Pi_z \right)^2, \tag{3.7}$$

$$s.t. \quad \mathbf{\Omega}_Z (\boldsymbol{\gamma}^T \mathbf{M}_p)^T = \mathbf{\Omega}_Z \mathbf{\Pi}, \tag{3.8}$$

where P_O^z and P_B^z are the highest offer and lowest bid accepted for zone z, respectively.

3.2.1 Inelastic Demand

We now show that when the demand is inelastic, the optimal solution is guaranteed to be cleared at uniform zonal prices, and further, the marginal prices given by that welfare maximisation problem solve the minimisation problem (3.7) and (3.8), can be obtained by simply taking the maximum over marginal prices of accepted bids for each zone.

Theorem 3.2.1. *Let the social welfare maximisation problem, its dual and the pricing problem be defined as above. Then, given inelastic demand,* $\Pi_z^* = \max_{o \in \mathcal{O}_z} \{P_o^z : x_o^z > 0\}$ *is the optimal solution to the optimisation problem given by* (3.7) *and* (3.8)*, and* Π^* *is guaranteed to clear the market at for the optimal solution.*

Proof. Let P_O^z and P_B^z denote the maximum and minimum prices corresponding to accepted offers and bids respectively. Then, we have that by definition $P_O^z = \max_{o \in \mathcal{O}_z} \{P_o^z : x_o^z > 0\}$ and $P_B^z = \min_{b \in \mathcal{B}_z} \{P_B^z : x_b^z > 0\}$. But since the demand is inelastic, $P_B^z := P_O^z$. Thus, by definition $P_O^z = \Pi_z$ and so the objective function (3.7) has a value of zero, which is the minimum attainable value since this is a sum of squares.

We next show that constraint (3.8) is satisfied. Since the demand is inelastic, the objective function of the primal problem becomes:

$$SW(x_\cdot) = -\sum_{z \in \mathcal{Z}} \sum_{b \in \mathcal{O}_z} Q_o^z P_o^z x_o^z, \tag{3.9}$$

the flow feasibility constraint becomes

$$\mathbf{M}_p \mathbf{E}_o \mathbf{x}_o \leq \mathbf{b}_p + \mathbf{M}_p \mathbf{E}_b \mathbf{x}_b =: \overline{\mathbf{r}}, \tag{3.10}$$

and the supply and demand balance:

$$\mathbf{e}_o^T \mathbf{x}_o = \mathbf{e}_b^T \mathbf{x}_b, \tag{3.11}$$

where $\mathbf{x}_o = ||_v(\mathbf{x}_o^z)$ is the concatenation of all offers for all zones (and similar for $\mathbf{x}_b$). Note that since the demand is inelastic, $x_b^z = 1$ for all b and z and thus these are not variables. The lagrangian of the primal and dual is

$$L = -SW(\mathbf{x}_o) - \boldsymbol{\gamma}^T(\overline{\mathbf{r}} - \mathbf{M}_p\mathbf{E}_o\mathbf{x}_o) - y(\mathbf{e}_b^T\mathbf{x}_b - \mathbf{e}_o^T\mathbf{x}_o) - \mathbf{p}^T(\mathbf{1} - \mathbf{x}_o) - \mathbf{w}^T\mathbf{x}_o. \tag{3.12}$$

Taking the partial derivative w.r.t. every offer i and setting to zero, we get

$$\frac{\partial L}{\partial x_i} = -\frac{\partial SW}{\partial x_i} + \boldsymbol{\gamma}^T(\mathbf{M}_p\mathbf{E}_o)_{:,i} - yQ_i^z + \tilde{p}_i = 0, \tag{3.13}$$

where $\tilde{p}_i = p_i - w_i$. These are the optimality conditions for the social welfare maximisation problem. We note that $(\mathbf{A}\mathbf{E}_o)_{:,i} = \mathbf{A}(\mathbf{E}_o)_{:,i}$, and that by definition of $\mathbf{E}_o$, $(\mathbf{E}_o)_{z,i} = Q_i^z$ if $i \in \mathcal{O}_z$ and $(\mathbf{E}_o)_{z,i} = 0$ otherwise. There is exactly one such nonzero entry for every i since an offer can only be placed in exactly one zone. Thus

$$\boldsymbol{\gamma}^T\mathbf{M}_p(\mathbf{E}_o)_{:,i} = \boldsymbol{\gamma}^T(\mathbf{M}_p)_{:,z}Q_i^z. \tag{3.14}$$

Finally, by differentiation of the objective function SW we get

$$-\frac{\partial SW}{\partial x_i} = Q_i^z P_i^z. \tag{3.15}$$

By virtue of (3.13), (3.14) and (3.15) we get that

$$Q_i^z P_i^z + \boldsymbol{\gamma}^T(\mathbf{M}_p)_{:,z}Q_i^z - yQ_i^z + \tilde{p}_i = 0. \tag{3.16}$$

By simplifying Q_i^z (since $Q_i^z > 0$), we get

$$P_i^z = -\boldsymbol{\gamma}^T(\mathbf{M}_p)_{:,z} + y - \tilde{p}_i/Q_i^z, \tag{3.17}$$

and by taking the difference for the indices $i_z^* = \arg\max_{o\in\mathcal{O}_z}\{P_o^z : x_o^z > 0\}$, we get that

$$P_{i_{z_1}^*}^{z_1} - P_{i_{z_2}^*}^{z_2} = \boldsymbol{\gamma}^T((\mathbf{M}_p)_{:,z_2} - (\mathbf{M}_p)_{:,z_1}) + \tilde{p}_{i_{z_1}^*}/Q_{i_{z_1}^*}^{z_1} - \tilde{p}_{i_{z_2}^*}/Q_{i_{z_2}^*}^{z_2}, \tag{3.18}$$

We next prove that for the maximal indices $\tilde{p}_{i_{z_1}^*}, \tilde{p}_{i_{z_2}^*} = 0$. For any non-trivial quantities traded, it must be the case that $w_{i_{z_1}^*}, w_{i_{z_2}^*} = 0$, since the corresponding quantities must be nonzero. We are left to next prove that for the maximal indices $p_{i_{z_1}^*}, p_{i_{z_2}^*} = 0$ for any z_k.

Suppose that this is not true, and thus $p_{i_{z_1}^*} > 0$, and so by complementarity slackness $x_{i_{z_1}^*}^{z_1} = 1$. Consider the two options:

(a) assume there exists an $x_i^{z_1} \in (0,1)$. Then this must correspond to the maximal price, since the optimality can be obtained via a greedy solution. However, we have that $x_{i_{z_1}^*}^{z_1} = 1$, implying that $i_{z_1}^* \neq \arg\max_{o \in \mathcal{O}_{z_1}} \{P_o^{z_1} : x_o^{z_1} > 0\}$. We have reached a contradiction.

(b) The only other alternative is that $x_i^{z_1} \in \{0,1\}$ for all $i \in \mathcal{O}_{z_1}$. But then consider $x_{i_{z_1}^*}^{z_1} \leq r_{i_{z_1}^*}^{z_1} = 1$. We have that

$$\frac{\partial L}{\partial r_{i_{z_1}^*}^{z_1}} = p_{i_{z_1}^*}.$$

Increasing $r_{i_{z_1}^*}^{z_1}$ for $i_{z_1}^*$ will not change the solution since $x_i^{z_1} = 1$ for $\forall i \in \mathcal{O}_{z_1} \setminus \{i_{z_1}^*\}$, and $i_{z_1}^*$ is the player with the maximum price. Thus $0 = \frac{\partial L}{\partial r_{i_{z_1}^*}^{z_1}} = p_{i_{z_1}^*}$.

Thus,

$$P_{i_{z_1}^*}^{z_1} - P_{i_{z_2}^*}^{z_2} = \boldsymbol{\gamma}^T((\mathbf{M}_p)_{:,z_2} - (\mathbf{M}_p)_{:,z_1}). \tag{3.19}$$

But this always implies (3.8) since this system is obtained by collecting all the equations (3.19) for all the possible combinations $\{z_1, z_2\}$. Thus Π^* is feasible reaching minimum objective value: an optimal solution to the minimisation problem given by (3.7) and (3.8). Since the objective is (strictly) convex, and the best possible value is bounded below zero, the zero objective value can be attained at most at one point. But Π^* yields this value and thus it is the unique optimal solution.

Finally, we note that all bids are accepted by definition of the problem. Further, all the offers accepted in the social welfare maximisation problem must have $P_i^z \leq \max\{P_i^z : x_o^z\} =: \Pi_z^*$ and thus they are below the unique zonal price, meaning that they will not be rejected after price determination. □

Since we are not mainly concerned with market design, Theorem 3.2.1 gives us a way to easily compute the market price without requiring another layer of optimisation as required by (3.7) and (3.8).

3.2.2 A New Proposed Mechanism for Day Ahead Spot Market

For convenience, from this point on we let $x_i \in [0, Q_i]$ represent accepted quantity instead of the fraction accepted for the corresponding bid. As seen above, under the social welfare maximisation (SWM) problem with multiple zones and inter-zonal constraints, zonal price computation is greatly simplified by taking demand as inflexible. For this reason, we make the pragmatic assumption of purely inelastic demand. Throughout this work we propose a cost minimisation model as an alternative to the SWM one. While, as we show, the cost minimisation model we propose is equivalent to the SWM one for the case of one zone, M player game, with inflexible demand, and continuous quantity variables, no network constraints, and no capacity constraints, changing any of the previous assumptions renders

the models different in principle and in practice. Further, for the case of two or more zones, our generalisation of cost minimisation for multiple zones is novel, and we show that this is the correct generalisation of the stack model for multiple zones [37]. An example illustrating the difference with other cost minimisation models in the literature is given in Section **??**. Throughout the thesis, we consider a range of variations for the proposed Cost Minimisation

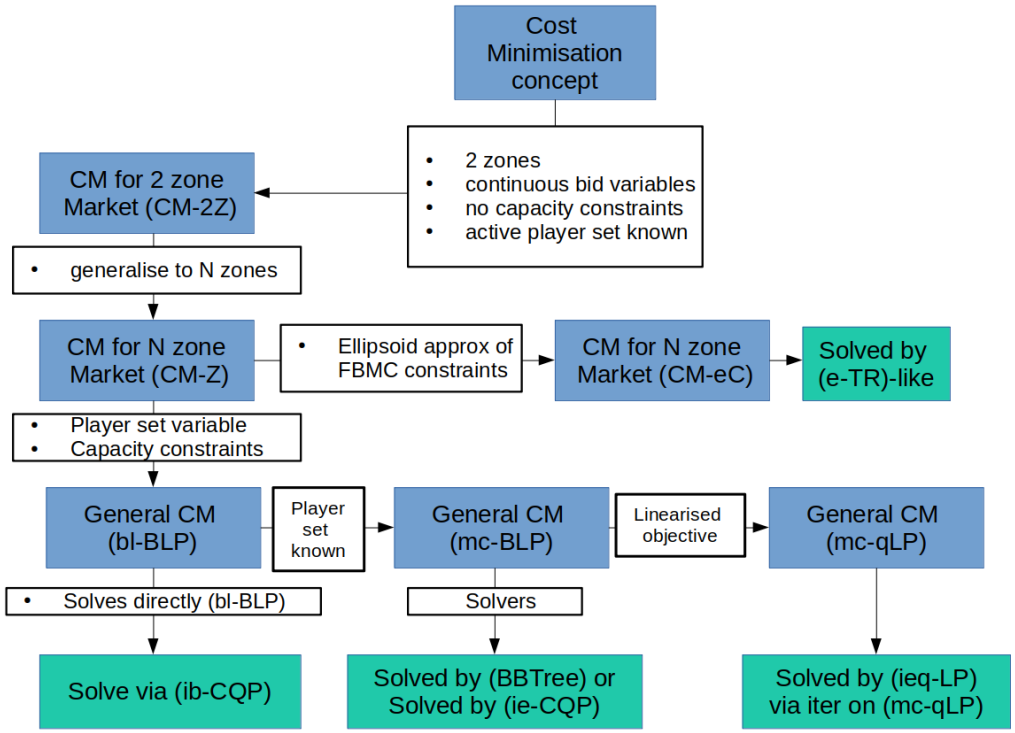


Figure 3.2: Variations of Cost Minimisation models considered. Richness and mathematical complexity is increased from top to bottom. Models are in blue while algorithms for solving them are in teal. White boxes explain changes between two linked model variations.

model, starting simple and building up complexity, and this is illustrated in Figure 3.2.

To simplify calculations, we employ a commonly used approach [85], [36], of considering a smooth offer (supply function) of the form $\lambda_i(x_i)$ where λ_i is the unit price required to produce x_i units of electricity. We make a commonly used simplification (as per [85], [41], [68], [38]), by parametrising the marginal asked price as $\lambda_i(x_i) = m_i x_i + a_i$ where $m_i, a_i \in \mathbb{R}^+$ are bidding constants chosen by player i. The Social Welfare Maximisation spot problem then reads

$$\begin{aligned} \min_x \sum_{i=\overline{1,M}} \int_0^{x_i} \lambda_i(\xi_i) d\xi_i &= \sum_{i=\overline{1,M}} \frac{1}{2} m_i x_i^2 + a_i x_i, \\ s.t. \sum_{i=\overline{1,M}} x_i = d \quad &: \quad (\gamma), \\ x_i \geq 0 \qquad\quad &: \quad (\theta_i), \quad \forall i, \end{aligned} \tag{SWM-1Z}$$

and the zonal price is given by $\rho_z = \rho := \max\{\lambda_i : x_i > 0\}$, since we considered a single zone. Another way to clear the market would be to minimise the total procurement cost of

electricity. This problem can be formulated as

$$\begin{aligned} &\min_x \rho \sum_i x_i = \rho d, \\ &s.t. \sum_{i \in \mathcal{P}} x_i = d, \ x_i \geq 0, \end{aligned} \tag{CM-1Z}$$

where ρ has the same definition as above, and since the demand level d is a constant, the problem is equivalent to price minimisation. However, this equivalence holds only for a zone market. We start by first showing that if the optimal active player sets $\mathcal{P}^{A,*}_{SWM} := \{i : x_i^{*,SWM} > 0\}$ and $\mathcal{P}^{A,*}_{CM} := \{i : x_i^{*,CM} > 0\}$ are the same, then (SWM-1Z) and (CM-1Z) have the same optimal solution. We then show that indeed that $\mathcal{P}^{A,*}_{SWM}$ and $\mathcal{P}^{A,*}_{CM}$ are identical.

Lemma 3.2.2. *Consider a one zone market with inflexible demand $d > 0$ and producer set $\mathcal{P}$. Assume that the submitted orders have $m_i > 0$ for all i, and that the optimal active sets $\mathcal{P}^{A,*}_{SWM} = \mathcal{P}^{A,*}_{CM} := \mathcal{P}^{A,*}$ are identical. Then, under the assumptions of no capacity and no network constraints employed in* (SWM-1Z) *and* (CM-1Z)*, the optimal solution of the two optimisation problems is the same, and is given by*

$$x_i^* = \frac{d + \sum_{j \in \mathcal{P}^{A,*} \setminus \{i\}} m_j^{-1}(a_j - a_i)}{m_i \sum_{j \in \mathcal{P}^{A,*}} \frac{1}{m_j}}, \ \ i \in \mathcal{P}^{A,*}, \tag{3.20}$$

and $x_i = 0$ if $i \notin \mathcal{P}^{A,*}$. Further, the marginal prices for any player in the active set $\mathcal{P}^{A,*}$ gives the zonal price, that is $\rho = \lambda_i = m_i x_i^* + a_i$.

Proof. Since we know $\mathcal{P}^{A,*}$, we can neglect all inequality constraints $x_i \geq 0$ and remove all indices $j \notin \mathcal{P}^{A,*}$ since all these players are irrelevant. Let us assume without loss of generality that player n belongs to $\mathcal{P}^{A,*}$. Problem (SWM-1Z) can be simplified by re-writing the balance constraint as $x_n = d - \sum_{i \in \mathcal{P} \setminus \{n\}} x_i$ and substituting this in the objective to yield

$$\begin{aligned} \min_{x_i : i \neq n} \sum_{i \in \mathcal{P}^{A,*} \setminus \{n\}} \left(\frac{1}{2} m_i x_i^2 + a_i x_i \right) + \frac{1}{2} m_n \left(d - \sum_{i \in \mathcal{P}^{A,*} \setminus \{n\}} x_i \right)^2 \\ + a_n \left(d - \sum_{i \in \mathcal{P}^{A,*} \setminus \{n\}} x_i \right) \end{aligned} \tag{3.21}$$

which is an unconstrained problem with one degree of freedom corresponding to x_n removed. We can set the gradient of this objective to zero to obtain the minimum. This gives us the

following system of equations

$$m_i x_i + a_i = m_n \left(d - \sum_{i \in \mathcal{P}^{A,*} \setminus \{n\}} x_i \right) + a_n \quad \forall i, \tag{3.22}$$

which tells us that at optimality the marginal price of all players with $x_i > 0$ is the same, and thus $\rho = \lambda_i = m_i x_i + a_i$, for all i for which $x_i > 0$. Now, given the optimal active set $\mathcal{P}^{A,*}$, (CM-1Z) is equivalent to

$$\begin{aligned} &\min_{x_i : i \in \mathcal{P}^{A,*}} \max_{i \in \mathcal{P}^{A,*}} \{m_i x_i + a_i\}, \\ &s.t. \sum_{i \in \mathcal{P}^{A,*}} x_i = d, \end{aligned} \tag{3.23}$$

and the minimum can only be achieved when there is indifference over the choice of player j from the $\mathcal{P}^{A,*}$ set, i.e. $m_j x_j + a_j = m_i x_i + a_i = \rho$, $\forall i \in \mathcal{P}^{A,*}$, $\forall j \in \mathcal{P}^{A,*}$, but this is equivalent to $\rho = \lambda_i = m_i x_i + a_i$, for all i for which $x_i > 0$, and thus both (SWM-1Z) and (CM-1Z) optimal solutions are given by solving this corresponding system, meaning that their solution is identical. System (3.22) can be solved by writing it as

$$\left(\hat{\mathbf{D}}_m + m_n \hat{\mathbf{e}} \hat{\mathbf{e}}^T \right) \hat{\mathbf{x}} = m_n d \hat{e} + a_n \hat{\mathbf{e}} - \hat{\mathbf{a}}, \tag{3.24}$$

where $\hat{\mathbf{x}}$, $\hat{\mathbf{a}}$, $\hat{\mathbf{m}}$ represent the vectors of quantities for all players except n, $\hat{e}$ is the vector of all ones of length $|\mathcal{P}| - 1$, and $\hat{\mathbf{D}}_m = diag(\hat{\mathbf{m}})$. This system is full rank since $m_i > 0$ $\forall i$, and an analytic solution can be obtained by applying Woodbury's matrix identity as an inversion formula which in this case leverages the diagonal structure of $\hat{\mathbf{D}}_m$ and the rank one of $\hat{\mathbf{e}}\hat{\mathbf{e}}^T$.

The optimal value of x_i for $i \neq n$ is then

$$x_i = \frac{d + \sum_{j \neq i} \frac{a_j - a_i}{m_j}}{m_i \sum_j \frac{1}{m_j}}. \tag{3.25}$$

However, the above equation does not contain n indices and there was no specific property of player n used in the derivation. Thus, by symmetry (3.25) holds for player n as well. □

Before proving the second part of the equivalence result, we need a simple lemma.

Lemma 3.2.3. *If $j \notin \mathcal{P}^A_{CM}$ but $a_j < \rho(\mathcal{P}^A_{CM})$, the solution of* (CM-1Z) *with this active set is not optimal.*

Proof. Assume that there exists such a j at optimality and that the solution is x. Then $\rho = m_i x_i + a_i$ for $i \in \mathcal{P}^A_{CM}$, but the point $\hat{x}$ defined as

$$\hat{x}_i = x_i - \frac{\Delta x}{|\mathcal{P}^A_{CM}|} > 0 \;\; x_j = \Delta x > 0, \tag{3.26}$$

satisfies the demand balance constraint and must be feasible for sufficiently small Δx. This point gives the price

$$\hat{\rho} = m_i \left(x_i - \frac{\Delta x}{|\mathcal{P}^A_{CM}|} \right) + a_i = \rho - \frac{\Delta x}{|\mathcal{P}^A_{CM}|} m_i < \rho, \tag{3.27}$$

which requires that $\lambda_j = m_j \Delta_x + a_j \leq \hat{\rho}$, and this is ensured for any $\Delta x \leq \frac{\rho - a_j}{m_j + m_i |\mathcal{P}^A_{CM}|^{-1}}$. Thus we have found an improvement to the initially claimed optimal solution, reaching the conclusion. □

Lemma 3.2.4. *The optimal active sets of* (SWM-1Z) *and* (CM-1Z) *are identical.*

Proof. The KKT conditions (see [44]) of (SWM-1Z) are

$$\begin{aligned} & m_i x_i + a_i - \gamma - \theta_i = 0, \; \forall i, \\ & \theta_i x_i = 0; \;\; \theta_i \geq 0; \;\; x_i \geq 0, \\ & \sum_i x_i = d. \end{aligned} \tag{3.28}$$

Let $\mathcal{P}^{A,*}_{SWM}$ be the optimal active set. Then

$$\forall i \in \mathcal{P}^{A,*}_{SWM} \implies x_i > 0 \implies \theta_i = 0 \implies m_i x_i + a_i = \gamma, \tag{3.29}$$

and thus $\gamma = \rho$ is the actual clearing price. Now, for any $j \notin \mathcal{P}^{A,*}_{SWM}$, we have that

$$j \notin \mathcal{P}^{A,*}_{SWM} \implies x_j = 0 \implies a_j - \lambda_j = \gamma > 0 \, (\text{since } m_j > 0, a_j > 0) \implies a_j \geq \gamma = \rho. \tag{3.30}$$

Thus, (3.29) and (3.30) give us that

$$x_i > 0 \Leftrightarrow a_i < \gamma = \rho^*(SWM), \tag{3.31}$$

$$x_i = 0 \Leftrightarrow a_j \geq \rho^*(SWM). \tag{3.32}$$

The rest of the proof is by contradiction and uses (3.31) and (3.32). Let us assume that $\mathcal{P}^{A,*}_{SWM} \neq \mathcal{P}^{A,*}_{CM}$. Then either (i) $\mathcal{P}^{A,*}_{CM} = \mathcal{P}^{A,*}_{SWM} \backslash \mathcal{P}'$ for some $\mathcal{P}' \neq \emptyset$ or (ii) $\mathcal{P}^{A,*}_{CM} = \mathcal{P}^{A,*}_{SWM} \cup \mathcal{P}'$

for some $\mathcal{P}' \neq \emptyset$. Consider (i), then the $m_i x_i + a_i = \rho^*_{CM}$ for all $i \in \mathcal{P}^{A,*}_{CM}$, but then there exists $j \in \mathcal{P}'$ such that

$$a_j < \rho^*(SWM) = \rho^*(CM; \mathcal{P}^{A,*}_{SWM}) \leq \rho^*(CM; \mathcal{P}^{A,*}_{CM}), \tag{3.33}$$

where the first inequality holds by (3.31), the equality holds by Lemma 3.2.2, and the last inequality holds since $a_j < \rho^*(CM; \mathcal{P}^{A,*}_{SWMM})$ and thus by the proof of Lemma 3.2.3 setting $x_j = 0$ cannot reduce $\rho^*(CM)$. Thus we have that $a_j < \rho^*(CM; \mathcal{P}^{A,*}_{CM})$ and thus by Lemma 3.2.3, the set $\mathcal{P}^{A,*}_{CM}$ cannot be optimal. We have reached a contradiction.

Now consider that (ii) $\mathcal{P}^{A,*}_{CM} = \mathcal{P}^{A,*}_{SWM} \cup \mathcal{P}'$, but then

$$\begin{aligned}
\rho^*_{CM} &= \max_{i \in \mathcal{P}^{A,*}_{CM}} m_i x_i + a_i = \max\{ \max_{i \in \mathcal{P}^{A,*}_{SWM}} m_i x_i + a_i, \max_{i \in \mathcal{P}'} m_i x_i + a_i \} \\
&> \max\{ \max_{i \in \mathcal{P}^{A,*}_{SWM}} m_i x_i + a_i, \max_{i \in \mathcal{P}'} a_i \} \\
&> \max_{i \in \mathcal{P}'} a_i > \rho^*(SWM) = \rho^*(SWM; \mathcal{P}^{A,*}_{SWM})
\end{aligned} \quad , \tag{3.34}$$

where the first equality holds by definition of $\mathcal{P}^{A,*}_{CM}$, the first inequality is due to $m_i > 0$, $x_i > 0$, the second inequality is by taking the maximum over a smaller set, and the last inequality is by the fact that $\mathcal{P}'$ is part of the inactive set at optimality for (SWM-1Z) and by (3.32).

Therefore, $\rho^*_{CM} > \rho^*(SWM; \mathcal{P}^{A,*}_{SWM})$, meaning that $\mathcal{P}^{A,*}_{CM} = \mathcal{P}^{A,*}_{SWM} \cup \mathcal{P}'$ cannot be the optimal set so long as $\mathcal{P}' \neq \emptyset$. Thus, it has to be that $\mathcal{P}^{A,*}_{CM} = \mathcal{P}^{A,*}_{SWM}$. □

We are now ready to state the final theorem showing equivalence of (SWM-1Z) and (CM-1Z).

Theorem 3.2.5. *Consider a one zone market with inflexible demand $d > 0$ and producer set $\mathcal{P}$ with submitted orders having $a_i > 0$, $m_i > 0$ for all i. Then, under the assumptions of no capacity and no network constraints employed in* (SWM-1Z) *and* (CM-1Z)*, the optimal solution of the two optimisation problems is the same, and is given by*

$$x^*_i = \frac{d + \sum_{j \in \mathcal{P}^{A,*} \setminus \{i\}} m_j^{-1}(a_j - a_i)}{m_i \sum_{j \in \mathcal{P}^{A,*}} \frac{1}{m_j}}, \;\; i \in \mathcal{P}^{A,*}, \tag{3.35}$$

and $x_i = 0$ if $i \notin \mathcal{P}^{A,*}$. Further, the marginal prices for any player in the active set $\mathcal{P}^{A,*}$ sets the zonal price, that is $\rho = \lambda_i = m_i x^*_i + a_i$.

Proof. By using Lemma 3.2.4, we obtain that the optimal active sets of (SWM-1Z) and (CM-1Z) are identical. By then applying Lemma 3.2.2, we obtain the desired result. □

We note that while Theorem 3.2.5 proves equivalence of the optimal solution of the two clearing mechanisms for a (simplified) one-zone market, this does not generalise to more general setups and to multiple-zones market. This is easy to show numerically and will be examined in detail in the numerical results section. However, the equivalence for the one-zone market suggests at least two ways to generalise the market clearing to multiple zones: (i) based on the Social Welfare Maximisation (SWM) view, and (ii) based on the Cost Minimisation (CM) view. The current market clearing mechanism used in the European markets uses the former, but we here focus the latter approach, the solution to more general such clearing mechanisms, and illustrate some possible benefits. Further, we consider the former approach for comparison. We also point out that the equivalence result is a consequence of allowing for clearing any desired fraction of the order book quantities.

3.3 A Cost Minimisation Two-Zone Market Model

While the concept of cost minimisation is well known and was studied extensively before (eg. see [64] or [5]), we introduce a novel type of consumer payment cost minimisation approach, that accounts for the true cost paid by the consumer as opposed to some form of approximated cost. The exact representation comes at increased mathematical complexity. To the best of author's knowledge this formulation is novel at least in the context of day ahead electricity markets with Zonal Marginal Pricing with Flow Based Market Coupling constraints. Further, analytic result in Section 3.5.2.4 reveal that the introduced cost minimisation approach is in fact the correct generalisation of the stack model for multiple zones [37]. Let us look at Example 3.3.1 to better understand the subtleties of our novelty.

Example 3.3.1. *Consider the following market setup, with the demand taken as inflexible as show in Figure 3.3. Consider the feasible solution* $x_1 = 4.5$ *and* $x_2 = 10.5$*, and let us*

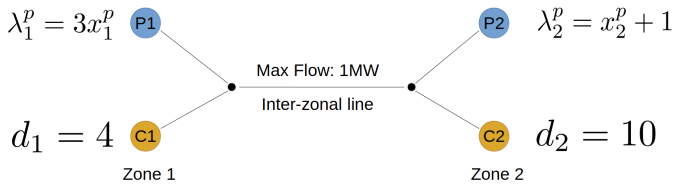


Figure 3.3: Market setup with inflexible demand.

compute the apparent cost paid by the demand, $C_a = \lambda_1 d_1 + \lambda_2 d_2 = 54 + 115 = 169$*. However, by balance of payments, the demand has to fully cover the compensation to suppliers which is* $C_r = \lambda_1 x_1 + \lambda_2 x_2 = 60.75 + 120.75 = 181.5$*, and this is the real cost that the consumers have to ultimately pay. We can see that the two costs are different, and this is generally the case so long as there are inter-zonal trading, since the zonal clearing price is unique, and the only way for the zonal costs based on demand and supply quantities to be equal for a zone is to have zero net exports. Further, the optimal solutions with the two objectives are*

$x_1^a = 3$, $x_2^a = 11$, $C_a^{*,a} = 146$, $C_r^{*,a} = 159$, *for the apparent cost as objective, and* $x_1^r = 3.625$, $x_2^a = 10.375$, $C_a^{*,r} = 157.25$, $C_r^{*,r} = 157.4375$ *for the true cost. The two solutions and the corresponding costs are different, meaning that even at optimality there is generally no equivalence.*

In contrast to the literature on cost minimisation that considers costs of the type C_a [64], we here consider the true cost that has to be paid by the consumers. While for markets with Locational Marginal Pricing with Optimum Power Flow the Social Welfare objective becomes the true cost under inflexible demand, this does not hold for Zonal Marginal Pricing since the price is always the maximum of the marginal prices in the zone, revealing another structural difference between ZMP and LMP. Thus for the case of Zonal Marginal Pricing, the cost objective we propose is novel and is neither a particular case of the usual Social Welfare objective, nor the apparent cost frequently used in other work [64]. Instead, as we show in sub-section 3.5.2 it is a natural generalisation of the usual stack model for one zone [37], which is essentially a cost minimisation model. If integer constraints of fill-or-kill type are imposed, a fundamental difference between the Cost Minimisation and Social Welfare maximisation objectives is revealed, as shown in Example 3.3.2

Example 3.3.2. *Consider the two order books shown in Figure 3.4. We can compute the*

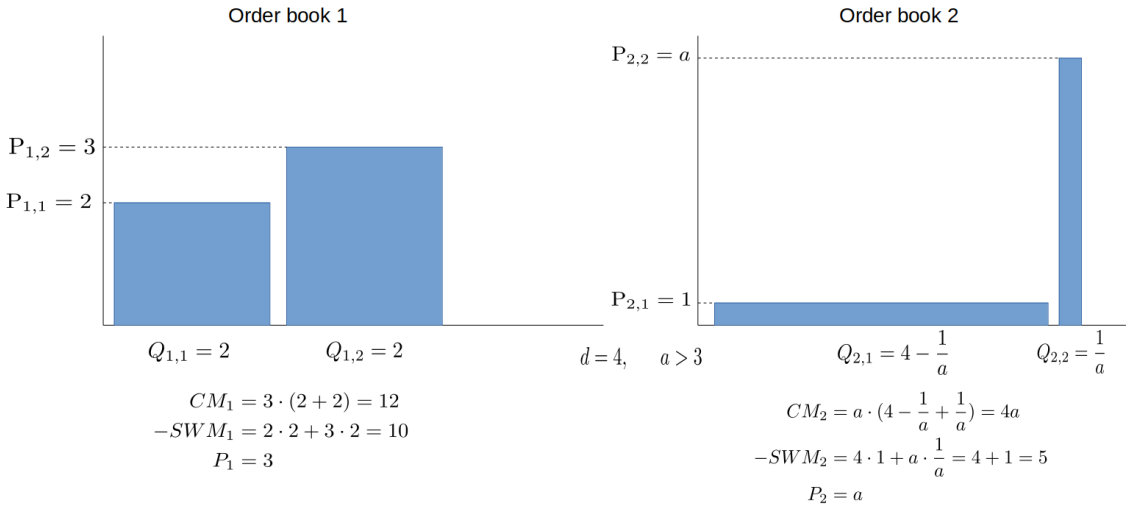


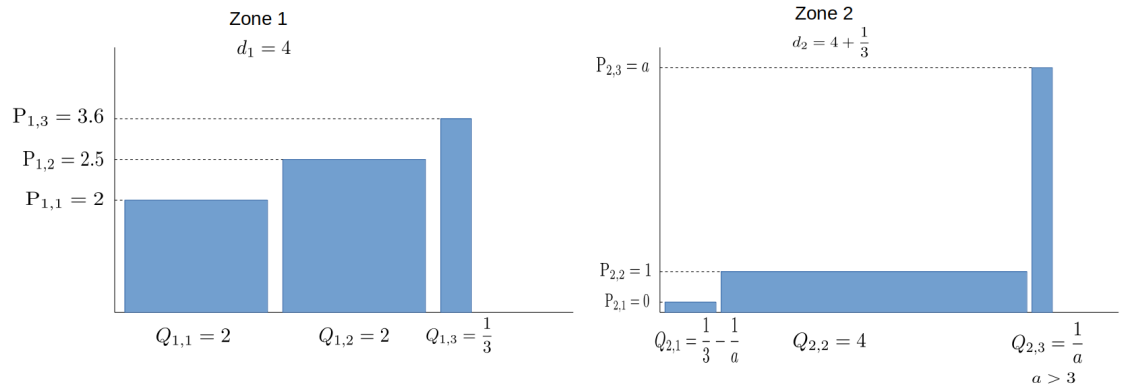
Figure 3.4: Order books of offers: optimal choices based on SWM and CM. Note that we compute the negative of SWM objective such that the optimal solution is obtained by minimisation, consistent with CM.

CM and SWM objective for each of the two order books, and conclude that the CM objective chooses Order book 1 as optimal, while SWM chooses Order book 2. We can clearly see that SWM chooses Order book 2 for any value of a. Thus, a, which is also the clearing price for Order book 2, can be taken as arbitrarily large and Order book 2 still remains optimal for SWM. This is clearly an undesirable effect, and it points to an inconsistency that the objective has with respect to the pricing scheme: the order book may be altered in such a way

that the SWM objective may not change at all, albeit the price may change arbitrarily much, which can be seen by swiping the value of a from 3 to plus infinity. On the other hand, the preference of CM objective is determined by area of the rectangle defined by the highest clearing price and the total volume actually cleared at that price. Thus, by definition of the CM objective, the clearing price and objective cannot change independently of one another, and they are in fact increasing functions of each other.

Example 3.3.3 shows how this preference over order books could translate to a real world scenario where all orders are fill-or-kill.

Example 3.3.3. *Consider a market with two zones,all orders submitted as fill or kill and network constraints that allow for a flow of* $\frac{1}{3}$ *between the two zones. We can see that the*



$$\text{solution 1 :}(x_{1,1} = 2, x_{1,2} = 2, x_{1,3} = 0) \ , P_1 = 2.5 \ , \qquad CM_1 = 10 + 4.33a > 23$$
$$(x_{2,1} = \frac{1}{3} - \frac{1}{a}, x_{2,2} = 4 - \frac{1}{a}, x_{2,3} = \frac{1}{a}) \ , P_2 = a \qquad -SWM_1 = 14 - \frac{1}{a} < 14$$
$$\text{solution 2 :}(x_{1,1} = 2, x_{1,2} = 2, x_{1,3} = \frac{1}{3}) \ , P_1 = 3.6 \ , \qquad CM_2 = 19.6 - \frac{1}{a} < CM_1$$
$$(x_{2,1} = 0, x_{2,2} = 4, x_{2,3} = 0) \ , P_2 = 1 \qquad -SWM_2 = 14.2 > -SWM_1$$

Figure 3.5: Example of market clearing for fill-or-kill orders based on CM and SWM

solution chosen by CM is $(x_{1,1} = 2, x_{1,2} = 2, x_{1,3} = \frac{1}{3})$ *and* $(x_{2,1} = 4, x_{2,2} = 0)$ *while SWM chooses* $(x_{1,1} = 2, x_{1,2} = 2, x_{1,3} = 0)$ *and* $(x_{2,1} = 4, x_{2,2} = \frac{1}{a})$*, for any* $a > 3$*. However, again the value of a, which is also the price in zone 2, can be arbitrarily large. Relaxing the integrality constraints would indeed resolve this problem and the two objectives would in this case converge to the same solution. Note that if Locational Marginal Pricing was used, the solution provided by the SWM is sensible, since the total cost does not explode with the value of a, and is in fact less than for solution 1.*

While it is true that Euphemia has heuristics to deal with this type of issues, for example by first relaxing the integrality constraints, we believe that using an objective that naturally and seamlessly guarantees to resolve this problem is desirable, and for this reason we propose a novel generalisation of cost minimisation to multiple zones in this thesis. Note however, that we do not observe these effects in the framework of our work, because we do not consider fill-or-kill types of orders. This is because solving the proposed CM model is

already challenging even when excluding integer constraints such as fill-or-kill or block bids. Nevertheless, we believe that this work could lay the foundation for clearing the market in practice via our proposed Cost Minimisation objective.

To gradually build up complexity, we start by considering a market with two zones, inflexible demand, and the objective of cost minimisation. Since the demand is inflexible, the zonal production levels y_1 and y_2 must satisfy

$$y_1 + y_2 = d_1 + d_2 = d, \tag{3.36}$$

where d_1 and d_2 are the demand levels in the two zones and d the total demand. The line-zonal PTDF constraints have the general form

$$\mathbf{q}_1 y_1 + \mathbf{q}_2 y_2 \leq \mathbf{r}_L, \tag{3.37}$$

where $\mathbf{q}_1$, $\mathbf{q}_2$ and $\mathbf{r}_L$ can be very high dimensional vectors. However, since we take the intersection of a line (equation (3.36)) with a 2D polytope ((3.37)), the polytope constraints can be simplified without loss of generality to

$$r_{LB} \leq y_1 - y_2 + d_2 - d_1 \leq r_{UB}, \tag{3.38}$$

for some r_{LB}, r_{UB} with $r_{LB} < r_{UB}$. We only make the simplifying assumption that $r_{LB} = -r_{UB} = -r$ (constraint symmetry), but this has no bearing on the solution procedure, although it allows for more compact notation and equations. We start with this simple model because as we shall see, it allows us to analytically track the impact of any bid on the auction solution: zonal prices and quantities allocated. As before, we assume that player i offers production level x_i for a price per unit λ_i, of the type $\lambda_i = m_i x_i + a_i$. The producer set in zone one and zone two are $\mathcal{Z}_1$ and $\mathcal{Z}_2$ respectively. The DAA solution given fixed bids, is independent of the cost structure of each player, and thus this is defined when we discussing players' strategies and the interaction between players. The market clearing problem then

reads

$$\begin{aligned}
&\min_{\mathbf{x}^T=(\mathbf{x}_1^T,\mathbf{x}_2^T)} \rho_1 y_1 + \rho_2 y_2, \\
&\quad s.t. \quad y_1 + y_2 = d_1 + d_2, \\
&\qquad\quad 1^T\mathbf{x}_1 = y_1; \quad 1^T\mathbf{x}_2 = y_2, \\
&\qquad\quad \rho_1 = \max_{i\in\mathcal{Z}_1} \left\{\lambda_i^1\left((\mathbf{x}_1)_i\right) : (\mathbf{x}_1)_i > 0\right\}, \\
&\qquad\quad \rho_2 = \max_{j\in\mathcal{Z}_2} \left\{\lambda_j^2\left((\mathbf{x}_2)_j\right) : (\mathbf{x}_2)_j > 0\right\}, \\
&\qquad\quad -r \le y_1 - y_2 + d_2 - d_1 \le r,
\end{aligned} \tag{CM-2Z}$$

where $y_1 \in \mathbb{R}_+$ and $y_2 \in \mathbb{R}_+$ are the total production level per zone, and $\mathbf{x}_1 \in \mathbb{R}^{n_1}$ and $\mathbf{x}_2 \in \mathbb{R}^{n_2}$ are the vectors of quantity allocated to each producer in zone 1 and zone 2 respectively. Demand levels per zone are given by d_1 and d_2 and the total imbalance of net production has to be bounded by r. This amounts to having a single line between the two zones, with capacity $2r$. The zonal prices ρ_1 and ρ_2 are given by the first marginal prices, that is, the price for the last unit of power dispatched in each zone. The value $\lambda_i^1\left((\mathbf{x}_1)_i\right)$ represents the price that player i from zone 1 charges currently for generating its power level $(\mathbf{x}_1)_i$. Note that players do not choose their production levels, or selling price, but only the bidding strategy (m_i, a_i), representing their supply function.

We solve the optimisation problem analytically in two steps: (i) first assume that y_1 and y_2 are fixed, and compute the optimal allocations $\mathbf{x}_1^*$ and $\mathbf{x}_2^*$, and (ii) find the optimal zonal productions y_1 and y_2 knowing their corresponding optimal allocations $\mathbf{x}_1^*$ and $\mathbf{x}_2^*$.

Let us now assume that y_1 and y_2 are fixed. Then the problem decouples for the two zones, and we have to find $\mathbf{x}_1$ such that ρ_1 is minimum, and $\mathbf{x}_2$ such that ρ_2 is minimum. Without loss of generality, we focus on zone 1, and by symmetry we then obtain the result for zone 2 as well. The resulting optimisation problem for zone 1 reads

$$\begin{aligned}
&\min_{x_1} \max_{i\in\mathcal{Z}_1} \left\{\lambda_i^1\left((\mathbf{x}_1)_i\right) : (\mathbf{x}_1)_i > 0\right\}, \\
&s.t. \quad 1^T\mathbf{x}_1 = y_1,
\end{aligned} \tag{CM-Z_1}$$

but we have seen this problem before. This is the CM problem and can be easily solved if we assume that the active player set $\mathcal{P}_z^A$ is known, i.e. that all the players have $(\mathbf{x}_1)_i > 0$, else they do not participate in the auction, and can be removed. The *"min player"* can achieve optimality only if it makes the *"max player"* indifferent amongst its choices, and thus we require that $\lambda_i^1\left((\mathbf{x}_1)_i\right) = \rho_1$ for all i. By using $\mathbf{1}^T\mathbf{x}_1 = y_1$ to eliminate $(\mathbf{x}_1)_{n_1}$ we obtain the linear system of equations

$$(\mathrm{diag}(\hat{\mathbf{m}}_1) + m_{n_1}\mathbf{1}\mathbf{1}^T)\hat{\mathbf{x}}_1 = m_{n_1} y_1 \mathbf{1} - \hat{a}_1 + a_{n_1}\mathbf{1}, \tag{3.39}$$

and by making use of Woodbury's inversion identity we obtain once more that

$$\hat{\mathbf{x}}_1^* = \left(\text{diag}(\hat{\mathbf{v}}_{m_1}) - \frac{m_{n_1}\hat{\mathbf{v}}_{m_1}\hat{\mathbf{v}}_{m_1}^T}{1 + m_{n_1}\hat{\mathbf{v}}_{m_1}^T\mathbf{1}}\right)(m_{n_1}y_1\mathbf{1} - \hat{a}_1 + a_{n_1}\mathbf{1}). \tag{3.40}$$

where $\hat{\mathbf{a}}_1^T = (a_1, a_2, ...a_{n_1-1})$, $\hat{\mathbf{m}}_1^T = (m_1, m_2, ...m_{n_1-1})$, $\hat{\mathbf{v}}_{m_1}^T = (m_1^{-1}, m_2^{-1}, ...m_{n_1-1}^{-1})$, and $\hat{\mathbf{x}}_1^T = (x_1, x_2, ...x_{n_1-1})$ are the corresponding quantities for zone 1, excluding the last player. Finally, since $(\mathbf{x}_1)_{n_1} = y_1 - 1^T\hat{\mathbf{x}}_1$, by performing algebraic calculations we obtain

$$\mathbf{x}_1^* = \frac{y_1 + \mathbf{v}_{m_1}^T\mathbf{a}_1}{\mathbf{1}^T\mathbf{v}_{m_1}}\mathbf{v}_{m_1} - \text{diag}(\mathbf{v}_{m_1})\mathbf{a}_1, \tag{3.41}$$

where the lack of hats represents inclusion of the n_1 element, and the result confirms player symmetry. By replacing the zonal indices an equivalent expression for zone 2 is obtained.

To find y_1, we must first understand the impact of y_1 under optimal distribution $\mathbf{x}_1^*$. To do this, we note that since $\lambda_i^1((\mathbf{x}_1)_i) = \rho_1$, then $\rho_1 = (n_1 - 1)^{-1}\sum_{i=1}^{n_1-1}\lambda_i^1((\mathbf{x}_1)_i)$ and therefore

$$\rho_1 = \frac{1}{n_1 - 1}\mathbf{1}^T(\text{diag}(\hat{\mathbf{m}}_1)\hat{\mathbf{x}}_1^* + \hat{\mathbf{a}}_1) = \frac{1}{n_1 - 1}\left(\hat{\mathbf{m}}_1^T\hat{\mathbf{x}}_1^* + \mathbf{1}^T\hat{\mathbf{a}}_1\right) \tag{3.42}$$

$$= \hat{\alpha}_1(\mathbf{m}_1)y_1 + \hat{\beta}_1(\mathbf{m}_1, \mathbf{a}_1), \tag{3.43}$$

and the coefficients $\hat{\alpha}_z(\mathbf{m}_z)$ and $\hat{\beta}_z(\mathbf{m}_z, \mathbf{a}_z)$ depend only on the strategies $(\mathbf{m}_z, \mathbf{a}_z)$, expressed as

$$\hat{\alpha}_1(\mathbf{m}_1) = \frac{m_{n_1}}{1 + m_{n_1}\hat{\mathbf{v}}_{m_1}^T\mathbf{1}} = \frac{1}{\mathbf{1}^T\mathbf{v}_{m_1}}, \tag{3.44}$$

$$\hat{\beta}_1(\mathbf{m}_1, \mathbf{a}_1) = \frac{a_{n_1}}{1 + m_{n_1}\hat{\mathbf{v}}_{m_1}^T\mathbf{1}} + \frac{m_{n_1}\hat{\mathbf{v}}_m^T\hat{\mathbf{a}}_1}{1 + m_{n_1}\hat{\mathbf{v}}_{m_1}^T\mathbf{1}} = \frac{\mathbf{a}_1^T\mathbf{v}_{m_1}}{\mathbf{1}^T\mathbf{v}_{m_1}}. \tag{3.45}$$

It is a rather remarkable result that given all players in zone 1 submit linear bids of the type $\lambda_i = m_i x_i + a_i$, then the zonal price ρ_1 is also a linear function with respect to the total produced quantity y_1, with coefficients $\hat{\alpha}_1(\mathbf{m}_1)$ and $\hat{\beta}_1(\mathbf{m}_1, \mathbf{a}_1)$ that depend purely on the strategies of each player. Further, ρ_1 does not depend on the explicit distribution of $\mathbf{x}_1^*$. Now that we understand the impact of y_1 on price, we can solve the outer optimisation

problem for y_1 and y_2 which is simply

$$\min_{y_1,y_2} \hat{\alpha}_1(\mathbf{m}_1)y_1^2 + \hat{\beta}_1(\mathbf{m}_1,\mathbf{a}_1)y_1 + \hat{\alpha}_2(\mathbf{m}_2)y_2^2 + \hat{\beta}_2(\mathbf{m}_2,\mathbf{a}_2)y_2 \tag{3.46}$$

$$s.t. \quad y_1 + y_2 = d_1 + d_2, \tag{3.47}$$

$$-r \leq y_1 - y_2 - d_1 + d_2 \leq r. \tag{3.48}$$

The main difficulty of solving this problem comes from the inequality constraint. Let us start by solving the problem assuming that the inequality constraint is inactive. This is a problem that we have solved before, and as in (3.25) we have that

$$y_1^I = \frac{\hat{\beta}_2(\mathbf{m}_2,\mathbf{a}_2) - \hat{\beta}_1(\mathbf{m}_1,\mathbf{a}_1) + 2\hat{\alpha}_2(\mathbf{m}_2)(d_1+d_2)}{2(\hat{\alpha}_1(\mathbf{m}_1) + \hat{\alpha}_2(\mathbf{m}_2))}, \tag{3.49}$$

where the superscript I refers to the solution in the case of unconstrained inter-zonal flows. For the problem to be unconstrained, we need

$$r \geq r^* = |2y_1 - 2d_1| = \frac{|\hat{\beta}_2 - \hat{\beta}_1 + 2(\hat{\alpha}_2 d_2 - \hat{\alpha}_1 d_1)|}{\hat{\alpha}_1 + \hat{\alpha}_2}, \tag{3.50}$$

where the right hand side is the absolute value of twice the inter-zonal flow $y_1 - y_2 - d_1 + d_2 = 2y_1 - 2d_1$. If $r \geq r^*$, then the problem is essentially unconstrained since the maximum capacity that can be transferred between zones is higher than the flow between zones at optimality. If the solution is not unconstrained, then it must be constrained and therefore $2y_1 - 2d_1 = r$ or $2y_1 - 2d_1 = -r$. This gives us that

$$\frac{\partial y_1}{\partial r} = \pm\frac{1}{2}, \tag{3.51}$$

and thus y_1 is a linear function of r, so long as $r < r^*$. All we need to ask now is what is the solution when $r = 0$. This is easy to solve since we then must have that

$$y_1 + y_2 = d_1 + d_2, \tag{3.52}$$

$$y_1 - y_2 = d_1 - d_2, \tag{3.53}$$

which gives the obvious solution that $y_1^{II} = d_1$ and $y_2^{II} = d_2$ since no inter-zonal flow is allowed. All we need to do is to recognise that for $r \leq r^*$

$$y_1 = \frac{r y_1^I + (r^* - r)y_1^{II}}{r^*}. \tag{3.54}$$

Thus, we are done since we already know the solution for $r \geq r^*$ and then y_1 can be expressed compactly as

$$y_1 = \begin{cases} \frac{\hat{\beta}_2 - \hat{\beta}_1 + 2\hat{\alpha}_2(d_1+d_2)}{2(\hat{\alpha}_1+\hat{\alpha}_2)}, & r \geq \frac{|\hat{\beta}_2 - \hat{\beta}_1 + 2(\hat{\alpha}_2 d_2 - \hat{\alpha}_1 d_1)|}{\hat{\alpha}_1+\hat{\alpha}_2} \\ \frac{\hat{\beta}_2 - \hat{\beta}_1 + 2(\hat{\alpha}_2 d_2 - \hat{\alpha}_1 d_1)}{2|\hat{\beta}_2 - \hat{\beta}_1 + 2(\hat{\alpha}_2 d_2 - \hat{\alpha}_1 d_1)|} r + d_1, & 0 \leq r \leq \frac{|\hat{\beta}_2 - \hat{\beta}_1 + 2(\hat{\alpha}_2 d_2 - \hat{\alpha}_1 d_1)|}{\hat{\alpha}_1+\hat{\alpha}_2} \end{cases}. \tag{3.55}$$

A similar expression can be obtained for y_2 by swapping the indices for zone 1 and zone 2.

$$y_2 = \begin{cases} \frac{\hat{\beta}_1 - \hat{\beta}_2 + 2\hat{\alpha}_1(d_1+d_2)}{2(\hat{\alpha}_1+\hat{\alpha}_2)}, & r \geq \frac{|\hat{\beta}_1 - \hat{\beta}_2 + 2(\hat{\alpha}_1 d_1 - \hat{\alpha}_2 d_2)|}{\hat{\alpha}_1+\hat{\alpha}_2} \\ \frac{\hat{\beta}_1 - \hat{\beta}_2 + 2(\hat{\alpha}_1 d_1 - \hat{\alpha}_2 d_2)}{2|\hat{\beta}_1 - \hat{\beta}_2 + 2(\hat{\alpha}_1 d_1 - \hat{\alpha}_2 d_2)|} r + d_2, & 0 \leq r \leq \frac{|\hat{\beta}_1 - \hat{\beta}_2 + 2(\hat{\alpha}_1 d_1 - \hat{\alpha}_2 d_2)|}{\hat{\alpha}_1+\hat{\alpha}_2} \end{cases}. \tag{3.56}$$

Note that $y_1 = y_1(\mathbf{m}_1, \mathbf{a}_1, \mathbf{m}_2, \mathbf{a}_2, r, d_2, d_1)$ and $y_2 = y_2(\mathbf{m}_2, \mathbf{a}_2, \mathbf{m}_1, \mathbf{a}_1, r, d_2, d_1)$, and thus the optimal production level in each zone also depends on the bids in the other zone, at least so long as $r > 0$. Thus, for a fixed $(\mathbf{m}_1, \mathbf{a}_1, \mathbf{m}_2, \mathbf{a}_2)$ strategy profile, margin r and demands d_1 and d_2 we can compute the optimal zonal production levels y_1, y_2 via (3.55) and (3.56), after which we can compute ρ_1 and ρ_2 by (3.43) and $\mathbf{x}_1$ and $\mathbf{x}_2$ by (3.41). The Spot Auction is now fully solved for the input $(\mathbf{m}_1, \mathbf{a}_1, \mathbf{m}_2, \mathbf{a}_2, r, d_1, d_2)$. The final step is to analyse players' interaction, given that they know the impact on the Spot Auction result of every other players' bid, demand levels, and transmission margin.

3.3.1 A Game Theoretic Resolution of the Spot Auction

To use the market clearing mechanism for analysis in practice, the submitted bids have to be known. However, these are not available for most markets, including European ones. As a result, it is often assumed that market participants place orders that fully represent their true costs, and this is known as truthful bidding (TB). However, market orders are each participant's choice and need not be given exclusively by the cost structure. Since each player has its own interest, they may consider bidding strategically instead. The TB assumptions may not be appropriate if the market mechanism does not incentivise players to bid truthfully, and this is not a guaranteed property [54]. In fact, achieving this and other desirable properties is a challenging auction design task [54], [62], [40]. For this reason, considering strategic bidding offers a more descriptive model of the electricity spot market. Using a game-theoretic framework, we analyse the case when players bid strategically to maximise their own profit knowing the market clearing mechanism, here given by (CM-2Z). We assume complete information for simplicity, which means that players know exactly the cost structure of all the players, as well as d_1, d_2 and r. We next consider the producers.

Each player tries to choose their strategies (m_i, a_i) such that the profits Π_i are maximised. Again, without loss of generality, we look at a producer from zone 1, and the problem reads

$$\max_{m_i, a_i} \rho_1(\mathbf{x}_1)_i - C\left((\mathbf{x}_1)_i\right), \tag{3.57}$$

where glstld:Costi$((\mathbf{x}_1)_i)$ is the cost for producing $(\mathbf{x}_1)_i$ units of electricity, which for simplicity we denote as x_i. Any continuous, monotonically increasing cost function can be used in this framework but for simplicity we assume that

$$C_i(x_i) = \frac{1}{2} c_i x_i^2 + b_i x_i, \tag{3.58}$$

which is commonly used in related literature [38], [36], [85]. The particular choice of the cost function does not change the general form of the system of equations that characterises the Nash Equlibria (which we obtain later), but it changes the solution to this system. For simplicity of notation we drop the sub- and super-scripts corresponding to zones, and this becomes implicit in the player index i.

We use the Nash Equilibria solution concept to solve the game, and we are only considering pure strategies (ignoring mixed strategies). As per Definition 3.3.4, a Nash Equilibrium is a set of strategies, one for each player, such that no player can have a unilateral profitable deviation by changing his strategy, when holding other players' strategies fixed.

Definition 3.3.4. *A set of strategies $\sigma_i^* = (m_i^*, a_i^*)$ is a Nash Equilibrium if for every player i we have that*

$$\Pi_i(\sigma_i^*, \sigma_{-i}^*) \geq \Pi_i(\sigma_i, \sigma_{-i}^*), \quad \forall \sigma_i \in \mathcal{S}_i, \tag{3.59}$$

where $\mathcal{S}_i$ is the feasible strategy space for player i, $\sigma_{-i} = \{\sigma_j : j \in \mathcal{P} \setminus \{i\}\}$ is the strategy profile of all players other than i, and $\mathcal{P}$ is the player set.

Since in our case each player has continuous unbounded strategy space, to ensure (3.59) holds, it is necessary that

$$\frac{\partial \Pi_i}{\partial m_i} = 0; \quad \frac{\partial \Pi_i}{\partial a_i} = 0, \tag{3.60}$$

for each player. To ensure that the supply functions are strictly increasing convex functions we only consider equilibrium strategies that have $m_i > 0$, $a_i \geq 0$ for all i.

The rest of this section is devoted to forming, via (3.60), the system of equations in (m_i, a_i) that characterises the Nash Equlibria, and solving this system. By expanding the partial derivatives we have that

$$\frac{\partial \Pi_i}{\partial m_i} = \left(\rho_1 - c_i x_i - b_i\right) \frac{\partial x_i}{\partial m_i} + \frac{\partial \rho_z}{\partial m_i} x_i, \tag{3.61}$$

where z is the zone index for player i. By using the fact that $\rho_z = m_i x_i + a_i$ for every player i in zone z, we have that

$$\frac{\partial \rho_z}{\partial m_i} = x_i + m_i \frac{\partial x_i}{\partial m_i}; \quad \frac{\partial \rho_z}{\partial a_i} = 1 + m_i \frac{\partial x_i}{\partial a_i}, \tag{3.62}$$

and thus we obtain

$$\frac{\partial \Pi_i}{\partial m_i} = (\rho_1 + m_i x_i - c_i x_i - b_i) \frac{\partial x_i}{\partial m_i} + x_i^2 = 0, \tag{3.63}$$

$$\frac{\partial \Pi_i}{\partial a_i} = (\rho_1 + m_i x_i - c_i x_i - b_i) \frac{\partial x_i}{\partial a_i} + x_i = 0. \tag{3.64}$$

We observe that bidding truthfully ($m_i = c_i$, $a_i = b_i$) gives $(\rho_1 + m_i x_i - c_i x_i - b_i) = c_i x_i$, $\frac{\partial \Pi}{\partial m_i} = c_i x_i \frac{\partial y_z}{\partial m_i} + x_i^2$ and $\frac{\partial \Pi}{\partial a_i} = c_i \frac{\partial y_z}{\partial m_i} + x_i$, but if the network is congested $\frac{\partial y_z}{\partial m_i} = 0$, yet $x_i > 0$ so long as player i is selling any quantity, so $\frac{\partial \Pi}{\partial m_i} > 0$ and $\frac{\partial \Pi}{\partial a_i} > 0$. The terms x_i^2 and x_i come from the fact that player i influences the market price via his bids. Thus truthful bidding cannot be an equilibrium, at least when the network is congested, so long as the players realise that their bids influence the market price. Note that if players assume they do not influence the market price, then $m_i = c_i$ and $a_i = b_i$ for all i is an equilibrium. However, in reality players' bids clearly influence the market price.

To solve the system, we need to express x_i in terms of y_z. By (3.41) we have that

$$x_i = \frac{y_z + \mathbf{v}_{m_z}^T \mathbf{a}_z}{m_i \mathbf{1}^T \mathbf{v}_{m_z}} - \frac{a_i}{m_i}. \tag{3.65}$$

We are now interested in the analytical form of $\frac{\partial x_i}{\partial m_i}$ for $i \neq n_z$ and $\frac{\partial x_{n_z}}{\partial m_{n_z}}$. After a series of calculations we obtain that for every i

$$\begin{aligned} \frac{\partial x_i}{\partial m_i} &= \frac{1}{m_i \mathbf{1}^T \mathbf{v}_{m_z}} \left(\frac{\partial y_z}{\partial \hat{\alpha}_i} \frac{\partial \hat{\alpha}_z}{\partial m_i} + \frac{\partial y_z}{\partial \hat{\beta}_i} \frac{\partial \hat{\beta}_z}{\partial m_i} \right) + \frac{y_z + \mathbf{v}_{m_z}^T (\mathbf{a}_z - a_i \mathbf{1})}{(m_i \mathbf{1}^T \mathbf{v}_{m_z})^2} (\mathbf{1}^T \mathbf{v}_{m_z} - 1) \\ &= \frac{1}{m_i \mathbf{1}^T \mathbf{v}_{m_z}} \left(\frac{\partial y_z}{\partial \hat{\alpha}_i} \frac{\partial \hat{\alpha}_z}{\partial m_i} + \frac{\partial y_z}{\partial \hat{\beta}_i} \frac{\partial \hat{\beta}_z}{\partial m_i} \right) + \frac{x_i}{m_i \mathbf{1}^T \mathbf{v}_{m_z}} \left(\frac{1}{m_i} - \mathbf{1}^T \mathbf{v}_{m_z} \right). \end{aligned} \tag{3.66}$$

In a similar way, we are interested in the analytical form of $\frac{\partial x_i}{\partial a_i}$ for every i, given by

$$\begin{aligned} \frac{\partial x_i}{\partial a_i} &= -\frac{1}{m_i} + \frac{1}{m_i^2} \frac{m_{n_z}}{1 + m_{n_z} \mathbf{1}^T \hat{\mathbf{v}}_{m_z}} + \left(\frac{m_{n_z}}{m_i} - \frac{(m_{n_z})^2 \hat{\mathbf{v}}_{m_z}^T \mathbf{1}}{m_i (1 + m_{n_z} \mathbf{1}^T \hat{\mathbf{v}}_{m_z})} \right) \frac{\partial y_z}{\partial \hat{\beta}_z} \frac{\partial \hat{\beta}_z}{\partial a_i} \\ &= \frac{1}{m_i \mathbf{1}^T \mathbf{v}_{m_z}} \left(\frac{\partial y_z}{\partial \hat{\beta}_z} \frac{\partial \hat{\beta}_z}{\partial a_i} + \frac{1}{m_i} - \mathbf{1}^T \mathbf{v}_{m_z} \right). \end{aligned} \tag{3.67}$$

We observe that five extra partial derivatives are involved: $\frac{\partial y_z}{\partial \hat{\alpha}_z}$, $\frac{\partial y_z}{\partial \hat{\beta}_z}$, $\frac{\partial \hat{\alpha}_z}{\partial m_i}$, $\frac{\partial \hat{\beta}_z}{\partial m_i}$, and $\frac{\partial \hat{\beta}_z}{\partial a_i}$. We therefore differentiate (3.44) with respect to m_i and (3.45) with respect to m_i and a_i to obtain the (player-symmetric) derivatives, expressed as

$$\frac{\partial \hat{\alpha}_z}{\partial m_i} = \frac{1}{m_i^2(\mathbf{1}^T \mathbf{v}_{m_z})^2}, \tag{3.68}$$

$$\frac{\partial \hat{\beta}_z}{\partial m_i} = \frac{\mathbf{a}_z^T \mathbf{v}_{m_z}}{m_i^2(\mathbf{1}^T \mathbf{v}_{m_z})^2} - \frac{a_i}{m_i^2(\mathbf{1}^T \mathbf{v}_{m_z})}, \tag{3.69}$$

$$\frac{\partial \hat{\beta}_z}{\partial a_i} = \frac{1}{m_i(\mathbf{1}^T \mathbf{v}_{m_z})}, \tag{3.70}$$

We now compute $\frac{\partial y_z}{\partial \hat{\alpha}_z}$ and $\frac{\partial y_z}{\partial \hat{\beta}_z}$, and restrict our attention on zone 1, without loss of generality

$$\frac{\partial y_1}{\partial \hat{\alpha}_1} = \begin{cases} \frac{\hat{\beta}_1 - \hat{\beta}_2 - 2\alpha(d_1+d_2)}{2(\hat{\alpha}_1+\hat{\alpha}_2)^2} & r \geq \frac{|\hat{\beta}_2 - \hat{\beta}_1 + 2(\hat{\alpha}_2 d_2 - \hat{\alpha}_1 d_1)|}{\hat{\alpha}_1+\hat{\alpha}_2} \\ 0 & \text{otherwise} \end{cases}, \tag{3.71}$$

and finally

$$\frac{\partial y_1}{\partial \hat{\beta}_1} = \begin{cases} -\frac{1}{2(\hat{\alpha}_1+\hat{\alpha}_2)} & r \geq \frac{|\hat{\beta}_2 - \hat{\beta}_1 + 2(\hat{\alpha}_2 d_2 - \hat{\alpha}_1 d_1)|}{\hat{\alpha}_1+\hat{\alpha}_2} \\ 0 & \text{otherwise} \end{cases}. \tag{3.72}$$

Note that all $\frac{\partial y_z}{\partial \hat{\alpha}_z}$, $\frac{\partial y_z}{\partial \hat{\beta}_z}$, $\frac{\partial \hat{\alpha}_z}{\partial m_i}$, $\frac{\partial \hat{\beta}_z}{\partial m_i}$, and $\frac{\partial \hat{\beta}_z}{\partial a_i}$ are purely functions of $(m_i, a_i)_{i \in \mathcal{P}}$, and thus so are $\frac{\partial x_i}{\partial m_i}$ and $\frac{\partial x_i}{\partial a_i}$. Thus, by substituting $\frac{\partial x_i}{\partial m_i}$ and $\frac{\partial x_i}{\partial a_i}$ into (3.100) and (3.101) and using (3.55), (3.43), so are $\frac{\partial \Pi_i}{\partial m_i}$ and $\frac{\partial \Pi_i}{\partial a_i}$, and we can now solve the system of equations given by

$$\mathcal{E} = \left\{ \left\{ \frac{\partial \Pi_i}{\partial a_i}(m_1, a_1, m_2, a_2) = 0, \quad \frac{\partial \Pi_i}{\partial m_i}(m_1, a_1, m_2, a_2) = 0 \right\} \text{ for all players } i \right\}, \tag{3.73}$$

and we denote its representation by $f_{\mathcal{E}}(\mathbf{m}_1, \mathbf{a}_1, \mathbf{m}_2, \mathbf{a}_2; d_1, d_2, r) = 0$. The resulting system of equations is very high order in $(\mathbf{m}_1, \mathbf{a}_1, \mathbf{m}_2, \mathbf{a}_2)$ and thus multiple Nash Equilibria are possible. We next describe the numerical solution to this problem.

3.3.2 Numerical Implementation

One could solve the system of equations via Newton's method, but obtaining an analytical formula for the Jacobian $f_{\mathcal{E}}$ is extremely involved. Automatic differentiation packages would require obtaining the gradient for each $(f_{\mathcal{E}})_k$ which is relatively computationally intensive,

especially when coupled with line search. We find that solving the problem

$$\min_{\boldsymbol{\omega}} \mathbf{f}_\epsilon(\boldsymbol{\omega}; d_1, d_2, r)^T \mathbf{f}_\epsilon(\boldsymbol{\omega}; d_1, d_2, r) \tag{3.74}$$

via gradient descent equipped with line search, where $\boldsymbol{\omega}^T = (\mathbf{m}_1^T, \mathbf{a}_1^T, \mathbf{m}_2^T, \mathbf{a}_2^T)$, is much faster. This approach is formalised in Algorithm 5, and gradients computed as per Algorithm 4. The vectors $\partial_{m_z}\mathbf{x}_z$ and $\partial_{a_z}\mathbf{x}_z$ have $[\partial_{m_z}\mathbf{x}_z]_i = \frac{\partial x_i}{\partial m_i}$, and $[\partial_{a_z}\mathbf{x}_z]_i = \frac{\partial x_i}{\partial a_i}$, and the vectors $\mathbf{c}_z$

Algorithm 4 Compute_Gradient_F

Require: input $\boldsymbol{\omega}$
  $\mathbf{m}_1$ $\mathbf{m}_2$, $\mathbf{a}_1$, $\mathbf{a}_2$ ←unpack($\boldsymbol{\omega}$)
  compute $\hat{\alpha}_1$, $\hat{\alpha}_2$, $\hat{\beta}_1$, $\hat{\beta}_2$ by (3.44), (3.45)
  compute y_1 and y_2 by (3.55)
  compute $\frac{\partial y_z}{\partial \hat{\alpha}_z}$ and $\frac{\partial y_z}{\partial \hat{\beta}_z}$ for $z \in \{1, 2\}$ by (3.71) and (3.72)
  compute $\nabla_{m_z}\hat{\alpha}_z$, $\nabla_{m_z}\hat{\beta}_z$ and $\nabla_{a_z}\hat{\beta}_z$ for $z \in \{1, 2\}$ by (3.68), (3.69), (3.70)
  compute $\partial_{m_z}\mathbf{x}_z$ and $\partial_{a_z}\mathbf{x}_z$ for $z \in \{1, 2\}$ by (3.66) and (3.67),
  $f^z_{m_z} \leftarrow (\rho_z \mathbf{1} + \mathbf{m}_z \odot \mathbf{x}_z - \mathbf{c}_z \odot \mathbf{x}_z - \mathbf{b}_z) \odot \partial_{m_z}\mathbf{x}_z + \mathbf{x}_z \odot \mathbf{x}_z$ for $z \in \{1, 2\}$
  $f^z_{a_z} \leftarrow (\rho_z \mathbf{1} + \mathbf{m}_z \odot \mathbf{x}_z - \mathbf{c}_z \odot \mathbf{x}_z - \mathbf{b}_z) \odot \partial_{a_z}\mathbf{x}_z + \mathbf{x}_z$ for $z \in \{1, 2\}$
  $F = \sum_{z=1}^{2} \|f^z_{m_z}\|_2^2 + \|f^z_{a_z}\|_2^2$
  use automatic differentiation on F to obtain ∇F
  return ∇F

and $\mathbf{b}_z$ represent the concatenation of all c_i and b_i respectively for all players in zone z.

Algorithm 5 Computation of a Nash Equilibrium

Require: hyper-parameters: $N_{\max} = 10000$, $\delta = 10^{-3}$, $N_{ls} = 7$, $\alpha = 0.4$ (example values)
Ensure: if not passed by the user, initialise $\mathbf{m}_1 \leftarrow 3\mathbf{c}_1$, $\mathbf{m}_2 \leftarrow 3\mathbf{c}_2$, $\mathbf{a}_1 \leftarrow \mathbf{b}_1$, $\mathbf{a}_2 \leftarrow \mathbf{b}_2$
  initialise $\boldsymbol{\omega}^T = (\mathbf{m}_1^T, \mathbf{a}_1^T, \mathbf{m}_2^T, \mathbf{a}_2^T)$, $F \leftarrow \|f(\boldsymbol{\omega})\|_2^2$
  for i in range($N_{\max}$) **do**
    $\nabla F \leftarrow$ Compute_ Gradient_F($\boldsymbol{\omega}$)
    for j in range(N_{ls}) **do**
      $\boldsymbol{\omega}' \leftarrow \boldsymbol{\omega} - \alpha^j \nabla F$
      if $F(\boldsymbol{\omega}') < F(\boldsymbol{\omega})$ **then**
        $\boldsymbol{\omega} \leftarrow \boldsymbol{\omega}'$, $F \leftarrow \|f(\boldsymbol{\omega})\|_2^2$
        break
      end if
    end for
    if $F < \delta$ **then return** solution $\mathbf{m}_1$, $\mathbf{a}_1$, $\mathbf{m}_2$, $\mathbf{a}_2$
  end for
  return solution $\mathbf{m}_1$, $\mathbf{a}_1$, $\mathbf{m}_2$, $\mathbf{a}_2$

3.4 Cost Minimisation Spot Model: Generalisation to any Number of Zones and Network Constraints

In this section we consider the case of N_c network constraints, and N_z zones, each of which must be cleared at a unique price, which is typical practice in industry. In European Power Markets, the auction mechanism is cleared based on a set of linear constraints known as the combination of PTDFs and RAMs which span a set of linear inequalities, as described below

$$\mathbf{M}_{PTDF}\Delta\mathbf{y} \leq \mathbf{b}_{RAM}, \tag{3.75}$$

where $\mathbf{M}_{PTDF} \in \mathbb{R}^{N_c \times N_z}$ is the linear constraint matrix with N_c the number of constraints to be imposed, and $\Delta\mathbf{y} \in \mathbb{R}^{N_z}$ is the vector of net production levels per zone. The vector of remaining available margins is $\mathbf{b}_{RAM}$, and by definition, if the network is not pre-congested [78] (i.e. $\mathbf{b}_{RAM} > 0$ component-wise) we have that $\Delta\mathbf{y} = \mathbf{0}$ is always a feasible point. Further in this case, there exists $\epsilon > 0$ such that $\mathbf{y} = \epsilon\mathbf{1}$ is also feasible, and strictly interior to the polyhedron $\mathcal{P}_{M,b} := \{\mathbf{y} \in \mathbb{R}^{N_z} : \mathbf{M}_p\Delta\mathbf{y} \leq \mathbf{b}_p\}$, with $\mathbf{M}_p = \mathbf{M}_{PTDF}$ and $\mathbf{b}_p = \mathbf{b}_{RAM}$. We know that the set of constraints given by $(\mathbf{M}_{PTDF}, \mathbf{b}_{PTDF})$ must yield a closed domain, for else there exist feasible points arbitrarily far from the origin, meaning that $\Delta\mathbf{y}$ has unbounded entries. This in turn would mean that the difference between production and consumption in certain zones can be arbitrarily large, and this should clearly be forbidden in any circumstances.

Just as before, here we work with inflexible demand, and thus the equivalent constraints for production levels become

$$\mathbf{M}_{PTDF}\mathbf{y} \leq \mathbf{b}_{RAM} + \mathbf{M}_{PTDF}\mathbf{d}, \tag{3.76}$$

where $\mathbf{d}$ is the vector of demand levels per zone. We denote this polyhedron as $\mathcal{P}_{M,b,d}$. Based on our discussion from before, $\mathbf{y} = \mathbf{d} + \epsilon\mathbf{1}$ with $\epsilon > 0$, is a strictly interior feasible point for ϵ sufficiently small. Further, the domain is convex and closed.

3.4.1 Introduction of Ellipsoid Network Constraints

Dealing with the set of linear equalities is complicated by two factors: (i) the number of corresponding Lagrangian multipliers is N_c which is generally large, thus making it difficult to track explicitly which constraints are active, and increase the dimensionality of the problem, and (ii) perhaps even worse, the corresponding spot market solution and its derivative are discontinuous as a function of problem parameters (bid strategies), which complicates the analysis via Game Theoretic framework, and can even result in no existence of pure strategy Nash Equilibria [38].

Because the constraints set gives a convex closed domain that has strictly interior points, we propose replacing this by the convex feasible set spanned the largest ellipsoid contained in the polyhedron. This ellipsoid can be computed since the polyhedron is fixed and assumed to be known in advance when solving the problem. Note that such an ellipse only needs to be computed once per problem. Let us for now assume that we have found such an ellipse, and discuss its computation later, in Section 3.4.5. The constraints can then be written as

$$\mathcal{E}_{A,p,r} := \{\mathbf{y} \in \mathbb{R}^{N_z} : \|\mathbf{A}_s\mathbf{y} - \mathbf{p}_s\|_2^2 \leq r_s^2\}. \tag{3.77}$$

Another advantage that $\mathcal{E}_{A,p,r}$ offers is the compactness of representation since $\mathbf{A}_s \in \mathbb{R}^{N_z \times N_z}$, $\mathbf{p}_s \in \mathbb{R}^{N_z}$, $r_s \in \mathbb{R}_+$. This yields only $N_z(N_z+1)+1$ parameters, a much smaller number than the $N_c(N_z+1)$ parameters given by $\mathcal{P}_{M,b}$, since $N_c \gg N_z$. We next define and analyse the spot auction mechanism for inflexible demand, and then consider competing players in a game theoretic framework, after which we devise an efficient algorithm for the computation of the Nash Equilibria.

Our spot model combined with the idea of ellipsoid constraints, allows us to formulate a system of equations that describes the Nash Equlibria, which can be then be solved efficiently by optimisation methods. This is in contrast with the other models proposed in the literature, where one obtains Nash Equilibria by solving EPECs, via the PATH solver [23], which are much more computationally intense [13], [85], [14]. Finally, consistent with the European methodology [78], our spot model yields a single zonal price, while the literature commonly uses Locational Marginal Prices ([85], [36], [55]), which define a potentially different price per each node. This is unrealistic for European markets, where zones contain hundreds if not thousands of nodes, and clear the market at a unique zonal price [78].

3.4.2 The Spot Auction Model

We consider a spot auction model of N_z zones, inflexible demand, with fixed demand levels d_z per zone, ellipsoid constraints as $\mathcal{E}_{A,p,r}$, and cost minimisation objective. The Cost Minimisation problem with ellipsoid constraints (CM-eC) then becomes

$$\begin{aligned} &\min_{\mathbf{x}} \sum_{z=1}^{N_z} \rho_z y_z, \\ &s.t.\ \ y_z = 1^T \mathbf{x}_z,\ \ \forall z; \quad \sum_{z=1}^{N_z} y_z = \sum_{z=1}^{N_z} d_z = d, \\ &\|\mathbf{A}_s\mathbf{y} - \mathbf{p}_s\|_2^2 \leq r_s^2; \quad \rho_z = \max_{j \in \mathcal{J}_z}\{\lambda_j\left((\mathbf{x}_z)_j\right) : (\mathbf{x}_z)_j > 0\},\ \ \forall z, \end{aligned} \tag{CM-eC}$$

where $\mathbf{x}^T = (\mathbf{x}_1^T, ...\mathbf{x}_{N_z}^T)$, $\mathbf{x}_z \in \mathbb{R}^{n_z}$ $d = \sum_{z=1}^{N_z} d_z$ and the bids are placed as $\lambda_j((x_z)_j) = m_j(\mathbf{x}_z)_j + a_j$. For simplicity of notation we will omit explicitly mentioning each player's zone and write $x_j = (\mathbf{x}_z)_j$ where possible, and z_j as the zone that contains player j, i.e. $j \in \mathcal{J}_{z_j}$.

We can approach this problem as before. For every vector $\mathbf{y}$, we can compute the optimal distribution of $\mathbf{x}$ that satisfies the equality constraint, and minimises the cost. This will give us ρ_z as a function strictly of y_z and bids in that zone. We can then find the optimal $\mathbf{y}$ by solving a constrained convex quadratic problem. Just as before, for each zone z, and for every y_z, the optimal distribution of $\mathbf{x}_z$ is given by

$$\mathbf{x}_z^* = \begin{pmatrix} \mathbf{I}_{n_z-1} \\ -\mathbf{1}^T \end{pmatrix} \left(\text{diag}(\hat{\mathbf{v}}_{m_z}) - \frac{m_{n_1} \hat{\mathbf{v}}_{m_z} \hat{\mathbf{v}}_{m_z}^T}{1 + m_{n_z} \mathbf{1}^T \hat{\mathbf{v}}_{m_z}} \right) (m_{n_z} y_z \mathbf{1} - \hat{\mathbf{a}}_z + a_{n_1} \mathbf{1}) + y_z \mathbf{1}, \tag{3.78}$$

which can be expressed in symmetric vector form as

$$\mathbf{x}_z = \frac{y_z + \mathbf{v}_{m_z}^T \mathbf{a}_z}{\mathbf{1}^T \mathbf{v}_{m_z}} \mathbf{v}_{m_z} - \text{diag}(\mathbf{v}_{m_z}) \mathbf{a}_z, \tag{3.79}$$

or written per entry as

$$x_i = \frac{y_{z_i} + \mathbf{v}_{m_{z_i}}^T (\mathbf{a}_{z_i} - a_i \mathbf{1})}{m_i \mathbf{1}^T \mathbf{v}_{m_{z_i}}}, \tag{3.80}$$

where $(\mathbf{v}_{m_{z_i}})_j = 1/m_j$ for all $j \in \mathcal{J}_{z_i}$ and $\mathbf{a}_{z_i}$ is the vector of all $\mathbf{a}_j$ for $j \in \mathcal{J}_{z_i}$. The zonal price can then be written as

$$\rho_z = \hat{\alpha}_z y_z + \hat{\beta}_z, \tag{3.81}$$

with

$$\hat{\alpha}_z = (\mathbf{1}^T \mathbf{v}_{m_z})^{-1} = \left(\sum_{j \in \mathcal{J}_z} \frac{1}{m_j} \right)^{-1} \tag{3.82}$$

$$\hat{\beta}_z = \frac{\mathbf{a}_z^T \mathbf{v}_{m_z}}{\mathbf{1}^T \mathbf{v}_{m_z}} = \left(\sum_{j \in \mathcal{J}_z} \frac{1}{m_j} \right)^{-1} \left(\sum_{j \in \mathcal{J}_z} \frac{a_j}{m_j} \right). \tag{3.83}$$

Since we have the optimal $\mathbf{x}_z$ distribution for every y_z, it only remains to find the optimal y values, where $\mathbf{x}_z$ variables can be eliminated by replacing them with the optimal values. The resulting problem is then

$$\min_{\mathbf{y}} \sum_{z=1}^{N_z} \hat{\alpha}_z y_z^2 + \hat{\beta}_z y_z,$$

$$s.t. \ \|\mathbf{A}_s \mathbf{y} - \mathbf{p}_s\|_2^2 \leq r_s^2; \quad \sum_{z=1}^{N_z} y_z = d,$$

which can be equivalently written in matrix form as

$$\begin{aligned} &\min_{\mathbf{y}} \sum_{z=1}^{N_z} \mathbf{y}^T \mathbf{D}\mathbf{y} + \hat{\boldsymbol{\beta}}^T \mathbf{y}, \\ &s.t.\ \mathbf{1}^T\mathbf{y} = d \qquad\qquad : \quad (\gamma), \\ &\qquad \|\mathbf{A}_s\mathbf{y} - \mathbf{p}_s\|_2^2 \leq r_s^2 \ : \quad (\lambda), \end{aligned} \tag{e-TR}$$

where $\mathbf{D}$ is a diagonal matrix with $\mathbf{D}_{z,z} = \hat{\alpha}_z$ and $\hat{\boldsymbol{\beta}}_z = \hat{\beta}_z$. The system is akin to a trust region optimisation problem, with the extra constraint that $\mathbf{1}^T\mathbf{y} = d$. Thus, we know that this does not have analytical solution in the general case [58], but can nevertheless, be solved efficiently by code since the number of $\mathbf{y}$ variables, N_z, is small and there are only two dual variables, γ and λ. By writing the KKT conditions we have that

$$\begin{aligned} &2\mathbf{D}\mathbf{y} + \hat{\boldsymbol{\beta}} + \gamma\mathbf{1} - \lambda(2\mathbf{A}_s^T\mathbf{A}_s\mathbf{y} - 2\mathbf{A}_s^T\mathbf{p}_s) = 0, \\ &\mathbf{1}^T\mathbf{y} = d; \quad \lambda(\|\mathbf{A}\mathbf{y} - \mathbf{p}_s\|_2^2 - r^2) = 0, \\ &\|\mathbf{A}_s\mathbf{y} - \mathbf{p}_s\|_2^2 \leq r_s^2, \quad \lambda \leq 0. \end{aligned} \tag{KKT-e-TR}$$

There are only two possible cases to this problem, namely that (i) the constraint is inactive, i.e. $\|\mathbf{A}_s\mathbf{y} - \mathbf{p}_s\|_2^2 < r^2$ which means that $\lambda = 0$, or that (ii) $\|\mathbf{A}_s\mathbf{y} - \mathbf{p}_s\|_2^2 = r^2$, in which case λ may be non-zero.

We start by considering (i). Since $\lambda = 0$, and the inequality is inactive, it can be removed, and thus we are left with a system of linear equations that has the solution

$$\begin{pmatrix} \mathbf{y} \\ \gamma \end{pmatrix} = \begin{pmatrix} 2\mathbf{D} & \mathbf{1} \\ \mathbf{1}^T & 0 \end{pmatrix}^{-1} \begin{pmatrix} -\hat{\boldsymbol{\beta}} \\ d \end{pmatrix}. \tag{3.84}$$

Otherwise we are in case (ii) and we can write $(\mathbf{y}^T, \gamma)$ as a function of λ

$$\begin{pmatrix} \mathbf{y} \\ \gamma \end{pmatrix} = \begin{pmatrix} 2\mathbf{D} - 2\lambda\mathbf{A}_s^T\mathbf{A}_s & \mathbf{1} \\ \mathbf{1}^T & 0 \end{pmatrix}^{-1} \begin{pmatrix} -\hat{\boldsymbol{\beta}} - 2\lambda\mathbf{A}_s^T\mathbf{p}_s \\ d \end{pmatrix}, \tag{3.85}$$

and let us denote

$$\hat{\mathbf{D}}(\lambda) := \begin{pmatrix} 2\mathbf{D} - 2\lambda\mathbf{A}_s^T\mathbf{A}_s & \mathbf{1} \\ \mathbf{1}^T & 0 \end{pmatrix}; \quad \mathbf{u}(\lambda) := \begin{pmatrix} -\hat{\boldsymbol{\beta}} - 2\mathbf{A}_s^T\mathbf{p}_s\lambda \\ d \end{pmatrix}. \tag{3.86}$$

In case (ii), we know that $\|\mathbf{A}_s\mathbf{y} - \mathbf{p}_s\|_2^2 = r_s^2$ and thus we have that

$$f(\lambda) = \frac{1}{||\overline{\mathbf{A}}\hat{\mathbf{D}}(\lambda)^{-1}\mathbf{u}(\lambda) - \mathbf{p}_s||_2^2} - \frac{1}{r^2} = 0, \tag{3.87}$$

is the secular equation that we are trying to solve for λ, where $\overline{\mathbf{A}} = (\mathbf{A}_s, \mathbf{0}) \in \mathbb{R}^{N_z \times N_z + 1}$, and we can use Newton-Raphson to solve this one dimensional problem. Once λ is found, $\mathbf{y}$ can be obtained by equation (3.85).

To be able to solve numerically a system of equations describing the Nash Equilibria, analogous to (3.73), we need to take partial derivatives of x_i with respect to player's strategy components m_i and a_i. This requires knowing $\partial y_{z_i}/\partial m_i$ and $\partial y_{z_i}/\partial a_i$, which can be computed by the chain rule as

$$\frac{\partial y_{z_i}}{\partial m_i} = \frac{\partial y_{z_i}}{\partial \alpha_{z_i}}\frac{\partial \alpha_{z_i}}{\partial m_i} + \frac{\partial y_{z_i}}{\partial \beta_{z_i}}\frac{\partial \beta_{z_i}}{\partial m_i}, \tag{3.88}$$

$$\frac{\partial y_{z_i}}{\partial a_i} = \frac{\partial y_{z_i}}{\partial \beta_{z_i}}\frac{\partial \beta_{z_i}}{\partial a_i}. \tag{3.89}$$

Thus, we also need to obtain the partial derivatives of y_{z_i} with respect to α_{z_i} and β_{z_i}. Before proceeding we note that

$$\frac{\partial(\hat{\mathbf{D}}(\lambda)^{-1})}{\partial \hat{\alpha}_z} = -\hat{\mathbf{D}}(\lambda)^{-1}\frac{\partial \hat{\mathbf{D}}(\lambda)}{\partial \hat{\alpha}_z}\hat{\mathbf{D}}(\lambda)^{-1} = -2\hat{\mathbf{D}}(\lambda)^{-1}\hat{\mathbf{e}}_z\hat{\mathbf{e}}_z^T\hat{\mathbf{D}}(\lambda)^{-1} + 2\hat{\mathbf{D}}(\lambda)^{-1}\overline{\mathbf{A}}^T\overline{\mathbf{A}}\hat{\mathbf{D}}(\lambda)^{-1}\frac{\partial \lambda}{\partial \hat{\alpha}_z},$$

$$\frac{\partial(\hat{\mathbf{D}}(\lambda)^{-1})}{\partial \hat{\beta}_z} = -\hat{\mathbf{D}}(\lambda)^{-1}\frac{\partial \hat{\mathbf{D}}(\lambda)}{\partial \hat{\beta}_z}\hat{\mathbf{D}}(\lambda)^{-1} = -2\hat{\mathbf{D}}(\lambda)^{-1}\overline{\mathbf{A}}^T\overline{\mathbf{A}}\hat{\mathbf{D}}(\lambda)^{-1}\frac{\partial \lambda}{\partial \hat{\beta}_z},$$

were $\overline{\mathbf{A}} = (\mathbf{A}_s, \mathbf{0}) \in \mathbb{R}^{N_z \times (N_z+1)}$ and similarly,

$$\frac{\partial \mathbf{u}(\lambda)}{\partial \hat{\alpha}_z} = \begin{pmatrix} -2\mathbf{A}_s^T\mathbf{p}_s \\ 0 \end{pmatrix}\frac{\partial \lambda}{\partial \hat{\alpha}_z} = \mathbf{w}_{A,p}\frac{\partial \lambda}{\partial \hat{\alpha}_z}; \quad \frac{\partial \mathbf{u}(\lambda)}{\partial \hat{\beta}_z} = -\hat{\mathbf{e}}_z + \mathbf{w}_{A,p}\frac{\partial \lambda}{\partial \hat{\beta}_z},$$

where $\hat{\mathbf{e}}_z^T = (\mathbf{e}_z^T, 0)$ is the indicator vector for position of zone z, extended for dimension $N_z + 1$. We now look at partial derivatives with respect to $\hat{\alpha}_z$

$$\frac{\partial}{\partial \hat{\alpha}_z}\begin{pmatrix} \mathbf{y} \\ \gamma \end{pmatrix} = \frac{\partial}{\partial \hat{\alpha}_z}\left(\hat{\mathbf{D}}(\lambda)^{-1}\mathbf{u}(\lambda)\right) = \frac{\partial(\hat{\mathbf{D}}(\lambda)^{-1})}{\partial \hat{\alpha}_z}\mathbf{u}(\lambda) + \hat{\mathbf{D}}(\lambda)^{-1}\frac{\partial \mathbf{u}(\lambda)}{\partial \hat{\alpha}_z}, \tag{3.90}$$

which, by using the previous equations can be expressed as

$$\frac{\partial}{\partial\hat{\alpha}_z}\begin{pmatrix}\mathbf{y}\\ \gamma\end{pmatrix} = -2\hat{\mathbf{D}}(\lambda)^{-1}\hat{\mathbf{e}}_z\hat{\mathbf{e}}_z^T\hat{\mathbf{D}}(\lambda)^{-1}\mathbf{u}(\lambda) + \left[2\mathbf{S}(\lambda)\mathbf{u}(\lambda)+\mathbf{w}(\lambda)\right]\frac{\partial\lambda}{\partial\hat{\alpha}_z}, \tag{3.91}$$

where $\mathbf{S}(\lambda) = \hat{\mathbf{D}}(\lambda)^{-1}\overline{\mathbf{A}}^T\overline{\mathbf{A}}\hat{\mathbf{D}}(\lambda)^{-1}$ and $\mathbf{w}(\lambda) = \hat{\mathbf{D}}(\lambda)^{-1}\mathbf{w}_{A,p}$, and let us further denote $\mathbf{Q}_z(\lambda) = \hat{\mathbf{D}}(\lambda)^{-1}\hat{\mathbf{e}}_z\hat{\mathbf{e}}_z^T\hat{\mathbf{D}}(\lambda)^{-1}$. We are now interested in $\frac{\partial y_z}{\partial\hat{\alpha}_z}$ only, but observe the dependence on $\frac{\partial\lambda}{\partial\hat{\alpha}_z}$, which can be obtained by differentiating $\lambda(\|\mathbf{A}\mathbf{y}-\mathbf{p}\|_2^2 - r^2) = 0$ to obtain that

$$\left(\|\mathbf{A}_s\mathbf{y}-\mathbf{p}_s\|_2^2 - r_s^2\right)\frac{\partial\lambda}{\partial\hat{\alpha}_z} + 2\lambda\left[\mathbf{A}_s^T(\mathbf{A}_s\mathbf{y}-\mathbf{p}_s)\right]^T\frac{\partial\mathbf{y}}{\partial\hat{\alpha}_z} = 0. \tag{3.92}$$

One can now write a linear system of N_z+2 equations with the N_z+2 partial derivatives as unknowns, by taking the z-th and last equation of (3.91)

$$\begin{pmatrix} I_{N_z} & \mathbf{0} & -\left[2\mathbf{S}(\lambda)\mathbf{u}(\lambda)+\mathbf{w}(\lambda)\right]_{1:N_z}\\ \mathbf{0}^T & 1 & -\left[2\mathbf{S}(\lambda)\mathbf{u}(\lambda)+\mathbf{w}(\lambda)\right]_{N_z+1}\\ 2\lambda\left[\mathbf{A}_s^T(\mathbf{A}_s\mathbf{y}-\mathbf{p}_s)\right]^T & 0 & \|\mathbf{A}_s\mathbf{y}-\mathbf{p}_s\|_2^2 - r_s^2\end{pmatrix}\begin{pmatrix}\frac{\partial\mathbf{y}}{\partial\hat{\alpha}_z}\\ \frac{\partial\gamma}{\partial\hat{\alpha}_z}\\ \frac{\partial\lambda}{\partial\hat{\alpha}_z}\end{pmatrix} = -2\begin{pmatrix}\left[\mathbf{Q}_z(\lambda)\mathbf{u}(\lambda)\right]_{1:N_z}\\ \left[\mathbf{Q}_z(\lambda)\mathbf{u}(\lambda)\right]_{N_z+1}\\ 0\end{pmatrix}, \tag{3.93}$$

which is just a linear system in $\frac{\partial\mathbf{y}}{\partial\hat{\alpha}_z}$, $\frac{\partial\gamma}{\partial\hat{\alpha}_z}$ and $\frac{\partial\lambda}{\partial\hat{\alpha}_z}$ since $\mathbf{y}$, γ and λ are known after solving the Trust Region problem. This is a $(N_z+2)\times(N_z+2)$ linear system that can be solved very efficiently and independently for every zone z.

We now concentrate on taking the partial derivative with respect to $\hat{\beta}_z$ and obtain

$$\begin{aligned}\frac{\partial}{\partial\hat{\beta}_z}\begin{pmatrix}\mathbf{y}\\ \gamma\end{pmatrix} &= \left[2\hat{\mathbf{D}}(\lambda)^{-1}\overline{\mathbf{A}}^T\overline{\mathbf{A}}\hat{\mathbf{D}}(\lambda)^{-1}\mathbf{u}(\lambda) + \hat{\mathbf{D}}(\lambda)^{-1}\mathbf{w}_{A,p}\right]\frac{\partial\lambda}{\partial\hat{\beta}_z} - \hat{\mathbf{D}}(\lambda)^{-1}\hat{\mathbf{e}}_z\\ &= \left[2\mathbf{S}(\lambda)\mathbf{u}(\lambda)+\mathbf{w}(\lambda)\right]\frac{\partial\lambda}{\partial\hat{\beta}_z} - \hat{\mathbf{D}}(\lambda)^{-1}\hat{\mathbf{e}}_z,\end{aligned} \tag{3.94}$$

which interestingly gives the same matrix for the linear system

$$\begin{pmatrix} I_{N_z} & \mathbf{0} & -\left[2\mathbf{S}(\lambda)\mathbf{u}(\lambda)+\mathbf{w}(\lambda)\right]_{1:N_z}\\ \mathbf{0}^T & 1 & -\left[2\mathbf{S}(\lambda)\mathbf{u}(\lambda)+\mathbf{w}(\lambda)\right]_{N_z+1}\\ 2\lambda\left[\mathbf{A}_s^T(\mathbf{A}_s\mathbf{y}-\mathbf{p}_s)\right]^T & 0 & \|\mathbf{A}_s\mathbf{y}-\mathbf{p}_s\|_2^2 - r_s^2\end{pmatrix}\begin{pmatrix}\frac{\partial\mathbf{y}}{\partial\hat{\beta}_z}\\ \frac{\partial\gamma}{\partial\hat{\beta}_z}\\ \frac{\partial\lambda}{\partial\hat{\beta}_z}\end{pmatrix} = -\begin{pmatrix}\left[\hat{\mathbf{D}}(\lambda)^{-1}\hat{e}_z\right]_{1:N_z}\\ \left[\hat{\mathbf{D}}(\lambda)^{-1}\hat{e}_z\right]_{N_z+1}\\ 0\end{pmatrix}, \tag{3.95}$$

but with different right hand side vector given by $\hat{\mathbf{D}}(\lambda)^{-1}\hat{\mathbf{e}}_z$. Now, given all the bids (m_i, a_i) we can solve the spot problem to obtain $\{x_i\}_{\forall i\in\cup_z\mathcal{J}_z}$, $\mathbf{y}$ via Algorithm 6, described below,

after which $\frac{\partial y_z}{\partial \hat{\alpha}_z}$ and $\frac{\partial y_z}{\partial \hat{\beta}_z}$ can be computed as described in Algorithm 7.

Algorithm 6 Solve Spot Mechanism

Require: input (m_i, a_i) for all $i \in \cup_z \mathcal{J}_z$
  compute all α_z and β_z based on $\{(m_i, a_i)\}_{i \in \cup_z \mathcal{J}_z}$, by (3.82) and (3.83)
  initialise $\lambda = 0$
  compute $\mathbf{y}$ and γ by (3.85)
  if $\|\mathbf{A}_s \mathbf{y} - \mathbf{p}_s\|_2^2 > r^2$ **then**
    obtain λ by solving (3.87) with Newton's Method
    obtain $\mathbf{y}$ and γ by solving (3.85), with λ from above
  end if
  for $z \in \{1, ..., N_z\}$ **do**
    obtain $\mathbf{x}_z$ by (3.79)
  end for
  return $\mathbf{y}$, $\mathbf{x}$, λ, γ

Algorithm 7 Get Gradients of Spot Solution

Require: input (m_i, a_i) for all $i \in \cup_z \mathcal{J}_z$, y, λ
  compute all α_z and β_z based on $\{(m_i, a_i)\}_{i \in \cup_z \mathcal{J}_z}$, by (3.82) and (3.83)
  if $\lambda = 0$ **then**
    for $z \in \{1, ..., N_z\}$ **do**
      obtain $\frac{\partial y_z}{\partial \hat{\alpha}_z}$ based on (3.91) using that $\lambda = 0$ and $\frac{\partial \lambda}{\partial \hat{\alpha}_z} = 0$
      obtain $\frac{\partial y_z}{\partial \hat{\beta}_z}$ based on (3.94) using that $\lambda = 0$ and $\frac{\partial \lambda}{\partial \hat{\beta}_z} = 0$
    end for
  else
    for $z \in \{1, ..., N_z\}$ **do**
      obtain $\frac{\partial y_z}{\partial \hat{\alpha}_z}$, $\frac{\partial \gamma}{\partial \hat{\alpha}_z}$, $\frac{\partial \lambda}{\partial \hat{\alpha}_z}$ by solving (3.93)
      obtain $\frac{\partial y_z}{\partial \hat{\beta}_z}$, $\frac{\partial \gamma}{\partial \hat{\beta}_z}$, $\frac{\partial \lambda}{\partial \hat{\beta}_z}$ by solving (3.95)
    end for
  end if
  for $i \in \cup_z J_z$ **do**
    compute $\frac{\partial \alpha_{z_i}}{\partial m_i}$, $\frac{\partial \beta_{z_i}}{\partial m_i}$ and $\frac{\partial \beta_{z_i}}{\partial a_i}$ by (3.68), (3.69), (3.70)
    obtain $\frac{\partial y_{z_i}}{\partial m_i} \leftarrow \frac{\partial y_{z_i}}{\partial \alpha_{z_i}} \frac{\partial \alpha_{z_i}}{\partial m_i} + \frac{\partial y_{z_i}}{\partial \beta_{z_i}} \frac{\partial \beta_{z_i}}{\partial m_i}$
    obtain $\frac{\partial y_{z_i}}{\partial a_i} \leftarrow \frac{\partial y_{z_i}}{\partial \beta_{z_i}} \frac{\partial \beta_{z_i}}{\partial a_i}$
  end for
  return $\{(\frac{\partial y_{z_i}}{\partial m_i}, \frac{\partial y_{z_i}}{\partial a_i})\}_{i \in \cup_z \mathcal{J}_z}$

Thus, although we do not have an analytical formula for the solution of the Spot Mechanism described by $\{\rho_z, y_z, \mathbf{x}_z\}_{z \in \mathcal{Z}}$, we can compute this numerically, as well as the derivatives $\left(\frac{\partial y_{z_i}}{\partial m_i}, \frac{\partial y_{z_i}}{\partial a_i}\right)$, meaning that the players can efficiently track the impact of their strategy changes on their profits. We next need to compute the second order derivatives of $\mathbf{y}$ with

respect to α and β, and by following the same approach we obtain

$$\begin{pmatrix} \mathbf{I}_{N_z} & \mathbf{0} & -\left[2\mathbf{S}(\lambda)\mathbf{u}(\lambda)+\mathbf{w}(\lambda)\right]_{1:N_z} \\ \mathbf{0}^T & 1 & -\left[2\mathbf{S}(\lambda)\mathbf{u}(\lambda)+\mathbf{w}(\lambda)\right]_{N_z+1} \\ 2\lambda\left[\mathbf{A}_s^T(\mathbf{A}_s\mathbf{y}-\mathbf{p}_s)\right]^T & 0 & \|\mathbf{A}_s\mathbf{y}-\mathbf{p}_s\|_2^2-r_s^2 \end{pmatrix} \begin{pmatrix} \frac{\partial^2\mathbf{y}}{\partial\alpha_{z_j}\partial\alpha_{z_i}} \\ \frac{\partial^2\gamma}{\partial\alpha_{z_j}\partial\alpha_{z_i}} \\ \frac{\partial^2\lambda}{\partial\alpha_{z_j}\partial\alpha_{z_i}} \end{pmatrix} = \begin{pmatrix} \left[\mathbf{r}_{\alpha_{z_j},\alpha_{z_i}}\right]_{1:N_z} \\ \left[\mathbf{r}_{\alpha_{z_j},\alpha_{z_i}}\right]_{N_z+1} \\ l_2(\alpha,\alpha,z_i,z_j) \end{pmatrix}, \tag{3.96}$$

where

$$\begin{aligned} l_2(q,v,z_i,z_j) =& -2(\mathbf{A}_s\mathbf{y}-\mathbf{p}_s)^T\mathbf{A}_s\left[\frac{\partial\lambda}{\partial q_{z_i}}\frac{\partial\mathbf{y}}{\partial v_{z_j}}+\frac{\partial\lambda}{\partial v_{z_j}}\frac{\partial\mathbf{y}}{\partial q_{z_i}}\right]-2\lambda\frac{\partial\mathbf{y}}{\partial v_{z_j}}^T\mathbf{A}_s^T\mathbf{A}_s\frac{\partial\mathbf{y}}{\partial q_{z_i}} \\ \mathbf{r}_{\alpha_{z_j},\alpha_{z_i}} =& -4\left(-\mathbf{Q}_{z_j}(\lambda)+\mathbf{S}(\lambda)\frac{\partial\lambda}{\partial\alpha_{z_j}}\right)\mathbf{D}(\lambda)\mathbf{Q}_{z_i}(\lambda)\mathbf{u}(\lambda) \\ & -4\mathbf{Q}_{z_i}(\lambda)\mathbf{D}(\lambda)\left(-\mathbf{Q}_{z_j}(\lambda)+\mathbf{S}(\lambda)\frac{\partial\lambda}{\partial\alpha_{z_j}}\right)\mathbf{u}(\lambda)-2\mathbf{Q}_{z_i}(\lambda)\mathbf{w}_{A,p}\frac{\partial\lambda}{\partial\alpha_{z_j}} \\ & +2\left(-\mathbf{Q}_{z_j}(\lambda)+\mathbf{S}(\lambda)\frac{\partial\lambda}{\partial\alpha_{z_j}}\right)\mathbf{D}(\lambda)\left(2\mathbf{S}(\lambda)\mathbf{u}(\lambda)+\mathbf{w}(\lambda)\right)\frac{\partial\lambda}{\partial\alpha_{z_i}} \\ & +4\mathbf{S}(\lambda)\mathbf{D}(\lambda)\left(\mathbf{Q}_{z_j}(\lambda)+\S(\lambda)\frac{\partial\lambda}{\partial\alpha_{z_j}}\right)\mathbf{u}(\lambda)\frac{\partial\lambda}{\partial\alpha_{z_i}}+2\mathbf{S}(\lambda)\mathbf{w}_{A,p}\frac{\partial\lambda}{\partial\alpha_{z_i}}\frac{\partial\lambda}{\partial\alpha_{z_j}} \end{aligned}$$

and note that the first order partial derivatives are known from before. Similarly

$$\begin{pmatrix} \mathbf{I}_{N_z} & \mathbf{0} & -\left[2\mathbf{S}(\lambda)\mathbf{u}(\lambda)+\mathbf{w}(\lambda)\right]_{1:N_z} \\ \mathbf{0}^T & 1 & -\left[2\mathbf{S}(\lambda)\mathbf{u}(\lambda)+\mathbf{w}(\lambda)\right]_{N_z+1} \\ 2\lambda\left[\mathbf{A}_s^T(\mathbf{A}_s\mathbf{y}-\mathbf{p}_s)\right]^T & 0 & \|\mathbf{A}_s\mathbf{y}-\mathbf{p}_s\|_2^2-r_s^2 \end{pmatrix} \begin{pmatrix} \frac{\partial^2\mathbf{y}}{\partial\beta_{z_j}\partial\beta_{z_i}} \\ \frac{\partial^2\gamma}{\partial\beta_{z_j}\partial\beta_{z_i}} \\ \frac{\partial^2\lambda}{\partial\beta_{z_j}\partial\beta_{z_i}} \end{pmatrix} = \begin{pmatrix} \left[\mathbf{r}_{\beta_{z_j},\beta_{z_i}}\right]_{1:N_z} \\ \left[\mathbf{r}_{\beta_{z_j},\beta_{z_i}}\right]_{N_z+1} \\ l_2(\beta,\beta,z_i,z_j) \end{pmatrix}, \tag{3.97}$$

with

$$\mathbf{r}_{\beta_{z_j},\beta_{z_i}} = 2\mathbf{S}(\lambda)\mathbf{D}(\lambda)\left(4\mathbf{S}(\lambda)\mathbf{u}(\lambda)+2\mathbf{w}(\lambda)\right)\frac{\partial\lambda}{\partial\beta_{z_j}}\frac{\partial\lambda}{\partial\beta_{z_i}}-2\mathbf{S}(\lambda)\left[\mathbf{e}_{z_i}\frac{\partial\lambda}{\partial\beta_{z_j}}+\mathbf{e}_{z_j}\frac{\partial\lambda}{\partial\beta_{z_i}}\right],$$

and finally

$$\begin{pmatrix} \mathbf{I}_{N_z} & \mathbf{0} & -\left[2\mathbf{S}(\lambda)\mathbf{u}(\lambda)+\mathbf{w}(\lambda)\right]_{1:N_z} \\ \mathbf{0}^T & 1 & -\left[2\mathbf{S}(\lambda)\mathbf{u}(\lambda)+\mathbf{w}(\lambda)\right]_{N_z+1} \\ 2\lambda\left[\mathbf{A}_s^T(\mathbf{A}_s\mathbf{y}-\mathbf{p}_s)\right]^T & 0 & \|\mathbf{A}_s\mathbf{y}-\mathbf{p}_s\|_2^2-r_s^2 \end{pmatrix} \begin{pmatrix} \frac{\partial^2 y}{\partial\alpha_{z_j}\partial\beta_{z_i}} \\ \frac{\partial^2\gamma}{\partial\alpha_{z_j}\partial\beta_{z_i}} \\ \frac{\partial^2\lambda}{\partial\alpha_{z_j}\partial\beta_{z_i}} \end{pmatrix} = \begin{pmatrix} \left[\mathbf{r}_{\alpha_{z_j},\beta_{z_i}}\right]_{1:N_z} \\ \left[\mathbf{r}_{\alpha_{z_j},\beta_{z_i}}\right]_{N_z+1} \\ l_2(\beta,\alpha,z_i,z_j) \end{pmatrix}, \tag{3.98}$$

where $r_{\alpha_{z_j},\beta_{z_i}}$ can be expressed as

$$\begin{aligned}\mathbf{r}_{\alpha_{z_j},\beta_{z_i}} =& 2\left(-\mathbf{Q}_{z_j}(\lambda)+\mathbf{S}(\lambda)\frac{\partial\lambda}{\partial\alpha_{z_j}}\right)\mathbf{D}(\lambda)\left[2\mathbf{S}(\lambda)\mathbf{u}(\lambda)+\mathbf{w}(\lambda)\right]\frac{\partial\lambda}{\partial\beta_{z_i}}+\\ &+4\mathbf{S}(\lambda)\mathbf{D}(\lambda)\left(-\mathbf{Q}_{z_j}(\lambda)+\mathbf{S}(\lambda)\frac{\partial\lambda}{\partial\alpha_{z_j}}\right)\mathbf{u}(\lambda)\frac{\partial\lambda}{\partial\beta_{z_i}}\\ &+2\mathbf{S}(\lambda)\mathbf{w}_{A,p}\frac{\partial\lambda}{\partial\alpha_j}\frac{\partial\lambda}{\partial\beta_i}-2\left(-\mathbf{Q}_{z_j}(\lambda)+\mathbf{S}(\lambda)\frac{\partial\lambda}{\partial\alpha_{z_j}}\right)\mathbf{e}_{z_i}.\end{aligned}$$

We are now ready to construct the system of equations that characterises the Nash Equilibria.

3.4.3 Game Theoretic Resolution of the N_z Zones Spot Auction

As before, player i in zone z_i solves the following profit maximisation problem

$$\max_{m_i,a_i}\rho_{z_i}x_i-\frac{1}{2}c_ix_i^2-b_ix_i, \tag{3.99}$$

and we are looking for the Nash Equilibria of the system, where no player can unilaterally perform a profitable deviation, by holding the strategies of the other players fixed. For this to happen, as before we have the necessary conditions that

$$\frac{\partial\Pi_i}{\partial m_i}=\left(\rho_{z_i}+m_ix_i-c_ix_i-b_i\right)\frac{\partial x_i}{\partial m_i}+x_i^2=0, \tag{3.100}$$

$$\frac{\partial\Pi_i}{\partial a_i}=\left(\rho_{z_i}+m_ix_i-c_ix_i-b_i\right)\frac{\partial x_i}{\partial a_i}+x_i=0, \tag{3.101}$$

for each player i, and thus we require $\frac{\partial x_i}{\partial m_i}$ and $\frac{\partial x_i}{\partial a_i}$, which can be expressed as

$$\frac{\partial x_i}{\partial m_i}=\frac{1}{m_i\mathbf{1}^T\mathbf{v}_{m_{z_i}}}\frac{\partial y_i}{\partial m_i}+\frac{x_i}{m_i(\mathbf{1}^T\mathbf{v}_{m_{z_i}})}\left(\frac{1}{m_i}-\mathbf{1}^T\mathbf{v}_{m_{z_i}}\right) \tag{3.102}$$

$$\frac{\partial x_i}{\partial a_i}=\frac{1}{m_i\mathbf{1}^T\mathbf{v}_{m_{z_i}}}\left(\frac{\partial y_{z_i}}{\partial a_i}+\frac{1}{m_i}-\mathbf{1}^T\mathbf{v}_{m_{z_i}}\right) \tag{3.103}$$

and we have already discussed how $\left(\frac{\partial y_{z_i}}{\partial m_i},\frac{\partial y_{z_i}}{\partial a_i}\right)$ and x_i are computed from before. The same system of equations to be solved numerically can be formed, namely

$$\mathcal{E}(N_z)=\left\{\left\{\frac{\partial\Pi_i}{\partial a_i}((m_j,a_j)_{j\in\cup_z\mathcal{J}_z})=0,\quad\frac{\partial\Pi_i}{\partial m_i}((m_j,a_j)_{j\in\cup_z\mathcal{J}_z})=0\right\}\text{ for all players }i\right\}. \tag{3.104}$$

If we could efficiently compute gradients with automatic differentiation, the system could be solved identically to the description in Algorithm 4 and Algorithm 5, with the only difference that y and $\left(\frac{\partial y_{z_i}}{\partial m_i}, \frac{\partial y_{z_i}}{\partial a_i}\right)$ are computed via Algorithm 6 and Algorithm 7 respectively, inside Algorithm 4. However, since the Spot Market Mechanism is solved iteratively, we compute gradients analytically. The task is just as demanding for computing the Jacobian of the system $\mathcal{E}(N_z) = \{\mathbf{f}_{\epsilon_N} = 0\}$, as is for computing the gradient of $F_{\epsilon_N} = \mathbf{f}_{\epsilon_N}^T \mathbf{f}_{\epsilon_N}$, but taking Newton steps for $\mathcal{E}(N_z) = \{\mathbf{f}_{\epsilon_N} = 0\}$ corresponds to taking Gauss-Newton steps for $F_{\epsilon_N} = \mathbf{f}_{\epsilon_N}^T \mathbf{f}_{\epsilon_N}$, which is expected to make more progress per iteration than taking gradient steps. For this reason we use Newton's method for root finding on $\mathcal{E}(N_z)$.

As before, let the intersection of the set of equations for each i

$$f_a^i := \frac{\partial \Pi_i}{\partial a_i} = (\rho_{z_i} + m_i x_i - c_i x_i - b_i) \frac{\partial x_i}{\partial a_i} + x_i = 0, \tag{3.105}$$

$$f_m^i := \frac{\partial \Pi_i}{\partial m_i} = (\rho_{z_i} + m_i x_i - c_i x_i - b_i) \frac{\partial x_i}{\partial m_i} + x_i^2 = 0, \tag{3.106}$$

define the system of equation $\mathcal{E}(N_z)$. To perform Newton steps we require $\frac{\partial f_m^i}{\partial m_j}$, $\frac{\partial f_m^i}{\partial a_j}$, $\frac{\partial f_a^i}{\partial m_j}$, and $\frac{\partial f_a^i}{\partial a_j}$, which can be expressed as

$$\frac{\partial f_m^i}{\partial m_j} = T_i \frac{\partial^2 x_i}{\partial m_j \partial m_i} + T_{i,j}^m \frac{\partial x_i}{\partial m_i} + 2 x_i \frac{\partial x_i}{\partial m_j}, \tag{3.107}$$

$$\frac{\partial f_m^i}{\partial a_j} = T_i \frac{\partial^2 x_i}{\partial a_j \partial m_i} + T_{i,j}^a \frac{\partial x_i}{\partial m_i} + 2 x_i \frac{\partial x_i}{\partial a_j}, \tag{3.108}$$

$$\frac{\partial f_a^i}{\partial m_j} = T_i \frac{\partial^2 x_i}{\partial m_j \partial a_i} + T_{i,j}^m \frac{\partial x_i}{\partial a_i} + \frac{\partial x_i}{\partial m_j}, \tag{3.109}$$

$$\frac{\partial f_a^i}{\partial a_j} = T_i \frac{\partial^2 x_i}{\partial a_j \partial a_i} + T_{i,j}^a \frac{\partial x_i}{\partial a_i} + \frac{\partial x_i}{\partial a_j}, \tag{3.110}$$

where $T_i = \rho_{z_i} + m_i x_i - c_i x_i - b_i$ and $T_{i,j}^m = \frac{\partial \rho_{z_i}}{\partial m_j} + m_i \frac{\partial x_i}{\partial m_j} - c_i \frac{\partial x_i}{\partial m_j}$, $T_{i,j}^a = \frac{\partial \rho_{z_i}}{\partial a_j} + m_i \frac{\partial x_i}{\partial a_j} - c_i \frac{\partial x_i}{\partial a_j}$, and $\frac{\partial \rho_{z_i}}{\partial m_j} = m_i \frac{\partial x_i}{\partial m_j} + \delta_{i,j} x_i$, $\frac{\partial \rho_{z_i}}{\partial a_j} = m_i \frac{\partial x_i}{\partial a_j} + \delta_{i,j}$. Thus, we require second order derivatives of x with respect to m and a, which can be obtained as

$$\frac{\partial^2 x_i}{\partial m_j \partial m_i} = \begin{cases} \frac{\upsilon_i}{m_i^2 (\mathbf{1}^T \mathbf{v}_{m_{z_i}})^2} \left(\frac{\partial y_{z_i}}{\partial m_i} + \upsilon_i x_i \right) + \frac{1}{m_i \mathbf{1}^T \mathbf{v}_{m_{z_i}}} \left(\frac{\partial^2 y_{z_i}}{\partial^2 m_i} + \upsilon_i \frac{\partial x_i}{\partial m_i} \right) & \text{if } j = i \\ \frac{1}{m_i m_j^2 (\mathbf{1}^T \mathbf{v}_{m_{z_i}})^2} \left(\frac{\partial y_i}{\partial m_i} + \upsilon_i x_i \right) + \frac{1}{m_i 1^T \mathbf{v}_{m_{z_i}}} \left(\frac{\partial^2 y_i}{\partial m_j \partial m_i} + \frac{1}{m_j^2} x_i + \upsilon_i \frac{\partial x_i}{\partial m_j} \right) & \text{if } j \neq i, j \in \mathcal{Z}_i \\ \frac{1}{m_i \mathbf{1}^T \mathbf{v}_{m_{z_i}}} \frac{\partial^2 y_i}{\partial m_j \partial m_i} + \frac{\upsilon_i}{m_i \mathbf{1}^T \mathbf{v}_{m_{z_i}}} \frac{\partial x_i}{\partial m_j} & \text{if } j \notin \mathcal{Z}_i \end{cases} \tag{3.111}$$

where $\upsilon_i = \frac{1}{m_i} - \mathbf{1}^T \mathbf{v}_{m_{z_i}}$, and $\mathcal{Z}_i$ is the set of players in the same zone as player i (including

itself). Similarly

$$\frac{\partial^2 x_i}{\partial m_j \partial a_i} = \begin{cases} \frac{1}{m_i \mathbf{1}^T \mathbf{v}_{m_{z_i}}} \left(\frac{\partial^2 y_i}{\partial m_j \partial a_i} + \upsilon_i \frac{\partial x_i}{\partial a_i} \right) & \text{if } j = i \\ \frac{1}{m_i \mathbf{1}^T \mathbf{v}_{m_{z_i}}} \left(\frac{\partial^2 y_i}{\partial m_j \partial a_i} + \frac{1}{m_j^2} \right) + \frac{1}{m_j^2 (1^T \mathbf{v}_{m_{z_i}})} \frac{\partial x_i}{\partial a_i} & \text{if } j \neq i, j \in \mathcal{Z}_i \\ \frac{1}{m_i \mathbf{1}^T \mathbf{v}_{m_{z_i}}} \frac{\partial^2 y_{z_i}}{\partial m_j \partial a_i} & \text{if } j \notin \mathcal{Z}_i \end{cases} \tag{3.112}$$

$$\frac{\partial^2 x_i}{\partial a_j \partial m_i} = \frac{1}{m_i \mathbf{1}^T \mathbf{v}_{m_{z_i}}} \left(\frac{\partial^2 y_{z_i}}{\partial a_j \partial m_i} + \upsilon_i \frac{\partial x_i}{\partial a_j} \right), \tag{3.113}$$

$$\frac{\partial^2 x_i}{\partial a_j \partial a_i} = \frac{1}{m_i \mathbf{1}^T \mathbf{v}_{m_{z_i}}} \frac{\partial^2 y_{z_i}}{\partial a_j \partial a_i} \tag{3.114}$$

for all j. We now require the second order derivatives of y with respect to a and m, and we can express these via the chain rule as

$$\frac{\partial^2 y_i}{\partial m_j \partial m_i} = \frac{\partial}{\partial m_j} \left(\frac{\partial y_{z_i}}{\partial \hat{\alpha}_{zi}} \frac{\partial \hat{\alpha}_{zi}}{\partial m_i} + \frac{\partial y_{z_i}}{\partial \hat{\beta}_{zi}} \frac{\partial \hat{\beta}_{zi}}{\partial m_i} \right), \tag{3.115}$$

which can be further expanded as

$$\begin{aligned} \frac{\partial^2 y_i}{\partial m_j \partial m_i} =& \frac{\partial y_{z_i}}{\partial \hat{\alpha}_{zi}} \frac{\partial^2 \hat{\alpha}_{zi}}{\partial m_j \partial m_i} + \frac{\partial y_{z_i}}{\partial \hat{\beta}_{zi}} \frac{\partial^2 \hat{\beta}_{zi}}{\partial m_j \partial m_i} + \frac{\partial \hat{\alpha}_{zi}}{\partial m_i} \left[\frac{\partial^2 y_i}{\partial \alpha_{z_j} \partial \alpha_{z_i}} \frac{\partial \alpha_{z_j}}{\partial m_j} + \frac{\partial^2 y_i}{\partial \beta_{z_j} \partial \alpha_{z_i}} \frac{\partial \beta_{z_j}}{\partial m_j} \right] \\ &+ \frac{\partial \beta_{z_i}}{\partial m_i} \left[\frac{\partial^2 y_i}{\partial \alpha_{z_j} \partial \beta_{z_i}} \frac{\partial \alpha_{z_j}}{\partial m_j} + \frac{\partial^2 y_i}{\partial \beta_{z_j} \partial \beta_{z_i}} \frac{\partial \beta_{z_j}}{\partial m_j} \right] \end{aligned}$$

and by replacing m_i and/or m_j with a_i and/or a_j we obtain

$$\begin{aligned} \frac{\partial^2 y_i}{\partial m_j \partial a_i} &= \frac{\partial y_{z_i}}{\partial \hat{\beta}_{zi}} \frac{\partial^2 \hat{\beta}_{zi}}{\partial m_j \partial a_i} + \frac{\partial \beta_{z_i}}{\partial a_i} \left[\frac{\partial^2 y_i}{\partial \alpha_{z_j} \partial \beta_{z_i}} \frac{\partial \alpha_{z_j}}{\partial m_j} + \frac{\partial^2 y_i}{\partial \beta_{z_j} \partial \beta_{z_i}} \frac{\partial \beta_{z_j}}{\partial m_j} \right], \\ \frac{\partial^2 y_i}{\partial a_j \partial m_i} &= \frac{\partial y_{z_i}}{\partial \hat{\beta}_{zi}} \frac{\partial^2 \hat{\beta}_{zi}}{\partial a_j \partial m_i} + \frac{\partial \hat{\alpha}_{zi}}{\partial m_i} \frac{\partial^2 y_i}{\partial \beta_{z_j} \partial \alpha_{z_i}} \frac{\partial \beta_{z_j}}{\partial a_j} + \frac{\partial \beta_{z_i}}{\partial m_i} \frac{\partial^2 y_i}{\partial \beta_{z_j} \partial \beta_{z_i}} \frac{\partial \beta_{z_j}}{\partial a_j}, \\ \frac{\partial^2 y_i}{\partial a_j \partial a_i} &= \frac{\partial y_{z_i}}{\partial \beta_i} \frac{\partial^2 \beta_{z_i}}{\partial a_j \partial a_i} + \frac{\partial \beta_{z_i}}{\partial a_i} \frac{\partial \beta_{z_j}}{\partial a_j} \frac{\partial^2 y_{z_i}}{\partial \beta_{z_j} \partial \beta_{z_i}} = \frac{\partial \beta_{z_i}}{\partial a_i} \frac{\partial \beta_{z_j}}{\partial a_j} \frac{\partial^2 y_{z_i}}{\partial \beta_{z_j} \partial \beta_{z_i}}. \end{aligned}$$

The second derivatives of α_z and β_z with respect to a and m are

$$\frac{\partial^2 \alpha_{z_i}}{\partial m_j \partial m_i} = \begin{cases} 2\left(\frac{1}{m_i} - \mathbf{1}^T \mathbf{v}_{m_{z_i}}\right) \frac{1}{m_i^3 (\mathbf{1}^T \mathbf{v}_{m_{z_i}})^3} & \text{if } j = i \\ \frac{2}{m_i m_j^3 (\mathbf{1}^T \mathbf{v}_{m_{z_i}})^3} & \text{if } j \neq i, j \in \mathcal{Z}_i \\ 0 & \text{if } j \notin \mathcal{Z}_i \end{cases}, \tag{3.116}$$

$$\frac{\partial^2 \beta_{z_i}}{\partial m_j \partial m_i} = \begin{cases} 2\upsilon_i \frac{\mathbf{a}_z^T \mathbf{v}_{m_{z_i}} - a_i \mathbf{1}^T \mathbf{v}_{m_{z_i}}}{m_i^3 (1^T \mathbf{v}_{m_{z_i}})^3} & \text{if } j = i \\ 2\frac{a_z^T \mathbf{v}_{m_{z_i}} - a_i \mathbf{1}^T \mathbf{v}_{m_{z_i}}}{m_i^2 m_j^2 (\mathbf{1}^T \mathbf{v}_{m_{z_i}})^3} + \frac{a_i - a_j}{m_i^2 m_j^2 (\mathbf{1}^T \mathbf{v}_{m_{z_i}})^2} & \text{if } j \in \mathcal{Z}_i \setminus \{i\} \\ 0 & \text{if } j \notin \mathcal{Z}_i \end{cases}, \tag{3.117}$$

$$\frac{\partial^2 \beta_{z_i}}{\partial a_j \partial m_i} = \begin{cases} \upsilon_i \frac{1}{m_i^2 (\mathbf{1}^T \mathbf{v}_{m_{z_i}})^2} & \text{if } j = i \\ \frac{1}{m_i^2 m_j (\mathbf{1}^T \mathbf{v}_{m_{z_i}})^2} & \text{if } j \in \mathcal{Z}_i \setminus \{i\} \\ 0 & \text{if } j \notin \mathcal{Z}_i \end{cases}, \tag{3.118}$$

$$\frac{\partial^2 \beta_{z_i}}{\partial m_j \partial a_i} = \begin{cases} \upsilon_i \frac{1}{m_i^2 (\mathbf{1}^T \mathbf{v}_{m_{z_i}})^2} & \text{if } j = i \\ \frac{1}{m_i m_j^2 (\mathbf{1}^T \mathbf{v}_{m_{z_i}})^2} & \text{if } j \in \mathcal{Z}_i \setminus \{i\} \\ 0 & \text{if } j \notin \mathcal{Z}_i \end{cases}, \tag{3.119}$$

and all the other ones are zero. These derivatives are used to compute the Jacobian of the $(\mathbf{f}_a^T, \mathbf{f}_m^T) = \mathbf{0}^T$ system, and we can now take Newton steps to obtain Nash stationary points.

3.4.4 A Mean-Variance Framework for Risk Averse Players

To justify this Subsection we start with a result with regards to the uniqueness of Nash Equilibria for our model. This sub-section is focused on theoretical results and is mostly addressed to a mathematically inclined reader, and the reader may otherwise skip to the main results given by Theorems 3.4.4 and 3.4.19.

Theorem 3.4.1. *For the case of two zones and any number of players per zone, consider the case of a congested market. If one Nash Equilibrium exists for the congested market, then there exist a continuum of such Nash Equilibria. In other words, there exist infinitely many, non-isolated local equilibria.*

Proof. At equilibrium, each player must satisfy the following equations

$$\frac{\partial \Pi_i}{\partial m_i} = \left[(2m_i - c_i)x_i + a_i - b_i\right] \frac{\partial x_i}{\partial m_i} + x_i^2 = 0, \tag{3.120}$$

$$\frac{\partial \Pi_i}{\partial a_i} = \left[(2m_i - c_i)x_i + a_i - b_i\right] \frac{\partial x_i}{\partial a_i} + x_i = 0. \tag{3.121}$$

The condition that the market is congested means that $y_{z_1} = \frac{1}{2}d \pm r$ and thus

$$\frac{\partial y_{z_i}}{\partial a_j} = \frac{\partial y_{z_i}}{\partial m_j} = 0. \tag{3.122}$$

Therefore, we have that

$$\frac{\partial x_i}{\partial a_i} = -\frac{\sum_{j \neq i} m_j^{-1}}{m_i \mathbf{1}^T \mathbf{v}_{m_{z_i}}}, \tag{3.123}$$

$$\frac{\partial x_i}{\partial m_i} = -\frac{x_i \sum_{j \neq i} m_j^{-1}}{m_i \mathbf{1}^T \mathbf{v}_{m_{z_i}}} = x_i \frac{\partial x_i}{\partial a_i}. \tag{3.124}$$

This means that $\frac{\partial \Pi_i}{\partial m_i} = x_i \frac{\partial \Pi_i}{\partial a_i}$ for any $(\mathbf{m}, \mathbf{a})$, which means that there are $2N$ strategy variables and only N distinct equations and thus there may exist infinitely many solutions. For fixed $\mathbf{m}$, equations (3.121) and (3.123) yield a full rank linear system of equations in $\mathbf{a}$ that has a unique solution. However, $\mathbf{a}$ is a function of $\mathbf{m}$, and the latter can be changed arbitrarily so long as $\mathbf{a}(\mathbf{m})$ solves (3.121) when (3.123) holds. By continuity, if one solution exists, then infinitely many have to exist. Further

$$\frac{\partial}{\partial q_k}\left(\frac{\partial \Pi_i}{\partial m_i}\right) = \frac{\partial}{\partial q_k}\left(x_i \frac{\partial \Pi_i}{\partial a_i}\right) = x_i \frac{\partial^2 \Pi_i}{\partial q_k a_i} + \frac{\partial x_i}{\partial q_k}\frac{\partial \Pi_i}{\partial a_i} = x_i \frac{\partial^2 \Pi_i}{\partial q_k a_i} \tag{3.125}$$

along the equilibrium lines since $\frac{\partial \Pi_i}{\partial a_i} = 0$. Thus, the Jacobian of the system of equations $\mathbf{f}_{\epsilon_N} = \mathbf{0}$ is

$$\nabla \mathbf{f}_{\epsilon_N} = \begin{pmatrix} \operatorname{diag}(\mathbf{x}) \\ \mathbf{I}_N \end{pmatrix} \mathbf{H}_a, \tag{3.126}$$

where $(\mathbf{H}_a)_{i,k} = \frac{\partial^2 \Pi_i}{\partial q_k \partial a_i}$, so $\mathbf{H}_a \in \mathbb{R}^{N \times 2N}$ and thus clearly $\mathbf{J}_{\epsilon_N} \in \mathbb{R}^{2N \times 2N}$ is at most rank N, and thus is not full rank, meaning that the Nash Equilibria are not isolated. □

Theorem 3.4.1 confirms that the Jacobian of $\mathbf{f}_{\epsilon_N}$, $\nabla \mathbf{f}_{\epsilon_N}$, is not full rank in general, and thus the local Nash Equilibria are not isolated. As we shall see, introducing risk aversion resolves this problem. From a practical point of view, in the CWE, observed strategic bidding is sanctioned by the regulators, while risk averse behaviour is permitted [39]. Here we look at players considering the possibility that the market does not have to clear exactly

as expected by them, that is, for each player, x_i has some uncertainty under their submitted strategy (m_i, a_i) and the others' expected strategy $(\mathbf{m}_{-i}, \mathbf{a}_{-i})$. One could see this as a very simplistic approach to incorporate incomplete information. Alternatively, let us imagine that the market operators solve the spot market problem in a randomized fashion, but the expected outcome is the one obtained by solving the optimisation problem to optimality. In other words, there is a probability distribution over possible outcomes, centered in the optimal outcome, even for fixed submitted bids $(\mathbf{m}, \mathbf{a})$. There are multiple reasons for which the outcome may be at least partially random and we mention three:

1. since the optimisation problem is in reality very large scale and contains more complex features, randomised algorithms might be employed to obtain the solution in feasible time, albeit at the cost of uncertain (sub-optimal) outcome. However, a desirable property is that in expectation, such algorithms give the actual optimal solution.

2. The operators cannot control the knowledge of other players about each other, and as we have seen, for inflexible demand and complete information, there are Nash Equilibria with arbitrarily large prices. Randomisation could then be used as a method to introduce uncertainty that will discourage risk averse players to bid arbitrarily high, due to higher bids having increased variance of profits. It is still desirable that the expected outcome is the optimal one, since this yields the highest social welfare. We will later show that under this type of randomisation, the NE become bounded.

3. The spot market clearing may be solved to optimality, but the submitted strategies may not be the ones under the considered NE, due to players mistaken submission of bids, multitude of equilibria, or intentional randomisation. It is very computationally intense to track the impact of mixed strategies $\Delta((\mathbf{m}, \mathbf{a}))$ on the distribution of $\mathbf{x}$. Further, it is extremely difficult (or perhaps impossible) for market players to obtain data on submitted bids, and thus may instead analyse the distribution of observed x_i.

Players might not know the randomisation strategy of the market operators, or the random component due to other participants' behaviour, but every player i can use historical data to estimate their uncertainty: for every time t use submitted bids $(m_i(t), a_i(t))$ to obtain the expected equilibrium value $x_i(t)$, and obtain the statistical properties of $x_i(t)$ by comparing with the actual spot resolution at time t which gives $\hat{x}_i(t)$. We assume that the following statistical properties are constant:

- Variance of x_i, $\mathbb{V}(x_i) = \sigma_i^2$, which can be estimated as $\hat{\mathbb{V}}(x_i) = \frac{1}{T}\sum_t (x_i(t) - \hat{x}_i(t))^2$,

- Variance of x_i^2, $\mathbb{V}(x_i^2) = \hat{\sigma}_i^2$, which can be estimated as $\hat{\mathbb{V}}(x_i^2) = \frac{1}{T}\sum_t (x_i(t)^2 - \hat{x}_i(t)^2)^2$,

- Co-Variance of x_i with x_i^2, $\text{Cov}(x_i, x_i^2) = \Gamma_i$, which can be estimated as $\hat{\text{Cov}}(x_i, x_i^2) = \frac{1}{T}\sum_t (x_i(t) - \hat{x}_i(t))(x_i(t)^2 - \hat{x}_i(t)^2)$.

The difficulty comes in estimating σ_i, $\hat{\sigma}_i$ and Γ_i for all players $i \in \mathcal{P}$. We further assume that each player uses a mean-variance risk aversion framework with risk aversion parameter $\eta_i > 0$. The objective function of each player i is then the utility U_i defined as

$$U_i = \mathbb{E}(\pi_i) - \eta_i \mathbb{V}(\pi_i). \tag{3.127}$$

We now have that

$$\begin{aligned} \mathbb{E}(\pi_i) &= \mathbb{E}\left(\left(m_i - \frac{1}{2}c_i\right)x_i^2 + (a_i - b_i)x_i\right) \\ &= \left(m_i - \frac{1}{2}c_i\right)\mathbb{E}(x_i)^2 + (a_i - b_i)\mathbb{E}(x_i) + \left(m_i - \frac{1}{2}c_i\right)\mathbb{V}(x_i), \end{aligned} \tag{3.128}$$

which can be re-written as

$$\tilde{\pi}_i := \mathbb{E}(\pi_i) = \left(m_i - \frac{1}{2}c_i\right)\overline{x}_i^2 + (a_i - b_i)\overline{x}_i + \left(m_i - \frac{1}{2}c_i\right)\sigma_i^2, \tag{3.129}$$

where $\overline{x}_i$ is the value obtained at the Nash Equilibrium point given by $(m_i^*, a_i^*, \mathbf{m}_{-i}^*, \mathbf{a}_{-i}^*)$. Similarly the variance of the profit can be written as

$$V_i(m_i, a_i) := \mathbb{V}(\pi_i) = \left(m_i - \frac{1}{2}c_i\right)^2 \hat{\sigma}_i^2 + (a_i - b_i)^2 \sigma_i^2 + 2\left(m_i - \frac{1}{2}c_i\right)(a_i - b_i)\,\Gamma_i. \tag{3.130}$$

Thus, the objective function of each player becomes

$$U_i = \left(m_i - \frac{1}{2}c_i\right)\overline{x}_i^2 + (a_i - b_i)\overline{x}_i + \left(m_i - \frac{1}{2}c_i\right)\sigma_i^2 - \eta_i V_i(m_i, a_i). \tag{3.131}$$

One can now proceed with these objective functions to find the Nash Equilibria, or we could imagine a more pessimistic player, that does not believe in the benefits of variance, introduced by $\left(m_i - \frac{1}{2}c_i\right)\sigma_i^2 \geq 0$ (since we expect each player to bid at least the marginal costs, thus $m_i \geq \frac{1}{2}c_i$). This pessimistic player will then maximise the lower bound on U_i

$$\tilde{U}_i = \left(m_i - \frac{1}{2}c_i\right)\overline{x}_i^2 + (a_i - b_i)\overline{x}_i - \eta_i V_i(m_i, a_i). \tag{3.132}$$

Since $\left(m_i - \frac{1}{2}c_i\right)\sigma_i^2$ is linear in m_i, the second order derivatives of U_i and $\tilde{U}_i$ with respect to strategies are the same, and thus this choice does not influence whether or not Nash

Equilibria are isolated, since this can be proved by showing that $\nabla f_{\epsilon_N,\eta}$ is full rank at any $(\mathbf{m}, \mathbf{a})$. We proceed with (3.131) since it is more general.

We denote $\overline{\pi}_i = \left(m_i - \frac{1}{2}c_i\right)\overline{x}_i^2 + (a_i - b_i)\overline{x}_i$, and thus $\tilde{\pi}_i = \overline{\pi}_i + \left(m_i - \frac{1}{2}c_i\right)\sigma_i^2$. We observe that $\overline{\pi}_i$ is the same as π_i from before, with the notation difference that x_i becomes $\overline{x}_i$. Thus, we can use the derivatives computed before for $\overline{\pi}_i$. We are interested in

$$\frac{\partial \tilde{\pi}_i}{\partial m_i} = \frac{\partial \bar{\pi}_i}{\partial m_i} + \sigma_i^2, \tag{3.133}$$

$$\frac{\partial \tilde{\pi}_i}{\partial a_i} = \frac{\partial \bar{\pi}_i}{\partial a_i}, \tag{3.134}$$

and the second order derivatives of $\tilde{\pi}_i$ are thus the same as $\overline{\pi}_i$, which have been computed before. Further,

$$\frac{\partial V_i}{\partial m_i} = 2\left(m_i - \frac{1}{2}c_i\right)\hat{\sigma_i}^2 + 2(a_i - b_i)\Gamma_i, \tag{3.135}$$

$$\frac{\partial V_i}{\partial a_i} = 2(a_i - b_i)\sigma_i^2 + 2\left(m_i - \frac{1}{2}c_i\right)\Gamma_i, \tag{3.136}$$

$$\frac{\partial^2 V_i}{\partial m_j \partial m_i} = 2\hat{\sigma_i}^2\delta_{i,j}, \tag{3.137}$$

$$\frac{\partial^2 V_i}{\partial a_j \partial a_i} = 2\sigma_i^2\delta_{i,j}, \tag{3.138}$$

$$\frac{\partial^2 V_i}{\partial m_j \partial a_i} = \frac{\partial^2 V_i}{\partial a_j \partial m_i} = 2\Gamma_i\delta_{i,j}, \tag{3.139}$$

which give

$$\frac{\partial U_i}{\partial m_i} = \frac{\partial \bar{\pi}_i}{\partial m_i} + \sigma_i^2 - 2\eta_i\left[\left(m_i - \frac{1}{2}c_i\right)\sigma_i^2 + (a_i - b_i)\Gamma_i\right], \tag{3.140}$$

$$\frac{\partial U_i}{\partial a_i} = \frac{\partial \bar{\pi}_i}{\partial a_i} - 2\eta_i\left[(a_i - b_i)\sigma_i^2 + \left(m_i - \frac{1}{2}c_i\right)\Gamma_i\right], \tag{3.141}$$

which must be zero at a Nash Equilibrium. The new set of equations that defines Nash Equilibria is then

$$\mathcal{E}(N_z) = \left\{\left\{\frac{\partial U_i}{\partial a_i}((m_j, a_j)_{j\in\cup_z\mathcal{J}_z}) = 0, \quad \frac{\partial U_i}{\partial m_i}((m_j, a_j)_{j\in\cup_z\mathcal{J}_z}) = 0\right\} \text{ for all players } i\right\}, \tag{3.142}$$

which we denote as $f_{\epsilon_N;\eta} = 0$. Thus,

$$\mathbf{J}_{f_{\epsilon_N;\eta}} = \nabla\mathbf{f}_{\epsilon_N} - 2\hat{\mathbf{R}}, \tag{3.143}$$

is the Jacobian of our system of equations with $\mathbf{J}_{f_{\epsilon_N;\eta}}(\mathbf{m},\mathbf{a}) \in \mathbb{R}^{2N\times 2N}$, and where

$$\hat{\mathbf{R}} = \begin{pmatrix} \text{diag}(\hat{\boldsymbol{\sigma}}^2 \odot \boldsymbol{\eta}) & \text{diag}(\boldsymbol{\Gamma} \odot \boldsymbol{\eta}) \\ \text{diag}(\boldsymbol{\Gamma} \odot \boldsymbol{\eta}) & \text{diag}(\boldsymbol{\sigma}^2 \odot \boldsymbol{\eta}) \end{pmatrix}, \tag{3.144}$$

with $\boldsymbol{\sigma}^T = (\sigma_1, \sigma_2, ...\sigma_N)$, $\boldsymbol{\Gamma}^T = (\Gamma_1, ..., \Gamma_N)$, and $\odot$ denotes the Hadamard product.

We next show that when all players are risk averse, the Nash Equilibria strategies are bounded, that is, there does not exist a player with arbitrarily large (m_i, a_i) at any Nash Equilibrium. We will next prove that in the case of two zones and two players per zone, for the case of risk averse players, are guaranteed to be isolated, given sufficiently large risk aversion of the least risk averse player. Since the proof is very involved, we simplify presentation by proving a number of lemmas first.

Lemma 3.4.2. *If all players are risk neutral, along the (linear) curve $\frac{da_i}{dm_i} = -x_i$, we have that x_i, Π_i and $\lambda_i = m_i x_i + a_i$ are constant.*

Proposition 3.4.3. *For any player i, with $\hat{\sigma}_i > 0$, $\sigma_i > 0$, $\Gamma_i \geq 0$ and $\eta_i > 0$, and any strategy of other players $(\mathbf{m}_{-i}, \mathbf{a}_{-i})$ we have that*

$$\lim_{m_i\to\infty} U_i(m_i, a_i, \mathbf{m}_{-i}, \mathbf{a}_{-i}) \to -\infty,$$

$$\lim_{a_i\to\infty} U_i(m_i, a_i, \mathbf{m}_{-i}, \mathbf{a}_{-i}) \to -\infty,$$

$$\lim_{a_i\to\infty; m_i\to\infty} U_i(m_i, a_i, \mathbf{m}_{-i}, \mathbf{a}_{-i}) \to -\infty.$$

Proof. Assume $\hat{\sigma}_i \neq 0$, $\sigma_i \neq 0$ and $\Gamma_i \geq 0$ for each player. For any opponent's strategy $(\mathbf{m}_{-i}, \mathbf{a}_{-i})$ and any (m_i, a_i), by the spot mechanism we have that $x_i \leq d$ where $d = \sum_z d_z$ is the total demand. Thus, for any $m_i > \frac{1}{2}c_i$ one can bound the utility of the i-th player by

$$\begin{aligned} U_i \leq B_i(m_i, a_i) := &\left(m_i - \frac{1}{2}c_i\right)(d^2 + \sigma_i^2 - 2\eta_i(a_i - b_i)\Gamma_i) + \max\{(a_i - b_i)d, 0\} \\ &- \eta_i\hat{\sigma}_i^2\left(m_i - \frac{1}{2}c_i\right)^2 - \eta_i(a_i - b_i)^2\sigma_i^2, \end{aligned} \tag{3.145}$$

and for fixed finite a_i, the term $d^2 + \sigma_i^2 - 2\eta_i(a_i - b_i)\Gamma_i$ is a finite constant. As $m_i \to \infty$, B_i is dominated by the $-\eta_i\hat{\sigma}_i^2\left(m_i - \frac{1}{2}c_i\right)^2$ term and since $\eta_i > 0$, $\hat{\sigma}_i^2 > 0$ we have that

$$\lim_{m_i\to-\infty} U_i \leq \lim_{m_i\to-\infty} B_i(m_i, a_i) = -\infty. \tag{3.146}$$

By an analogous argument it can be shown that

$$\lim_{a_i \to -\infty} U_i \leq \lim_{a_i \to -\infty} B_i(m_i, a_i) = -\infty. \tag{3.147}$$

Finally when both $m_i, a_i \to \infty$ all the three terms that dominate have non-positive coefficients, with only the term that involves Γ_i that could be zero, and the other two strictly negative. Thus $B_i \to -\infty$ in this case too. □

We now show that there are no with arbitrary large entries in the strategy set (m^*, a^*), and we give upper bounds on the equilibria strategy set.

Theorem 3.4.4. *Consider the market clearing problem* (CM-eC) *with parameters* $\hat{\sigma}_i > 0$, $\sigma_i > 0$, $\Gamma_i \geq 0$ *and* $\eta_i > 0$ *for each player. Then the set of all Nash Equilibria* (m^*, a^*) *are found in a bounded space* $\mathcal{F}^K = \times_i \mathcal{F}_i^K$ *where* $\mathcal{F}_i^K := \{(m_i, a_i) : m_i < \frac{1}{2} K_i^m c_i;\ a_i < K_i^a b_i\}$, *for any* K_i *s.t.*

$$K_i^m \geq 1 + \frac{2d^2 + 2\sigma_i^2 + \sigma_i^{-1} d\hat{\sigma}_i}{2\eta_i c_i \hat{\sigma_i}^2} =: 1 + \frac{\nu_i^m}{\eta_i}, \tag{3.148}$$

$$K_i^a \geq 1 + \frac{2d + \hat{\sigma}_i^{-1}(d^2 + \sigma_i^2)\sigma_i}{2\eta_i b_i \sigma_i^2} =: 1 + \frac{\nu_i^a}{\eta_i}. \tag{3.149}$$

Further, the zonal prices and the profits are also bounded, that is $\rho_z \leq R_z$ *and* $\pi_i \leq L_i$ *for some finite* R_z *and* L_i.

Proof. First, let us observe that when $m_i = c_i$, $a_i = b_i$ we have that

$$U_i = \left(m_i - \frac{1}{2}c_i\right) x_i^2 + (a_i - b_i) + \left(m_i - \frac{1}{2}c_i\right) \sigma_i^2 - \eta V_i(m_i, a_i) = 0, \tag{3.150}$$

since $V_i(c_i, b_i) = 0$. This is the case for any strategies of other players $(\mathbf{m}_{-i}, \mathbf{a}_{-i})$. Thus, if any strategy profile $(\mathbf{m}, \mathbf{a}) \in \mathcal{S}$ has $U_i < 0$ for any player i, then $(\mathbf{m}, \mathbf{a})$ cannot be a Nash Equilibrium, as player i can improve by unilaterally changing the strategy to $m_i = \frac{1}{2}c_i$, $a_i = b_i$, which gives $U_i = 0$. The rest of the proof therefore shows that any point $(\mathbf{m}, \mathbf{a})$ such that there exists i for which $(m_i, a_i) \notin \mathcal{F}_i^K$, cannot be a Nash Equilibrium, by showing that in this case, the utility of player i for such a point is strictly negative.

When $m_i > c_i$ and $\Gamma_i \geq 0$ we have that

$$\begin{aligned} U_i \leq & -\eta_i \left(m_i - \frac{1}{2}c_i\right)^2 \hat{\sigma}_i^2 - \eta_i (a_i - b_i)^2 \sigma_i^2 + \\ & + \max\{\left(m_i - \frac{1}{2}c_i\right)(d^2 + \sigma_i^2), 0\} + \max\{(a_i - b_i)d, 0\} \quad =: \hat{B}_i(m_i, a_i). \end{aligned} \tag{3.151}$$

The case when $m_i > c_i$ and $a_i > b_i$ gives the largest bound $\hat{B}_i(m_i, a_i)$ since otherwise the corresponding terms $(m_i - c_i)(d^2 + \sigma_i^2) < 0$ or $(a_i - b_i)d < 0$ and thus can be removed from

the bound. Thus, it is sufficient to consider $m_i > c_i$ and $a_i > b_i$. Let us take $m_i = 2^{-1}K_i^m c_i$ and $a_i = K_i^a b_i$, with $K_i^a > 1$, $K_i^m > 1$, which is not restrictive, so long as K_i^m and K_i^a are free. Then equation (3.151) gives us that

$$\hat{B}_i(K_i^m, K_i^a) = (K_i^a - 1)b_i d - \eta_i(K_i^a - 1)^2\sigma_i^2 b_i^2 + \frac{1}{2}(K_i^m - 1)c_i(d^2 + \sigma_i^2) - \frac{1}{4}\eta_i(K_i^m - 1)^2 c_i^2\hat{\sigma}_i^2 \tag{3.152}$$

and denote

$$B_a(K_i^a - 1) = (K_i^a - 1)b_i d - \eta_i(K_i^a - 1)^2\sigma_i^2 b_i^2, \tag{3.153}$$

$$B_m(K_i^m - 1) = \frac{1}{2}(K_i^m - 1)c_i(d^2 + \sigma_i^2) - \frac{1}{4}\eta_i(K_i^m - 1)^2 c_i^2\hat{\sigma}_i^2, \tag{3.154}$$

which are both concave quadratic functions of $K_i^a - 1$ and $K_i^m - 1$ respectively, and thus the maximum that they can attain are

$$\max_{K_i^a} B_a(K_i^a - 1) = \frac{d^2}{4\eta_i\sigma_i^2}, \tag{3.155}$$

$$\max_{K_i^m} B_m(K_i^m - 1) = \frac{(d^2 + \sigma_i^2)^2}{4\eta_i\hat{\sigma}_i^2}. \tag{3.156}$$

By using the maximum of $B_a(K_i^a - 1)$ to bound $\hat{B}_i(m_i, a_i)$ we get that

$$\hat{B}_i(m_i, a_i) \leq \frac{d^2}{4\eta_i\sigma_i^2} + (K_i^m - 1)c_i(d^2 + \sigma_i^2) - \eta_i(K_i^m - 1)^2 c_i^2\hat{\sigma}_i^2 := Q_m(K_i^m - 1), \tag{3.157}$$

whose right hand side is still a concave quadratic in $K_i^m - 1$, and thus for any value of $K_i^m - 1$ greater than the largest root, the right hand side $Q_m(K_i^m - 1) < 0$. Thus, for any K_i^m such that

$$K_i^m - 1 > \frac{d^2 + \sigma_i^2 + \sqrt{(d^2 + \sigma_i^2)^2 + \sigma_i^{-2}d^2\hat{\sigma}_i^2}}{2\eta_i c_i\hat{\sigma}_i^2} = K_i^{m^+} - 1, \tag{3.158}$$

where $K_i^{m^+} - 1$ denotes the largest root of $Q_m(K_i^m - 1)$, $Q_m(K_i^m - 1) < 0$. We can simplify the expression by requiring that K_i^m is slightly larger, namely

$$K_i^m > 1 + \frac{d^2 + \sigma_i^2 + \sqrt{(d^2 + \sigma_i^2 + \sigma_i^{-1}d\hat{\sigma}_i)^2}}{2\eta_i c_i\hat{\sigma}_i^2} = 1 + \frac{2d^2 + 2\sigma_i^2 + \sigma_i^{-1}d\hat{\sigma}_i}{2\eta_i c_i\hat{\sigma}_i^2} =: K_i^M, \tag{3.159}$$

is a sufficient condition such that $Q_m(K_i^m - 1) < 0$, but $Q_m(K_i^m - 1) > \hat{B}_i > U_i$ and thus $U_i < 0$, meaning that points with $m_i = K_i^m c_i$ and K_i^m satisfying (3.159) cannot be Nash

Equilibria. Similarly, we have that

$$\hat{B}_i(m_i, a_i) \leq \frac{(d^2+\sigma_i^2)^2}{4\eta_i\hat{\sigma}_i^2} + (K_i^a - 1)b_i d - \eta_i(K_i^a-1)^2\sigma_i^2 b_i^2 =: Q_a(K_i^a - 1), \tag{3.160}$$

and an analogous calculation gives that $Q_a(K_i^a - 1) < 0$ for every K_i^a such that

$$K_i^a > 1 + \frac{2d + \hat{\sigma}^{-1}(d^2+\sigma_i^2)\sigma_i}{2\eta_i b_i \sigma_i^2} =: K_i^A, \tag{3.161}$$

and thus for any point $(\mathbf{m}, \mathbf{a})$, with $a_i = K_i^a b_i$ and K_i^a satisfying (3.161), no Nash Equilibrium exists. Note that since $K_i^M > 1$ and $K_i^A > 1$, the assumptions that $a_i > b_i$ and $m_i > c_i$ are not restrictive in the proof of the theorem. Thus, all Nash Equilibria must have that $(m^*, a^*) \in \mathcal{F}^K$. Now clearly $\rho_z \leq \delta_m d + \delta_a$, with $\delta_m = \max_j K_j^M c_j$ and $\delta_a = \max_j K_j^A b_j$ and so Π_i must also be finite since at equilibrium

$$\eta_i V(m_i, c_i) \leq \Pi_i < \frac{1}{4}(K_i^M - 1)d^2 + (K_i^A - 1)d, \tag{3.162}$$

and $V(m_i, a_i)$ is bounded for $(m_i, a_i) \in \mathcal{F}_i^K$. Even more, for $m_i > \frac{1}{2}c_i$ and $a_i > b_i$ or $\Gamma_i \geq 0$, we must have that $\Pi_i \geq 0$ at equilibrium. □

Remark 3.4.5. *We note that as η_i increases, K_i^m and K_i^a decrease, and thus as risk aversion increases, the upper bound on the equilibrium price decreases. In particular as $\eta_i \to \infty$, then $K_i^A \to 1$ and $K_i^M \to 1$ and thus $m_i \to \frac{1}{2}c_i$, $a_i \to b_i$, meaning that the players bid below marginal costs, just enough to cover the production costs. Increasing the uncertainty has a similar effect. To see this consider the case where $\hat{\sigma}_i = 2\sigma_i^2$, as is the case for normal distributions (and in general $\hat{\sigma}_i \sim \sigma_i^2$). As $\sigma_i \to \infty$ we still have that $K_i^A \to 1$ and $K_i^M \to 1$.*

Definition 3.4.6. *The matrix $(\mathbf{H}_a)_{i,k} = \frac{\partial^2 \Pi_i}{\partial q_k \partial a_i}$ can be written as $\mathbf{H}_a = (\hat{M}_m; M_a)$ where $\hat{\mathbf{M}}_m$ and $\mathbf{M}_a$ are $N \times N$ matrices defined by $(\hat{\mathbf{M}}_m)_{i,k} = \frac{\partial^2 \Pi_i}{\partial m_k \partial a_i}$ and $(\mathbf{M}_a)_{i,k} = \frac{\partial^2 \Pi_i}{\partial a_k \partial a_i}$.*

Lemma 3.4.7. *In the case of two zones, and two players per zone with congested network, the matrices $\hat{M}_m$ and M_a can be written as*

$$\mathbf{M}_a = \begin{pmatrix} \mathbf{M}_a^{z_1} & \mathbf{0} \\ \mathbf{0} & \mathbf{M}_a^{z_2} \end{pmatrix}, \quad \hat{\mathbf{M}}_m = \begin{pmatrix} \mathbf{M}_m^{z_1} & \mathbf{0} \\ \mathbf{0} & \mathbf{M}_m^{z_2} \end{pmatrix}, \tag{3.163}$$

where $\mathbf{M}_a^{z_1}$ are 2×2 matrices defined as

$$\mathbf{M}_a^{z_1} = \frac{1}{(m_1+m_2)^2} \begin{pmatrix} -(2m_2 + c_1) & m_2 - m_1 + c_1 \\ m_1 - m_2 + c_2 & -(2m_1 + c_2) \end{pmatrix}, \tag{3.164}$$

$$\mathbf{M}_m^{z_1} = \begin{pmatrix} \frac{a_1-b_1+(m_1-3m_2-2c_1)x_1}{(m_1+m_2)^2} & \frac{a_1-b_1+2(m_1-c_1)x_1+2(m_2-m_1+c_1)x_2}{(m_1+m_2)^2} \\ \frac{a_2-b_2+2(m_2-c_2)x_2+2(m_1-m_2+c_2)x_1}{(m_1+m_2)^2} & \frac{a_2-b_2+(m_2-3m_1-2c_2)x_2}{(m_1+m_2)^2} \end{pmatrix}, \tag{3.165}$$

and analogously for $\mathbf{M}_a^{z_2}$ *and* $\mathbf{M}_m^{z_2}$.

Definition 3.4.8. *In the case of two players per zone, let* $\mathcal{I}_m = \mathcal{I}_m^{z_1} \times ... \times \mathcal{I}_m^{z_{|\mathcal{Z}|}} \times$ *with* $\mathcal{I}_m^z := \{(m_1^z, m_2^z) : m_2^z - m_1^z > -c_1^z; m_1^z - m_2^z > -c_2^z\}$.

Lemma 3.4.9. *For the case of two zones, two players per zone and a congested network,* M_a *is strictly row diagonally dominant (SRDD) for any* $(\mathbf{m}, \mathbf{a})$ *with* $\mathbf{m} \in \mathcal{I}_m$.

Proof. Due to the block diagonal structure, it is sufficient to show that each block is SRDD. By symmetry it is sufficient to show that $\mathbf{M}_a^{z_1}$ is SRDD. Since $m \in \mathcal{I}_m$ we have that the numerators of the off-diagonal elements of $\mathbf{M}_a^{z_1}$ satisfy $m_2 - m_1 + c_1 > 0$ as well as $m_1 - m_2 + c_2 > 0$, and the diagonal elements are clearly negative since $m_i > 0$ and $c_i > 0$ for each i. Thus we have that

$$|(\mathbf{M}_a^{z_1})_{1,1}| - |(\mathbf{M}_a^{z_1})_{1,2}| = \frac{1}{m_1 + m_2} > 0, \tag{3.166}$$

and

$$|(\mathbf{M}_a^{z_1})_{2,1}| - |(\mathbf{M}_a^{z_1})_{2,2}| = \frac{1}{m_1 + m_2} > 0, \tag{3.167}$$

and therefore $M_a^{z_1}$ is SRDD. □

Remark 3.4.10. *Note that since* $\mathbf{M}_a$ *is SRDD, it is full rank by Gershgorin's Circle Theorem. Further, note that it is not necessary that* $m \in \mathcal{I}_m$. *Assume for example that* $m_2 - m_1 + c_1 < 0$, *in which case* $m_1 > m_2 + c_1$ *and* $|(\mathbf{M}_a^{z_1})_{1,1}| - |(\mathbf{M}_a^{z_1})_{1,2}| = (m_1+m_2)^{-2}(3m_2+2c_1-m_1)$. *This can still be positive if* m_1 *is bounded above by a sufficiently small number. This can be obtained for sufficiently high risk aversion, as per Theorem 3.4.4.*

Lemma 3.4.11. *For a two zone model with two players per zone and congested network, the Jacobian of* $\mathbf{x}$ *with respect to* $\mathbf{a}$, $\mathbf{J}_a^x$, *defined as* $(\mathbf{J}_a^x)_{i,k} = \frac{\partial x_i}{\partial a_k}$, *has the eigen-decomposition*

$$\mathbf{J}_a^x = \mathbf{P}_a \mathbf{D}_a \mathbf{P}_a^T, \tag{3.168}$$

where

$$\mathbf{P}_a = \frac{\sqrt{2}}{2} \begin{pmatrix} 1 & 0 & 1 & 0 \\ -1 & 0 & 1 & 0 \\ 0 & 1 & 0 & 1 \\ 0 & -1 & 0 & 1 \end{pmatrix}, \tag{3.169}$$

and $\mathbf{D}_a = -\text{diag}(2(m_1 + m_2)^{-1}, 2(m_3 + m_4)^{-1}, 0, 0)$.

Proof. When the network is congested, $\frac{\partial y_{z_i}}{\partial a_i} = 0$, and thus by differentiating (3.80), J_a^x has the form

$$\mathbf{J}_a^x = \begin{pmatrix} -\frac{1}{m_1+m_2} & \frac{1}{m_1+m_2} & 0 & 0 \\ \frac{1}{m_1+m_2} & -\frac{1}{m_1+m_2} & 0 & 0 \\ 0 & 0 & -\frac{1}{m_4+m_3} & \frac{1}{m_4+m_3} \\ 0 & 0 & \frac{1}{m_4+m_3} & -\frac{1}{m_4+m_3} \end{pmatrix} \tag{3.170}$$

and we right multiply $\mathbf{J}_a^x$ by $\mathbf{P}_a$ to see that $\mathbf{J}_a^x\mathbf{P}_a = \mathbf{D}_a\mathbf{P}_a$. □

Definition 3.4.12. *Let the feasible equilibrium strategy set be defined as* $\mathcal{F}_m^{z_i} = \mathcal{I}_m^{z_i} \cap \mathcal{F}_i^K$.

Lemma 3.4.13. *For the case of two zones, with congested network, when* $\Gamma_i = 0$, $\sigma_i > 0$ *and* $\hat{\sigma}_i > 0$, *the Jacobian of the regularised system of equations, denoted* $J_{\mathbf{f}_{\epsilon_N}}$, *has the determinant*

$$|\mathbf{J}_{\mathbf{f}_{\epsilon_N}}| = -2\prod_j(\sigma_j^2 + \sigma_j^2 x_j)\eta_j \left| \left(\mathbf{M}_a - 2\text{diag}(\boldsymbol{\eta} \odot \boldsymbol{\sigma}^2)\right)(I - \text{diag}(\mathbf{x})\mathbf{S}) - \hat{\mathbf{M}}_m S \right|, \tag{3.171}$$

where

$$\mathbf{S} = \text{diag}\left(\frac{\boldsymbol{\sigma}^2 \odot \mathbf{x}}{\hat{\boldsymbol{\sigma}}^2 + \boldsymbol{\sigma}^2 \odot \mathbf{x}^2}\right) + \text{diag}\left(\frac{(\mathbf{a}-\mathbf{b}) \odot \boldsymbol{\sigma}^2}{\hat{\boldsymbol{\sigma}}^2 + \boldsymbol{\sigma}^2 \odot \mathbf{x}^2}\right)\mathbf{J}_a^x, \tag{3.172}$$

and the division is performed element-wise.

Proof. As before, we have that

$$\frac{\partial}{\partial q_k}\left(\frac{\partial \Pi_i}{\partial m_i}\right) = \frac{\partial}{\partial q_k}\left(x_i \frac{\partial \Pi_i}{\partial a_i}\right) = x_i \frac{\partial^2 \Pi_i}{\partial q_k a_i} + \frac{\partial x_i}{\partial q_k}\frac{\partial \Pi_i}{\partial a_i}, \tag{3.173}$$

and since $\frac{\partial U_i}{\partial a_i} = 0$ at a Nash Equilibrium, this implies we have that $\frac{\partial \Pi_i}{\partial a_i} = 2\eta_i(a_i - b_i)\sigma_i^2$,

$$\frac{\partial}{\partial q_k}\left(\frac{\partial \Pi_i}{\partial m_i}\right) = x_i \frac{\partial^2 \Pi_i}{\partial q_k a_i} + 2\eta_i(a_i - b_i)\sigma_i^2 \frac{\partial x_i}{\partial q_k}, \tag{3.174}$$

and thus by Theorem 3.4.1 we have that

$$\mathbf{J}_{\mathbf{f}_{\epsilon_N}} = \nabla \mathbf{f}_{\epsilon_N} - 2\hat{\mathbf{R}} = \begin{pmatrix} \text{diag}(\mathbf{x}) \\ \mathbf{I} \end{pmatrix} \mathbf{H}_a + 2\mathbf{D}_\eta(\mathbf{J}_m^x; \mathbf{J}_a^x) - 2\hat{\mathbf{R}}, \tag{3.175}$$

where $\mathbf{D}_\eta = \text{diag}(\boldsymbol{\eta} \odot (\mathbf{a} - \mathbf{b}) \odot \boldsymbol{\sigma}^2)$. For the case of a congested network, one can observe that

$$\frac{\partial x_i}{\partial m_j} = x_i \frac{\partial x_i}{\partial a_j} \tag{3.176}$$

and therefore $\mathbf{J}^x_m = \text{diag}(\mathbf{x})\mathbf{J}^x_a$. Thus the determinant has the form

$$|\mathbf{J}_{\mathbf{f}_{\epsilon_N};\eta}| = \begin{vmatrix} \text{diag}(\mathbf{x})\hat{\mathbf{M}}_m + 2\mathbf{D}_\eta\mathbf{J}^x_m - 2\text{diag}(\hat{\boldsymbol{\sigma}}^2 \odot \boldsymbol{\eta}) & \text{diag}(\mathbf{x})\mathbf{M}_a + 2\mathbf{D}_\eta\mathbf{J}^x_a \\ \hat{\mathbf{M}}_m & \mathbf{M}_a - 2\text{diag}(\boldsymbol{\sigma}^2 \odot \boldsymbol{\eta}) \end{vmatrix}. \tag{3.177}$$

We now perform determinant operations to obtain a convenient form, in which the block on the first row and first column is easily invertible. We start by subtracting a $\text{diag}(x)$ multiple of the bottom blocks from the top ones to obtain

$$|\mathbf{J}_{\mathbf{f}_{\epsilon_N};\eta}| = \begin{vmatrix} 2\mathbf{D}_\eta\mathbf{J}^x_m - 2\text{diag}(\hat{\boldsymbol{\sigma}}^2 \odot \boldsymbol{\eta}) & 2\mathbf{D}_\eta\mathbf{J}^x_a + 2\text{diag}(\mathbf{x} \odot \boldsymbol{\eta} \odot \boldsymbol{\sigma}^2) \\ \hat{\mathbf{M}}_m & \mathbf{M}_a - 2\text{diag}(\boldsymbol{\sigma}^2 \odot \boldsymbol{\eta}) \end{vmatrix}, \tag{3.178}$$

and we then subtract from the left blocks a $\text{diag}(x)$ multiple of the right blocks to obtain

$$|J_{\mathbf{f}_{\epsilon_N};\eta}| = \begin{vmatrix} -2\text{diag}(\boldsymbol{\eta} \odot (\hat{\boldsymbol{\sigma}}^2 + \boldsymbol{\sigma}^2 \odot \mathbf{x}^2)) & 2\mathbf{D}_{\boldsymbol{\eta}}\mathbf{J}^x_a + 2\text{diag}(\mathbf{x} \odot \boldsymbol{\eta} \odot \boldsymbol{\sigma}^2) \\ \hat{\mathbf{M}}_m - \text{diag}(\mathbf{x})\mathbf{M}_a + 2\text{diag}(\mathbf{x} \odot \boldsymbol{\eta} \odot \boldsymbol{\sigma}^2) & \mathbf{M}_a - 2\text{diag}(\boldsymbol{\sigma}^2 \odot \boldsymbol{\eta}) \end{vmatrix}. \tag{3.179}$$

We now use the well known fact that, as per [63], for an invertible matrix $\mathbf{A}$ we have that

$$\begin{vmatrix} \mathbf{A} & \mathbf{B} \\ \mathbf{C} & \mathbf{D} \end{vmatrix} = \det(\mathbf{A})\det(\mathbf{D} - \mathbf{C}\mathbf{A}^{-1}\mathbf{B}), \tag{3.180}$$

which we can use since $\eta_j > 0$, $x_j \geq 0$, $\hat{\sigma}_j > 0$, $\forall j$, and we thus obtain that

$$|\mathbf{J}_{\mathbf{f}_{\epsilon_N};\eta}| = -2\prod_j \eta_j(\sigma_j^2 x_j^2 + \hat{\sigma}_j)\det\left[\mathbf{M}_a - 2\text{diag}(\boldsymbol{\sigma}^2 \odot \boldsymbol{\eta}) + \mathbf{T}^1_J \cdot \mathbf{T}^2_J\right], \tag{3.181}$$

where

$$\mathbf{T}^1_J = \hat{\mathbf{M}}_m - \text{diag}(\mathbf{x})\mathbf{M}_a + 2\text{diag}(\mathbf{x} \odot \boldsymbol{\eta} \odot \boldsymbol{\sigma}^2), \tag{3.182}$$

$$\mathbf{T}^2_J = \text{diag}(\boldsymbol{\eta} \odot (\hat{\boldsymbol{\sigma}}^2 + \boldsymbol{\sigma}^2 \odot \mathbf{x}^2))^{-1}(2\mathbf{D}_\eta\mathbf{J}^x_a + 2\text{diag}(\mathbf{x} \odot \boldsymbol{\eta} \odot \boldsymbol{\sigma}^2)). \tag{3.183}$$

By rearrangement we obtain the desired result. □

The proof showing that NE are isolated relies on showing that the Jacobian of the system $f_{\epsilon_N;\eta}(\mathbf{m}, \mathbf{a}) = 0$ is full rank, at a Nash Equilibrium point. To do this, we bound the smallest singular value above zero. This requires finding bounds on the largest singular values of

$\hat{\mathbf{M}}_m$ and $\hat{\mathbf{S}}$ and the smallest singular values of $\mathbf{M}_a - 2\text{diag}(\boldsymbol{\eta} \odot \boldsymbol{\sigma}^2)$ and $\mathbf{I} - \text{diag}(\mathbf{x})\mathbf{S}$. We address this in the next four lemmas. Let $K_M = \max_j K_j^M$, $c_{\max} = \max_j c_j$, $c_{\min} = \min_j c_j$. To avoid confusion we denote singular values by ς and standard deviations by σ.

Lemma 3.4.14. *For the case of two zones and two players per zone, in the congested case, when $m \in \mathcal{I}_m$, we have that the minimum singular value of $\tilde{\mathbf{M}}_a := \mathbf{M}_a - 2\text{diag}(\boldsymbol{\sigma}^2 \odot \boldsymbol{\eta})$ satisfies*

$$\varsigma_{\min}\left(\mathbf{M}_a - 2\text{diag}(\boldsymbol{\sigma}^2 \odot \boldsymbol{\eta})\right) \geq \min_j \left(\sqrt{4\eta_j^2\sigma_j^4 + \frac{1}{K_M c_{\max}}\eta_j\sigma_j^2}\right) > 2\min_j \eta_j\sigma_j^2. \tag{3.184}$$

Proof. First of all we have that, $\sigma_{\min} = \min\{\sigma^1_{\min}, \sigma^2_{\min}\}$, where $\sigma^i_{\min}$ corresponds to the i-th diagonal block of $\tilde{\mathbf{M}}_a$. Thus, we concentrate on the first block, since the form of the bound will be the same for both blocks, and we take the minimum across blocks. Further, by using the smallest singular value lower bound from [67] (Theorem V), we have that

$$\varsigma_{\min} \geq \left(\min_{k\in\{1,2\}} \left[|(\mathbf{M}_a)_{k,k} - 2\sigma_k^2\eta_k| - |(\mathbf{M}_a)_{k,k+1}|\right]\right)^{\frac{1}{2}} \left(\min_{k\in\{1,2\}} \left[|(\mathbf{M}_a)_{k,k} - 2\sigma_k^2\eta_k| - |(\mathbf{M}_a)_{k+1,k}|\right]\right)^{\frac{1}{2}}, \tag{3.185}$$

and since $\mathbf{m} \in \mathcal{I}_m$, $m_2 - m_1 + c_1 > 0$ and $m_1 - m_2 + c_2 > 0$ we have that the off-diagonals of M_a are positive while the diagonal entries are strictly negative. Thus we have that

$$\begin{aligned} |(\mathbf{M}_a)_{1,1} - 2\sigma_k^2\eta_k| - |(\mathbf{M}_a)_{1,2}| &= 2\sigma_1^2\eta_1 + \frac{2m_2 + c_1 - m_2 + m_1 - c_1}{(m_1+m_2)^2} = 2\sigma_1^2\eta_1 + \frac{1}{m_1+m_2} \\ &\geq 2\sigma_1^2\eta_1 + \frac{1}{K_M c_{\max}}. \end{aligned} \tag{3.186}$$

Similarly, we can compute that

$$|(\mathbf{M}_a)_{1,1} - 2\sigma_k^2\eta_k| - |(\mathbf{M}_a)_{1,2}| = 2\sigma_1^2\eta_1 + \frac{m_2 - m_1 + 2c_1 + 2(m_2 - c_2)}{(m_1+m_2)^2} \geq 2\sigma_1^2\eta_1. \tag{3.187}$$

By noting that for every diagonal entry we obtain the same type of bounds, we have that for each block

$$\varsigma_{\min}(\mathbf{M}_a^{z_i}) \geq \min_{j\in N_{z_i}} \left(\sqrt{4\eta_j^2\sigma_j^4 + \frac{1}{K_M c_{\max}}\eta_j\sigma_j^2}\right), \tag{3.188}$$

where N_{z_i} is the index set of players in zone z_i. Clearly, the minimum singular value is the minimum amongst $\varsigma_{\min}$ of each block, yielding the desired result. Note that $\frac{1}{K_M c_{\max}}\eta_j\sigma_j^2 > 0$ since we assumed $\eta_j > 0$ and $\sigma_j > 0$, and therefore the bound is not tight since we drop strictly positive terms in the process, but we do so for simplicity of expression. □

Lemma 3.4.15. *For the case of two zones and two players per zone, in the congested case,*

we have that a lower bound on the smallest singular value of $I - diag(x)S$ is

$$\varsigma_{\min}\left(\mathbf{I} - \operatorname{diag}(\mathbf{x})\mathbf{S}\right) \geq r_1 - d_r \frac{\nu_A^{\max} M_\sigma}{c_{\min}\eta_{\min}}, \tag{3.189}$$

where $d_r = d/2 + r$, $M_\sigma = \max_j \sigma_j^2/\hat{\sigma}_j^2$, $\nu_A^{\max} = \max_j \nu_i^a$, with ν_i^a as per Theorem 3.4.4 and $r_1 = \min_j \frac{\hat{\sigma}_j^2}{\hat{\sigma}_j^2 + \sigma_j^2 d_r^2}$.

Proof. We have that

$$\mathbf{I} - \operatorname{diag}(\mathbf{x})\mathbf{S} = \operatorname{diag}\left(\frac{\hat{\boldsymbol{\sigma}}^2}{\hat{\boldsymbol{\sigma}}^2 + \boldsymbol{\sigma}^2 \odot \mathbf{x}^2}\right) + \mathbf{D}_x \mathbf{P}_a \mathbf{D}_a \mathbf{P}_a^T, \tag{3.190}$$

with $\mathbf{D}_x = \operatorname{diag}\left(\frac{\mathbf{x}\odot(\mathbf{a}-\mathbf{b})\odot\boldsymbol{\sigma}^2}{\hat{\boldsymbol{\sigma}}^2+\boldsymbol{\sigma}^2\odot\mathbf{x}^2}\right)$, and thus we have that

$$\varsigma_{\min}(\mathbf{I} - \operatorname{diag}(\mathbf{x})\mathbf{S}) \geq \varsigma_{\min}\left(\operatorname{diag}\left(\frac{\hat{\boldsymbol{\sigma}}^2}{\hat{\boldsymbol{\sigma}}^2 + \boldsymbol{\sigma}^2 \odot \mathbf{x}^2}\right)\right) - \varsigma_{\max}(\mathbf{D}_x \mathbf{P}_a \mathbf{D}_a \mathbf{P}_a^T), \tag{3.191}$$

$$\varsigma_{\min}(\mathbf{I} - \operatorname{diag}(\mathbf{x})\mathbf{S}) \geq \varsigma_{\min}\left(\operatorname{diag}\left(\frac{\hat{\boldsymbol{\sigma}}^2}{\hat{\boldsymbol{\sigma}}^2 + \boldsymbol{\sigma}^2 \odot \mathbf{x}^2}\right)\right) - \varsigma_{\max}(\mathbf{D}_x)\varsigma_{\max}(\mathbf{D}_a), \tag{3.192}$$

and since $\varsigma_{\max}(\mathbf{D}_a) \leq c_{\min}^{-1}$, by Lemma 3.4.11

$$\varsigma_{\min}(\mathbf{I} - \operatorname{diag}(\mathbf{x})\mathbf{S}) \geq \min_j \frac{\hat{\sigma}_j^2}{\hat{\sigma}_j^2 + \sigma_j^2 x_j^2} - (K_A - 1) d_r \max_j \frac{\sigma_j^2}{\hat{\sigma}_j^2 + \sigma_j^2 x_j^2} \frac{1}{c_{\min}}, \tag{3.193}$$

and by using that $K_A \leq \frac{\nu_A^{\max}}{\eta_{\min}} + 1$, and $x_j < d_r$ we obtain the desired result. □

Lemma 3.4.16. *For the case of two zones and two players per zone, in the congested case, we have that*

$$\varsigma_{\max}(\mathbf{S}) \leq d_r M_\sigma + \frac{K_A - 1}{c_{\min}\hat{\sigma}_{\min}^2} M_b \leq d_r M_\sigma + \frac{M_b}{\hat{\sigma}_{\min}^2 c_{\min}} \frac{\nu_A^{\max}}{\eta_{\min}} \tag{3.194}$$

where $M_b = \max_j b_j \sigma_j^2$.

Proof.

$$\varsigma_{\max}(S) \leq \varsigma_{\max}\left(\operatorname{diag}\left(\frac{\hat{\boldsymbol{\sigma}}^2}{\hat{\boldsymbol{\sigma}}^2 + \boldsymbol{\sigma}^2 \odot \mathbf{x}^2}\right)\right) + \varsigma_{\max}\left(\operatorname{diag}\left(\frac{(\mathbf{a} - \mathbf{b}) \odot \boldsymbol{\sigma}^2}{\hat{\boldsymbol{\sigma}}^2 + \boldsymbol{\sigma}^2 \odot \mathbf{x}^2}\right) \mathbf{J}_a^x\right), \tag{3.195}$$

$$\varsigma_{\max}(S) \leq \varsigma_{\max}\left(\operatorname{diag}\left(\frac{\hat{\boldsymbol{\sigma}}^2}{\hat{\boldsymbol{\sigma}}^2 + \boldsymbol{\sigma}^2 \odot \mathbf{x}^2}\right)\right) + \varsigma_{\max}\left(\operatorname{diag}\left(\frac{(\mathbf{a} - \mathbf{b}) \odot \boldsymbol{\sigma}^2}{\hat{\boldsymbol{\sigma}}^2 + \boldsymbol{\sigma}^2 \odot \mathbf{x}^2}\right)\right) \varsigma_{\max}\left(\mathbf{J}_a^x\right), \tag{3.196}$$

and by using that $a_i \leq K_A b_i$ we get that

$$\varsigma_{\max}(S) \leq \max_j \frac{\sigma_j^2 x_j}{\hat{\sigma}_j^2 + \sigma_j^2 x_j^2} + \frac{K_A - 1}{\hat{\sigma}_{\min}^2} \max_j (b_j \sigma_j^2) \varsigma_{\max}\left(\mathbf{J}_a^x\right). \tag{3.197}$$

Finally, by using that $x_j < d_r$ for all j, the result of Lemma 3.4.11 and the previous definitions of M_b and M_σ we get the desired result. □

Lemma 3.4.17. *Consider the case of two zones and two players per zone, in the congested case, and assume that for all i, $m_i \in \mathcal{F}_m^{z_i}$. Then we have that*

$$\varsigma_{\max}(\hat{M}_m) \leq 2\frac{b_{\max}(K_A - 1)}{(c_1 + c_2)^2} + \frac{5 d_r K_M}{c_{min}} \leq \frac{2 b_{\max} \nu_A^{\max}}{c_{\min}^2 \eta_{\min}} + \frac{5 d_r}{c_{\min}} + \frac{5 d_r \nu_M^{\max}}{c_{\min} \eta_{\min}}. \tag{3.198}$$

Proof. Since $\hat{M}_m$ is block diagonal we start by looking at the singular value of the first block $\hat{M}_m^{z_1}$. By symmetry across zones, the maximum singular value can be expressed as $\varsigma_{\max}(\hat{M}_m) = \max\{\varsigma_{\max}(\hat{\mathbf{M}}_m^{z_1}), \varsigma_{\max}(\hat{\mathbf{M}}_m^{z_2})\}$. We next decompose $\hat{\mathbf{M}}_m^{z_1}$ as

$$\hat{\mathbf{M}}_m = \begin{pmatrix} \frac{a_1 - b_1}{(m_1+m_2)^2} & \frac{a_1 - b_1}{(m_1+m_2)^2} \\ \frac{a_2 - b_2}{(m_1+m_2)^2} & \frac{a_2 - b_2}{(m_1+m_2)^2} \end{pmatrix} + \begin{pmatrix} 0 & \frac{(m_2 - m_1 + c_1)x_1}{(m_1+m_2)^2} \\ \frac{(m_1 - m_2 + c_2)x_2}{(m_1+m_2)^2} & 0 \end{pmatrix} + \begin{pmatrix} \frac{(m_1 - 3m_2 - 2c_1)x_1}{(m_1+m_2)^2} & \frac{(2m_1 - c_1)x_1}{(m_1+m_2)^2} \\ \frac{(2m_2 - c_2)x_2}{(m_1+m_2)^2} & \frac{(m_2 - 3m_1 - 2c_2)x_2}{(m_1+m_2)^2} \end{pmatrix}. \tag{3.199}$$

We will then take the two-norm and apply triangular inequality to bound $\hat{\mathbf{M}}_m$, but we bound each term individually first. We have

$$\begin{aligned} \left\| \begin{pmatrix} \frac{a_1 - b_1}{(m_1+m_2)^2} & \frac{a_1 - b_1}{(m_1+m_2)^2} \\ \frac{a_2 - b_2}{(m_1+m_2)^2} & \frac{a_2 - b_2}{(m_1+m_2)^2} \end{pmatrix} \right\|_2 &\leq \sqrt{2} \max \left\{ \left\| \begin{pmatrix} \frac{a_1 - b_1}{(m_1+m_2)^2} \\ \frac{a_1 - b_1}{(m_1+m_2)^2} \end{pmatrix} \right\|_2, \left\| \begin{pmatrix} \frac{a_2 - b_2}{(m_1+m_2)^2} \\ \frac{a_2 - b_2}{(m_1+m_2)^2} \end{pmatrix} \right\|_2 \right\} \\ &\leq 2 \max_j b_j \frac{K_A - 1}{(\frac{1}{2}c_1 + \frac{1}{2}c_2)^2} \leq 2 \max_j b_j \frac{K_A - 1}{c_{min}^2}, \end{aligned} \tag{3.200}$$

and

$$\begin{aligned} \left\| \begin{pmatrix} 0 & \frac{(m_2 - m_1 + c_1)x_1}{(m_1+m_2)^2} \\ \frac{(m_1 + c_2)x_2}{(m_1+m_2)^2} & 0 \end{pmatrix} \right\|_2 &\leq \max \left\{ \frac{(m_1 - m_2 + c_2)x_2}{(m_1+m_2)^2}, \frac{(m_2 - m_1 + c_1)x_1}{(m_1+m_2)^2} \right\} \\ &\leq 2 \frac{d_r}{(\frac{1}{2}c_1 + \frac{1}{2}c_2)^2} \max \left\{ \frac{K_M}{2} c_1 + \frac{1}{2} c_2, \frac{K_M}{2} c_2 + \frac{1}{2} c_1 \right\} \\ &< 2 \frac{d_r}{c_{min}} K_M. \end{aligned} \tag{3.201}$$

Finally, the third matrix clearly has negative diagonal entries since $m_1 - m_2 - c_1 < 0$ and

$m_2 - m_1 - c_2 < 0$ and positive off diagonal entries since $m_i > \frac{1}{2}c_i$. We have the bounds

$$\frac{(3m_2 + 2c_1 - m_1)x_1}{(m_1 + m_2)^2} \leq \frac{3(\frac{K_M}{2}c_2 + \frac{1}{2}c_1)}{(\frac{1}{2}c_1 + \frac{1}{2}c_2)^2}d_r < 3\frac{K_M d_r}{c_{min}}, \tag{3.202}$$

and

$$\frac{(2m_2 - c_2)x_2}{(m_1 + m_2)^2} \leq \frac{(K_M - \frac{1}{2})c_2}{(c_1 + c_2)^2}d_r < \frac{3(K_M c_2 + \frac{1}{2}c_1)}{(c_1 + c_2)^2}d_r < 3\frac{K_M d_r}{c_{min}}, \tag{3.203}$$

and thus we can write the bound

$$\left\| \begin{pmatrix} \frac{(m_1 - 3m_2 - 2c_1)x_1}{(m_1+m_2)^2} & \frac{2(m_1-c_1)x_1}{(m_1+m_2)^2} \\ \frac{2(m_2-c_2)x_2}{(m_1+m_2)^2} & \frac{(m_2-3m_1-2c_2)x_2}{(m_1+m_2)^2} \end{pmatrix} \right\|_2 < 3\frac{K_M d_r}{c_{min}}. \tag{3.204}$$

Collecting all these bounds gives the desired result. □

Lemma 3.4.18. *A quadratic function ax^2+bx+c with $a > 0$, $b < 0$ and $c < 0$ is guaranteed to be positive for any $x \geq -\frac{b}{a} + \sqrt{\frac{-c}{a}}$.*

Proof. The largest root has the form

$$x_+ = -\frac{b}{2a} + \frac{\sqrt{b^2 - 4ac}}{2a}, \tag{3.205}$$

where $-4ac > 0$. By using that

$$b^2 - 4ac < (-b + 2\sqrt{-ac})^2, \tag{3.206}$$

where the strict inequality holds since $a \neq 0$ and $c \neq 0$, and thus have that

$$x_+ < x_0 = \frac{-b}{2a} + \frac{-b + 2\sqrt{-ac}}{2a} = -\frac{b}{a} + \sqrt{\frac{-c}{a}}. \tag{3.207}$$

Since x_0 is at least as large as the biggest root x_+, and $a > 0$, then it has to be that $ax_0^2 + bx_0 + c > 0$, and $x^2 + bx + c > 0$ for all $x \geq x_0$. □

Theorem 3.4.19. *For the case of two zones and two players per zone, for the case of risk averse players, within the zone $\mathcal{F}_m := \mathcal{F}_m^{z_1} \times \mathcal{F}_m^{z_2}$, for $\eta_i > 0$, $\sigma_i > 0$, and $\hat{\sigma}_i > 0$, $\Gamma_i = 0$, all Nash Equilibria that occur with a congested network are isolated, for any regularisation*

parameter vector η that satisfies

$$\eta_{\min} \geq \frac{(\sigma_{\min}^2 \nu_A^{\max} + \frac{5}{2} d_r) d_r M_\sigma}{c_{\min} \sigma_{\min}^2 r_1} + \\ + \sqrt{\frac{\frac{5}{2} d_r M_b \nu_A^{\max}}{c_{\min}^3 r_1 \sigma_{\min}^2 \hat{\sigma}_{\min}^2} + \frac{b_{\max} \nu_A^{\max} + \frac{5}{2} d_r \nu_M^{\max} c_{\min}}{\sigma_{\min}^2 c_{\min}^2 r_1} \left(d_r M_\sigma + \frac{M_b \nu_A^{\max}}{\hat{\sigma}_{\min}^2 c_{\min} \eta_0} \right)} =: \eta_\uparrow, \tag{3.208}$$

for each player i, where

$$\eta_0 = \frac{(\sigma_{\min}^2 \nu_A^{\max} + \frac{5}{2} d_r) d_r M_\sigma}{c_{\min} \sigma_{\min}^2 r_1} + \sqrt{\frac{\frac{5}{2} d_r M_b \nu_A^{\max}}{c_{\min}^3 r_1 \sigma_{\min}^2 \hat{\sigma}_{\min}^2} + \frac{b_{\max} \nu_A^{\max} + \frac{5}{2} d_r \nu_M^{\max} c_{\min}}{\sigma_{\min}^2 c_{\min}^2 r_1} d_r M_\sigma}. \tag{3.209}$$

Proof. If $\mathbf{J}_{\epsilon_N;\eta}$ is full rank at a Nash Equilibrium point ($\mathbf{f}_\epsilon(\mathbf{m}, \mathbf{a}) = \mathbf{0}$), then it must be isolated since a change in $(\mathbf{m}, \mathbf{a})$ along any direction will result in entries in $\mathbf{f}_\epsilon$ to become nonzero. The conditions of this theorem satisfy the conditions of Lemma 3.4.13, and therefore $\mathbf{J}_{\epsilon_N;\eta}$ is full rank if and only if $(\mathbf{M}_a - 2\text{diag}(\boldsymbol{\eta} \odot \boldsymbol{\sigma}^2))(\mathbf{I} - \text{diag}(\mathbf{x})\mathbf{S}) - \hat{\mathbf{M}}_m \mathbf{S}$ is full rank. For this matrix to be full rank, it is sufficient to show that the smallest singular value is strictly bounded above zero. We have that

$$\varsigma_{\min}\left(\left(\mathbf{M}_a - 2\text{diag}(\boldsymbol{\eta} \odot \boldsymbol{\sigma}^2)\right)(\mathbf{I} - \text{diag}(\mathbf{x})\mathbf{S}) - \hat{\mathbf{M}}_m \mathbf{S}\right) \geq \varsigma_{\min}\left(\left[\mathbf{M}_a - 2\text{diag}(\boldsymbol{\eta} \odot \boldsymbol{\sigma}^2)\right][\mathbf{I} - \text{diag}(\mathbf{x})\mathbf{S}]\right) \\ - \varsigma_{\max}(\hat{\mathbf{M}}_m \mathbf{S}) \tag{3.210}$$

and by using that for any matrices $\mathbf{A}$ and $\mathbf{B}$ we have that $\varsigma_{\max}(\mathbf{AB}) \leq \varsigma_{\max}(\mathbf{A})\varsigma_{\max}(\mathbf{B})$ and that

$$\varsigma_{\min}(\mathbf{AB}) = \min_x \frac{\|\mathbf{ABx}\|}{\|\mathbf{x}\|} = \min_{\mathbf{x}} \frac{\|\mathbf{ABx}\|}{\|\mathbf{Bx}\|} \frac{\|\mathbf{Bx}\|}{\|\mathbf{x}\|} \geq \min_{\mathbf{x}} \frac{\|\mathbf{ABx}\|}{\|\mathbf{Bx}\|} \min_{\mathbf{x}} \frac{\|\mathbf{Bx}\|}{\|\mathbf{x}\|} = \varsigma_{\min}(\mathbf{A})\varsigma_{\min}(\mathbf{B}), \tag{3.211}$$

we obtain

$$\varsigma_{\min}^* \geq \varsigma_{\min}\left(\mathbf{M}_a - 2\text{diag}(\eta \odot \sigma^2)\right) \varsigma_{\min}\left(\mathbf{I} - \text{diag}(\mathbf{x})\mathbf{S}\right) - \varsigma_{\max}(\hat{\mathbf{M}}_m)\varsigma_{\max}(\mathbf{S}), \tag{3.212}$$

where $\varsigma_{\min}^* = \varsigma_{\min}\left((\mathbf{M}_a - 2\text{diag}(\boldsymbol{\eta} \odot \boldsymbol{\sigma}^2))(\mathbf{I} - \text{diag}(\mathbf{x})\mathbf{S}) - \hat{\mathbf{M}}_m \mathbf{S}\right)$. We need to find the values of $\eta_{\min} = \min_j \eta_j$ such that $\varsigma_{\min}^* > 0$. We now use the results from Lemmas 3.4.14, 3.4.15, 3.4.16, 3.4.17 and inequality (3.212), to obtain

$$\varsigma_{\min}^* \geq 2\eta_{\min}\sigma_{\min}^2 \left(r_1 - \frac{d_r \nu_A^{\max} M_\sigma}{c_{\min}\eta_{\min}}\right) - \left(\frac{5d_r}{c_{\min}} + \frac{2b_{\max}\nu_A^{\max} + 5d_r\nu_M^{\max}c_{\min}}{c_{\min}^2 \eta_{\min}}\right)\left(d_r M_\sigma + \frac{M_b \nu_A^{\max}}{\hat{\sigma}_{\min}^2 c_{\min}\eta_{\min}}\right). \tag{3.213}$$

We next multiply the right hand side by $\eta_{\min} > 0$, and group the terms by the powers of $\eta_{\min}$. Note that it is necessary that $\eta_{\min} > \frac{d_r \nu_A^{\max} M_\sigma}{c_{\min} r_1}$, for else all the terms on the right hand side are negative, and we cannot bound $\varsigma^*_{\min}$ above zero in this case. Thus, we obtain the sufficient condition that

$$\kappa_1 \eta_{\min}^2 + \kappa_2 \eta_{\min} + \kappa_3 + \kappa_4 \eta_{\min}^{-1} > 0, \tag{3.214}$$

which guarantees that $\varsigma^*_{\min} > 0$, where

$$\kappa_1 = 2\sigma_{\min}^2 r_1 > 0, \tag{3.215}$$

$$\kappa_2 = -\left(\frac{2\sigma_{\min}^2 d_r \nu_A^{\max} M_\sigma}{c_{\min}} + \frac{5 d_r^2 M_\sigma}{c_{\min}} \right) = -\frac{(2\sigma_{\min}^2 \nu_A^{\max} + 5 d_r) d_r M_\sigma}{c_{\min}} < 0, \tag{3.216}$$

$$\kappa_3 = -\left(\frac{5 d_r M_b \nu_A^{\max}}{c_{\min}^3 \hat{\sigma}_{\min}^2} + \frac{2 b_{\max} \nu_A^{\max} + 5 c_{\min} d_r \nu_M^{\max}}{c_{\min}^2} d_r M_\sigma \right) < 0, \tag{3.217}$$

$$\kappa_4 = -\frac{2 b_{\max} \nu_A^{\max} + 5 c_{\min} d_r \nu_M^{\max}}{c_{\min}^3 \sigma_{\min}^2} M_b \nu_A^{\max} < 0. \tag{3.218}$$

Thus the left hand side of inequality (3.214) is essentially a cubic in $\eta_{\min}$, since $\eta_{\min} > 0$ is guaranteed. Thus, for sufficiently large $\eta_{\min}$, inequality (3.214) must hold. Since $\kappa_4 < 0$ and $\eta_{\min} > 0$, a necessary condition for $\eta_{\min}$ is that

$$\kappa_1 \eta_{\min}^2 + \kappa_2 \eta_{\min} + \kappa_3 > 0, \tag{3.219}$$

which by Lemma 3.4.18 is guaranteed for any $\eta_{\min}$ satisfying

$$\eta_{\min} \geq -\frac{\kappa_2}{\kappa_1} + \sqrt{\frac{-\kappa_3}{\kappa_1}} \tag{3.220}$$

And by replacing κ_1, κ_2 and κ_3 we get that

$$\eta_{\min} \geq \frac{(\sigma_{\min}^2 \nu_A^{\max} + \frac{5}{2} d_r) d_r M_\sigma}{c_{\min} \sigma_{\min}^2 r_1} + \sqrt{\frac{\frac{5}{2} d_r M_b \nu_A^{\max}}{c_{\min}^3 r_1 \sigma_{\min}^2 \hat{\sigma}_{\min}^2} + \frac{b_{\max} \nu_A^{\max} + \frac{5}{2} d_r \nu_M^{\max} c_{\min}}{\sigma_{\min}^2 c_{\min}^2 r_1} d_r M_\sigma}. \tag{3.221}$$

Let $\eta_0 = -\frac{\kappa_2}{\kappa_1} + \sqrt{\frac{-\kappa_3}{\kappa_1}}$. Since $\kappa_4 < 0$, and based on (3.221) a sufficient condition is then that

$$\kappa_1 \eta_{\min}^2 + \kappa_2 \eta_{\min} + \kappa_3 + \kappa_4 \eta_0^{-1} > 0, \tag{3.222}$$

which is still a quadratic in $\eta_{\min}$, and we apply Lemma 3.4.18 which gives us that

$$\eta_{\min} \geq -\frac{\kappa_2}{\kappa_1} + \sqrt{-\frac{\kappa_3 + \kappa_4 \eta_0^{-1}}{\kappa_1}}, \tag{3.223}$$

to obtain the desired result that

$$\begin{aligned}\eta_{\min} \geq & \frac{(\sigma_{\min}^2 \nu_A^{\max} + \frac{5}{2} d_r) d_r M_\sigma}{c_{\min} \sigma_{\min}^2 r_1} + \\ & + \sqrt{\frac{\frac{5}{2} d_r M_b \nu_A^{\max}}{c_{\min}^3 r_1 \sigma_{\min}^2 \hat{\sigma}_{\min}^2} + \frac{b_{\max} \nu_A^{\max} + \frac{5}{2} d_r \nu_M^{\max} c_{\min}}{\sigma_{\min}^2 c_{\min}^2 r_1} \left(d_r M_\sigma + \frac{M_b \nu_A^{\max}}{\hat{\sigma}_{\min}^2 c_{\min} \eta_0} \right)},\end{aligned} \tag{3.224}$$

whose right hand side is strictly greater than η_0. Therefore for any such $\eta_{\min}$, $\varsigma_{\min}^* > 0$, meaning that $J_{\epsilon_N;\eta}$ is full rank. □

Remark 3.4.20. *Since the bound is rather complex, let us examine what the bound would be, when $1/\eta_{\min}$ is very small and thus can be neglected. In this case, we get that*

$$2\sigma_{\min}^2 r_1 \eta_{\min} - 5\frac{d_r^2}{c_{\min}} M_\sigma - \frac{2\sigma_{min}^2 \nu_A^{max} d_r M_\sigma}{c_{min}} > 0 \tag{3.225}$$

is required to hold. Exactly the same inequailty can be obtained by imagining that $\sigma_{\min} \to \infty$, and retaining only the leading order terms. Thus, an approximate, oversimplified bound, for the case of large noise is

$$\eta_{\min} > \frac{\frac{5}{2} d_r^2 M_\sigma + \sigma_{min}^2 \nu_A^{max} d_r M_\sigma}{c_{\min} \sigma_{\min}^2 r_1} \approx \frac{d_r \nu_A^{\max}}{4 c_{\min} \sigma_{min}^2}, \tag{3.226}$$

where the approximation uses that $\hat{\sigma}_{\min} \approx 2\sigma_{\min}^2$ and $r_1 \approx 1$ when $\sigma_{\min}$ is very large. Since $\nu_A^{\max} \sim \sigma_i^{-1}$, the larger the noise, the smaller the value of η_{min} required to ensure Theorem 3.4.19 holds.

Remark 3.4.21. *When $\sigma_{\min} \to \infty$, we have that $\hat{\sigma}_{\min} \sim \sigma_{\min}^2$, $M_\sigma \sim \sigma_{\min}^{-2} \to 0$, $\nu_M^{\max} \sim \sigma_{\min}^{-2}$, $\nu_A^{\max} \sim \sigma_{\min}^{-1}$, $M_b \sim \sigma_{\min}^2$ and thus*

$$\eta_0 \sim \sigma_{\min}^{-5/2} \to 0, \tag{3.227}$$

which gives us that

$$\eta_\uparrow \sim \sigma_{\min}^{-5/2} \to 0, \tag{3.228}$$

meaning that any positive risk aversion is sufficient to make the equilibria isolated, if the noise is very large.

3.4.5 Solving the Market Problem over the Polytope via Iterative Elliptical Constraints

Thus far we have seen how to solve the market clearing problem if the physical constraints are elliptical, i.e. if $\|\mathbf{A}_s\mathbf{y} - \mathbf{p}_s\|_2 \leq r_s$ is imposed, but in reality the form of the constraints for European spot markets [78] is of linear type, i.e. $\mathcal{P}(\mathbf{y}) := \{\mathbf{y} : \mathbf{M}_p\mathbf{y} \leq \mathbf{b}_p\}$. Note that $\mathcal{P}(\mathbf{y})$ must be a polytope since arbitrarily large y values for any entry cannot physically be permitted. To revert to the problem we can solve fast, (e-TR), we can think of finding the largest ellipse enclosed in the polytope $\mathcal{P}(\mathbf{y})$, replace the polytope constraint with the resulting ellipsoid constraint, and solve within the ellipse as we did for (e-TR). Although obtaining the largest enclosed ellipse is a challenging problem, given an interior point of $\mathcal{P}(\mathbf{y})$, $\mathbf{y}_c$, we can cheaply obtain an ellipse that is *"close"* to the maximum one, as per [66]. This ellipse can be obtained by writing the log barrier function based on the linear constraints

$$f_b(\mathbf{y}) = -\sum_k \ln\left((\mathbf{b}_p)_k - (\mathbf{M}_p)_{k,:}\mathbf{y}\right), \tag{3.229}$$

which is only defined inside the polytope $\mathcal{P}(\mathbf{y})$. The Hessian of this function can be obtained as

$$\mathbf{H}_b(\mathbf{y}) = \nabla^2 f_b = -\mathbf{M}_p^T \mathrm{diag}(\mathbf{g}_b(y))^2 \mathbf{M}_p, \tag{3.230}$$

where $\mathbf{g}_b(\mathbf{y}) := \nabla f_b(\mathbf{y})$ with

$$(\mathbf{g}_b)_k(\mathbf{y}) = \frac{1}{(\mathbf{b}_p)_k - (\mathbf{M}_p)_{k,:}\mathbf{y}}. \tag{3.231}$$

As per [66], if $\mathbf{y}_c$ is an interior point of $\mathcal{P}(\mathbf{y})$, the ellipse

$$\mathrm{EL}(\mathbf{y}_c, \mathbf{M}_p, \mathbf{b}_p) := \{\mathbf{y} : (\mathbf{y} - \mathbf{y}_c)^T \mathbf{H}_b(\mathbf{y}_c)(\mathbf{y} - \mathbf{y}_c) \leq 1\} \tag{3.232}$$

is guaranteed to lie inside the polytope $\mathcal{P}(\mathbf{y})$. One can now simply use this ellipsoid constraint in (e-TR), or can reduce it to the standard form by performing the Cholesky decomposition $\mathbf{H}_b = \mathbf{L}\mathbf{L}^T = \mathbf{A}_s^T\mathbf{A}_s$, and so $\mathbf{A}_s = \mathbf{L}^T$, $\mathbf{p}_s = \mathbf{A}_s\mathbf{y}_c$, $r = 1$, and the ellipse can then be re-written as

$$\mathrm{EL}(\mathbf{y}_c, \mathbf{M}_p, \mathbf{b}_p) := \{\mathbf{y} : \|\mathbf{A}_s\mathbf{y} - \mathbf{p}_s\|_2 \leq r\}. \tag{3.233}$$

Let us denote this procedure of obtaining $\mathbf{A}_s$, $\mathbf{p}_s$ and r based on $\mathbf{y}_c$, $\mathbf{M}_p$, $\mathbf{b}_p$ as $\mathrm{EL}(\mathbf{y}_c, \mathbf{M}_p, \mathbf{b}_p)$. Although the dimensionality of y is small, and thus we expect the ellipse $\mathrm{EL}(\mathbf{y}_c, \mathbf{M}_p, \mathbf{b}_p)$ to cover most of $\mathcal{P}(\mathbf{y})$ for a well chosen $\mathbf{y}_c$, there exist points in $\mathcal{P}(\mathbf{y})$ that are not in $\mathrm{EL}(\mathbf{y}_c, \mathbf{M}_p, \mathbf{b}_p)$, and thus by replacing $\mathcal{P}(\mathbf{y})$ with $\mathrm{EL}(\mathbf{y}_c, \mathbf{M}_p, \mathbf{b}_p)$, the obtained solution may not be a local minimum on $\mathcal{P}(\mathbf{y})$. This approximation becomes increasingly worse as the dimensionality of y increases.

We can control the approximation error, or indeed reduce it to zero, by generating a sequence of ellipses as follows: (i) given an interior point $\mathbf{y}_c$, compute the ellipse , (ii) solve the corresponding (e-TR) on this ellipse to obtain a solution $\mathbf{y}^*$, and (iii) replace $\mathbf{y}_c$ by $\mathbf{y}^*$ and go to (i), or stop if $\mathbf{y}^*$ lies strictly inside $\text{EL}(\mathbf{y}_c, \mathbf{M}_p, \mathbf{b}_p)$, or if a specific convergence criterion is met. This is described in Algorithm 8.

Algorithm 8 Iterative elliptically Constrained Quadratic Programming (ie-CQP)

Require: input (m_i, a_i) for all $i \in \cup_z \mathcal{J}_z$, maximum number of iterations N^e_{max}, tolerance δ
  Use an initial guess $\mathbf{y}_c = \mathbf{d}$ or the Chebychev centre of the $(\mathbf{M}_p, \mathbf{b}_p)$ polytope.
  for $i \in \{1, ..., N^e_{max}\}$ **do**
    obtain $\mathbf{A}_s, \mathbf{p}_s, r \leftarrow \text{EL}(\mathbf{y}_c, \mathbf{M}_p, \mathbf{b}_p)$
    obtain y^*_i and derivatives by solving e-TR with the ellipse given by $\|\mathbf{A}_s\mathbf{y} - \mathbf{p}_s\| \leq r$
    compute $\Delta y = \|\mathbf{y}^*_i - \mathbf{y}_c\|_2$
    if $\Delta y < \delta$ **then**
      return $\mathbf{y}^*_i$, $\Delta\mathbf{y}$
    end if
    $\mathbf{y}_c \leftarrow \mathbf{y}^*_i$
  end for
  return $\mathbf{y}^*_i$, Δy

To obtain an initial interior point, one can simply try the demand vector $\mathbf{d}$. However, this may be infeasible or too close to the boundary. An alternative to this is to find the Chebyshev centre of the polytope $\mathcal{P}(\mathbf{y})$ as

$$\begin{aligned} &\max_{\mathbf{y}_c, r_c} r_c, \\ &s.t.\ \mathbf{M}_p\mathbf{y}_c + r_c\mathbf{w}_m \leq b_p, \\ &\quad r_c \geq 0, \end{aligned} \tag{Cheb-C}$$

where $(\mathbf{w}_m)_i = \|(\mathbf{M}_p)_{i,:}\|_2$, and let us denote this procedure by $\text{ChebC}(\mathbf{M}_p, \mathbf{b}_p)$, and it returns $\mathbf{y}_c$, r_c.

3.5 The general Cost Minimisation model with capacity constraints

In this section we again look at the situation of N_z zones, N_p players, and N_c linear constraints. In addition, we introduce capacity constraints for the electricity providers, which have a critical impact on the price formation. If the active player set was known, this results in the market clearing problem being a linearly constrained problem with strictly bilinear terms in the objective. We introduce four approaches for solving the market clearing given bids $(\mathbf{m}, \mathbf{a})$, with capacity constraints $\mathbf{Q}$, each with different trade-offs between convergence guarantees and computational cost:

1. Iterative enhanced quasi-LP solution (ieq-LP) aims to solve sequential LPs obtained by approximating the zonal quantities in the objective only. This method cannot guarantee convergence to even a local minimum but is the fastest approach.

2. Iterative ellipsoidal constrained quadratic programming (ie-CQP), uses the ideas in Section 3.4.5, by solving a series of Quadratic Programs as in Section 3.4.2, although the objective function is now not convex. The ellipses now ensure capacity constraints are also enforced. This approach is relatively fast and can guarantee asymptotic convergence to a local minimum. Obtaining a global minimum cannot be guaranteed.

3. A Branch and Bound Tree (BBTree) approach is used to guarantee convergence to the global minimum. This uses ideas from ieq-LP and ie-CQP and can guarantee obtaining the global minimum within a pre-specified optimality gap. However, this convergence guarantee comes at the cost of increased computational cost.

4. Iteratively bounded Convex Quadratic Programs (ib-CQP) approach uses strong (but partial) analytical results to iteratively solve linearly constrained CQPs over $\mathbf{y}$ variables to obtain the solution. The method appears to offer the best trade-off between convergence speed, computational cost, and convergence guarantees and it can guarantee global convergence on sub-intervals defined by capacity constraints (instead of on the whole space).

We next give a detailed explanation of these methods and explain how they are used. We first note that the problem of non-isolated Nash Equilibria that can be arbitrarily far from the origin persists in the case of risk neutral players. To this end, we introduce a Robust Strategy Selection (RSS) approach for each player in Section 3.5.4, although the framework in Section 3.4.4 could in principle also be used. However, RSS is preferred because it reduces the search space and allows for discretisation, reducing the computational cost. This partially compensates for increased computational cost as a result of bilinear objective for the market clearing mechanism.

3.5.1 A Bilinear Formulation for the Market Clearing Problem

We consider an optimisation problem similar to the one in Section 3.4.2, but with polytope constraints on the zonal variables and capacity constraints for production level of the type $0 \leq x_i \leq Q_i$ for all i. The problem to be solved then becomes:

$$\begin{aligned}
&\min_{\mathbf{x},\mathbf{y}} \sum_{z=1}^{N_z} \rho_z y_z, \\
&s.t.\ \ y_z = \mathbf{1}^T \mathbf{x}_z, \quad \forall z, \\
&\qquad \rho_z = \max_{j \in \mathcal{P}_z} \{\lambda_j \left((\mathbf{x}_z)_j\right) : (\mathbf{x}_z)_j > 0\}, \\
&\qquad \sum_{z=1}^{N_z} y_z = \sum_{z=1}^{N_z} d_z = d, \\
&\qquad x_i \geq 0; \ \ Q_i - x_i \geq 0, \quad \forall i, \\
&\qquad \mathbf{M}_p \mathbf{y} \leq \mathbf{b}_p,
\end{aligned} \tag{bl-BLP}$$

where $\lambda_i = m_i x_i + a_i$ is the bid price as a function of assigned production quantity x_i. With this formulation we have nested optimisation problems due to the max function. However, one can note that ρ_z can be expressed as:

$$\rho_z = \min_{v_z} \{v_z : \ v_z \geq \ m_i x_i + a_i; \quad \forall i \in \mathcal{J}_z\},$$

which says that ρ_z is the smallest price that is larger than all the bid prices at assigned quantities x_i. The market clearing bilinear problem (mc-BLP) then becomes

$$\begin{aligned}
&\min_{\mathbf{x},\mathbf{v},\mathbf{y}} \sum_{z=1}^{N_z} v_z y_z, \\
&s.t.\ \ \mathbf{y} = \mathbf{E}\mathbf{x}, \\
&\qquad v_z \geq m_i x_i + a_i, \ \ \forall i \in \mathcal{J}_z, \ \forall z, \\
&\qquad \mathbf{1}^T \mathbf{x} = d, \\
&\qquad x_i \geq 0; \ \ Q_i - x_i \geq 0, \quad \forall i, \\
&\qquad \mathbf{M}_p \mathbf{E}\mathbf{x} \leq \mathbf{b}_p,
\end{aligned} \tag{mc-BLP}$$

since given we have that $\min_{x,y} \sum_{z=1}^{N_z} \min_{v_z} \{v_z\} y_z = \min_{x,v,y} \sum_{z=1}^{N_z} v_z y_z$. The (mc-BLP) formulation still requires that the sets $\mathcal{J}_z = \{i : \ x_i > 0, \ i \in \mathcal{P}_z\}$ are known, since $v_{z_i} \geq a_i$ is

not required when $x_i = 0$, but does allow for $v_{z_i} > m_i x_i + a_i$ which could happen if $x_i = Q_i$. Thus, $\mathcal{J}_z$ sets have to be known in advance, and we discuss this how these can be obtained in Section 3.5.5, but for now we assume $\mathcal{J}_z$ are known. The zonal price is now denoted as v_z instead of ρ_z, to distinguish the different properties of prices when introducing capacity constraints. The matrix $\mathbf{E} \in \mathbb{R}^{N_z \times N_p}$ maps player quantities $\mathbf{x}$ to the zonal quantities $\mathbf{y}$ by summing all the produced quantities x_i with $i \in \mathcal{P}_z$ in each zone z.

It is worth observing that if the zonal quantities $\mathbf{y}$ were known, then the problem becomes an LP for $(\mathbf{x}, \mathbf{v})$, since the only nonlinear (bilinear) terms are the $v_z y_z$ ones in the objective. However, the problem is nonlinear in general and the computational cost for solving an optimisation problem with bilinear objective can be rather high.

3.5.2 Market Clearing Solutions

In this section we devise four methods to solve the (bl-BLP) formulation of the Cost Minimisation spot model, which is central to obtaining the market clearing prices and quantities. This sub-section is mostly of interest for the numerically oriented reader. The methods are presented in the order of increasingly stronger exploitation of problem structure, and for the first three, also based on convergence properties that come at the cost of increased complexity. The last method we propose is perhaps the most elegant, and makes the most use of analytical results. It perhaps offers the best trade-off between convergence speed and computational complexity, although strictly speaking it can only guarantee global convergence on sub-intervals generated by capacity constraints, instead of the whole space.

3.5.2.1 Iterative Enhanced quasi-LP Solution

This approach observes that if $\mathbf{y}$ was approximated just in the objective, then mc-BLP becomes an LP. This observation is important because the zonal production vector $\mathbf{y}$ is much lower dimensional, and fractional changes are expected to be lower than $\mathbf{x}$ values, when the objective is approximated. Further, the constraint $\mathbf{y} = \mathbf{E}\mathbf{x}$ becomes redundant and can be removed. Thus, given a guess value for the zonal quantities, $\hat{y}$ we solve the following LP:

$$
\begin{aligned}
&\min_{\mathbf{x},\mathbf{v}} \sum_{z=1}^{N_z} v_z \hat{y}_z, \\
s.t.\ \ & v_z \geq m_i x_i + a_i, \ \ \forall i \in \mathcal{J}_z, \ \forall z, \\
& \mathbf{1}^T \mathbf{x} = d, \\
& x_i \geq 0; \ \ Q_i - x_i \geq 0, \quad \forall i, \\
& \mathbf{M}_p \mathbf{E}\mathbf{x} \leq \mathbf{b}_p.
\end{aligned}
\tag{mc-qLP}
$$

Once mc-qLP is solved, we update $\hat{\mathbf{y}} = \mathbf{E}\mathbf{x}$, and repeat the process until converged. Note that it is key to remove the constraint $\hat{\mathbf{y}} = \mathbf{E}\mathbf{x}$, to allow for updates in $\hat{\mathbf{y}}$, for else this is constant and an iterative approach cannot improve the solution. This approach is denoted as iterative quasi-LP (iq-LP).

Unfortunately, this approach is not guaranteed to converge and it can be observed that the actual objective function $\mathbf{v}^{*T}\mathbf{E}\mathbf{x}^*$ can increase from one iteration to another. To resolve this problem, instead of retaining the solution given by the last iteration, the solution with the minimum actual objective function, $\mathbf{v}^{*T}\mathbf{E}\mathbf{x}^*$, is always stored, and a maximum number of iterations, N^q_{max}, is imposed. This is described in Heuristic 9, and its aim is then not

Heuristic 9 Iterative enhanced quasi LP (ieq-LP)

Require: input (m_i, a_i) for all $i \in \cup_z \mathcal{J}_z$, maximum iterations N^q_{max}, and tolerance δ
  use an initial guess $\mathbf{y}^0 = \mathbf{d}$ or the Chebychev centre of the $(\mathbf{M}_p, \mathbf{b}_p)$ polytope
  initialise best solution as $\mathbf{x}, \mathbf{v}, \mathbf{y} \leftarrow$ None, and $f_{\text{best}} \leftarrow \infty$
  for $i \in \{1, ..., N^q_{max}\}$ **do**
    obtain $\mathbf{x}^i, \mathbf{v}^i$ by solving mc-qLP($\mathbf{y}^{i-1}$)
    obtain $\mathbf{y}^i \leftarrow \mathbf{E}\mathbf{x}^i$
    if $\mathbf{v}^{iT}\mathbf{E}\mathbf{x}^i < f_{\text{best}}$ **then**
      $f_{\text{best}} \leftarrow \mathbf{v}^{iT}\mathbf{E}\mathbf{x}^i$
      $\mathbf{x} \leftarrow \mathbf{x}^i$, $\mathbf{v} \leftarrow \mathbf{v}^i$, $\mathbf{y} \leftarrow \mathbf{y}^i$
    end if
    if $\|\mathbf{x}^i - \mathbf{x}^{i-1}\|_2^2 / \|\mathbf{x}^i\| < \delta$ **then**
      return $\mathbf{x}, \mathbf{v}, \mathbf{y}, f_{\text{best}}$
    end if
  end for
  return $\mathbf{x}$, $\mathbf{v}$, $\mathbf{y}$, f_{best}

to obtain a global or even local minimizer, but rather to quickly obtain a feasible solution that has the objective function as small as possible. We also consider the case of updating $\mathbf{y}^i$ as $\mathbf{y}^i \leftarrow \alpha_y \mathbf{y}^{i-1} + (1 - \alpha_y)\mathbf{E}\mathbf{x}^i$, with $0 < \alpha_y < 1$ which is an exponentially moving average approach, and we denote the corresponding algorithm as (ieq-LP-ma). As discussed in the numerical results section, the idea is to avoid cycling between different points by changing $\mathbf{y}^i$ *"sufficiently slow"*.

3.5.2.2 Iterative Ellipsoid Constraints Solution

The idea is analogous to the one in Section 3.4.2, but the difference is that the ellipsoid constraints are set on $\mathbf{x}$ instead of $\mathbf{y}$. Clearly, the dimensionality of $\mathbf{x}$ is much higher than that of $\mathbf{y}$, since generally we expect the number of players to be much larger than the number of zones. This will increase the computational cost, but is required to guarantee that the capacity constraints on $\mathbf{x}$ are satisfied. We begin by looking at (mc-BLP) and eliminating the zonal quantities $\mathbf{y}$, using the constraint that $\mathbf{y} = \mathbf{E}\mathbf{x}$, and obtain an analogous problem

to (mc-BLP) but with the y variables removed:

$$\begin{aligned}
&\min_{\mathbf{x},\mathbf{v}} \mathbf{v}^T\mathbf{E}\mathbf{x}, \\
&s.t.\ v_z \geq m_i x_i + a_i,\ \ \forall i \in \mathcal{J}_z,\ \ \forall z, \\
&\quad \mathbf{1}^T\mathbf{x} = d, \\
&\quad x_i \geq 0;\ \ Q_i - x_i \geq 0, \quad \forall i, \\
&\quad \mathbf{M}_p\mathbf{E}\mathbf{x} \leq \mathbf{b}_p.
\end{aligned} \tag{mc-BLP(x,v)}$$

Note that this formulation is not approximate, unlike (mc-qLP). We define $\mathbf{z}^T = (\mathbf{x}^T, \mathbf{v}^T)$, which avoids confusion with zonal indices z due to bolded vector notation, and we rearrange the system to obtain

$$\begin{aligned}
&\min \mathbf{z}^T\mathbf{G}\mathbf{z}, \\
&s.t.\ \mathbf{A}_I\mathbf{z} \leq \mathbf{b}_I, \\
&\quad \overline{\mathbf{e}}_E^T\mathbf{z} = d,
\end{aligned} \tag{mc-QP}$$

where d is the total demand, $\overline{\mathbf{e}}_E^T = (\mathbf{e}_x^T, \mathbf{0}^T) \in \mathbb{R}^{1\times(N_p+N_z)}$, with $\mathbf{e}_x \in \mathbb{R}^{N_p}$ the vector of all ones, and

$$\mathbf{G} = \begin{bmatrix} \mathbf{0} & \frac{1}{2}\mathbf{E}^T \\ \frac{1}{2}\mathbf{E} & \mathbf{0} \end{bmatrix}; \quad \mathbf{A}_I = \begin{bmatrix} \mathbf{D}_m & -\mathbf{E}^T \\ -\mathbf{I} & \mathbf{0} \\ +\mathbf{I} & \mathbf{0} \\ \mathbf{M}_p\mathbf{E} & \mathbf{0} \end{bmatrix}; \quad \mathbf{b}_I = \begin{bmatrix} -\mathbf{a} \\ \mathbf{0} \\ \mathbf{Q} \\ \mathbf{b}_p \end{bmatrix}, \tag{3.234}$$

where $\mathbf{D}_m = \text{diag}(\mathbf{m})$. One could also introduce regularisation by replacing $\mathbf{G}$ by some $\hat{\mathbf{G}} = \mathbf{G} + \text{diag}(\boldsymbol{\delta})$ for some vector $\boldsymbol{\delta} > 0$. We can observe that this problem is very similar to (e-TR), with the linear term in the objective being zero, and the ellipsoid constraints replaced by the linear constraints $\mathbf{A}_I\mathbf{z} \leq \mathbf{b}_I$. Problem (mc-QP) is difficult to solve in general, because the objective is not strictly convex (for which fast algorithms exist), but rather indefinite. However, we have seen how to solve (e-TR) before. Thus, Algorithm 8 can be applied, and an initial interior point can be obtained by using (Cheb-C). The apparent difference between $\mathbf{G}$ in (mc-QP) and $\mathbf{D}$ in (e-TR) is irrelevant, since the structure of $\mathbf{D}$ is not used to solve (e-TR) with the iterative ellipsoids approach. Further, the lack of a linear term in (mc-QP) is simply equivalent to setting $\hat{\boldsymbol{\beta}} = \mathbf{0}$ in (e-TR). The derivatives of $\mathbf{z}$ with respect to parameters can also be computed in a similar way to the approach in Section 3.4.2, although in this case the difference in the structure of $\mathbf{G}$ and $\mathbf{D}$ matters.

However, in practice we observe that the ellipsoid constraints $\|\mathbf{A}_s\mathbf{z} - \mathbf{p}_s\|_2 \leq r_s$ can

have an increasingly ill conditioned $\mathbf{A}_s$, as the solution iterate $\mathbf{x}_l^*$ approaches the boundaries of the $\mathbf{A}_I\mathbf{x} \leq \mathbf{b}_I$ polytope. This results in very little progress per outer iteration and longer solution times for an individual Trust-Region problem. To resolve this problem, when inequality constraints become *"close to equalities"* we transform these constraints to equality constraints, and search for solutions in the resulting subspace. To this end, we are now required to solve

$$\begin{aligned} &\min_{\mathbf{z}} \mathbf{z}^T\mathbf{G}\mathbf{z}, \\ &s.t.\ \|\mathbf{A}_s\mathbf{z} - \mathbf{p}_s\|_2 \leq r_s, \\ &\mathbf{M}_e\mathbf{z} = \mathbf{b}_e, \end{aligned} \tag{em-TR}$$

which can be solved perfectly analogously to how (e-TR) is solved. The KKT system is then

$$\begin{aligned} &2\mathbf{G}\mathbf{z} + \mathbf{M}_e^T\boldsymbol{\gamma} - \lambda(2\mathbf{A}_s^T\mathbf{A}_s\mathbf{z} - 2\mathbf{A}_s^T\mathbf{p}_s) = 0, \\ &\mathbf{M}_e\mathbf{z} = \mathbf{b}_e, \\ &\|\mathbf{A}_s z - \mathbf{p}_s\|_2^2 \leq r_s^2, \\ &\lambda(\|\mathbf{A}_s\mathbf{z} - \mathbf{p}_s\|_2^2 - r_s^2) = 0;\ \ \lambda \leq 0. \end{aligned}$$

The first solution step is to then solve

$$\begin{pmatrix} \mathbf{z}^* \\ \boldsymbol{\gamma}^* \end{pmatrix} = \begin{pmatrix} 2\mathbf{G} & \mathbf{M}_e^T \\ \mathbf{M}_e & \mathbf{0} \end{pmatrix}^{-1} \begin{pmatrix} \mathbf{0} \\ \mathbf{b}_e \end{pmatrix}. \tag{3.235}$$

If $\|\mathbf{A}_s\mathbf{z}^* - \mathbf{p}_s\|_2 > r_s$, then the solution must be on the ellipsoid boundary and we can write

$$\begin{pmatrix} \mathbf{z} \\ \boldsymbol{\gamma} \end{pmatrix} = \begin{pmatrix} 2\mathbf{G} - 2\lambda\mathbf{A}_s^T\mathbf{A}_s & \mathbf{M}_e^T \\ \mathbf{M}_e & \mathbf{0} \end{pmatrix}^{-1} \begin{pmatrix} -2\mathbf{A}_s^T\mathbf{p}_s\lambda \\ \mathbf{b}_e \end{pmatrix}, \tag{3.236}$$

and as before, let us denote

$$\hat{\mathbf{D}}(\lambda) := \begin{pmatrix} 2\mathbf{G} - 2\lambda\mathbf{A}_s^T\mathbf{A}_s & \mathbf{M}_e^T \\ \mathbf{M}_e & \mathbf{0} \end{pmatrix};\quad \mathbf{u}(\lambda) := \begin{pmatrix} -2\mathbf{A}_s^T\mathbf{p}_s\lambda \\ \mathbf{b}_e \end{pmatrix}. \tag{3.237}$$

We know that $\|\mathbf{A}_s\mathbf{z} - \mathbf{p}_s\|_2^2 = r^2$ and thus we have that $f(\lambda) = \frac{1}{||\mathbf{A}_0\hat{\mathbf{D}}(\lambda)^{-1}\mathbf{u}(\lambda) - \mathbf{p}||_2^2} - \frac{1}{r^2} = 0$, which is a one dimensional problem that can be solved with Newton-Raphson. Finally, if

the equality system $\mathbf{M}_e\mathbf{z} = \mathbf{b}_e$ becomes full rank, there is no need to continue, as a unique solution exists, and this can be computed as $\mathbf{z}^* = (\mathbf{M}_e^T\mathbf{M}_e)^{-1}\mathbf{M}_e^T\mathbf{b}_e$. The algorithm for obtaining the market solution is described in Algorithm 10 where $||_v$ represents vertical concatenation of matrices or vectors.

Algorithm 10 ie-CQP with reconditioning (ie-CQP-wr)

Require: input (m_i, a_i, Q_i) for all $i \in \cup_z \mathcal{J}_z$, maximum number of iterations N_{max}, total demand d, convergence tolerance δ, and boundary tolerance δ_B.
  compute the Chebychev centre $\mathbf{z}_c$ of the $(\mathbf{A}_I, \mathbf{b}_I)$ polytope.
  initialise $\mathbf{M}_e \leftarrow (\mathbf{1}_{N_p}^T, \mathbf{0}_{N_z}^T)$, $\mathbf{b}_e \leftarrow d$
  for $k \in \{1, ..., N_{max}\}$ **do**
    obtain $\mathbf{A}_s, \mathbf{p}_s, r_s \leftarrow \text{EL}(\mathbf{z}_c, \mathbf{A}_I, \mathbf{b}_I)$ as described in Section 3.4.5
    obtain $\mathbf{z}_i^*$ (and derivatives) by solving the (em-TR) problem, using ellipsoid $(\mathbf{A}_s, \mathbf{p}_s, r_s)$
    compute $\Delta z = \|\mathbf{z}_k^* - \mathbf{z}_c\|_2$
    if $\Delta z < \delta$ **then**
      return $\mathbf{z}_k^*$, Δz
    end if
    $\mathbf{z}_c \leftarrow \mathbf{z}_k^*$
    let $\mathcal{L} := \overline{1, \dim(\mathbf{b}_I)}$, $\mathcal{E} := \{l : (\mathbf{b}_I)_l - (\mathbf{A}_I)_{l,:}\mathbf{z}_k^* < \delta_B, l \in \mathcal{L}\}$
    $\mathbf{A}_I \leftarrow \mathbf{A}_I[\mathcal{L} \setminus \mathcal{E}, :]$, $\mathbf{b}_I \leftarrow \mathbf{b}_I[\mathcal{L} \setminus \mathcal{E}]$
    $\mathbf{M}_e \leftarrow ||_v(\mathbf{M}_e, \mathbf{A}_I[\mathcal{E}, :])$, $\mathbf{b}_e \leftarrow ||_v(\mathbf{b}_e, \mathbf{b}_I[\mathcal{E}])$
    if $\text{rank}(\mathbf{M}_e) = \dim(\mathbf{z})$ **then**
      $\mathbf{z}_k^* \leftarrow (\mathbf{M}_e^T\mathbf{M}_e)^{-1}\mathbf{M}_e^T\mathbf{b}_e$, $\Delta z \leftarrow \|\mathbf{z}_k^* - \mathbf{z}_c\|_2$
      return $\mathbf{z}_k^*$, Δz
    end if
  end for
  return $\mathbf{z}_k^*$, Δz

3.5.2.3 Branch and Bound Tree Based Solution

The intuition behind using a Branch and Bound approach can be understood by looking at (mc-BLP) and observing that if $\mathbf{y}$ was known, the problem becomes an LP which is easy to solve. Thus, one might consider trying *all the possible values* for $\mathbf{y}$, solve the corresponding LP with fixed $\mathbf{y}$, and retain the solution with the minimum objective value. However, since $\mathcal{P}(\mathbf{y})$ is a continuous space, the number of values of $\mathbf{y}$ to try is infinite. One could consider a discretisation but even for $N_z = 5$, and the number of discretisation points for each zone $N_{dc} = 10$, the number of problems to be solved is $N_{dc}^{N_z} = 10^5 = 100,000$ which is prohibitively large.

Therefore, a Branch and Bound Tree (BBTree) based approach is proposed here, that leverages more information about the problem to *try to group similar* $\mathbf{y}$ *subspaces together*, such that early elimination of sub-optimal $\mathbf{y}$ values is possible. For the BBTree approach the following are required:

1. a method to compute an upper bound (UB) of the optimal solution on the feasible (sub-)space given,
2. a method to compute a lower bound (LB) on the given feasible (sub-)space,
3. a method to branch (split) the feasible (sub-)space considered into at least two regions, ideally in such a way to facilitate rapid elimination of sub-optimal (sub-)spaces,
4. and a rule to choose the next tree node (defined by its feasible subspace), which is then to be processed.

Obtaining an Upper Bound (UB) on a feasible subspace given by $(\mathbf{M}_p^j, \mathbf{b}_p^j)$ at node j is achieved by using Heuristic 9 (ieq-LP). Since the resulting solution is feasible, it offers an upper bound on the optimal objective. This approach is used because it is fast, and it has been observed that often times it obtains a local or even global minimum. While this is not a guarantee, it is a useful property, since Heuristic 9 (ieq-LP) is called many times inside BBTree, once for each node, and therefore achieving a tight UB often, helping with pruning. Using Algorithm 10 (ie-CQP) to obtain an UB was also considered, but the computational time is significantly increased, and the increased UB tightness does not compensate for this, generally yielding a much slower BBTree when using ie-CQP when compared to ieq-LP. The UB for a tree node j is thus updated as $f_{\text{UB}}(j) \leftarrow f_{\text{best}}(\text{ieq-LP}(j))$, and the corresponding quantities and prices returned by ieq-LP(j) are denoted as $\mathbf{x}_{\text{sol}}(j)$, $\mathbf{v}_{\text{sol}}(j)$, $\mathbf{y}_{\text{sol}}(j)$.

Obtaining a Lower Bound (LB) that is fast to compute and tight is rather challenging since it requires solving a (sufficiently) simplified problem that guarantees a (tight) lower bound. Multiple approaches were tried, but a variation of McCormick envelopes [61] appeared to perform best. To obtain the McCormick envelopes, we first need to compute $v_z^{\min}$, $v_z^{\max}$, $y_z^{\min}$, $y_z^{\max}$, for each zone z, and this can be achieved by solving the LP obtained by replacing the objective in (mc-BLP) with v_z, $-v_z$, y_z and $-y_z$. The resulting problems are indeed LPs since both the objective and constraints are linear and we denote them by LP-vm$(z, \mathbf{M}_p^j, \mathbf{b}_p^j)$, LP-vM$(z, \mathbf{M}_p^j, \mathbf{b}_p^j)$, LP-ym$(z, \mathbf{M}_p^j, \mathbf{b}_p^j)$, LP-yM$(z, \mathbf{M}_p^j, \mathbf{b}_p^j)$ respectively, and let us denote by LPVY$(z, \mathbf{M}_p^j, \mathbf{b}_p^j)$ the process of computing all four quantities. Note that the problems for $\mathbf{y}^{\min}$ and $\mathbf{y}^{max}$ can be further simplified by using that $\mathbf{Ex} = \mathbf{y}$ and removing all the other constraints for $\mathbf{x}$, as well as removing $\mathbf{v}$.

The McCormick envelopes can now be obtained by using that given

$$v_z^{min} \leq v_z \leq v_z^{max}, \tag{3.238}$$

$$y_z^{min} \leq y_z \leq y_z^{max}, \tag{3.239}$$

we have that

$$v_z y_z \geq v_z^{min} y_z + y_z^{min} v_z - v_z^{min} y_z^{min} =: w_z^{LB,1}, \tag{3.240}$$

$$v_z y_z \geq v_z^{max} y_z + y_z^{max} v_z - v_z^{max} y_z^{max} =: w_z^{LB,2}, \tag{3.241}$$

and so by summing over all zones we get that

$$\sum_z v_z y_z \geq w_z^{LB,1}; \quad \sum_z v_z y_z \geq w_z^{LB,2} \tag{3.242}$$

and by taking the maximum

$$\sum_z v_z y_z \geq \max \left\{ \sum_z w_z^{LB,1}, \sum_z w_z^{LB,2} \right\}. \tag{3.243}$$

A tighter bound could be obtained as

$$\sum_z v_z y_z \geq \max \sum_z \left\{ w_z^{LB,1}, w_z^{LB,2} \right\}, \tag{3.244}$$

but then the resulting problem is a Mixed Integer Linear Program (MILP) instead of LP, which is much harder to solve. Note that v_z^{min}, v_z^{max}, y_z^{min} and y_z^{max} are a function of $\mathbf{M}_p^j$ and $\mathbf{b}_p^j$ and thus are updated for each node j. Given the bounds on y and v, one can now compute the lower bounds on the objective over the domain $(\mathbf{M}_p^j, \mathbf{b}_p^j)$ as

$$\begin{aligned} \min_{\mathbf{x},\mathbf{v},\mathbf{y},\mathbf{w}^{LB,l}} \; & \sum_{z=1}^{N_z} w_z^{LB,l}, \\ s.t. \; & \mathbf{y} = \mathbf{E}\mathbf{x}, \\ & v_z \geq m_i x_i + a_i, \;\; \forall i \in \mathcal{J}_z, \; \forall z \\ & \mathbf{1}^T \mathbf{x} = d, \\ & x_i \geq 0; \;\; Q_i - x_i \geq 0, \quad \forall i, \\ & \mathbf{M}_p \mathbf{E}\mathbf{x} \leq \mathbf{b}_p, \end{aligned} \tag{Env-LP(l)}$$

for $l \in \{1, 2\}$. The lower bound for node j is then updated as $f_{\text{LB}}(j) = \max \left\{ \sum_z w_z^{LB,1}, \sum_z w_z^{LB,2} \right\}$.

Branching at a Node is a key component to facilitate fast pruning and therefore convergence speed. Branching is achieved in three steps, as explained below:

1. Compute the Chebyshev centre $\mathbf{y}_c(j)$ of node j, and the corresponding radius $r_c(j)$ using (Cheb-C). This point is chosen such that the size of the two resulting branches are balanced.

2. Determine a cutting plane, which is chosen by finding a *"global"* descent direction $\mathbf{s}_D(j)$ and cutting at $\mathbf{y}_c(j)$ via a hyperplane perpendicular to it. The intuition behind choosing such a direction is that if the objective function is approximately linear, then the branch including all points containing negative directions along $\mathbf{s}_D(j)$ should be pruned fast, as its LB is expected to be higher than the UB of the other branch.

3. Perform the cut and form the new branches.

The mathematics required to perform these steps is now explained. Finding the Chebyshev centre was already explained in (Cheb-C). The *"global descent"* direction is obtained as

$$s_D = \frac{1}{\|\mathbf{y}_{\text{sol}}(j) - \mathbf{y}_c(j)\|} \left(\mathbf{y}_{\text{sol}}(j) - \mathbf{y}_c(j)\right). \tag{3.245}$$

Using the local steepest descent at $y_c(j)$ was considered, but based on numerical experiments we observe that the cutting plane is rather ineffective, and the BBTree algorithm makes much slower progress in this case. Plane cutting is then performed by splitting the domains as

$$\mathcal{P}_1^j := \{\mathbf{y} : (\mathbf{y} - \mathbf{y}_c(j))^T \mathbf{s}_D \geq 0\}; \quad \mathcal{P}_2^j := \{\mathbf{y} : (\mathbf{y} - \mathbf{y}_c(j))^T \mathbf{s}_D \leq 0\}, \tag{3.246}$$

where the subscripts on $\mathcal{P}^j$ refer to child 1 and 2 of node j. This results in the need to add the following constraint line to each of the two branches:

$$\mathbf{M}_p^j(l) \begin{bmatrix} \mathbf{M}_p^j \\ (-1)^l \mathbf{s}_D(j)^T \end{bmatrix}; \ \mathbf{b}_p^j(l) = \begin{bmatrix} \mathbf{b}_p^j \\ (-1)^l \mathbf{s}_D(j)^T \mathbf{y}_c(j) \end{bmatrix}, \tag{3.247}$$

for $l = \{1, 2\}$. Algorithm 11 describes computing the required node quantities.

Algorithm 11 Compute Node Quantities (CNQ)

Require: input (m_i, a_i) for all $i \in \cup_z \mathcal{J}_z$, $(\mathbf{M}_p^j, \mathbf{b}_p^j)$, and domain size tolerance r_δ
  compute the Chebychev centre $y_c(j)$ and the radius $r_c(j)$ of the $(\mathbf{M}_p, \mathbf{b}_p)$ polytope.
  compute $\mathbf{x}_{\text{UB}}$, $\mathbf{v}_{\text{UB}}$, $\mathbf{y}_{\text{UB}}$ and f_{UB} as per ieq-LP, given $(\mathbf{M}_p^j, \mathbf{b}_p^j)$ as polytope constraints.
  $\mathbf{x}_{\text{sol}} \leftarrow \mathbf{x}_{\text{UB}}$, $\mathbf{v}_{\text{sol}} \leftarrow \mathbf{v}_{\text{UB}}$, $\mathbf{y}_{\text{sol}} \leftarrow \mathbf{y}_{\text{UB}}$
  if $r_c < r_\delta$ **then**
    set LB values to the UB values (since the distance $|\mathbf{y}_{\text{sol}} - \mathbf{y}_{opt}|$ must be very small)
  else
    for all z compute $(\mathbf{v}_z^{\min}, \mathbf{v}_z^{\max}, \mathbf{y}_z^{\min}, \mathbf{y}_z^{\max})$ via LPVY$(z, \mathbf{M}_p^j, \mathbf{b}_p^j)$
    compute $\mathbf{x}_{\text{LB}}$, $\mathbf{v}_{\text{LB}}$, $\mathbf{y}_{\text{LB}}$, f_{LB} via (Env-LP(l)), with $l = \{1, 2\}$
  end if
  $\mathbf{s}_D(j) \leftarrow \frac{1}{\|\mathbf{y}_{\text{sol}}(j) - \mathbf{y}_c(j)\|} \left(\mathbf{y}_{\text{sol}}(j) - \mathbf{y}_c(j)\right)$
  compute branching domains for children, $(\mathbf{M}_p^j(l), \mathbf{b}_p^j(l)$ as per (3.247)
  store all computed quantities at node level

Choosing the next node to process is also important in achieving convergence speed. The considerations for deciding which node to process next are: (i) not to neglect any leaf for a very large number of iterations, relative to the number of active leaves generated before it, (ii) to reduce the global UB *"as much as possible"*, (iii) to increase the global LB *"as much as possible"*, and (iv) to explore new leaves to avoid getting stuck in a bad pattern. To this end, node choice is performed as follows, although the exact percentages could be changed:

- Choose the oldest active (yet unprocessed and unpruned) leaf, 60% of the time. This is because the oldest active leaf is expected to be amongst the largest based on feasible domains, and thus it might include the global minimum with higher likelihood.
- With 10% probability, choose the node that contains the incumbent (best available solution) to be processed if it is a leaf. Note that unless ieq-LP fails to achieve solutions at least as good as the parent for the children, the incumbent must be a leaf. Non-leaf incumbent was observed almost not at all, but the implementation of the algorithm safeguards against branching an already branched node.
- With 20% probability, choose the node with the lowest global LB, to try to maximise the lower bound and therefore reduce the optimality gap. More time is spent on the LB, as in practice we observe that the UB is significantly tighter than the LB.
- With 10% probability, choose uniformly at random an active leaf.

We call this rule the Randomised Node Selection rule (RNS). The pseudocode for the BBTree is presented in Algorithm 12.

Algorithm 12 Branch and Bound Tree (BBTree)

Require: input (m_i, a_i, Q_i) for all $i \in \cup_z \mathcal{J}_z$, demand vector d, $\mathbf{E}$, $(\mathbf{M}_p, \mathbf{b}_p)$, domain size tolerance r_δ, optimality gap δ_o
  initialise root $\mathcal{R}_n$ of tree $\mathcal{T}$, on whole domain by calling CNQ$(\mathbf{M}_p, \mathbf{b}_p)$
  set the active set of leaves $\mathcal{L}_A = \{\mathcal{R}_n\}$, $\delta_T \leftarrow \infty$
  while $\delta_T > \delta_o$ **do**
    choose pointer p to branch at, based on the RNS rule,
    use CNQ to process both nodes (branches) generated by pointer p
    $\mathcal{L}_A \leftarrow \mathcal{L}_A \cup \{c_p^1\} \cup \{c_p^2\} \setminus \{p\}$, where c_p^l are the children of p.
    update global upper bound $f_{\text{UB}}^G \leftarrow \min\{f_{\text{UB}}(j) : j \in \mathcal{L}_A\}$, and retain best node s_n
    update global lower bound $f_{\text{UB}}^G \leftarrow \min\{f_{\text{LB}}(j) : j \in \mathcal{L}_A\}$ and retain lowest lower bound node l_n
    for all active leaves $j \in \mathcal{L}_A$ remove node j from active leaves if $f_{\text{LB}}(j) > f_{\text{UB}}^G$.
    compute $\delta_T = 2(f_{\text{UB}}^G - f_{\text{LB}}^G)/(f_{\text{UB}}^G + f_{\text{LB}}^G)$
  end while
  fetch x_{best}, y_{best}, v_{best}, f_{best} based on best current node s_n,
  return x_{best}, y_{best}, v_{best}, f_{best}, δ_T

3.5.2.4 Iteratively Bounded Convex Quadratic Programming solution (ib-CQP)

The intuition behind this method is that for each zone, the price function $v_z(y_z^*)$ is piecewise linear at optimality. This can be understood as following: if there are no capacity constraints, we have seen that the optimal price takes the form $v_z^* = \alpha_z y_z + \beta_z$. Thus, the same must be true if solving over regions of $\mathbf{x} \in \mathcal{X}$ (that map to regions over $\mathbf{y} \in \mathcal{Y}$), where no capacity constraints change state - that is, player sets $\mathcal{P}_z^I := \{i \in \mathcal{Z} : x_i = 0\}$, $\mathcal{P}_z^M := \{i \in \mathcal{Z} : 0 < x_i < Q_i\}$ and $\mathcal{P}_z^F := \{i \in \mathcal{Z} : x_i = Q_i\}$ remain unchanged within each of these sub-domains of $\mathcal{X}$. For such a sub-domain players in $\mathcal{P}_z^I$ can be simply disregarded, while players in $\mathcal{P}_z^F$ can be eliminated by reducing the production levels as $\hat{y}_z = y_z - \sum_{i \in \mathcal{P}_z^F} Q_i$. When these three player sets change, a change may occur in the price function, but this still remains linear between change points. However, by considering $v(y)$, it is not trivial to devise a method to directly find the three $\mathcal{P}_z^{\cdot}$ sets for each y in a computationally efficient way. For this reason we propose an alternative view, that enables making analytical progress: instead of trying to compute $\mathbf{v}(\mathbf{y})$ for fixed y at optimality, let us fix $\mathbf{v}$, and compute the corresponding optimal $\mathbf{x}$ and $\mathbf{y}$. This might seem naive or counter-intuitive at first, as $\mathbf{v}$ is perhaps the variable that has the greatest impact on the objective.

However, this way of thinking allows us to make the following observation: for each zone, if the corresponding v_z^* is the optimal value, then it has to be that (for $\forall i \in \mathcal{Z}$): (i) a player has $a_i > v_z^*$ if and only if it belongs to the inactive set, $i \in P_z^I$, (ii) a player does not sell at full capacity ($i \in \mathcal{P}_z^M$) if and only if $v_z = \lambda_i$, and (iii) a player sells at full capacity ($i \in \mathcal{P}_z^F$) if and only if $v_z \geq \lambda_i$. Note that the exact location of placing the equality signs is somewhat irrelevant. By computing the maximum price that a player asks for, $\lambda_i^{max} = m_i Q_i + a_i$ we

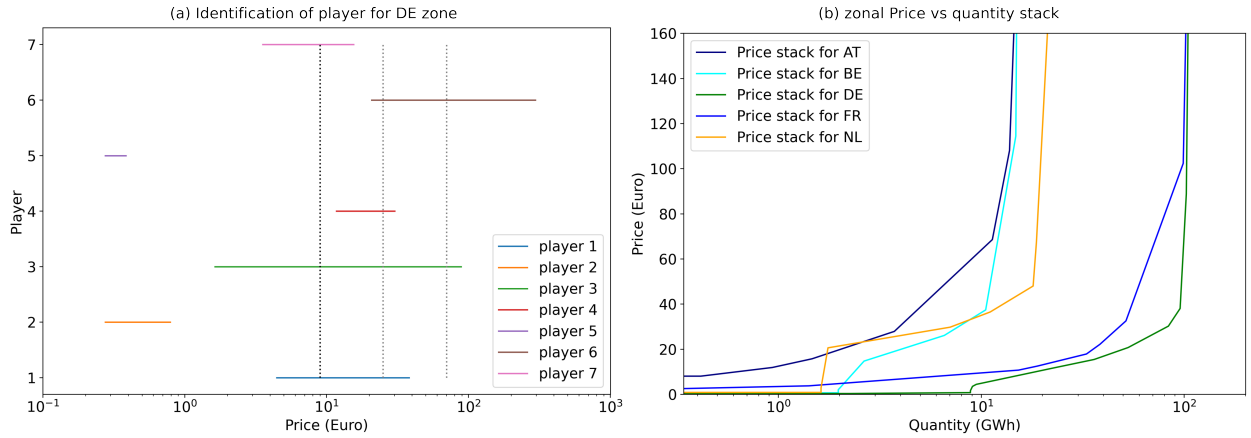


Figure 3.6: Obtaining the optimal price function: (a) visualisation of player sets identification, and (b) the resulting (optimal) zonal stack curves

can re-state the result in the following simplified form. At optimality we must have that (for all $i \in \mathcal{Z}$): (i) $v_{z_i} > a_i$ if and only if $x_i = 0$, (ii) $a_i \leq v_{z_i} < m_i Q_i + a_i$ if and only if $0 < x_i < Q_i$, and (iii) $v_{z_i} \geq m_i Q_i + a_i$ if and only if $x_i = Q_i$. This makes identifying the three player sets trivial for each v_z. The value of v_z can then be swept across $[0, \max_{i \in \mathcal{J}_z} \lambda_i^{max}]$

to obtain all discontinuity points, as illustrated in Figure 3.6 (a). The price range shown for each player is the the range of market clearing prices for which the player is effectively on the margin and thus impacts the price (makes the price), if the market clearing price is lower than the lowest point in the range, the player is out of the market, while a clearing price above the highest end of the range means that the player is selling at full capacity.

In fact, one can simply get all price points $\mathcal{V}_z := \{a_i : i \in \mathcal{Z}\} \cup \{m_i Q_i + a_i : i \in \mathcal{Z}\} \cup \{0\}$, sort them and then compute the player set for each interval only when required. By using the results from the Section 3.4.2, for each $\nu_z \in \mathcal{V}_z^D$, one can obtain the corresponding y_z value as

$$y_z(\nu_z) = (\nu_z - \beta_z(\nu_z))/\alpha_z(\nu_z) + \sum_{i \in \mathcal{P}_z^F(\nu_z)} Q_i, \tag{3.248}$$

where $\mathcal{P}_z^F(\nu_z) := \{i \in \mathcal{Z} : \nu_z > m_i Q_i + a_i\}$ is the player set in zone z that has the maximum offered price below the current price ν_z, and $\alpha_z(\nu_z))$ and $\beta_z(\nu_z))$ are computed as per Section 3.4.2, equations (3.83), (3.82), by assuming the player set to be $\mathcal{J}_z \leftarrow \mathcal{P}_z^M(\nu_z) := \{i \in \mathcal{Z} : a_i < \nu_z < m_i Q_i + a_i\}$. Let us denote the point set of all $y_z(\nu_z)$ corresponding to $\mathcal{V}_z^D$ as $\mathcal{Y}_z^D$. Let us further denote the total production offered by players in zone z at full capacity as $Q_z^s(\mathcal{Y}_z^D) = \sum_{i \in \mathcal{P}_z^F(\nu_z)} Q_i$. Note that there is a one-to-one mapping between the two sets. Thus, for each y_z, we can find y_z^L and y_z^U such that $y_z^L \leq y_z < y_z^U$, with $y_z^L, y_z^U \in \mathcal{Y}_z^D$, and let us denote this interval $\mathcal{Y}_z^I(y_z)$. Further we can now obtain the $\alpha_z(\mathcal{Y}_z^I(y_z))$ and $\beta_z(\mathcal{Y}_z^I(y_z))$ corresponding to the $\mathcal{Y}_z^I(y_z)$ interval. Note that $\alpha_z(\mathcal{Y}_z^I(y_z))$ and $\beta_z(\mathcal{Y}^I(y_z))$ are fixed on each interval. This gives us the outstanding property that the cost minimisation objective $\sum_z v_z y_z$ is in fact piece-wise quadratic. Given any $\mathcal{Y}^I = \cup_z \mathcal{Y}_z^I$, the objective function can be exactly expressed for any $y \in \mathcal{Y}^I$ as

$$\sum_z v_z y_z = \alpha_z(\mathcal{Y}_z^I) y_z^2 + \left[\beta_z(\mathcal{Y}_z^I) - \alpha_z(\mathcal{Y}_z^I) Q_z^s(\mathcal{Y}_z^I)\right] y_z \tag{3.249}$$

when optimality over $\mathbf{x}_z$ s.t. $\mathbf{x}_z$ satisfies $\mathbf{1}^T \mathbf{x}_z = y_z$ and the capacity constraints. This is a rather remarkable result that allows us to solve strictly convex quadratic problems over polytope constraints, which are fast to solve [34]. By constraining $\mathbf{y} \in \mathcal{Y}^I$ plugging in (3.249) in mc-BLP and removing the already optimised $\mathbf{x}$ variables, we obtain

$$\begin{aligned} &\min_y \sum_{z=1}^{N_z} \alpha_z(\mathcal{Y}_z^I) y_z^2 + \left[\beta_z(\mathcal{Y}_z^I) - \alpha_z(\mathcal{Y}_z^I), Q_z^s(\mathcal{Y}_z^I)\right] y_z, \\ &s.t. \quad \mathbf{M}_p \mathbf{y} \leq \mathbf{b}_p; \quad \mathbf{y} \in \mathcal{Y}^I; \quad \mathbf{1}^T \mathbf{y} = d, \end{aligned} \tag{sub-CQP($\mathcal{Y}^I$)}$$

which is a much simpler problem to solve since $\mathcal{Y}^I$ is just a box constrained domain. The naive way of obtaining the global solution would then be to solve sub-CQP($\mathcal{Y}^I$) for all possible $\mathcal{Y}^I$, and simply choose the best solution. However, their number can be fairly large.

For the real world case of CWE, we observe about 11 (including $(0, 0)$) discontinuity points per zone, giving about $10^5 = 100,000$ combinations which is extremely large. This is in fact much more computationally expensive than the BBTree approach, that also guarantees global convergence. However, a compromise can be obtained by iteratively updating the considered box location $\mathcal{Y}^I$ based on the previous result. The solution idea is as follows:

1. Pick a feasible $\mathbf{y}$, and solve sub-CQP($\mathcal{Y}^I$) over the $\mathcal{Y}^I$ interval,

2. if for any zone z the corresponding optimal y_z^* is on the boundary, then switch the bounds to be the other set of bounds $\mathcal{Y}_z^{I\prime}$ that includes y_z^*. For example imagine that the initial domain for y_z was $[y_z^{l_1}, y_z^{u_1}]$ and the next domain in increasing order is $[y_z^{l_2}, y_z^{u_2}]$ (with $y_z^{l_2} = y_z^{u_1}$). Then if the optimal solution with the $[y_z^{l_1}, y_z^{u_1}]$ bound gives $y_z^* = y_z^{u_1}$, the interval to solve over at the next iteration is updated to $[y_z^{l_2}, y_z^{u_2}]$. Interval updates for all zones are performed simultaneously if necessary.

3. Iterate until the optimal solution over some $\mathcal{Y}_z^{I\prime}$ lies strictly inside the domain, or the change in y between two consecutive (outer) iterations is zero.

Note that in a strict sense, this approach does not guarantee global convergence, but it guarantees something close: global convergence over the domain $\mathcal{Y}^I$ in which the solution y^* lies. This is a much stronger result than purely local convergence, although not as strong as purely global convergence. We refer to this type of optimality as sub-domain optimal, to distinguish it from the weaker counterpart of purely local optimality.

Algorithm 13 Iteratively Bounded CQP(ib-CQP)

Require: input (m_i, a_i) for all $\forall i$, $(\mathbf{M}_p, \mathbf{b}_p)$, and demand d.
compute the Chebychev centre $\mathbf{y}_c$ and the radius r_c of the $(\mathbf{M}_p, \mathbf{b}_p)$ polytope.
$\mathbf{y} \leftarrow \mathbf{y}_c$ and set $\Delta y = 1$
while $\Delta y > 0$ **do**
get the domain $\mathcal{Y}^I$ that contains $\mathbf{y}$ and the corresponding α, β
obtain $\mathbf{y}'$ and $\mathbf{v}'$ by solving sub-CQP($\mathcal{Y}^I$) and compute $\delta y = \|\mathbf{y} - \mathbf{y}'\|_2$
$\mathbf{y} \leftarrow \mathbf{y}'$, $\mathbf{v} \leftarrow \mathbf{v}'$
If $\mathbf{y}'$ not on boundary of $\mathcal{Y}^I$, **then** break
update $\mathcal{Y}^I$ for all z where y_z is on the boundary
end while
use equation (3.80) to compute $\mathbf{x}$ knowing $\mathbf{y}$, $\mathbf{v}$ and the active player set $\mathcal{P}^F \cup \mathcal{P}^M$
return $\mathbf{x}$, $\mathbf{y}$, $\mathbf{v}$

Note that since sub-CQP($\mathcal{Y}^I$) makes no assumption with regards to the set of active players, this is obtained as part of the solution, instead of requiring any assumption or pre-computation as for the previously devised methods. This is a great advantage over the other proposed methods. However, as we discuss in Subsection 3.5.5, we also propose rather efficient methods to obtain the active player set for the other three approaches.

3.5.3 Coupled and Decoupled Market Outcomes

So far we looked at the situation where each zone has an individual zonal price, that is to say, the market is decoupled. Market decoupling given a solution $(\mathbf{x}, \mathbf{v}, \mathbf{y})$, refers to the situation where power exchanges between at least two zones cannot be adjusted in both directions, without violating the network constraints. In this case, different zonal prices are to be set. If market decoupling does not occur, then a single electricity price is set across the entire network. For the case of inflexible demand, as considered here, the price-decoupling case is by far the more challenging one, while the coupled case can be obtained by simply solving an LP. If the market outcome is coupled, then all zones have the same price v. Assuming that the market outcome is coupled, the resulting market clearing problem becomes

$$\begin{aligned} &\min_{\mathbf{x},v} \; v\mathbf{1}^T\mathbf{x} = vd, \\ &s.t \;\; x_i \geq 0; \;\; Q_i - x_i \geq 0, \quad \forall i, \\ &\quad \mathbf{M}_p\mathbf{E}\mathbf{x} \leq \mathbf{b}_p; \quad \mathbf{1}^T\mathbf{x} = d, \\ &\quad v - m_i x_i - a_i \geq 0; \quad \forall i \in \mathcal{J} := \cup_z \mathcal{J}_z, \end{aligned} \tag{3.250}$$

which is just a linear program since $\mathbf{1}^T\mathbf{x} = d$ and so the objective can be written simply as v, since d is a constant. The idea of the market clearing solution process is to start by assuming that the market outcome is coupled, and solve the corresponding problem. Let us denote this solution as $v^{*,c}$ and $\mathbf{x}^{*,c}$, where the star indicates optimality and the superscript c indicates that the solution is optimal for the coupled problem. If there exists one active PTDF-RAM constraint, i.e. if $\min_j\{[\mathbf{b}_p]_j - [\mathbf{M}_p\mathbf{x}^{*,c}]_j\} = 0$, then we know that the solution is not coupled, and we proceed by solving the decoupled problem, (mc-BLP), described in detail before, using any of the methods described before. Otherwise, if $\min_j\{[\mathbf{b}_p]_j - [\mathbf{M}_p\mathbf{x}]_j\} > \delta_{tol}$ for some small tolerance $\delta_{tol} > 0$, then the market clearing solution is coupled, and we are done, not requiring solving (mc-BLP). This case is fortunate, because we only need to solve an LP to obtain the market clearing solution, as opposed to using the ieq-LP method, the ie-CQP method, or the BB-Tree method, all of which require solving multiple LPs or Trust region like problems, with different trade-offs between computational speed and convergence guarantees.

3.5.4 Robust Strategy Selection as a Risk Aversion Model

It is apparent that the multiplicity of equilibria is a result of the fact that players have *"too much choice"*. Strategising over $(\mathbf{m}, \mathbf{a})$ instead of only a increases the strategy space but does not intensify the competition accordingly. A rational player may recognize that due to multiplicity of equilibria, playing a Nash Equilibrium strategy does not guarantee that

the outcome will correspond to this particular equilibrium point. Since negative profits are possible when players play different Nash Equilibria strategies (if $m_i < c_i$ or $a_i < b_i$), a risk averse player may take extra precautions in selecting the strategy played. First, they could observe that playing strategies only of the form $\mathcal{S}_R(i) = \{(m_i, a_i) : m_i \geq \frac{1}{2}c_i,\ a_i \geq b_i\}$, would guarantee that the profit is non-negative as per Result 3.5.1.

Result 3.5.1. *Under the market clearing given by* (bl-BLP)*, player i is guaranteed non-negative profit by playing any $\sigma_i \in \mathcal{S}'_R(i) := \{(m_i, a_i) : m_i \geq \frac{1}{2}c_i,\ a_i \geq b_i\}$, for any $(\mathbf{m}_{-i}, \mathbf{a}_{-i})$.*

Proof. If the player plays strategy $\sigma_i \in \mathcal{S}_R(i)$ and he is out of the market ($x_i = 0$), then $\pi_i = 0 \geq 0$. Let us consider the case of $x_i > 0$. By definition of $v_{z_i} = \max\{m_j x_j + a_j : x_j > 0; j \in \mathcal{P}_{z_i}\}$ and since $i \in \mathcal{P}_{z_i}$, $x_i > 0$ we have that the profit of player i can then be lower bounded as

$$\pi_i = v_{z_i} x_i - \frac{1}{2}c_i x_i^2 - b_i x_i \geq \left[(2m_i - c_i)x_i + (a_i - b_i)\right] x_i \tag{3.251}$$

where the inequality comes by using that $v_{z_i} \geq m_i x_i + a_i$. Since $x_i \geq 0$ is guaranteed by (bl-BLP), and $m_i \geq \frac{1}{2}c_i$, $a_i \geq b_i$ by the fact that $(m_i, a_i) \in \mathcal{S}_R(i)$, we conclude that $\pi_i \geq 0$. The choice of $\mathbf{m}_{-i}$ and $\mathbf{a}_{-i}$ is absolutely irrelevant for the argument, and thus this must be the case for any such values. □

Next, the player could assign probabilities to every possible combination of equilibrium strategies that a player may play, and maximise the expected (risk adjusted) profit. However, estimating such probabilities is a very difficult task and wrong estimation could have a detrimental impact on the actual outcome. Thus, instead of considering a mean-variance approach that adjusts the utility function to account for risk, a conservative player may wish to first ensure a minimum profit level in a *worst case scenario*. Note that according to Result 3.5.1, such a guarantee with non-negative profit is always possible. If multiple equivalent such strategies exist, then the player may use this choice to maximise his actual profit (as opposed to the worst case). Further, let us assume that all players behave in this way, and that this is common knowledge. The worst case optimisation problem is then

$$\max_{\sigma_i \in \mathcal{S}_R(i)} \min_{\sigma_{-i} \in \mathcal{S}_R(-i)} \pi_i(\sigma_i; \sigma_{-i}), \tag{WCP(i))}$$

and let us denote $\mathcal{B}_{LB}(i)$ the set of all solutions to (WCP(i)). The advantage of this approach is the lack of parameters or required estimates, at least when assuming complete information. Unfortunately (WCP(i)) is very difficult to solve since an analytical form for π_i as a function of strategy vector σ cannot generally be obtained under the (bl-BLP) market clearing model. Due to (bl-BLP) yielding the value of π_i, (WCP(i)) is a tri-level optimisation problem. Solving this is clearly very challenging. However, players may be willing to simplify (WCP(i)) to enable for progress, to at least estimate strategies that perform well

under the *worst case*. One such simplification would be to consider ignoring the capacity and network constraints. As we shall see, this allows for an analytic closed form for the resulting optimal set of strategies $\mathcal{B}_{LB}(i)$.

Let us now look at how this simplifies the problem. To begin with, under these assumptions we have a unique price that satisfies

$$v = m_i x_i + a_i, \ \forall i : x_i > 0. \tag{3.252}$$

By taking derivatives of π_i with respect to a_j and m_j for any $j \neq i$ we get that

$$\begin{aligned} \frac{\partial \pi_i}{\partial a_j} &= [(2m_i - c_i)x_i + (a_i - b_i)] \frac{\partial x_i}{\partial a_j}, \\ \frac{\partial \pi_i}{\partial m_j} &= [(2m_i - c_i)x_i + (a_i - b_i)] \frac{\partial x_i}{\partial m_j}, \end{aligned} \tag{3.253}$$

where

$$\frac{\partial x_i}{\partial a_j} = \frac{1}{m_j} \geq 0; \quad \frac{\partial x_i}{\partial m_j} = \frac{m_i x_i + a_i - a_j}{m_j^2 m_i \sum_k \frac{1}{m_j}} \geq 0, \tag{3.254}$$

where the inequality for $\frac{\partial x_i}{\partial m_j}$ holds since $m_i x_i + a_i = v = m_j x_j + a_j > a_j$ if player j is active i.e. $x_j > 0$. If player j is inactive, then $\frac{\partial x_i}{\partial a_j} = 0$. At the boundary between active and inactive, we have that $a_j = v$. Either way, $\frac{\partial x_i}{\partial m_j} \geq 0$ and $\frac{\partial x_i}{\partial a_j} \geq 0$, and strict inequalities hold if player j is active. This means that π_i is increasing function of a_j and m_j, for any $j \neq i$. Thus, the worst case for player i, regardless of its strategy is when all other players bid their minimum acceptable values, i.e. $a_j = b_j$ and $m_j = \frac{1}{2}c_j$ for all $j \neq i$. This essentially removes the min optimisation problem from (WCP(i)). Further, the resulting cost minimisation problem can be solved analytically, and thus we are left with the following maximisation problem for player i:

$$\max_{(m_i, a_i) \in \mathcal{S}_R(i)} \pi_i(m_i, a_i; \frac{1}{2}c_{-i}, b_{-i}). \tag{3.255}$$

As a final simplification, player i can make the conservative assumption that in the worst case scenario they cannot influence the price, i.e. $\frac{\partial v_{z_i}}{\partial m_i}$ and $\frac{\partial v_{z_i}}{\partial a_i}$. Thus, the *worst case* price can be computed by solving (bl-BLP) with bids $(\frac{1}{2}\mathbf{c}, \mathbf{b})$, and we denote this as s_z^{min} for each zone z.

Although player i cannot control at all the price v_{z_i}, or his quantity x_i directly, he can control the bid strategy, and therefore (partially) control x_i, given that the price and other players' bids are known. There are three possible options, namely: (i) $\lambda_i = a_i > s_{z_i}^{min}$ and $x_i = 0$, (ii) $\lambda_i = s_{z_i}^{min}$ and $0 < x_i \leq Q_i$, or (iii) $\lambda_i < s_{z_i}^{min}$ and $x_i = Q_i$. Option (i) is clearly sub-optimal for player i, for any $a_i > b_i$, because bidding (c_i, b_i) guarantees non-negative profit and has a non-zero probability of strictly positive profit, while under (i), the profit is always zero. Let us consider (ii) and compare later with (iii).

Since we are under possibility (ii) for player i, we have that

$$m_i x_i + a_i = s_{z_i}^{min}, \tag{3.256}$$

which can be rearranged for x_i to give

$$x_i = \frac{s_{z_i}^{min} - a_i}{m_i}. \tag{3.257}$$

The profit of player i can now be expressed as

$$\Pi_i^{LB} = (m_i - \frac{1}{2}c_i)x_i^2 + (a_i - b_i)x_i = \frac{m_i - \frac{1}{2}c_i}{m_i^2}(s_{z_i}^{min} - a_i)^2 + (a_i - b_i)\frac{s_{z_i}^{min} - a_i}{m_i}, \tag{3.258}$$

and the superscript indicates that this is the lowest possible profit under branch (ii). The equation can be rearranged as

$$\Pi_i^{LB} = -\frac{c_i}{2m_i^2}(s_{z_i}^{min} - a_i)^2 + \frac{1}{m_i}(s_{z_i}^{min} - a_i)(s_{z_i}^{min} - b_i). \tag{3.259}$$

For the profit to be non-negative, we need $s_{z_i}^{min} \geq b_i$, and for strictly positive profit we require $a_i < s_z^{min}$ and $b_i < a_i$, since $m_i \geq \frac{1}{2}c_i$, or $a_i < s_z^{min}$ and $\frac{1}{2}c_i < m_i$. We delay the discussion of what the strategies should be if $s_{z_i}^{min} < b_i$ until we also evaluate case (iii). For now, let us assume this is not the case, and thus player i can obtain positive profit. In this case, we observe that Π_i^{LB} is marginally concave quadratic in a_i, and it also reaches a maximum over $m_i > 0$ for every a_i. Thus, let us take the partial derivatives to obtain the location of the potential maxima:

$$\frac{\partial}{\partial a_i}\Pi_i^{LB} = \frac{c_i}{m_i^2}(s_z^{min} - a_i) - \frac{1}{m_i}(s_z^{min} - b_i) = 0, \tag{3.260}$$

$$\frac{\partial}{\partial m_i}\Pi_i^{LB} = \frac{c_i}{m_i^3}(s_z^{min} - a_i)^2 - \frac{1}{m_i^2}(s_z^{min} - b_i)(s_z^{min} - a_i) = 0, \tag{3.261}$$

and for the case where strictly positive profit is allowed, both equations are identical, since $s_z^{min} - a_i > 0$, and $m_i > 0$ always. Thus, we obtain the best responses to worst case scenario to be a (linear) curve along which Π_i^{LB} is maximum, and the curve is given by

$$\mathcal{B}_{LB}(i) := \{(m_i, a_i) : c_i s_{z_i}^{min} = c_i a_i + (s_{z_i}^{min} - b_i)m_i;\ m_i \geq c_i;\ a_i \geq b_i\}, \tag{3.262}$$

which can be rearranged to express a_i or m_i as a function of the other as

$$a_i = s_{z_i}^{min} - \frac{s_{z_i} - b_i}{c_i} m_i, \tag{3.263}$$

$$m_i = \frac{c_i s_{z_i}^{min}}{s_{z_i}^{min} - b_i} - \frac{c_i}{s_{z_i}^{min} - b_i} a_i. \tag{3.264}$$

Let us recall that $a_i \geq b_i$ and $m_i \geq c_i$ is required, and since on the optimal curve increasing a_i decreases m_i and vice versa, the bids cannot be arbitrarily large. Using (3.262) we obtain that $m_i \in [\frac{1}{2}c_i, c_i]$ and $a_i \in [b_i, \frac{s_{z_i}^{min}}{2} + \frac{b_i}{2}]$, which is a nonempty interval if and only if $b_i < s_{z_i}^{min}$, as required before. The corresponding Π_i^{LB} is then

$$\Pi_i^{LB,(ii)} = \frac{1}{2c_i}(s_{z_i}^{min} - b_i)^2 > 0, \tag{3.265}$$

which is strictly positive, and therefore by playing a strategy on the $\mathcal{B}_{LB}(i)$ curve, so long as $s_{z_i}^{min} > b_i$, the player is guaranteed strictly positive profit. Let us now evaluate option (iii). In this case, we have that

$$\Pi_i^{LB,(iii)} = s_{z_i}^{min} Q_i - \frac{1}{2} c_i Q_i^2 - b_i Q_i = (s_{z_i}^{min} - b_i) Q_i - \frac{1}{2} c_i Q_i^2. \tag{3.266}$$

Similarly, $\Pi_i^{LB,(iii)} \geq 0$ if

$$s_{z_i}^{min} \geq m_i Q_i + a_i \geq \frac{1}{2} c_i Q_i + b_i, \tag{3.267}$$

and thus $s_{z_i}^{min} - b_i \geq \frac{1}{2} c_i Q_i$ is required to guarantee $\Pi_i^{LB,(iii)} \geq 0$, which is much more restrictive than $s_{z_i}^{min} - b_i \geq 0$, especially for large capacity. Therefore, we assume that players aim for bidding to fall under case (ii), and thus to maximising $\Pi_i^{LB,(ii)}$. Finally, if $s_{z_i}^{min} \leq b_i$, then the player cannot guarantee that $\Pi_i^{LB,(ii)} > 0$ for any $x_i > 0$ and the profit may be strictly negative. Thus the player should not bid strategically, but play (c_i, b_i), since the profit cannot be negative in this case. Alternatively, if $s_{z_i}^{min} > b_i$, it should play from the strategy set $\mathcal{B}_{LB}(i)$. Note that $a_i = b_i$ and $m_i = c_i$ is a point in $\mathcal{B}_{LB}(i)$, thus this approach is guaranteed to be superior for player's i profit when compared to simply taking $a_i = b_i$, $m_i = c_i$ because the extra choice can be used to play a game of profit maximisation.

Therefore, risk aversion to *"worst case scenario"* (under a set of conditions) has eliminated the possibility of arbitrarily large *equilibrium* prices, which is clearly beneficial for the Game theoretic approach. Further, it has reduced the search space for each player from two dimensions to only one, with both upper and lower bounds on the strategies possible. This clearly reduces the computational cost of finding Nash Equilibria, and allows for efficient discretisation of the strategy spaces, along a one dimensional space, instead of two dimensional one.

3.5.5 Finding the Feasible Active Player Sets

Up until this point, and in Section 3.5.1, we assumed that the optimal set of active players for each zone is known, and solved the resulting problem using various methods such as ieq-LP, ie-CQP and BBTree. Here we discuss two ways to obtain the set of active players: (i) a simple heuristic that we observe to work very well in practice, (ii) an approach that computes a subset of all *possible* optimal combinations of active players.

Due to its simplicity, we start with the heuristic. The idea is very simple, namely that by solving a simpler problem that approximates the Cost Minimisation problem we may obtain an estimate of (or perhaps even the true) active player set at optimality. To this end, for ieq-LP, ie-CQP, BBTree we use the active player set obtained by solving the SWM problem (discussed in Section 3.6). As we shall see, solving the SWM problem requires solving a strictly convex quadratic program on the same feasible domain as the CM problem (excluding the zonal prices constraints), and thus the only change is the objective function. This problem is much faster to solve, and the optimal active player set is obtained as part of the solution. The SWM objective can in fact be viewed as an approximation of the CM one, in the sense that for inflexible demand, the SWM objective represents the *apparent cost* if everyone was paid according to a pay-as-bid (note that the pricing is uniform zonal marginal price)mechanism, while CM accounts for zonal marginal pricing. We observe that using the SWM optimal active player set works very well in practice, on both the synthetic and the real dataset.

We next discuss finding a set of all *"plausible"* combinations of active players. Once these are known, one can then solve each problem independently and take the solution with the smallest objective function. The total number of possible combinations for N_z zones and N_p^z players per zone is $\prod_z 2^{N_p^z}$, which is very large, but the idea is to remove a very large fraction of these combinations, by showing that they cannot be optimal. To this end, we present two results and then based on these, an algorithm that finds all potentially optimal active player sets. A player k is said to be active if $x_k > 0$ and inactive if $x_k = 0$.

Theorem 3.5.2. *Consider the (mc-BLP) problem, but with $\mathcal{J}_z$ being a set to optimise over, here denoted as $\mathcal{A}_z$. Let $m_i > 0$ and $Q_i > 0$ for each player i, and assume that for each zone the player indices are sorted such that $a_1^z \leq a_2^z \leq ... \leq a_{N_p^z}^z$. Then, for each zone z, at optimality, the set of active players for zone z, $\mathcal{A}_z := \{j : x_j^z > 0\}$ must be of the form $\mathcal{A}_z = \{1, 2, ..., k_{max}^z\} = \overline{1, k_{max}^z}$ for some $k_{max} \in \mathbb{N}^*$.*

Proof. Recall that the definition of v_z is $v_z = \max_j\{m_j x_j + a_j : j \in A_z\}$. We prove the result by contradiction. Assume that the optimal solution, (y^*, v^*, x^*), does not have this form. Then there must exist a zone z and an index $k_z < k_{max}^z$ such that $x_{k^z}^z = 0$ and $x_{k_{max}^z} > 0$ at optimality. Since $x_{k_z}^z = 0$, player k_z cannot determine the price. Thus, there must exist a non-empty set of players $\mathcal{R}_z = \{j : v_z^* = m_j x_j + a_j\}$ that sets the price of the zone. Now, there are two possibilities:

1. Either $v_z \leq a_{k_z}$, which implies that $m_j x_j + a_j \leq a_{k_z}$, $\forall j \in \mathcal{R}_z$. But $m_j > 0$ by assumption and $x_j > 0$ since j can only set the price if it is active. Thus, $a_k > a_j$ for $j \in \mathcal{P}$. Next, we look at how a_k compares to active players that do not set the price. If a player is inactive and does not set the price, at optimality, then it has to be that $x_i = Q_i$ for $i \in \mathcal{A}_z \setminus \mathcal{R}_z$. Further, it has to be that $m_i Q_i + a_i < v_z \leq a_{k_z}$, where the last part holds by assumption of this possibility. Since $Q_i > 0$ and $m_i > 0$, it has to be that $a_{k_z} > a_i$, $\forall i \in \mathcal{A}_z \setminus \mathcal{R}_z$. But then it means that $a_k > a_l$ for $\forall l \in \mathcal{A}_z$. This contradicts the assumption about the solution form, and thus we cannot have $k_z < k_{max}$ with $a_{k_z} \geq v_z^*$ at optimality.

2. The only possible alternative is that $a^z_{k_z} < v_z^*$. In this case, consider the adjustment in quantities assigned to players, defined by $\{\varepsilon_j\}_{j \in \mathcal{P}_z}$ such that:

$$\begin{aligned} &0 < \varepsilon_j < x_j; \quad \sum_{j \in P_z} \varepsilon_j < Q_k, \\ &m_{k_z} \sum_{j \in P_z} \varepsilon_j + \max_j \{m_j \varepsilon_j\} < v_z^* - a^z_{k_z}. \end{aligned} \tag{3.268}$$

   System (3.268) is always feasible, if $x_j > 0$, $Q_k > 0$, as per our assumptions, and since $v_z^* - a_{k_z} > 0$. To see this, let us take an example of $\varepsilon_j = \varepsilon$, in which case the system becomes

$$\begin{aligned} &0 < \varepsilon < \min_j x_j; \quad N^z_p \varepsilon < Q_k, \\ &m_{k_z} N^z_p \varepsilon + \max_j \{m_j\} \varepsilon < v_z^* - a^z_{k_z}, \end{aligned} \tag{3.269}$$

   which has solutions $\varepsilon^* \in (0, \epsilon_M)$ with

$$\epsilon_M = \min \left\{ \frac{Q_k}{N^z_p}, x_j, \frac{v_z^* - a^z_{k_z}}{N^z_p m_{k_z} + \max_j \{m_j\}} \right\}, \tag{3.270}$$

and the interval is clearly non-empty since all terms under the min function are strictly positive. Thus, there exists a solution to system (3.268). Then, consider the adjustment of solution $\hat{x}_j \leftarrow x_j - \varepsilon_j$ and thus $\hat{x}_j < x_j$, and $\hat{x}_{k_z} = \sum_j \varepsilon_j$. Now, k_z becomes active. Thus, the zonal quanitity $\hat{y}_z = \sum_{j \in \hat{\mathcal{A}}_z} \hat{x}_j = y_z$, remains unchanged. Let us now look at what happens to the zonal price. The last equation in (3.268) can be rearranged to give us

$$\lambda_k = m_{k_z} \hat{x}_{k_z} + a_{k_z} < v_z^* - \max_j m_j \varepsilon_j = \min_j \{m_j (x_j - \varepsilon_j) + a_j\} \leq \max_j \{m_j (x_j - \varepsilon_j) + a_j\}. \tag{3.271}$$

The new zonal price following the adjustment is

$$\hat{v}_z^* = \max\{\lambda_k, \max_j\{m_j(x_j - \varepsilon_j) + a_j\}\} = \max_j\{m_j(x_j - \varepsilon_j) + a_j\}, \tag{3.272}$$

where the last part holds by (3.271). But $\max_{j\in_z}\{m_j(x_j - \varepsilon_j) + a_j\} < v_z^*$ since $\varepsilon_j > 0$ and $v_z^* = m_j x_j + a_j$ for all $j \in \mathcal{R}_z$, and therefore $\hat{v}_z^* < v_z^*$. Thus, since the zonal quantity is left unchanged, the cost term for zone z has changed from $y_z v_z^*$ to a strictly smaller one, namely $y_z \hat{v}_z^*$. This means that we have found an improvement, by introducing $x_{k_z} > 0$, and thus the initially proposed solution is not optimal. We have reached a contradiction, meaning that the optimal solution must have the form stated. □

This result gives us some intuition on how to construct the feasible player sets for each zone: find the smallest k_{max}^z such that $\sum_{i=1}^{k_{max}} Q_i \geq y_{min}^z$, with y_{min}^z being the minimum quantity that must be produced in zone z to ensure feasibility (which is usually much larger than 0). Then all the feasible active player sets sets are $\mathcal{S}_z = \{\{1, 2, ..., l^z\} : l^z \in \overline{k_{max}^z, N_p^z}\}$. However, this may still be rather large, and the next result leverages further problem specific knowledge to try to reduce this set.

Theorem 3.5.3. *Under the conditions of Theorem 3.5.2, for all z, any player k_z with $k_z \notin \mathcal{A}_z$ ($x_{k_z} = 0$), that has $a_{k_z} < \hat{v}_{min}^z(\mathbf{y}_{min}, k_z, \mathcal{A}_z)$, where $\hat{v}_{min}^z(\mathbf{y}_{min}, k_z, \mathcal{A}_z)$ is obtained as*

$$\begin{aligned} &\min_{\mathbf{x}, v_z} v_z, \\ &s.t. \sum_{i\in\mathcal{P}_z} x_i = y_{min}^z, \\ &\quad v_z - m_i x_i - a_i \geq 0, \quad \forall i \in \mathcal{A}_z, \end{aligned} \tag{3.273}$$

must reduce the objective value by setting $x_{k_z} > 0$, and the active set $\mathcal{A}_z$ cannot be optimal.

Proof. We first start by making a claim, namely that $\hat{v}_{min}^z(\mathbf{y}_{min}, k_z, \mathcal{A}_z) \leq \hat{v}_{min}^z(\mathbf{y}, k_z, \mathcal{A}_z)$. Clearly since $\mathbf{y}_{min}$ is the absolute smallest feasible value, any other y_z must satisfy $y_z = y_{min}^z + \delta$, with $\delta > 0$. The extra quantity δ, cannot be distributed amongst any players and reduce the price, since the players' marginal prices $\lambda_j(a_j) = m_j x_j + a_j$ are strictly increasing functions. But then we have that $a_{k_z} < \hat{v}_{min}^z(\mathbf{y}_{min}, k_z, \mathcal{A}_z) \leq \hat{v}_{min}^z(\mathbf{y}^*, k_z, \mathcal{A}_z) \leq v_z^*$, where the last inequality holds because the objective is to minimise exactly v_z instead of the global cost $\sum_z y_z v_z$. But we are now in the conditions of the second branch of proof of Theorem 3.5.2, meaning that an improvement can be found by setting $x_{k_z} > 0$, concluding the proof. □

Algorithm 14 summarises finding the feasible active players sets for a zone z.

Algorithm 14 Compute Potential Optimal Sets of zone z

Require: input (m_i, a_i, Q_i) for all $i \in \mathcal{P}_z$, vector of the minimum feasible quantities y_{min},
sort players in zone z in increasing order of a_i.
find $k^z_{max} = \arg\min_k \sum_{i=1}^{k} Q_i \geq y^z_{min}$
while $\hat{v}^z_{min}(y_{min}, k_z, \mathcal{A}_z) > a_{k_{max}+1}$ and $k_{max} < N^z_p$ **do**
$\mathcal{A}_z \leftarrow \mathcal{A}_z \cup \{k^z_{max} + 1\}$
$k^z_{max} \leftarrow k^z_{max} + 1$
recompute $\hat{v}^z_{min}(y_{min}, k_z, \mathcal{A}_z)$
end while
return $S_z = \{\{1, ..l^z\} : l^z \in \overline{k_{max}, N^z_p}\}$

3.5.6 Nash Equilibria Computation

The approach we use for finding Nash Equilibria differs from the one used in Section 3.4.3, because: (i) the approach used before only finds stationary points (also known as *stationary Nash points*), which are weaker than local Nash Equilibria [85], and here we aim to compute (approximate) global Nash Equilibria, (ii) Robust Strategy Selection reduces the strategy space to one (bounded) dimension for each player, making it much cheaper to compute best responses using grid search.

Instead of computing derivatives and updating an estimate of a local Nash point until convergence, we consider iteratively improving each player's best response function given other players' strategies. Let us denote the best response function for player i, given other players' strategies $(\mathbf{m}_{-i}, \mathbf{a}_{-i})$ as $B_i(\mathbf{m}_{-i}, \mathbf{a}_{-i}; \omega_i)$ where the problem parameters for player i are $\omega_i = (c_i, b_i, Q_i, d, \mathbf{M}_p, \mathbf{b}_p)$. Since $(m_i, a_i) \in \mathcal{B}_{LB}(i)$, we drop a_i and only denote the strategy of player i by m_i, with the implicit corresponding a_i value given by (3.263). Further, we have that $\frac{1}{2}c_i \leq m_i \leq c_i$ and therefore the feasible strategy space is bounded when using RSS. Thus, to compute an approximate best response function, $\hat{B}_i(m_i; \omega_i, N_{pts})$ we discretise the domain in N_{pts} equispaced points over $[\frac{1}{2}c_i, c_i]$, and for each strategy point solve the CM market clearing problem via ieq-LP, ie-CQP, BBTree or ib-CQP and use the result to evaluate Π_i, as formally explained in Algorithm 15. Note that our idea for computation of (approximate) global Nash Equilibria remains the same regardless of the market clearing mechanism used. Thus the same algorithms are applied to the SWM market clearing case presented in Section 3.6 for the computation of SWM-based Nash Equilibria.

Given an algorithm to compute an (approximate) best response function $\hat{B}_i(m_i; \omega_i, N_{pts})$, one can now obtain an (approximate) global Nash Equilibrium point by iteratively updating strategies until no further improvement is possible for any player. Iterative updates over players can be done in at least two ways: (i) a Gauss-Seidel type of approach (GS), where each player uses the most recent information about other players' strategies, and (ii) a Jacobi type of approach (JS), where each player is updated simultaneously using last time point with synchronised information. Due to the large computational expense associated with the problem, both approaches have their strengths and limitations, and both are relevant here.

Algorithm 15 Compute approximate best response function $\hat{B}_i(m_i; \omega_i, N_{pts}, \mathcal{M})$ under RSS (a-BRF-RSS)

Require: input (m_k, a_k, Q_k) for all $k \in \cup_z \mathcal{J}_z \setminus \{i\}$, (c_i, b_i), N_{pts}
Require: market clearing solution method $\mathcal{M}$ (ieq-LP, ie-CQP or BBTree)
  if $b_i > s_{z_i}^{min}$ **then**
    return (c_i, b_i) (there is no opportunity for gaming, so bid marginal costs only)
  end if
  for $l = 1, 2, ..., N_{pts}$ **do**
    get player's i strategy $m_i(l) = \frac{1}{2}c_0 + \frac{l-1}{N_{pts}-1}\frac{1}{2}c_0$
    compute the corresponding $a_i(l)$ using $(m_i(l), a_i(l)) \in \mathcal{B}_{LB}(i)$
    solve the market clearing problem using $\mathcal{M}$, and obtain x^*, v^* and y^*
    compute $\Pi_i(x_i^*, m_i(l), a_i(l), c_i, b_i)$
  end for
  $m_i^B \leftarrow \arg\max_{m_i(l); l \in \overline{1, N_{pts}}} \Pi_i(x_i^*, m_i(l), a_i(l), c_i, b_i)$
  return (m_i^B, a_i^B)

The main advantage of GS is that the most recent information is always used, potentially requiring fewer iterations, but paralellisation can only be done across N_{pts} different tasks, as each player has to wait for the previous one's best response function to be updated. On the

Algorithm 16 Compute cycle strategy update by JS (C-JS)

Require: input strategies m_i $\forall i$, N_{pts}
Require: market clearing solution method $\mathcal{M}$
  for $(i, l) \in \mathcal{P} \times \{1, 2, ..., N_{pts}\}$ **do**
    get player's i strategy $m_i(l) = \frac{1}{2}c_0 + \frac{l-1}{N_{pts}-1}\frac{1}{2}c_0$
    compute the corresponding $a_i(l)$ using $(m_i(l), a_i(l)) \in \mathcal{B}_{LB}(i)$
    solve the market clearing problem using $\mathcal{M}$, for $(m_i(l), \mathbf{m}_{-i})$ and obtain x^*, v^* and y^*
    compute $\Pi_i(x_i^*, m_i(l), a_i(l), c_i, b_i)$
  end for
  for $i \in \{1, 2, ...N_p\}$ **do**
    $m_i^B \leftarrow \arg\max_{m_i(l); l \in \overline{1, N_{pts}}} \Pi_i(x_i^*, m_i(l), a_i(l), c_i, b_i)$
  end for
  return $\{(m_i^B, a_i^B)\}_{i \in \mathcal{P}}$

other hand, JS does not make best use of the last available iterations, and thus may require more iterations, but it has the big advantage that it can be parallelised across $(i, l) \in \mathcal{P} \times \{1, 2, ...N_{pts}\}$, i.e. across both the player set and discretisation points indepedently. Thus, $N_p N_{pts}$ tasks can be solved simultaneously, instead of just N_{pts} and assuming identical computational time for each task, and sufficiently many cores to perform independent tasks, it can take N_p times more iterations when compared to GS to achieve the same computational time, albeit at a larger energy usage. Performing a detailed numerical analysis is very time and energy consuming. Thus, we just use this simple analysis to conclude that JS is more appropriate when sufficiently many cores are available, while GS is more appropriate when running on a machine with few cores (≤ 32). The two ideas are formalised in Algorithm 16

Algorithm 17 Compute cycle strategy update by GS (C-GS)

Require: initial strategies $m_i \ \forall i$, N_{pts}
Require: market clearing solution method $\mathcal{M}$
  for $i \in \{1, 2, ...N_p\}$ **do**
    compute (m_i^B, a_i^B) using $\hat{B}_i(m_i; \omega_i, N_{pts}, \mathcal{M})$
    $m_i \leftarrow m_i^B$
  end for
  return $\{(m_i^B, a_i^B)\}_{i \in \mathcal{P}}$

and 17. To perform intensive computations (Section 3.7.2.3) we use *DescartesLabs*'s cloud computing services provided by *Macquarie Group*, while the less intensive computations (Section 3.7.2.1 and Section 3.7.2.2) are performed on a machine with 8 cores.

Finally, one can now obtain a Nash equilibrium by repeatedly using C-GS or C-JS using the previous strategy output as input, until convergence, as shown in Algorithm 18. When

Algorithm 18 Compute Nash Equilibrium Point (CNEP-Q)

Require: initial strategies $m_i^{(0)} \ \forall i$, N_{pts}, maximum cycles number N_{max}^C, tolerance $\delta_{NE} \geq 0$
Require: market clearing solution method $\mathcal{M}$
  for $k \in \{1, 2, ...N_{max}^C\}$ **do**
    compute $\{(m_i^{(k)}, a_i^{(k)})\}_{i \in \mathcal{P}}$ using C-GS or C-JS and $\{(m_i^{(k-1)}, a_i^{(k-1)})\}_{i \in \mathcal{P}}$ as strategies
    if $m_i^{(k-1)} = m_i^{(k)}$ (or less strictly $\|m_i^{(k-1)} - m_i^{(k-1)}\|_2 < \delta_{NE}$) **then** break
    end if
  end for
  return $\{(m_i^{(k)}, a_i^{(k)})\}_{i \in \mathcal{P}}$

running CNEP-Q using the cloud services, we presolve by using CNEP-Q with $\mathcal{M}$ =*ieq-LP-ma* first, and use this result as input to presolve using CNEP-Q with $\mathcal{M}$ =*ie-CQP-wr*. In both stages we fairly coarse algorithm specific tolerances and rather small N_{max}^C. Only then, we use CNEP-Q with $\mathcal{M} = BBTree$ on the previous outputs. Under the limited runs performed, we find this approach to give the shortest computational time, as well as the smallest number of iterations performed using CNEP-Q with $\mathcal{M} = BBTree$. Note that we can always get a reasonable initial point by choosing any point in the feasible domain, due to the boundedness of our strategy domain, and our pre-solvers as well as main solvers are always observed to converge, revealing the robustness of our approach, perhaps owed to the low dimensionality of the strategy space (1D for each player) and bounded domain.

3.6 The Social Welfare Maximisation Spot Model

In the CWE Day Ahead Auction market, the clearing mechanism is based on the idea of *Social Welfare Maximisation*, which defines the objective to maximise as the sum of total apparent benefits obtained by the consumer minus the total apparent costs of the producer.

Unlike in the usual literature, we point out that the quantities used are *apparent* because they neglect the possibility of un-truthful bidding and the effect of marginal pricing. The SWM optimisation problem can then be written as

$$\begin{aligned} &\min_x \frac{1}{2}\sum_i m_i x_i^2 + a_i x_i = \frac{1}{2}\mathbf{x}^T\mathbf{D}_m\mathbf{x} + \mathbf{a}^T\mathbf{x}, \\ &s.t.\ x_i \geq 0;\ \ Q_i - x_i \geq 0, \quad \forall i, \\ &\quad \mathbf{M}_p\mathbf{E}\mathbf{x} \leq \mathbf{b}_p, \\ &\quad \mathbf{1}^T\mathbf{x} = d, \end{aligned} \tag{SWM}$$

since considering the form of the bids we assumed, and inflexible demand, the objective is given by

$$F_{SWM} = -\sum_i \int_0^{x_i} (m_i\zeta_i + a_i)d\zeta_i = -\sum_i \frac{1}{2}m_i x_i^2 + a_i x_i. \tag{3.274}$$

Note that there are no price variables in either the objective or constraint set. As per the market solution in practice and according to Theorem 3.2.1, the prices can be computed after solving the SWM problem and the largest price in each zone (with corresponding strictly positive production) is retained. Further, the optimal active player set is simply the set of players $\mathcal{P}^A := \{i : x_i^* > 0\}$, which can be trivially computed once the optimal solution of SWM is obtained. Note that SWM is a linearly constrained strictly convex quadratic program, which can be solved very effectively numerically. While this problem is simple to solve, obtaining its solution is important for the following reasons:

1. The solution is fast, and gives an active player set that can be used as an input for our methods when solving the Cost Minimisation (CM) problem. This heuristic drastically reduces the total computational effort and generally the optimal active player set of the SWM is observed to coincide with the CM one.

2. A SWM-based mechanism is used in practice, thus we expect our SWM to represent the market outcome in the CWE more accurately than a CM based approach, allowing us to better analyse the truthful-bid versus game-theoretic models' performance against the real world price data.

3. To be able to show the potential benefits of using a Cost Minimisation objective, this has to be compared with the approach currently used in the CWE, which is a variant of a Social Welfare Maximisation (SWM) optimisation problem.

Finally, the SWM optimisation problem introduced here was solved via the *quadprog* package in *Python 3*.

3.7 Numerical Results

3.7.1 Synthetic Data Experiments (no capacity constraints)

Since the model is a complex multi-level optimisation, possessing features such as non-uniqueness of equilibria, and non-concavity of the utility functions, we perform numerical experiments on simple synthetic data to better understand the features of the model and the market it represents.

3.7.1.1 Risk Neutral Players

We only briefly review numerical results for the case of no capacity constraints and risk-neutral players under our model. We run the procedure described in Section 3.4.3 first from a random starting point and then choosing as new starting point $\mathbf{m}_0^{(k)} \leftarrow \mathbf{m}_{NE}^{(k-1)} + \varepsilon_m \mathbf{1}$ and $\mathbf{a}_0^{(k)} \leftarrow \mathbf{a}_{NE}^{(k-1)} - \varepsilon_m \mathbf{x}_{NE}^{(k-1)}$, as per Lemma 3.4.2. We only have a limited look at numerical results because, as can be seen in Figure 3.7, the number of local equilibria is very large and it indeed appears that these equilibria may not be isolated, since points that are very close together can be found. This is consistent with the theoretical results we obtain and

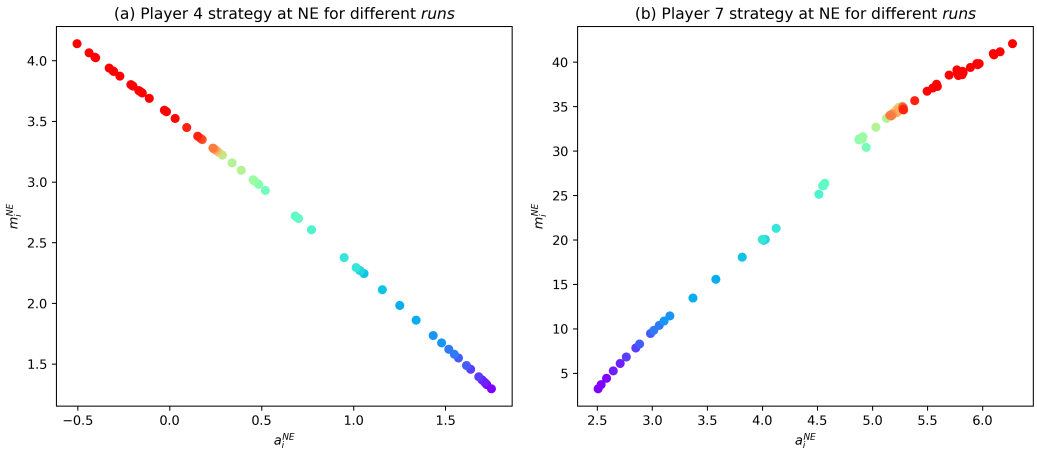


Figure 3.7: Local Nash Equilibria found: colored by numbers for comparison across players. The strategy set for each shown player is plotted in each subfigure, and the colorbar indicates the profit level for each player.

confirms the need to introduce risk aversion.

3.7.1.2 Risk Averse Players

We have shown in Section 3.4.4 that if all players are risk averse, and $\Gamma_i \geq 0$ for all i, then the equilibrium strategies are bounded above. Further, we have shown that for the particular case of two zones and two players per zone, if the risk aversion of the least risk averse player is *sufficiently high*, the local Nash Equilibria become isolated. It would be

instructive for practical applications to obtain a bound on the minimum distance between two such equilibria, and/or on their number. However, we have not obtained theoretical results for this, and to get a better understanding of this issue we perform a numerical experiment. We consider a synthetic market with two zones, $\mathcal{Z} = \{z_1, z_2\}$ and two players per zone, that is $i = \overline{1,4}$ and the zonal player sets are $\mathcal{P}_{z_1} = \{1, 2\}$, $\mathcal{P}_{z_2} = \{3, 4\}$. Players' costs and risk parameters are set based on the parameters in Table 3.1 below. The demand

	$i=1$	$i=2$	$i=3$	$i=4$
c_i	0.1	0.1	0.2	0.2
b_i	1.5	1.3	0.63	0.65
σ_i	0.15	0.15	0.45	0.55
$\hat{\sigma}_i$	0.425	0.369	0.24	0.24
Γ_i	0	0	0	0
η_i	3	3	3	3

Table 3.1: Example problem parameters for numerical experiment on NE isolation.

levels are $\mathbf{d}^T = (d_1, d_2)$ with $d_1 = 10$ and $d_2 = 6$, and the feasible domain is given by the ellipsoid constraints with $r = 1$, centered in the demand levels, i.e. $\mathbf{p}_s = \mathbf{A}_s\mathbf{d}$ and

$$\mathbf{A}_s = \begin{pmatrix} 1.535 & 0.318 \\ 0 & 1.1 \end{pmatrix}. \tag{3.275}$$

We obtain the Local Nash Equilibria, by performing a grid search over multiple starting points, for each starting point solving via the method described in Section 3.4. Since we have 8 variables, a full grid search would be computationally prohibitive and thus we search over the space (K_1, K_2) where $\mathbf{m} = K_1\mathbf{c}$ and $\mathbf{a} = K_2\mathbf{b}$. It is worth noting that we do not guarantee finding all the equilibria in this way.

From Figure 3.8, we can see that the equilibria we obtain are bounded and isolated, although their number is fairly large, and some are rather close to each other. The latter could also be because of numerical stopping criterion. By looking at the profit value for each player, for each equilibria, we observe that many contain players with negative profits, and thus negative utility, since the regularisation term is non-positive. We know that players can guarantee non-negative profit and zero utility by bidding exactly the marginal costs, and thus these local Nash Equilibria cannot be globally optimal, and since a better solution, that is trivial to find (bidding the marginal costs) is available, we remove these.

Once we perform this operation we are left with the equilibria presented in Figure 3.9. We can see that in this case, the number of local NE is reduced drastically, and they become relatively more isolated although the distance between them remains rather small. We conclude that although in theory the stationary points should be isolated, in practice

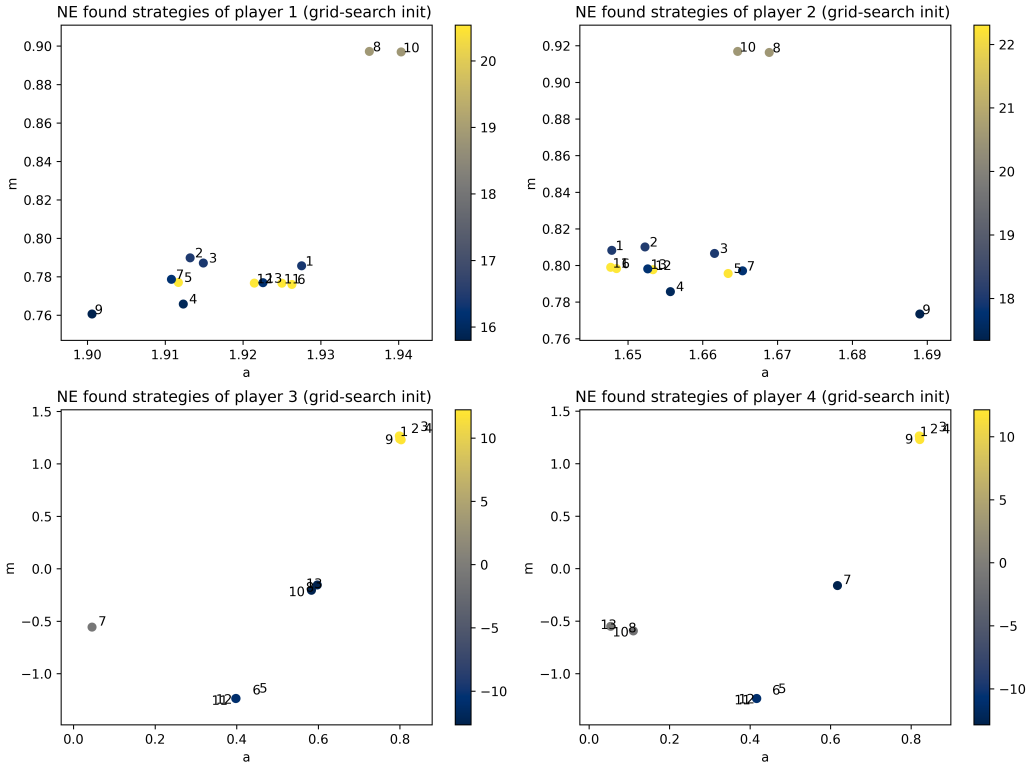


Figure 3.8: Local Nash Equilibria found: indexed by numbers for comparison across players. The strategy set for each player is plotted in each subfigure, and the colorbar indicates the profit level for each player.

they can be very close to each other. This motivates the introduction of a different type of risk aversion, which we called *Robust Strategy Selection (RSS)*, introduced in Section 3.5.4.

3.7.2 Synthetic Data Experiments for Capacity Constrained Model and Algorithms

We now look at numerical results for the case where capacity constraints are considered for each player, as discussed in Section 3.5. We first evaluate the computational performance and convergence properties of the four proposed market clearing solution approaches: (i) ieq-LP, (ii) ie-CQP and ie-CQP-wr, (iii) BBTree and (iv) ib-CQP. Using each of the three methods, we then consider the computation of the profit function under the Robust Strategy Subspace for each player, and other market solution variables, as well as the computational time required. Lastly, we compute Nash Equilibria for this problem and investigate some properties of this solution.

We now define the synthetic problem to be solved. We consider a market with $N_z = 3$ zones and $N_p = 6$, having two players per zone. The zonal demand vector is $d^T = [10, 6, 6]$.

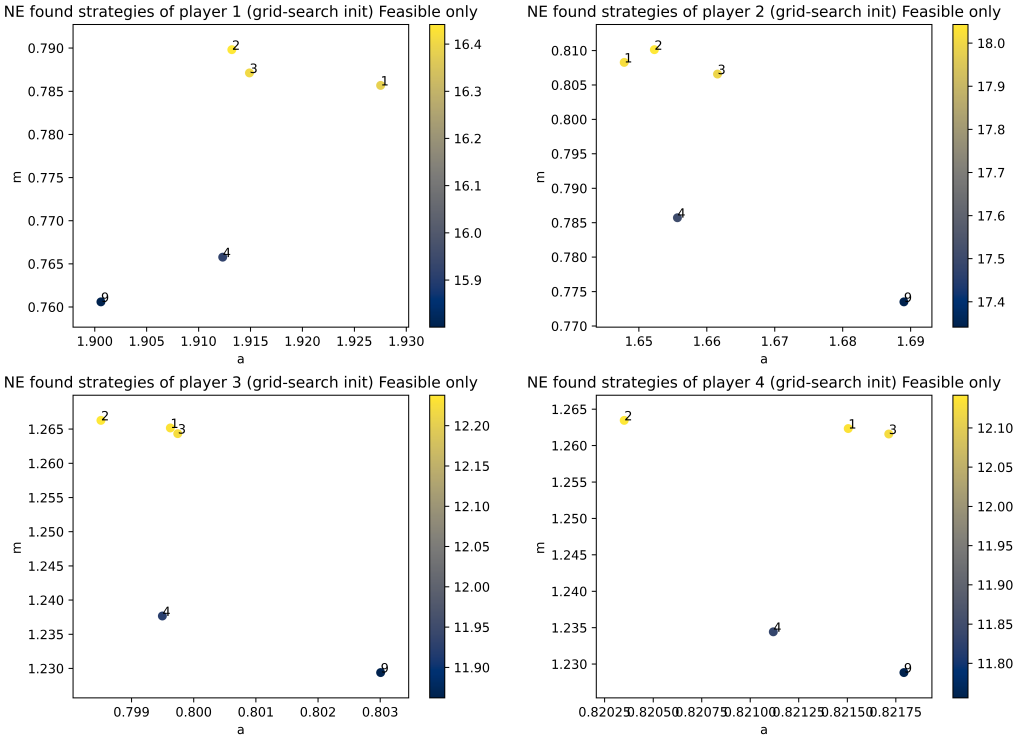


Figure 3.9: Local Nash Equilibria found satifying the condition that the profit of all players is non-negative. Local Nash Equilibria are indexed by numbers for comparison across players. The strategy set for each player is plotted in each subfigure, and the colorbar indicates the profit level for each player.

The production costs, capacity constraints and network constraints are defined by

$$\mathbf{c}^T = \begin{bmatrix} 1.0 & 1.0 & 0.8 & 0.8 & 1.0 & 1.0 \end{bmatrix}, \quad \mathbf{b}^T = \begin{bmatrix} 1.50 & 1.30 & 0.80 & 0.63 & 0.20 & 0.40 \end{bmatrix},$$
$$\mathbf{Q}^T = \begin{bmatrix} 4.0 & 5.5 & 4.0 & 4.0 & 3.0 & 4.0 \end{bmatrix},$$
$$\mathbf{M}_p^T = \begin{bmatrix} 1.0 & 1.0 & 0.0 & 1.0 & 0.0 & 0.0 & -1.0 & 0.0 & 0.0 \\ -1.0 & 0.0 & 1.0 & 0.0 & 1.0 & 0.0 & 0.0 & -1.0 & 0.0 \\ 0.0 & -1.0 & -1.0 & 0.0 & 0.0 & 1.0 & 0.0 & 0.0 & -1.0 \end{bmatrix},$$
$$\mathbf{b}_p^T = \begin{bmatrix} 5.0 & 5.0 & 2.5 & 12.0 & 8.0 & 8.0 & -8.0 & -4.0 & -4.0 \end{bmatrix}.$$

We further define two strategy cases where $\mathbf{m}^I = 0.675\mathbf{c}$, $\mathbf{a}^I = 1.02\mathbf{b} + 0.2$ and $\mathbf{m}^{II} = \mathbf{c}$, $\mathbf{a}^{II} = \mathbf{b}$, where the first strategy, $(\mathbf{m}^I, \mathbf{a}^I)$, is a fairly arbitrary one, while the second strategy, $(\mathbf{m}^{II}, \mathbf{a}^{II}) \in \times_i \mathcal{B}_{LB}(i)$, is the point with the largest value of m_i in the Robust Strategy space, for each player i.

3.7.2.1 Evaluation of Approaches for Solving the Market Clearing

For the initial evaluation of the four solution methods and their variations, we use $(\mathbf{c}, \mathbf{b})$ as the bids for simplicity, and run each of the four approaches independently on this problem. From Figure 3.10, we can clearly see that for ieq-LP, by using a moving averaging update the

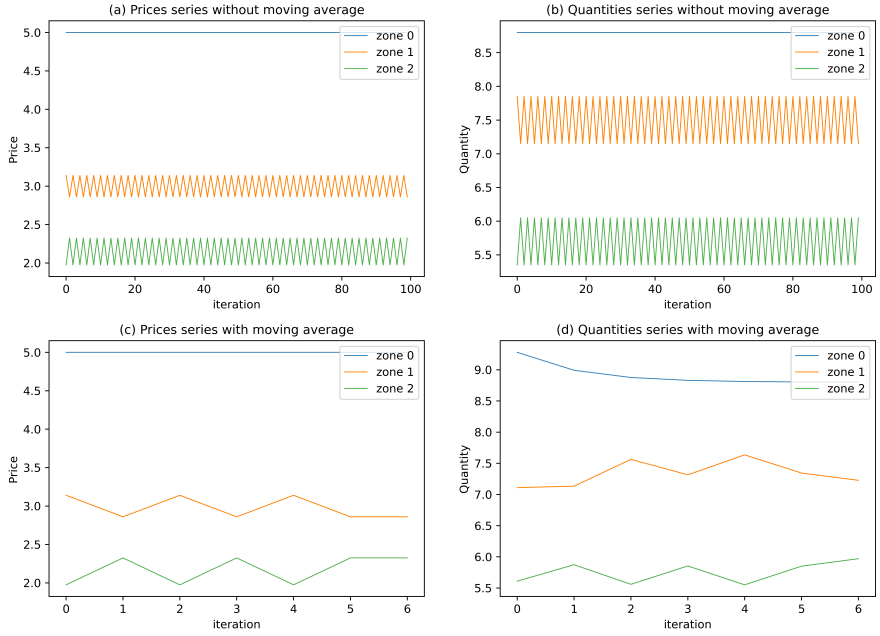


Figure 3.10: Zonal price and zonal quantity estimator $\hat{y}_z$ vs number of iterations for ieq-LP and ieq-LP-ma with $\alpha = 0.5$.

number of iterations is greatly reduced, although the quality of the solution is virtually the same. Since the computational time is proportional to the number of iterations, ieq-LP-ma is much faster in this case. However, much of the inefficiency of ieq-LP comes from the fact that the maximum number of iterations was set to $N_{max} = 100$. If this was set to $N_{max} = 6$ for example, the computational time of the two variants will be roughly the same. While we cannot guess the ideal value of N_{max} for each problem, one could remember all the previous solutions and stop ieq-LP when the current solution is *"very close"* to one of the previous solutions. This is somewhat more memory and computationally intense than ieq-LP-ma, since it requires storing all past solutions and computing norms of differences between the current solution and the past ones. For this reason, we use ieq-LP-ma.

We now focus on ie-CQP an ie-CQP-wr. In our definition of ellipse $(\mathbf{A}_s, \mathbf{p}_s, r_s)$, $r_s = 1$ always, but the scale of $\mathbf{A}_s$ changes accordingly, resulting in a smaller effective radius. In this sense, by normalising $\mathbf{A}_s$ to have norm 1, $r_s \sim \|\mathbf{A}_s\|_2^{-1}$, is an indication of the ellipse size. From Figure 3.11, we see that as r_s becomes smaller, the condition number of $\mathbf{A}_s$ sharply increases past a specific r_s value, and with it, so does the computational time taken.

Since r_s decreases, it must mean that the maximum singular value $\varsigma_{\max}(\mathbf{A}_s) = \|\mathbf{A}_s\|_2$ increases, but $\varsigma_{\min}$ may increase at a slower rate, resulting in an increased condition number. This can only happen if the ellipsoid is very flat in some particular directions, meaning that

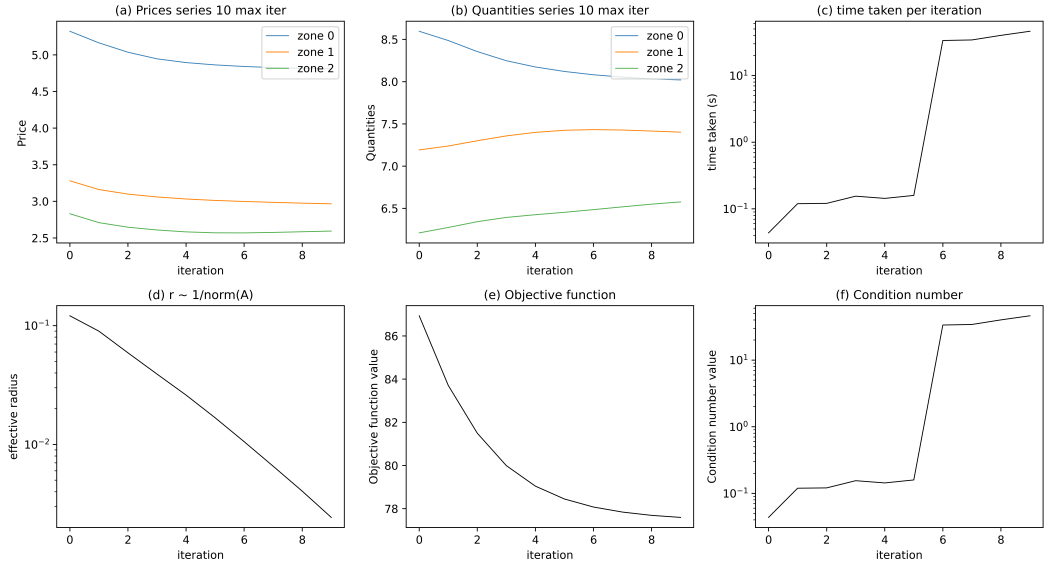


Figure 3.11: ie-CQP: Zonal price, quantities, and convergence parameters for each iteration.

we have reached a solution close to the boundary, as we can see from Figure 3.12. To deal with this issue, ie-CQP-wr was introduced. By contrast with ie-CQP, ie-CQP-wr obtains

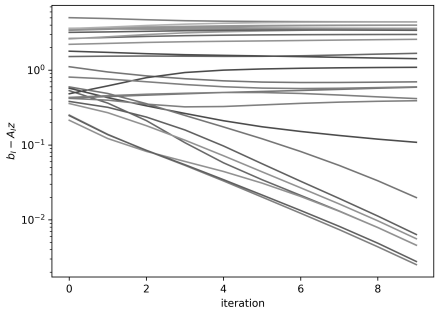


Figure 3.12: Constraints value. Each $(\mathbf{b}_I)_l - (\mathbf{A}_I)_l \mathbf{z}^j$ represents a plot line, evaluated at the solution obtained at iteration j, $\mathbf{z}^j$.

a larger r_s, much smaller condition number, and takes less time towards the end stages of the algorithm. This is because the generated ellipses can be larger, and better conditioned, allowing for faster solution of (em-TR). Thus, we can clearly see that ie-CQP-wr is superior to ie-CQP, requiring much smaller computational time, and with the potential to obtain much more accurate solutions asymptotically.

Next, when running the BBTree algorithm, we find that branching and pruning are in general really effective, with many branches being pruned very early, as seen in Figure 3.14. Since at every branching, the domain size is roughly halved, we can see that after a small number of nodes is processed, the remaining feasible domain size is fairly small.

We now look at the performance of ib-CQP on the test problems mentioned here. Since $\mathbf{y}$ is three dimensional, but constrained to a 2D subspace by the supply and demand balance constraint $\mathbf{1}^T\mathbf{y} = d$, we can plot the shape of the objective function as a function of the first two components of $\mathbf{y}$, given the optimal allocation of $\mathbf{x}$ for each fixed $\mathbf{y}$. This function is

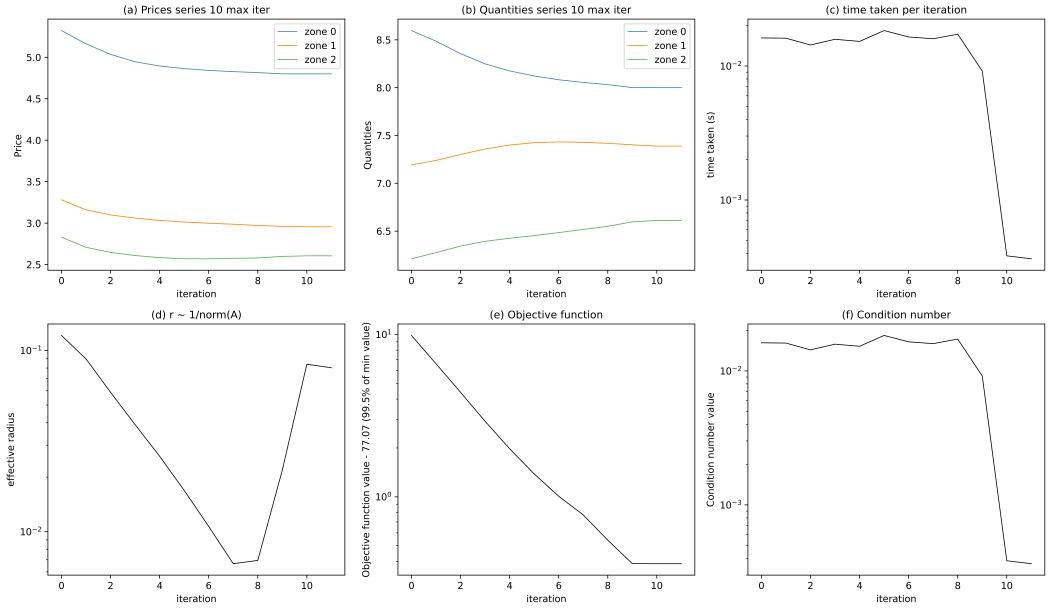


Figure 3.13: ie-CQP-wr: Zonal price, quantities, and convergence parameters for each iteration.

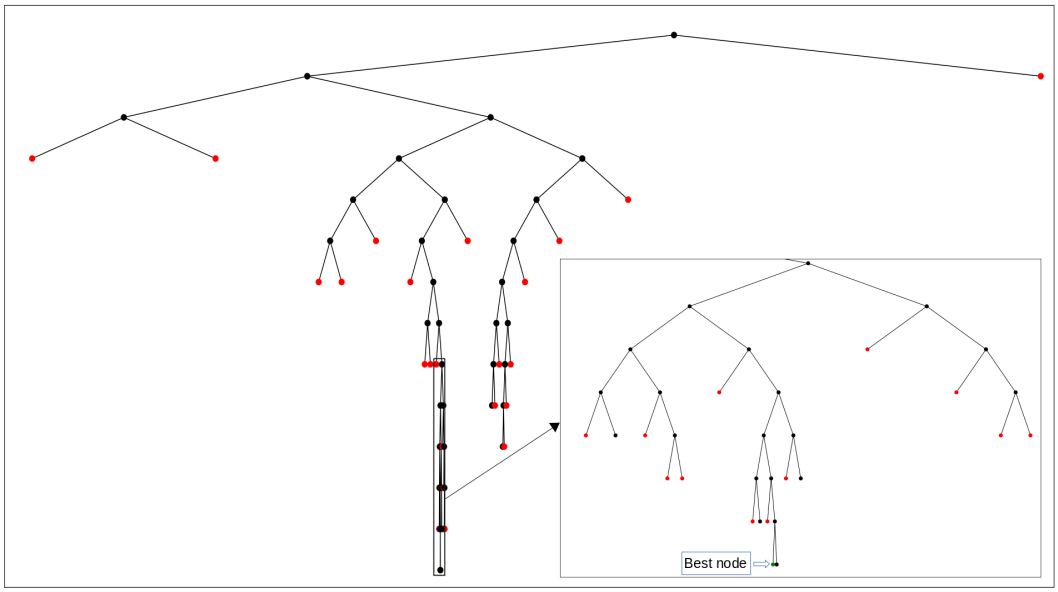


Figure 3.14: Convergence of the BBTree algorithm. Red nodes represent pruning, while the active nodes with the smallest lower bound and the best feasible solutions are represented by yellow and blue respectively. If the two coincide, they are represented in green.

shown in Figure 3.15. In practice we observe that the number of outer iterations (number of times sub-CQP problems are solved) is generally 2, often with very little change between the iterates, and the solution often lies on an internal boundary of a sub-CQP($\mathbf{y}$) problem. This is also the case in Figure 3.15, where the solution $\mathbf{y}^*$ effectively belongs to either of the two sub-CQP domains. However, we can observe that BBTree finds a different (and slightly better) solution, on a boundary given by the polytope constraints, $(\mathbf{M}_p, \mathbf{b}_p)$, which can never be a sub-CQP internal boundary. The difference could occur due to the flat

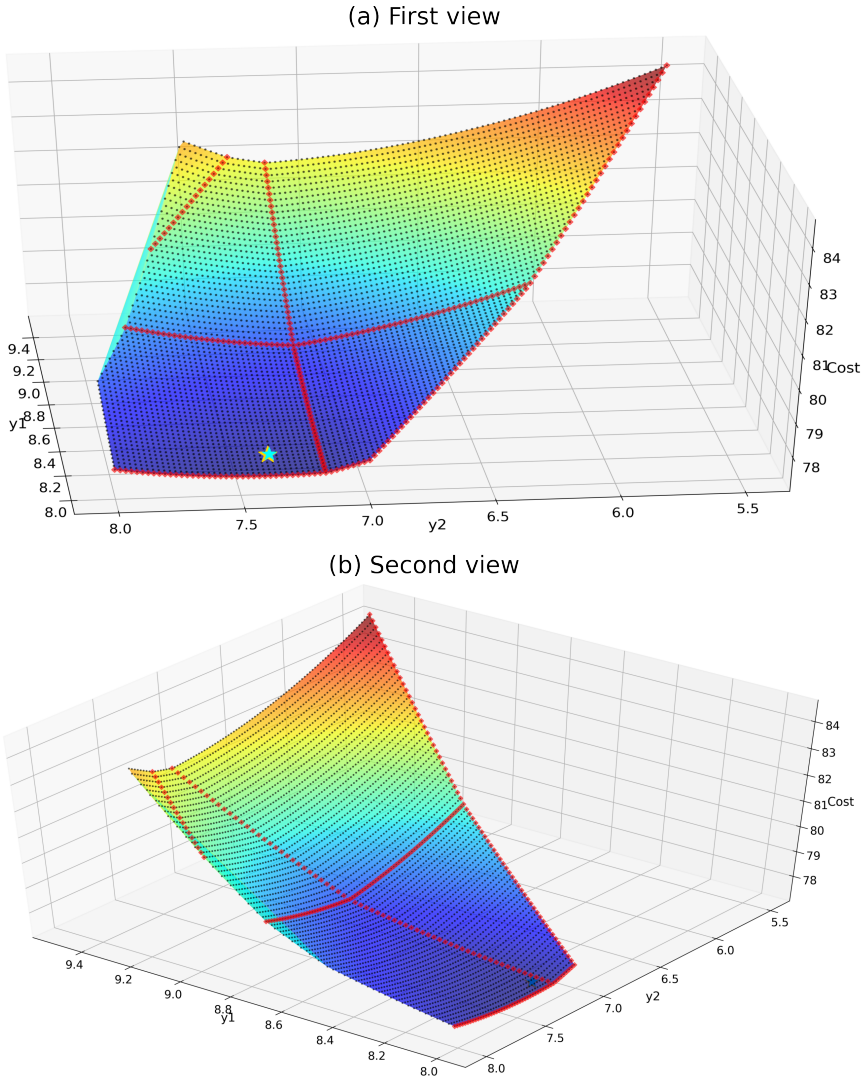


Figure 3.15: Total cost (objective function) for the three-zone problem, given optimal $\mathbf{x}$ for every $\mathbf{y}$. Across the lines formed by the red points are the changes in the three player sets (at optimal $\mathbf{x}$ given $\mathbf{y}$): $\mathcal{P}^I$, $\mathcal{P}^M$, $\mathcal{P}^F$, highlighting the boundaries between which the objective function is continuous, quadratic and strictly convex. The golden and cyan stars represent the optimal points found by ib-CQP and BBTree respectively.

landscape around the region, and the stopping criterion when solving the sub-CQP with Convex Quadratic Programming sub-routines. We can confirm that reducing the tolerance improves the ib-CQP solution which in this case concides with the BBTree one, but this also requires more outer iterations in general, and on larger problems could possibly drastically increase the computational time due to ill-conditioning when trying to improve in regions that are very weakly convex. Figure 3.15 gives us an idea of the landscape of the cost function in the $\mathbf{y}$ space given optimal choice of $\mathbf{x}$ for each $\mathbf{y}$, and thus gives us some intuition as to why ib-CQP works well in practice: if the solution of a sub-CQP problem lies on an internal boundary, improvement may be possible by solving the corresponding sub-CQP problem over neighbouring domains. If the solution to a sub-CQP sub-problem does not lie on the boundary, this is not only the global solution for this sub-CQP (by strict convexity) but

also a local solution over the whole domain. Note that this solution is globally optimal for a much larger domain than the usual infinitesimally small neighbourhood that is standard to local optimality.

However, the limitations of the method may also become apparent: when the number of sub-domains corresponding to sub-CQP problems is very large many sub-CQP problems need to be solved and the computational cost per problem remains just as high. As the number of sub-domains increases, the method becomes more *"myopic"*, and this could further result in tracing a path that leads to a solution that is very different than the global optimum. Further if the domain size of ib-CQP is very small, or elongated along one axis, then ill-conditioning of the sub-CQP problem may occur. For this reason, ib-CQP cannot guarantee any form of proximity to global optimum for its solution, although it does offer stronger than (purely) local convergence guarantees. The method also becomes increasingly slow as the number of players increases. Finally, although not observed in this example, discontinuities across internal boundaries can have a strong adverse impact on the ib-CQP solution, when compared to the true global one. Across an internal boundary, it may be possible for a strong drop in price to occur for some zone z and thus total cost, as y_z is reduced, if players with high initial cost become inactive at optimal x given y. However, the ib-CQP algorithm may give a different sub-CQP to solve next, based on the best solution when solving the current sub-CQP, since no information about the discontinuity magnitudes is used when solving sub-CQP.

We finally look at the objective function values, computational times taken, and convergence indicators in Table 3.2.

Method	Objective	Time taken	Convergence indicator
ieq-LP	78.51	1.46s	None, $i = N^q_{max} = 100$
ieq-LP-ma	78.56	0.12s	$\|\mathbf{x}^i - \mathbf{x}^{i-1}\|_2^2 / \|\mathbf{x}^i\|_2 < 10^{-6}$
ie-CQP	77.59	161.1s	$\Delta z / \|\mathbf{z}_c\|_2 < 2 \cdot 10^{-3}$
ie-CQP-wr	77.463	0.21s	$\Delta z / \|\mathbf{z}_c\|_2 < 2 \cdot 10^{-3}$
BBTree	77.463	37.3s	$\delta_T < 10^{-5}$
ib-CQP (CQP tol 10^{-2})	77.512	≈0.005s	$\|\mathbf{y}^i - \mathbf{y}^{i-1}\|_2 / \|\mathbf{y}^i\|_2 < 10^{-3}$
ib-CQP (CQP tol 10^{-4})	77.463	≈0.01s	$\|\mathbf{y}^i - \mathbf{y}^{i-1}\|_2 / \|\mathbf{y}^i\|_2 < 10^{-3}$

Table 3.2: Objective functions, times taken and convergence indicators for ieq-LP, ie-CQP, BBTree, ib-CQP and their variants.

We can see that the computational times of ieq-LP-ma and ie-CQP-wr are drastically reduced when compared to their counterparts, and this effect is especially pronounced for ie-CQP-wr. We note that although ieq-LP-ma is much faster than ieq-LP, in this case, the objective is a bit worse. However, the reverse is true for ie-CQP-wr when compared to ie-CQP. Further, ie-CQP-wr achieves the same solution as BBTree in this case, i.e the global optimum, within an objective optimality gap of 10^{-5}. On the other hand ib-CQP offers a solution only slightly worse than the global minimum, at a a very low computational cost,

and the same solution as the BBTree at the expense of slightly increased computational cost, which is nonetheless much smaller than for any other of the methods introduced here.

In the next subsection, we show numerically that indeed ie-CQP-wr and ib-CQP can generally obtain solutions very close to the ones obtained by BBTree (which can be seen as the global optimum within a tolerance). While ie-CQP-wr and ib-CQP are much faster than BBTree, at least in this case, the latter method may still be desirable because it offers a certificate of global optimality, while the solutions of ie-CQP-wr and ib-CQP can only be guaranteed to be locally optimal and sub-domain optimal respectively. Further, for more difficult problems, the time taken by ie-CQP-wr may also increase significantly, while the time taken by BBTree algorithm, albeit larger in general, may be less sensitive to specific problem details. In the light of the results presented here, one may be tempted to just use ib-CQP and discard all other methods. While the ib-CQP makes best use of the problem structure, and thus is indeed expected to be superior in general, this may not be the case if strong discontinuities in the zonal optimal stack (price-quantity) curves exist, if the number of players is very high (especially with respect to the total feasible domain size), or if the sub-domains corresponding to sub-CQP are very elongated along one axis. Further, as the problem size becomes increasingly large, solving CQPs becomes much more expensive than solving LPs, and thus the CQP based methods may become relatively slower. Since BBTree uses ieq-LP-ma as a way to find an upper bound, BBTree is more agnostic to size increase. Note that BBTree could be equipped with ib-CQP as well, and this may outperform the current form of BBTree in certain cases, but may become increasingly expensive at larger problem sizes. Nevertheless, heuristics may be used to reduce the time spent finding an upper bound. However, due to time limitations, equipping BBTree with ib-CQP was not investigated. Ultimately, the choice of solution method depends on the problem size and structure (number of constraints relative to number of players, cost structure), and the trade-off between computational resources and time available, when compared to the desired convergence guarantees. Clearly, BBTree is generally the slowest method but provides a global convergence guarantee, while ib-CQP provides sub-domain optimality and is expected to be fastest for well behaved zonal stack curves, at least if the problem size is not *very large*. Further, ie-CQP-wr can be much faster than BBTree and even outperform ib-CQP if the zonal stack curves are not well behaved, but only provides a local convergence guarantee, while ieq-LP-ma may be the fastest on large scale problems, but provides no convergence guarantee. In our situation, when concerned with the CWE 2019 (real world) data, we have found ib-CQP to give us the best trade-off between speed, results accuracy and convergence guarantees, while BBTree may give a slightly better objective function at the expense of greatly increased computational cost.

3.7.2.2 Evaluation of Approaches for Computation of Profit Function and Best Responses

In this subsection, we take a closer look at the typical profit functions for each player i, in the subspace $\mathcal{B}_{LB}(i)$. Clearly, the profit function $\Pi_i(m_i, a_i; \mathbf{m}_{-i}, \mathbf{a}_{-i}, \mathbf{M}_p, \mathbf{b}_p, \mathbf{Q}, d)$ depends on other players' strategies. When considering a player, for the purpose of this Subsection,

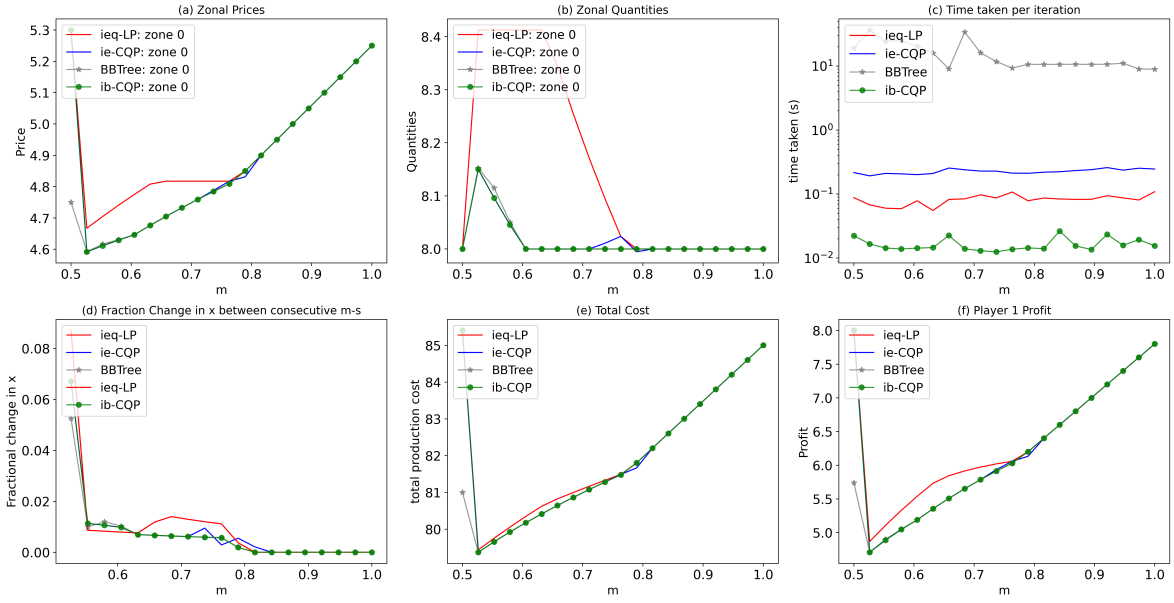


Figure 3.16: Player 1: Zonal price and quantity, time taken for ieq-LP-ma, ie-CQP-wr, BBTree, ib-CQP, fractional change in quantities, total cost and player profit under $(\mathbf{m}^I, \mathbf{a}^I)$.

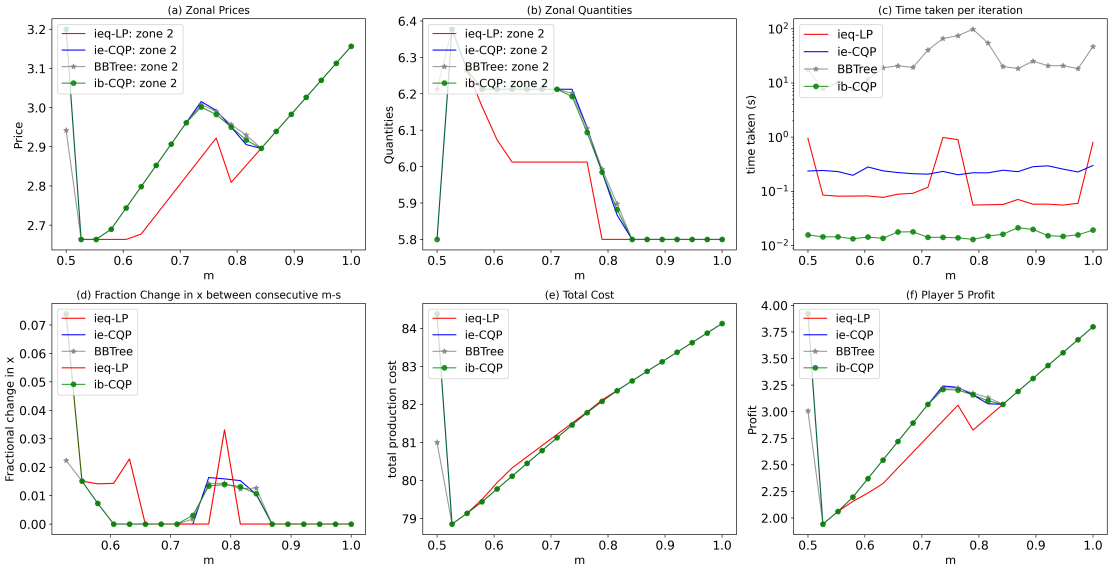


Figure 3.17: Player 5: Zonal price and quantity, time taken for ieq-LP-ma, ie-CQP-wr, BBTree, ib-CQP, fractional change in quantities, total cost and player profit under $(\mathbf{m}^I, \mathbf{a}^I)$.

we thus assume that all the other players play strategy $(\mathbf{m}^I, \mathbf{a}^I)$ or $(\mathbf{m}^{II}, \mathbf{a}^{II})$. The former is just an arbitrary one, while the latter is, as we shall see, in some sense *close* to a Nash Equilibrium. We use ieq-LP-ma, ie-CQP-wr, BBTree and ib-CQP to solve the market

clearing problem for every player, over the range $m_i \in [\frac{1}{2}c_i, c_i]$ with $(m_i, a_i) \in \mathcal{B}_{LB}(i)$, at $N_{pts} = 20$ discrete and equally spaced points. We randomly chose players 0, 1 and 5 to play against $(\mathbf{m}^I, \mathbf{a}^I)$ strategy, and the other three against $(\mathbf{m}^{II}, \mathbf{a}^{II})$.

For each player, we look at the zonal prices and quantities, time taken by each solution method, fractional change in assigned quantities x, total cost and profit function. To avoid congestion on the plot, the zonal prices and quantities are only shown for the zone to which the player belongs. For $(\mathbf{m}^I, \mathbf{a}^I)$ we show the results for player 1 and player 5 in Figure 3.16 and Figure 3.17 respectively. We first observe that when using $(\mathbf{m}^I, \mathbf{a}^I)$ as base strategy,

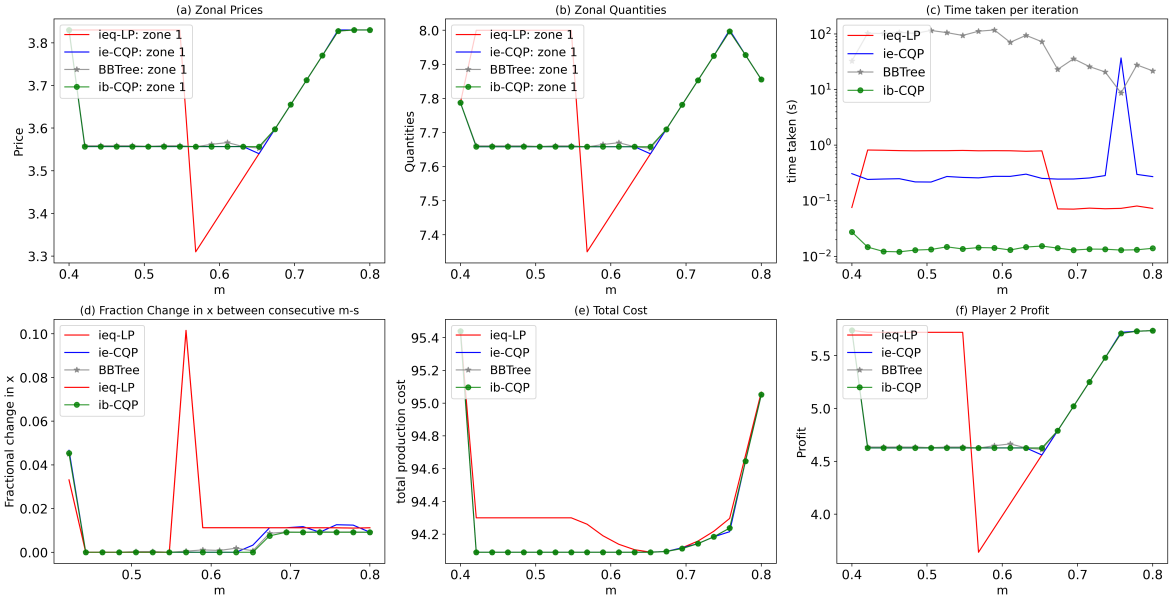


Figure 3.18: Player 2: Zonal price and quantity, time taken for ieq-LP-ma, ie-CQP-wr, BB-Tree, ib-CQP, fractional change in quantities, total cost and player profit under $(\mathbf{m}^{II}, \mathbf{a}^{II})$.

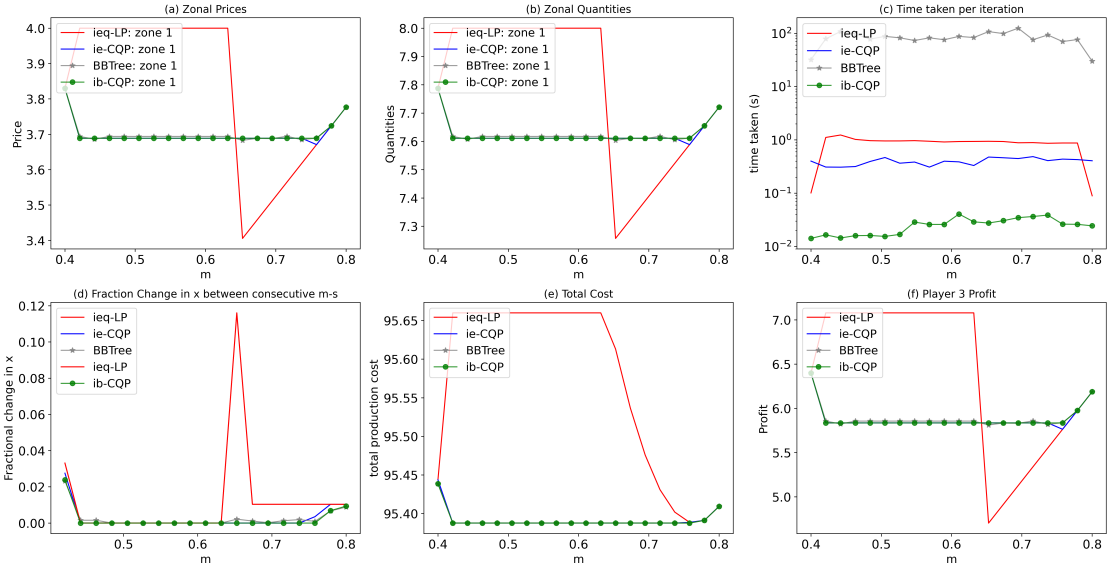


Figure 3.19: Player 3: Zonal price and quantity, time taken for ieq-LP-ma, ie-CQP-wr, BB-Tree, ib-CQP, fractional change in quantities, total cost and player profit under $(\mathbf{m}^{II}, \mathbf{a}^{II})$.

ib-CQP takes the least time to reach a solution, since it generally requires only two outer

iterations for convergence. However, the solution overshoots for both player 1 and 5 at $m_i = c_i$. The ieq-LP-ma method takes the second least time to reach a solution, but the solution is not always very accurate, although it is reasonable for reproducing the total cost $(v^*)^T y^*$, and player's profit Π_i, while the zonal quantities may be fairly inaccurate. On the other hand ie-CQP-wr is still fast and obtains results that are in general very close to BBTree ones (which can be assumed as the ground truth). When considering the best response function for player i, either of ieq-LP-ma, ie-CQP-wr or ib-CQP may give different best responses when compared to BBTree (ground truth), as seen for player 5, but this may be more pronounced for ieq-LP-ma.

The results for player 2 and player 3 when using $(\mathbf{m}^{II}, \mathbf{a}^{II})$ as base strategy are shown in Figure 3.18 and Figure 3.19. One can observe that the problems at hand are generally more difficult in this case. We observe that ib-CQP is still the fastest approach, and the solution is generally very accurate. The ieq-LP-ma is generally the second fastest, but not always, and we actually observe that when the method is slowest, the obtained solution is also poor, by comparison to the BBTree one. This could be because ill-conditioning may arise in the obtained LPs, for specific iterate values due to large number of (almost) redundant constraints. By contrast, ie-CQP-wr remains generally fast, and the results remain very close to the BBTree ones. However, in one instance we can observe a sharp computational cost increase from $0.2s$ to $21s$. The best response implied by ieq-LP is very different than the one implied by BBTree, while the best responses implied by ie-CQP-wr and ib-CQP are the same as BBTree for both player 2 and 3. However, both ib-CQP and ie-CQP-wr occasionally show minor undershoot or overshoot, and this is an indication that it is not guaranteed that the methods always give the same results as BBTree. Different results for a single point $(\mathbf{m}, \mathbf{a})$ may result in a totally different best response function. This motivates the need for the BBTree algorithm, when computing best responses or Nash Equilibria. This method comes with global guarantees, albeit at increased computational costs. Further, for player 2 at $m_i \approx 0.75$, ie-CQP-wr requires even more time than BBTree to obtain a solution, and the convergence guarantee is poorer. This could be because the ellipses become increasingly ill-conditioned but inequality constraints are concluded to be equalities at optimality at a much slower rate. This depends on the tolerance chosen and indicates that choosing a generally cheaper method does not guarantee lower computational time or cost in every instance. Table 3.3 shows the computational times taken for each method to obtain the best

	Player 0	Player 1	Player 2	Player 3	Player 4	Player 5
ieq-LP-ma	1.42s	4.45s	1.44s	1.51s	0.98s	1.4s
ie-CQP-wr	4.5s	4.32s	25.1s	5.4s	4.2s	5.55s
BBTree	112s	154s	456s	611s	556s	63s
ib-CQP	0.33s	0.25s	0.51s	0.61s	0.78s	0.31s

Table 3.3: Time taken to compute profit functions for each player, with $N_{pts} = 20$ discretisation points on $\mathcal{B}_{LB}(.)$

response function. Since our numerical experiments are somewhat limited in number and size, it is difficult to conclude the performance of each method by ranking them according to different criteria. However, for the benefit of the reader we give some indication based on theoretical properties, numerical experiments on the synthetic and real data, as well as our expectations. The results are presented below, but they should be understood as indicative as opposed to concluded based on an exhaustive set of experiments:

1. **Accuracy of solution when compared to global optimum (better first)**: BB-Tree, ib-CQP, ie-CQP-wr, ieq-LP-ma. This indication is based on numerical experiments on synthetic and real world data, as well as theoretical convergence guarantees.

2. **Computational effort for small and medium size problems (low is first)**: ib-CQP, ieq-LP-ma, ie-CQP-wr, BBTree. This indication is based on numerical experiments on synthetic and real world data, as well as expectations based on theoretical complexity.

3. **Computational effort for large scale problems (low is first)**: ieq-LP-ma, ib-CQP, ie-CQP-wr, BBTree. This indication is mostly based on expectations given by theoretical complexity of CQP and LP problems.

4. **Computational cost robustness to ill-conditioned problems**: ib-CQP, BBTree, ie-CQP-wr, ieq-LP. This indication is based on numerical experiments on synthetic and real world data, as well as expectations based on theoretical properties of each method. We observe ib-CQP to perform best in practice, followed by BBTree, while ie-CQP-wr and ieq-LP perform rather poor if strict convergence criteria are set (to ensure good quality of results). Note that ib-CQP is much less affected by ill-conditioning due to only solving CQPs in a much lower dimensional space of N_z dimensions (5 in our case). The BBTree method is somewhat more prone to cost increase, but we observe this to be rather mild if a smaller maximum number of iterations is set for obtaining the nodal upper bounds with ieq-LP-ma, and unlike for outright ieq-LP-ma, this does not have a large (or often any) impact on the final solution.

The general conclusion is to use BBTree if the highest standards of accuracy are required, while ib-CQP may generally offer the best trade-off between computational cost and quality of the solution, but the method may perform poorly if the zonal optimal stack has large discontinuities, large number of players relative to domain size, or very elongated subdomains. Nevertheless, by leveraging (partial) analytical results, ib-CQP is the only method that can quickly obtain the optimal active player set without requiring heuristics or intense computation. The ie-CQP-wr method is generally also offering a solution of comparable quality with ib-CQP, although the theoretical guarantee is slightly weaker, and the computational time may also be higher. For the capacity constrained case, the method relies on building high dimensional ellipses and thus it can become ill-conditioned before ib-CQP does. The

restriction to relevant subspaces by increasing the equality set close to a solution attenuates this problem, but finding the optimal threshold may prove challenging. However, the method is likely not drastically affected by strong discontinuities in the zonal optimal stack curve, since this is smoothed out when variation over x is considered. Finally, ieq-LP-ma is of great importance as a mechanism for finding upper bounds in BBTree, but it may be replaced by any other method (ib-CQP for example). Our choice for the mechanism finding the UB comes as a result of simplicity of the method, and because we expect ieq-LP-ma to require the least computational time for large scale problems, at least if the maximum number of iterations set is appropriate. Due to time constraints, equipping BBTree with ib-CQP to obtain upper bounds is left as future work.

3.7.2.3 Computation of Nash Equilibria and Evaluation of its Properties

In this section we evaluate the results obtained by using the BBTree algorithm for the computation of a global Nash Equilibrium point, with ieq-LP-ma and ie-CQP-wr used as pre-solvers to obtain a good initial estimate of the Nash Equilibrium point. We evaluate a range of discretisations for $N_{pts} \in \{4, 8, 12, 16, 24, 32, 64\} =: \mathcal{N}_{disc}$. We leave numerical evaluation of how Nash Equilibrium points change with parameters $\omega = (\mathbf{c}, \mathbf{b}, \mathbf{Q}, \mathbf{d}, \mathbf{M}_p, \mathbf{b}_p)$ as future work.

For the pre-solving steps, we observed using just ieq-LP-ma to usually require significantly many more iterations of C-JS under the Nash equilibrium computation algorithm (CNEP-Q), than when pre-solving with the ie-CQP-wr method. However, using only ie-CQP-wr as pre-solver on this problem required between $240s$ and $400s$ while pre-solving with ieq-LP-ma and then ie-CQP-wr required about $25s$ to $40s$ and $75s$ respectively ($100 - 115s$ combined). Since pre-solving is done on a local machine, in a sequential manner, the market solution from the *closest* available point that was solved for is used as initial guess, and thus we observe the total time taken to solve ie-CQP-wr in this case to be very similar (around $75s$) regardless of the value of N_{pts} chosen from $\mathcal{N}_{disc}$.

We only show detailed results for the final solution step, after pre-solving as described. Figure 3.20 shows the equilibrium strategy for player 5 for different levels of discretisations. We show player 5 because the biggest fractional changes in NE strategy occur in this case. We can see that the changes are significant but rather small and that in this case, one can obtain a very accurate estimate of the equilibrium strategies by choosing $N_{pts} = 32$ which is fairly small. It is also interesting to observe that the total computational time is roughly constant for small N_{pts} values and then increases linearly with N_{pts} for larger values. This is because the initial build-up cost is relatively constant irrespective of how many independent tasks are solved. However, once this cost is overcame, given sufficient independent processing units, the average time spent per problem solved should be the same, but the number of iterations of C-JS required to settle to an equilibrium may be higher for finer grids. In this case we observe this number of iterations to increase slower than linear, close to logarithmic.

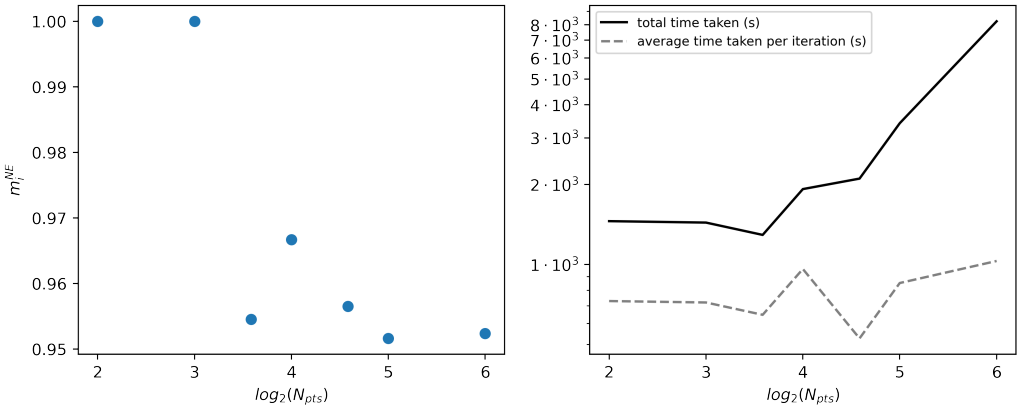


Figure 3.20: Change in optimal strategy of player 5 at NE (left) and total and average run times (right) for different discretisation levels.

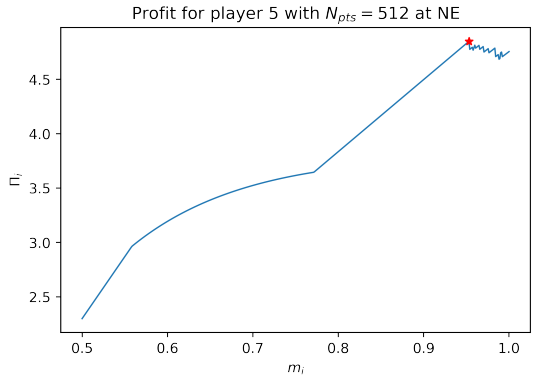


Figure 3.21: Profit function for player 5 at NE (at N_{pts}), computed with 512 discretisation points. The red star indicates the exact location of the best response on this plot.

As shown in Figure 3.21, to further gauge the quality of our global NE estimate, we look at the profit function of player 5 computed for $N_{pts} = 512$ discretisation points, at the NE solution given by $N_{pts} = 64$. This is not excessively expensive since it is done for only one player, only once.

We can observe that the best response given $N_{pts} = 64$ is about $m_5^B(N_{pts} = 64) = 0.952$ while when using $N_{pts} = 512$, it is $m_5^B(N_{pts} = 512) = 0.931$, giving a relative difference of about 2.2%, which is acceptable for most practical applications. Indeed, when the number of players N_p and number of zones N_z are larger, reaching this level of confidence may require a larger N_{pts}. Further, the specific parameters of the problem, ω, may also play a role in this.

Finally, we look at how m_i, computational time, and largest optimality gap change over C-JS iterations performed by CNEP-Q, as show in Figure 3.22. We can see that players' strategies change over C-JS iterations but not by very large amount. This is mainly due to starting at a *"good"* initial estimate given by our pre-solve approach. One can also observe that the computational time per iteration is fairly constant across both iterations and N_{pts},

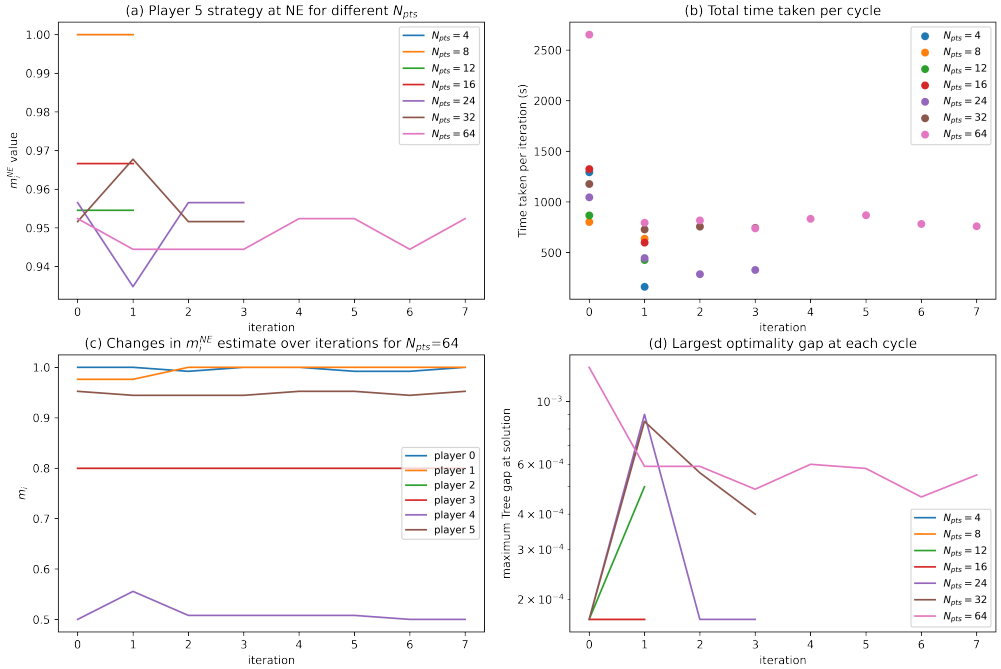


Figure 3.22: Strategy updates, computational times and optimality gaps for C-JS iterations under CNEP-Q

and that the first iteration always requires more time, due to the build-up cost. This cost takes a very large fraction of the total time for N_{pts}. Finally, the largest optimality gap (over all tasks solved at a C-JS iteration), gives an indication of how close the obtained market solution was to the true global solution. We can see that the largest optimality gap is rather small and does not change drastically across C-JS iterations or N_{pts}. This gives us a certificate that our NE estimate is close to the true NE, at least when assuming that the only possible strategies are the discretised ones. Since the impact of discretisation of NE was also discussed, we conclude that in this case we can obtain an estimate of a global Nash Equilibrium point (under RSS) fairly accurately, which is a very strong result. Finally, we ran multiple starting points for N_{pts} and convergence to the same Nash Equilibrium was obtained, but further analysis is required to verify if the chosen N_{pts} or pre-solving have any impact on this. Unfortunately, even for small N_{pts}, obtaining the whole pay-off matrix of the game is computationally infeasible, and thus we cannot yet confirm numerically that NE is unique (under RSS), even just for this problem.

3.7.3 Application to Real World Data (CWE Market $2019-2020$)

Our approach was developed with the Central Western European Day Ahead Auction in mind, and therefore naturally, we are interested in applying this methodology to CWE DAA data to obtain forecasts of market outcome and prices based on fundamental inputs. To evaluate the suitability of our proposed model, the obtained prices are then be compared to the actual real world prices, referred to as *target prices* from here on. Before arriving at results, a significant number of difficulties and limitations had to be overcome:

(a) the computational cost of the *full scale* CWE problem is very large, even when simplifying the set of market participants,

(b) although in Chapter 2 we have reconstructed the PTDF and RAMs, the polytope constraints $(\mathbf{M}_p, \mathbf{b}_p)$ may still be fairly inaccurate or ill-conditioned at times, potentially impacting the end results,

(c) we have considered each (hourly) time period independently, but in reality, Euphemia solves the market over a one day horison with hourly resolution, and market participants may also consider multiple time periods together due to ramping constraints, but also game-theoretic considerations, resulting in a larger market clearing problem, and a game with multiple time steps,

(d) complex bids such as for example fill-or-kill or parent-child block bids [9] are not considered here, due to increased computational burden, but these may sometimes have an important effect on the market outcome,

(e) obtaining representative and accurate fuel prices and power plants' cost for each producer is a very labour- and thought-intensive task,

(f) in particular, quantifying the cost of hydro storage power plants should ideally be done based on opportunity cost in the future, but this may be achieved by solving an optimisation problem for each hydro power plant individually, and this would greatly increase the complexity of our model, and is outside the scope of this work,

(g) we have only considered bids with linearly increasing price as a function of produced quantity.

A description of how most of these limitations are addressed is given in Subsections 3.7.3.1 and 3.7.3.2, but we focus on applying the current framework to the real data with minimum extra work. To this end, the model has to be calibrated to the data, and we do this by fitting only two scalars per zone, representing the cost scales for b and c entries, as described in subsection 3.7.3.2. The calibration is only done to SWM-TB and CM-TB, since SWM-GT and CM-GT are too computationally intense to be used in the fitting process. Nevertheless,

we perform a one iteration update of the TB fitted parameters to obtain better estimates of the GT models parameters.

We show in Subsection 3.7.3.3 that, while the SWM market clearing model better represents the market, for the same cost structure, the CM market clearing model proposed by us, generally offers a significant reduction in prices, and the total cost paid to suppliers is guaranteed to be lower. This can be used as a means to limiting producers' market power, and thus may be of interest to the market operators. In Subsection 3.7.3.4, using the SWM problem as the market clearing mechanism, we evaluate the performance of the truthful bidding (TB) and the game theoretic (GT) assumptions against the real world price data. We show that while both models perform relatively well on training and test sets, the SWM-TB one slightly outperforms the SWM-GT model. However, this could be due to the fact that both SWM-TB and SWM-GT use parameters fit to the data via SWM-TB. We finally devise a method based on hypothesis testing to evaluate (in hindsight) at each hour if players were bidding truthfully or gaming (bidding untruthfully/strategically).

We show that in fact, while for a large majority of times we cannot say with high confidence whether the players are gaming or bidding truthfully, the number of times we are confident that players are gaming is much higher than the number of times we are confident that the players are bidding truthfully. Our results show that, in general, gaming appears to be especially pronounced at intervals around the peak demand hours: 8am−1pm and 5pm−9pm. Another regime, where renewable energy influx appears to dominate the price action, is also identified and this effect is generally more pronounced at off-peak morning hours: 0am−6am. Our model can thus be used as a fundamental approach for market outcome and price prediction, understanding the impact various fundamental factors on the price, understanding of producers' behaviour, and identifying if and when players are bidding strategically instead of truthfully.

3.7.3.1 Input Data

For every time index representing one hour interval, our model requires the following inputs: (i) zonal demand for every country, (ii) network constraints given by the PTDF-RAM combination, (iii) cost structure (c_i, b_i) and production capacity limit (Q_i) for every player (producer) i.

First, the zonal demand for every country is obtained by using the day ahead forecast of demand available at ENtoE [29]. If forecasts further into the future are desired, then one needs a means to forecast the demand curve in advance.

Second, the reconstructed PTDFs and RAMs hourly data, obtained in Chapter 2 is used. Note that a forecasting method for the constraints could in principle be built based on the GSKs obtained in Chapter 2, but that we did not use such a method here. Instead, we confine ourselves to the first 5040 hours of 2019, and use the reconstructed PTDFs and

RAMs already obtained in Chapter 2. Recall that for each time t and each scenario s the network constraints can be written as

$$\mathbf{r}_{s,t} := -\mathbf{F}_{s,t}^{max} - \mathbf{F}_{s,t}^{ref} \leq \text{PTDF}_{s,t}(\mathbf{y}_t - \mathbf{d}_t) \leq \mathbf{F}_{s,t}^{max} - \mathbf{F}_{s,t}^{ref} =: \mathbf{R}_{s,t}, \tag{3.276}$$

where $\dot{t}$ and $\mathbf{y}_t$ are the zonal demand and production vectors. Further, $\mathbf{F}_{s,t}^{max}$ and $\mathbf{F}_{s,t}^{ref}$ are $|\mathcal{L}_{\text{cne}}|$-dimensional vectors, with each entry corresponding to a critical line $l \in \mathcal{L}_{\text{cne}}$, and in our case $|\mathcal{L}_{\text{cne}}| = 102$. Further recall that the reconstructed matrix $\text{PTDF}_{s,t} \in \mathbb{R}^{|\mathcal{L}_{\text{cne}}| \times N_z}$ where N_z is the number of zones, needs to be obtained from the centered version by adding back the mean as following $\text{PTDF}_{s,t} = \text{PTDF}_{s,t}^{c} + Y$. Based on our methodology, the PTDFs and reference flows are used to generate the polytope constraints (defined as $\mathbf{M}_p x \leq \mathbf{b}_p$), for each time t as following:

$$\mathbf{M}_p(t) = \begin{bmatrix} -\text{PTDF}_t^{\mathcal{LS}} \\ +\text{PTDF}_t^{\mathcal{LS}} \end{bmatrix}; \quad \mathbf{b}_p(t) = \begin{bmatrix} -\mathbf{r}_t^{\mathcal{LS}} - \text{PTDF}_t^{\mathcal{LS}} \mathbf{d}_t \\ +\mathbf{R}_t^{\mathcal{LS}} + \text{PTDF}_t^{\mathcal{LS}} \mathbf{d}_t \end{bmatrix} \tag{3.277}$$

where the argument t in $\mathbf{M}_p(t)$ and $\mathbf{b}_p(t)$ indicates that constraints are changing with time t, and $\text{PTDF}_t^{\mathcal{LS}}$, $\mathbf{r}_t^{\mathcal{LS}}$ and $\mathbf{R}_t^{\mathcal{LS}}$ are defined as

$$\text{PTDF}_t^{\mathcal{LS}} := ||_v \{[\text{PTDF}_{s,t}]_l : (l,s) \in \mathcal{LS}\} \in \mathbb{R}^{|\mathcal{LS}| \times N_z},$$

$$\mathbf{r}_t^{\mathcal{LS}} = ||_v \{[\mathbf{r}_{s,t}]_l : (l,s) \in \mathcal{LS}\}; \quad \mathbf{R}_t^{\mathcal{LS}} = ||_v \{[\mathbf{R}_{s,t}]_l : (l,s) \in \mathcal{LS}\},$$

where $\mathcal{LS}$ is the set of line-scenario pairs (l,s) that is observed in the data. Note that this is performed instead of simply concatenating all the corresponding vectors or matrices (e.g $\text{PTDF}_{s,t}$) for all scenarios $s \in \mathcal{S}$ at each time t. This is done to keep the number of constraints as small as possible, as an attempt to reduce ill-conditioning and computational cost. The added benefit of the method introduced in Chapter 2 is still large, since the method offers constraints data for all $(l,s) \in \mathcal{LS}$ pairs for all times t, instead of a much sparser subset of this. To resemble the approach of the TSOs and ensure a closed domain, the final version of $\mathbf{M}_p$ and $\mathbf{b}_p$ are obtained by adding box constraints that force each zone to cover at least 40% of their own demand, and export at most 60% of their base demand. These extra requirements can be justified by the need for energy security of every country, and the fact that higher production generally leads to higher prices. Further, the operators also impose these types of box constraints in practice, and are likely much more restrictive than the ones we propose.

We next need to obtain input data corresponding to each player i, for each time t, namely (c_i, b_i, Q_i). However, we need to first define the player set. To retain computational tractability, inspired by the work of [77], for each country, we define each player to represent

all power plants for a specific type of production (e.g. one player for all Gas plants in Austria), and consider all main production types as per the ENTSOE data on *Installed Capacity per Production Type*. While this is a strong simplification, it is crucial to allowing for tractable numerical solution for the Strategic Bidding case, since the computational complexity rapidly explodes with the number of players. Perhaps a better parametrisation of players would be to group the power plants by commercial producer, but this is a much more challenging data gathering exercise, and the large number of small commercial producers present in some countries (eg. Germany) would have to be aggregated in some way, perhaps by grouping these by geographical location. This would give us around 11 players per

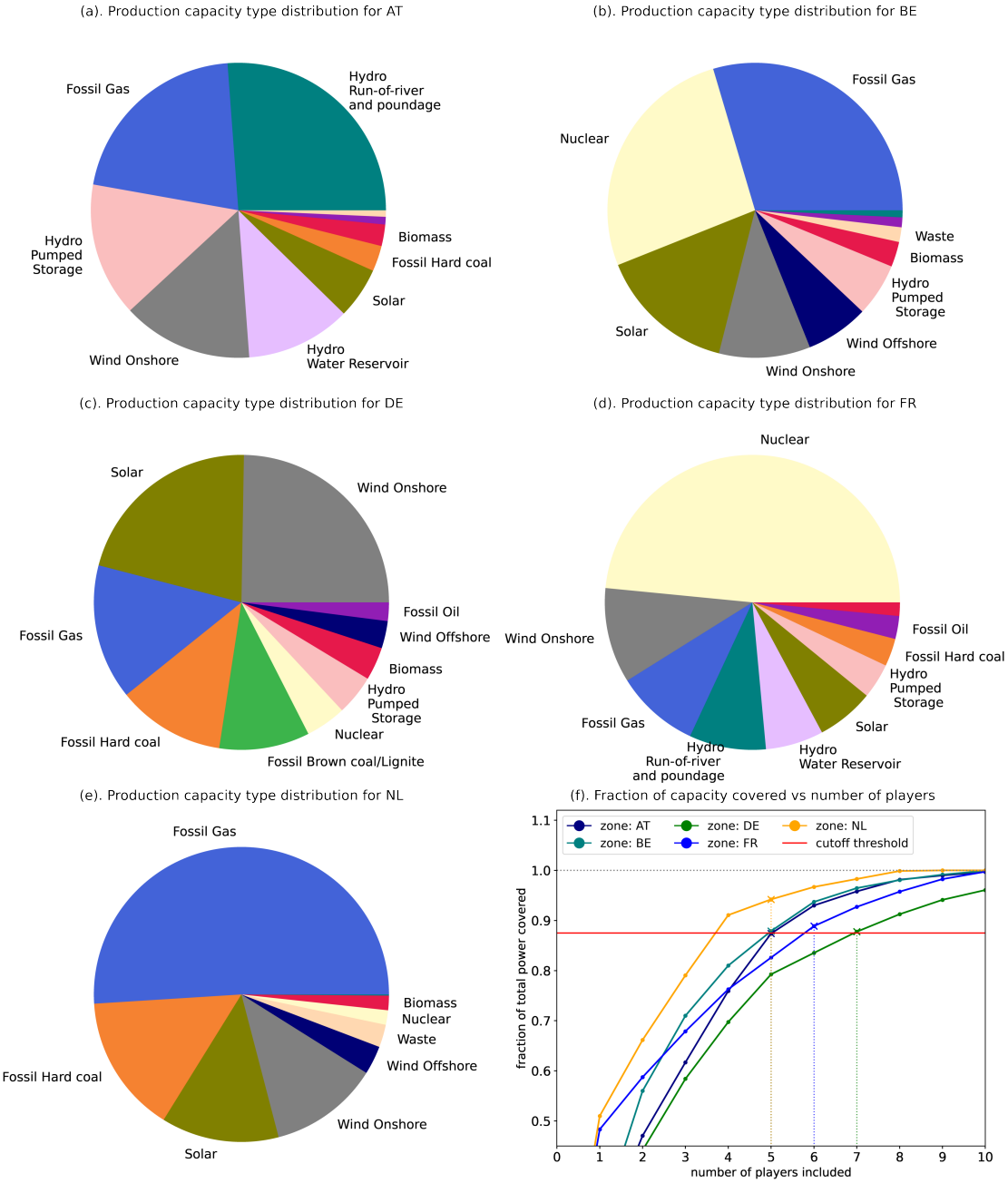


Figure 3.23: Capacity per production types per country, and illustration of player choice. Sub-figures (a)-(e) show the largest 10 production types per country. Sub-figure (f) illustrates the thresholding process.

country, and thus 55 players in total. However, some of these players would have very small capacity for some countries, and thus essentially do not affect the market outcome, but significantly increase the computational cost. Since we are required to solve for thousand of time indexes and the set of network constraints is composed of more than 600 rows, the total computational cost can grow very large. Therefore, we take a very parsimonious approach and restrict the player set, in an attempt to minimise computational effort while retaining the dominant fundamental factors. To this end, for each zone, we retain the top n_z players that cover at least $\theta = 88\%$ of the total installed capacity in the country, but require that $n_z \geq 5$, to retain most of the diversity of production types as well.

In other words, if $\phi_z(n_z)$ is the fraction of total capacity covered by the largest n_z players, then for each z we choose $n_z^* = \min\{n_z : \phi_z(n_z) \geq 0.88, n_z \geq 5, , n_z \in \mathbb{N}\}$. Figure 3.23 (a)-(e) show the top 10 production types for each country, while sub-figure 3.23.(f) summarises the approach for deciding the number of players. By using the numbers shown in this sub-plot, the reader can obtain exactly the types of production considered for each country, with the mentioning that On- and Off-shore wind, Hydro Pumped Storage and Hydro Water Reservoir, as well as Hard Coal and Lignite types are combined together in one player where possible, due to their similarity of cost and actual capacity structures. In terms of total capacity considered, this has the effect of lifting the lowest $\phi_z(n_z^*)$ to at least 91%. For example Belgium retains 5 players, including: (i) Fossil Gas, (ii) Nuclear, (iii) Solar, (iv) Wind Onshore plus Wind Offshore, and (v) Hydro Pumped Storage. In this way we get 5 players for the AT, BE, NL zones, 6 for the FR zone, and 7 for the DE zone, and thus the total number of players is 28, about half of the initial number.

With the player sets well defined, we can now proceed to gathering the cost data for each player. Note that in principle, for each player, we require a time series $(c_i(t), b_i(t))$. For the final series used as inputs, the same type in different zones may have the same or different cost values depending on the properties of the type and available data. We construct the players' cost per type, and the types to be considered are: (i) Fossil Gas, (ii) Coal, (iii) Nuclear, (iv) Solar, (v) Wind, (vi) Hydro Pumped Storage (vii) Hydro Water Reservoir, (viii) Hydro Run-of-river and poundage. For simplicity, for each player, the two cost parameters are obtained by extrapolating from a representative value indicating the production cost per MWh, for each time index t. This could (but does not have to) be the corresponding fuel cost for one MWh of production. Let this cost for type θ in zone z at time t be $k_{\theta,z}(t)$. Note that θ, z define a player, and call it j. To obtain two parameters we then define the cost function for player j as

$$\lambda_{j,t}(x_j) := k_{\theta,z}(t)\left(1 - \frac{f_\theta}{1-f_\theta}n_\theta\right) + n_\theta \frac{k_{\theta,z}}{(1-f_\theta)Q_j}x_j = b_j + c_j x_j, \tag{3.278}$$

where $\lambda_{j,t}(x_j)$ is the price asked at quantity x_j, f_θ is the fraction of total capacity at which the price asked is exactly $k_{\theta,z}(t)$, and $n_\theta + 1$ is the number of times the production cost is

higher at full capacity when compared to the base average level, $k_{\theta,z}(t)$. We take the cost to be $k_{\theta,z}(t)$ at 50% capacity level, i.e. $f_\theta = 0.5$ for all types for simplicity and $n_\theta \in [0, 1]$, to guarantee that $b_j \geq 0$, with the exact value of n_θ depending on the fuel type. We are now left with obtaining $k_{\theta,z}(t)$ and n_θ. Since it is hard to obtain n_θ, we just assign sensible values based on judgement. In this context when n_θ is close to 1 we say that the cost per MWh increases very fast with produced quantity, while a value close to 0 represents slow cost per MWh increase. We now discuss how $k_{\theta,z}$ is obtained and the n_θ values are assigned for each type:

1. For gas power plants we use the daily time series of spot gas prices at the Dutch Title Transfer Facility (TTF) hub, available at EEX, [26]. These are conveniently priced in $€/MWh$ of production, and thus requires no conversion. Although gas prices depend on location and delivery time we only consider the TTF hub for simplicity. Since we do not expect cost per MWh to increase rapidly with output we take $n_{gas} = 0.2$. Finally, the daily time series is expanded to hourly by assuming constant values during all hours of the corresponding day.

2. Coal prices are not so readily available, and data frequency is usually weekly in the futures market. To improve the granularity of our data, we use the daily spot coal price data available at Argus [6], and pad the weekends (when trading is closed) with the Friday value. The prices are stated in \$/ton and we convert this to $€/MWh$ by using the fact that 0.55tons of coal generate $1MWh$ on average, and a $\$/€ = 0.89$, thus requiring a scale-up of the value by multiplying by 1.62. We choose $n_{coal} = 0.4$ since production cost may increase due to requirement to purchase Global Emissions Offset on the spot.

3. Nuclear power plants' production cost is taken as the average cost per MWh, quoted at about 31\$, or about 27.6€ using the same conversion rate. However, because nuclear power plants cannot easily switch on and off, we assume that they are prepared to sell at a loss of 50% and thus their switch-off cost is $k_{nuclear,z}(t) = 13.8€/MWh \ \forall t$, for the purpose of this model, since we do not consider ramping constraints. In practice they may even sell at much lower prices for short periods of time just to avoid switching off. Since these power plants can only change their output very slowly, producing very close to max capacity runs the risk of being forced to sell at a much lower price later, effectively resulting in increased cost. Thus, we choose $n_{nuclear} = 0.8$.

4. For Wind and Solar energy, we take a very low value of $k_{nuclear,z}(t) = 0.5€/MWh$ for all t, and $n_\cdot = 0.05$ since increasing output is not expected to increase costs per MWh significantly. While the cost per MWh may seem very low in comparison to the usual quotes, we stick to this number due to the awareness that renewable energy influx was subsidised by the European Government for the year of 2019, meaning that the net cost was likely close to zero or even negative. To avoid modelling issues where

Wind and Solar are just as reliable as nuclear, the capacity is given by the day-ahead daily forecast for wind and solar generation available at ENTSOE [29]. Thus, for these types of players, while their cost is constant, their capacity changes rather erratically with time.

5. Hydro Pumped Storage cost is obtained by taking for each day, the average base load electricity price (for the off-peak hours) over a running window including the past week. This is because Hydro Pumped Storage plants operate like a battery: loading when electricity prices are cheap, and selling when prices are high. This gives a daily time series that is expanded to hourly by taking all hours within the day as identical. Producing at maximum capacity may result in low storage levels left for later hours, and thus the possibility of missing opportunities or requiring to load at a higher average price. However, these effects may be rather small under proper management and planning, and thus we assign $n_{hydro-s} = 0.2$.

6. Finally, the Hydro Run-of-river power plants generally have a levelised cost of energy (LCOE) between $2\$/MWh-$ and $7\$/MWh$. Taking an average value and converting it we obtain a cost of about $k_{hydro-r,z} = 8.45€/MWh$, $\forall t$. We choose $n_{hydro-r} = 0.1$.

The approach employed here for obtaining time series of the cost parameters for each player is admittedly very simplistic and perhaps naive. We attempt to compensate for this by performing a simple calibration of costs to better represent prices in Subsection 3.7.3.2. Although simplistic, due to time constraints, we use this approach to facilitate focusing on the formulation, analysis, and solution of the market clearing and game theoretic models, which also require intense implementations. Nevertheless, we show that with minimal fitting (of only 1 parameter per zone), we obtain results that capture well the main features of the actual prices time series, with train and test errors of only 17.9% and 24.5% on average, even for large test window (28 days or 672 hours). This reveals the robustness of our fundamental model and suggests that the reconstructed network constraints (from Chapter 2) offer a satisfactory representation of the true constraints, at least for this application.

3.7.3.2 Model Calibration

The calibration approach is very simple and is constrained to adjusting $(\mathbf{c}, \mathbf{b})$ values only. This is to minimise computational cost but also the number of fitted parameters, as in principle, our fundamental model should be representative of the market without requiring any fitting, if the cost structure and other inputs are descriptive. Thus, we use this mostly as a simple way to improve our guess on the cost structure.

Since production costs may change we can still consider the cost to depend on the changing fuel prices and fit only the power plants' characteristics. To this end, for each zone

z we simply fit a scale parameter for each $\mathbf{c}$ and $\mathbf{b}$ variables

$$c_i^{final} = s_z^c c_i^{initial};\ b_i^{final} = s_z^b b_i^{initial}\ \forall i \in \mathcal{P}_z, \tag{3.279}$$

giving a total of 10 parameters to fit, and we initialise $s_z^{\cdot} = 1$, for all z. As we shall see immediately, this also has the major benefit of drastically simplifying the optimisation problem by allowing to easily track and compute derivatives. Since the optimisation process requires solving the underlying model a very large number of times, even with these simplifications, fitting the Game-Theoretic (GT) models would be very computationally intense. For this reason we only fit the SWM and CM models under the Truthful Bids (TB) assumption, and explain later how the parameters for the GT models are adjusted. We fit the zonal cost scales $\mathbf{s}^c$ and $\mathbf{s}^b$ to the price data. Regardless of whether CM or SWM market clearing is used, the model price can be expressed as $v_z = s_z^c c_{k_z} x_{k_z} + b_{k_z}$ for each zone z, where k_z is the player with the highest marginal price in the zone and $x_{k_z} > 0$. The advantage of defining the cost scales is that $\frac{\partial v_z}{\partial s_z^{\cdot}}$ can be easily computed, regardless of the fact that k_z changes. The optimisation objective is then

$$F(s) = \frac{1}{N_T} \sum_{t=1}^{N_T} \sum_{z} (v_{z,t} - P_{z,t})^2, \tag{3.280}$$

where $v_{z,t}$ and $P_{z,t}$ are the model and target prices respectively, at zone z for time t. Note that the scale parameters $\mathbf{s}^T = (\mathbf{s}^{cT}, \mathbf{s}^{bT})$ are not dependent on time, and thus have a very strongly over-determined Nonlinear Least Squares Problem. Let

$$F_t(s) = \sum_{z} (v_{z,t} - P_{z,t})^2. \tag{3.281}$$

We then have that

$$\frac{\partial F_t}{\partial s_z^c} = 2(v_{z,t} - P_{z,t}) c_{k_z} x_{k_z};\ \ \frac{\partial F_t}{\partial s_z^b} = 2(v_{z,t} - P_{z,t}) b_{k_z}, \tag{3.282}$$

which by summation, and collecting for all zones z, gives $\nabla_s F(s)$. The second derivatives can be similarly computed as

$$\frac{\partial^2 F_t}{\partial^2 s_z^c} = c_{k_z}^2 x_{k_z}^2;\quad \frac{\partial^2 F_t}{\partial^2 s_z^b} = b_{k_z}^2;\quad \frac{\partial^2 F_t}{\partial s_z^b \partial s_z^c} = b_{k_z} c_{k_z} x_{k_z}, \tag{3.283}$$

with all other entries in the $\nabla_s^2 F$ being 0. Both Gradient Descent and Newton's Method with line-search as globalisation method were tried, and Gradient Descent appears to be able to obtain lower values of the objective function value. Thus, we stick to Gradient Descent,

and summarise the fitting algorithm below:

Algorithm 19 Cost Structure Calibration

Require: input $(\mathbf{c}(t), \mathbf{b}(t), \mathbf{M}_p(t), \mathbf{b}_p(t), d_t, P_t)$ for $t \in \mathcal{T}$
  initialise $\mathbf{s}^c \leftarrow \mathbf{1}$, $\mathbf{s}^b \leftarrow \mathbf{1}$, error threshold δ, $\eta = 0.65$, $\alpha = 1$, $K = 20$
  set initial error $\epsilon = 10\delta$ (to guarantee first iteration)
  while $\epsilon > \delta$ **do**
    compute $\nabla_z F(s)$ as per (3.282), $\psi \leftarrow$ False
    for $k = \overline{1, K}$ **do**
      $\mathbf{s}' = \mathbf{s} - \alpha\eta^k \nabla_s F(\mathbf{s})$
      if $F(\mathbf{s}') < F(\mathbf{s})$ **then** $\psi \leftarrow$ True and Break
    end for
    if $\psi =$ False **then** Break
    $\mathbf{s} \leftarrow \mathbf{s}'$; $\epsilon \leftarrow F(\mathbf{s}')$
  end while
  return $\mathbf{s}$

Finally, this procedure is applied for fitting parameters for the SWM and CM models on a training data with times set $\mathcal{T}_{train} = [24, 2040] \cup \mathbb{N}$, and a test set 28 days, $\mathcal{T}_{test} = [2040, 2712] \cup \mathbb{N}$. We refer to this fit for the cost scales as SWM-fit. The SWM-GT and CM-GT models are too computationally intense to be fit to the price data with the same procedure. Thus, we take the SWM-TB fitted parameters, run the SWM-GT model to obtain the prices $v_{z,t}^{SWM-GT}$ for a subset $\mathcal{T}_{GT} = \overline{24, 672}$, and re-scale the s_z^c by dividing them by the average value over $\mathcal{T}_{GT}$ of $v_{z,t}^{SWM-GT}/P_{z,t}$, denoted as ρ_z, i.e. $s_z^c(GT) \leftarrow s_z^{c*}(TB)/\rho_z$, $\forall z$. We do not re-scale s_z^b, i.e. $s_z^b(GT) \leftarrow by s_z^b(TB)$. This is not a calibration of the GT models in the true sense, but rather a one iteration improvement of the available fitted parameters for the Truthful Bidding case.

In the next two subsections we review numerical results to reveal some market properties. In subsection 3.7.3.3, we perform a comparison between the SWM-TB and the CM-TB models, and reveal that whereas SWM-TB better represents the data, under the same circumstances, CM-TB generally offers significant reduction in prices, and the total cost is confirmed to be always lower. This reduces the ability of producers to exercise market power, and thus changing the market clearing to a Cost Minimisation approach might be of interest to regulators or operators. In subsection 3.7.3.4 we compare the performance of the SWM-TB and SWM-GT models, not only as a numerical experiment, but also in an attempt to reveal if and when the producers might have bid untruthfully. We conclude that SWM-TB performs better on average, but there exist times where the SWM-GT model is clearly much more representative. We devise a simple method based on hypothesis testing to recognise times when players are gaming, and observe that we can say much more often with high confidence that the players are gaming, than that they are bidding truthfully, albeit for a large majority of times we cannot distinguish between the two modes with high confidence.

3.7.3.3 Truthful Bidding: Social Welfare Maximisation vs Cost Minimisation

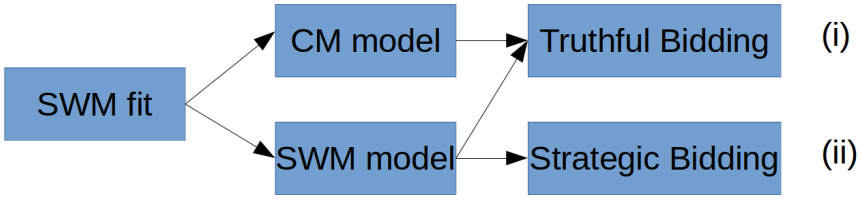


Figure 3.24: Type of runs considered for the SWM and CM models.

As shown in Figure 3.24, we perform two types of runs that are of interest for the focus of this subsection, on both $\mathcal{T}_{train}$ and $\mathcal{T}_{test}$: (i) we run SWM-TB with the SWM-fit parameters and call these results SWM-TB (SWM-fit), and (ii) we run CM-TB with the SWM-fit parameters and call these results CM-TB (SWM-fit). The comparison between (i) and (ii) reveals the potential benefits of Cost Minimisation over Social Welfare Maximisation, since we require exactly the same circumstances for a direct comparison. We compute the average error as $e_z(\mathcal{T}) = \frac{1}{|\mathcal{T}|}\sum_{t\in\mathcal{T}} |v_{z,t}^{model} - P_{z,t}|$, and the relative average error as $\overline{e}_z(\mathcal{T}) = e_z/\mu_{t\in\mathcal{T}}(P_{z,t})$, where $\mu_{t\in\mathcal{T}}(P_{z,t})$ represents the mean of $P_{z,t}$ over the $\mathcal{T}$ time indexes set.

	AT	BE	DE	FR	NL	Aggregate
SWM-TB (SWM-fit)	20.3%	14.2%	26.1%	14.5%	13.6%	17.9%
CM-TB (SWM-fit)	27.4%	38.8%	35.6%	15.5%	32.8%	30.2%

Table 3.4: Results for $\overline{e}_z(\mathcal{T}_{train})$ for each zone and aggregate.

	AT	BE	DE	FR	NL	Aggregate
SWM-TB (SWM-fit)	28.8%	22.8%	30.5%	19.6%	18.5%	24.6%
CM-TB (SWM-fit)	33.1%	40.8%	49.7%	31.6%	36.1%	38.2%

Table 3.5: Results for $\overline{e}_z(\mathcal{T}_{test})$ for each zone and aggregate.

As it can be observed from Tables 3.4 and 3.5, the CM-TB (SWM-fit) generally gives larger error but this is expected since these results use the SWM obtained parameters, instead of optimal parameters for the CM-TB model. We can also observe that the test error is generally larger for the SWM when compared to the train set, and thus one might argue that the model has been slightly over-fit to the training data. However, while this hypothesis cannot be fully disproved, the number of parameters is very small in relation to the complexity of the problem, and the SWM-TB (SWM-fit) model still has the best generalisation error. Further, as can be seen in Figure 3.25, the test set is quite challenging. First we observe that on the second part of the test set, while gas and coal prices steadily

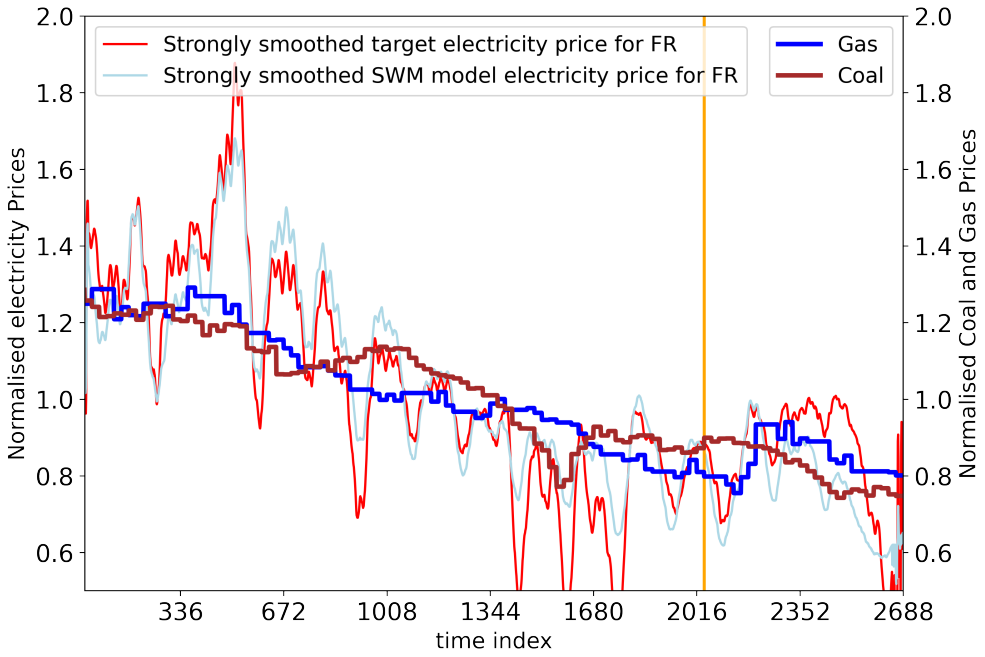


Figure 3.25: Trends Comparison: electricity, gas and coal price vs SWM-TB model prediction, for the $\mathcal{T}_{train}$ (left of orange line), and $\mathcal{T}_{test}$ (right of orange line). Electricity prices are smoothed by taking an exponentially weighted average over 49 hours centered in the point of interest. Only FR electricity prices are shown for better visualisation.

decrease, on average, the electricity prices remain elevated and then suddenly drop. As a thought exercise, if we assume that all the other inputs remain constant, reduction in coal and gas prices will result (under TB) in our model predicting a reduction in electricity prices (as observed), especially since coal and gas power plants are often on the margin. Thus, this may increase the discrepancy between our prediction and the price target data. This behaviour of (smoothed) electricity prices suggests that producers may price their fuel costs in a rather conservative way, by taking higher and/or older prices as reference.

We next look at detailed results of the SWM-TB (SWM-fit) and (CM-TB (SWM-fit) models for the price time series and total costs, and compare this to the observed data. We only focus on the first 672 and 336 hours of the train and test sets respectively, for better visualisation of details. From Figure 3.26 we observe that the CM-TB model generally gives lower prices than the SWM-TB one, and that the total cost is always lower. The latter is expected, since by definition the CM optimisation problem is minimising this cost, while the SWM problem minimises some form of apparent cost. Further, CM gives much flatter price profiles, suggesting that when compared to SWM it reduces the impact that a single producer has on the final zonal price. We can further observe that the CM model price closely follows the SWM model price for France, revealing robustness of prices in this zone, with respect to the market clearing method, especially when compared to Belgium and the Netherlands, where the price reductions obtained via CM market clearing are very large. This reveals high price sensitivity of the Belgian and Dutch zones with respect to the market clearing rule. Since the Netherlands rely heavily on gas power plants, it also indicates that

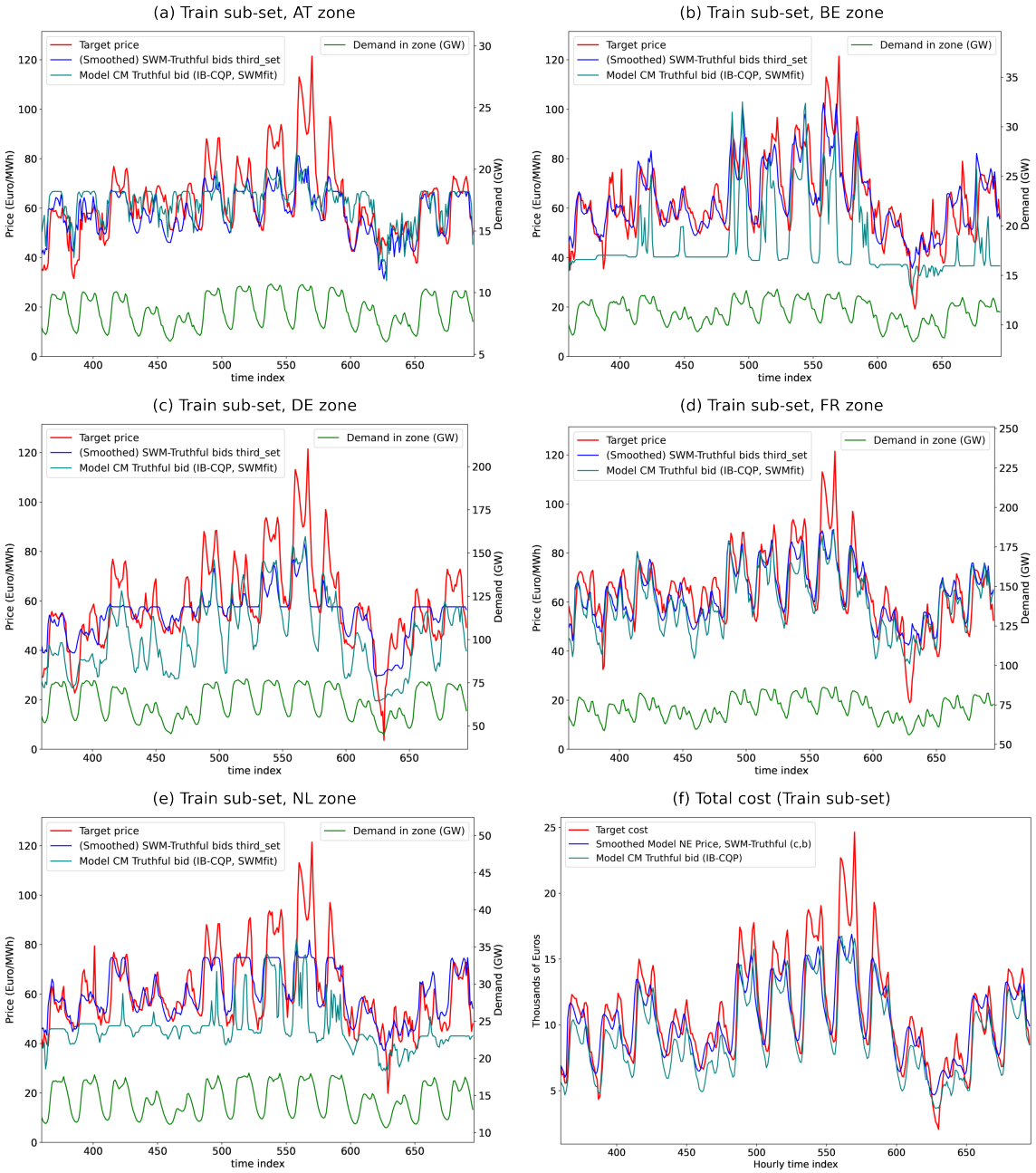


Figure 3.26: Training set: SWM-TB and CM-TB model results comparison with target prices, with indicative demand series.

using the CM model (instead of SWM) could reduce the price impact of this reliance. One can also observe that CM often gives higher prices than SWM for the Austrian zone. This is not an inconsistency, as the cost minimisation problem guarantees that the total cost of electricity procurement is minimised, not the individual zonal costs or prices. It thus appears that if switching to Cost Minimisation, Austria may pay the price for obtaining cheaper electricity for the whole market on average. This is perhaps due to the large hydro storage capacity in this zone, which is optimally used by the clearing mechanism to minimise the total cost, instead of the zonal price in Austria, at least if producers bid truthfully. We note that the approach used for valuation of hydro stored power is likely to significantly

impact this conclusion.

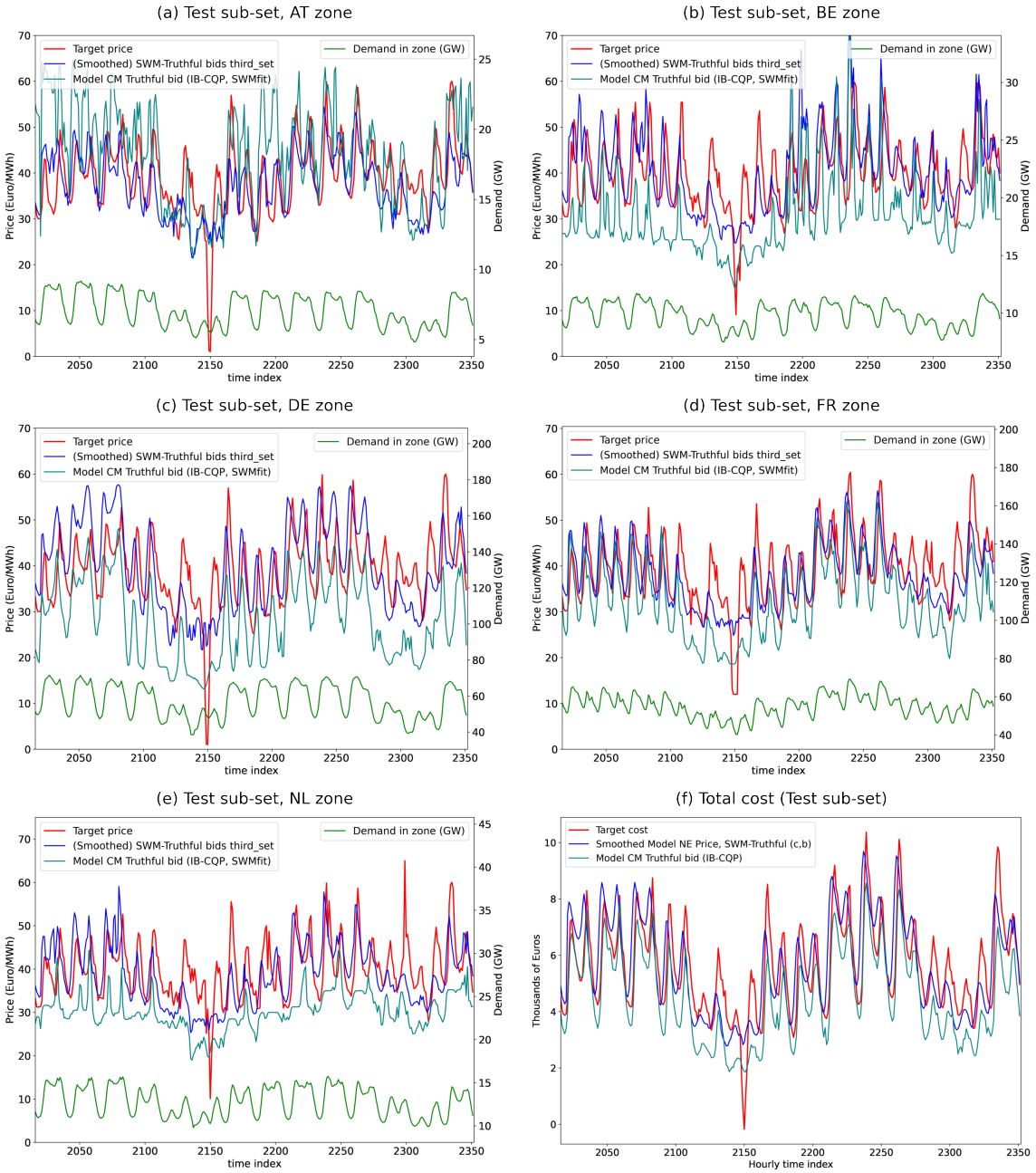


Figure 3.27: Test set: SWM-TB and CM-TB model results comparison with target prices, with indicative demand series.

By now focusing on the comparison of SWM-TB with the target prices, we observe that often the SWM-TB model under-predicts the real price, despite the fact that no demand spike is recorded. The price spikes could therefore be a consequence of supply shortage or strongly constrained network. While we assume constant supply, variation in network constraints is included in the model. Assuming accurate network constraints, this suggests that players may bid strategically at times to maximise profits, despite the fact that they may often bid truthfully. Note that in practice it may be difficult to distinguish between the case of capacity reduction due to outages and capacity reduction as a strategic tool for

increasing profit.

We finally observe that our results are worst for the German zone, and this could be due to the very complex nature of this region, including a very diversified portfolio of power plants, large grid with multiple operators, and large renewable energy but also coal plants capacity. The nature of renewable production via wind and solar is very unpredictable, while the extent to which coal power plants are used may not be a function purely of market price, but also of environmental conscience, and our model for incorporating the cost of emissions may be too simplistic. Further error could be introduced by the modelling of participants, as the number we consider for Germany is only seven, while in reality there is a much larger number of market participants.

From Figure 3.27 we can observe that SWM-TB generally performs well on the test set, that the CM-TB (SWM-fit) gives more frequent spikes than for the training set, suggesting that this set might have more erratic features.

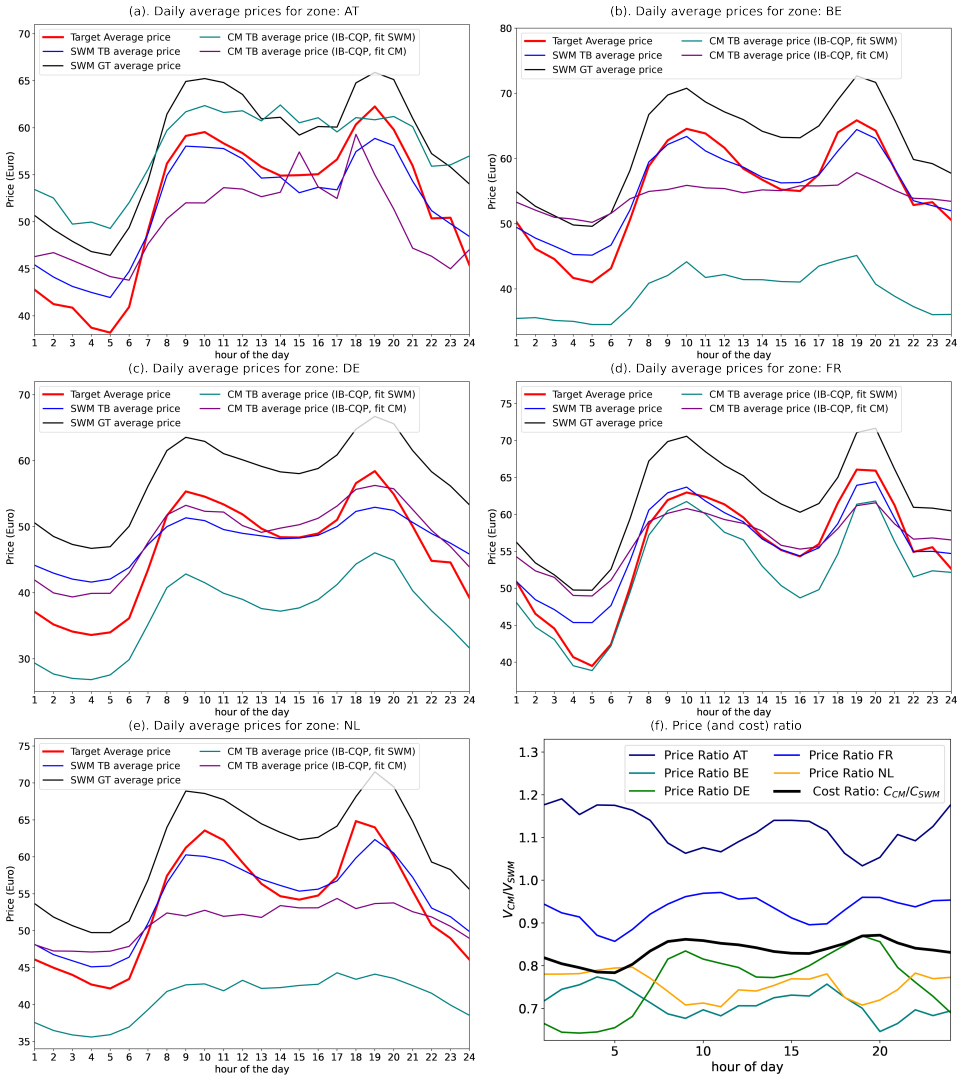


Figure 3.28: Average daily profile for each country: sub-figures (a) - (e) and (f) the ratio of the CM profile to SWM profile, as well as the total cost ratio.

We finally look at the average daily price profile for each zone, and the corresponding

ratio of the CM-TB (SWM-fit) to SWM-TB (SWM-fit), as per Figure 3.28. First, note that when considering a country, under inflexible demand, the price and cost ratio for that country is the same. We observe that indeed the CM model decreases the average total cost, and that the average daily prices for all zones except Austria are also reduced, for each hour. We can observe that Belgium, France and the Netherlands obtain the most drastic price reduction at hours of peak demand. This is because both France and Belgium have rather large production (nuclear) capacity at low prices. When compared to SWM, CM allocates power plant production levels much more effectively, by reducing the impact that small but expensive units can have on the zonal price, and the effect of this allocation is more pronounced when demand levels are high. This is because the zonal price is set by the power plant producing at the highest cost, and thus reducing the allocation to expensive plants even by a small amount can have a large impact on the price. It is interesting to observe that the Netherlands also benefits of this effect. This could be due to cross-border flows from Belgium and France, as well as coal power plants which may produce at lower price levels than gas plants.

We finally note that the CM-TB (SWM-fit) and SWM-GT (SWM-fit) models respectively, act as lower and upper bounds to the target price, confirming that bidding strategically is generally increasing the prices, while using a CM market clearing model generally results in price reduction. We also observe that the CM-TB (CM fit model) gives a much flatter price profile, especially for Belgium and the Netherlands, suggesting that the CM model is more robust to underlying changes when compared to the SWM model.

Thus, we conclude that the SWM-TB (SWM-fit) model is generally most representative for the price data, while using a CM market clearing model may generally give lower prices, the corresponding total electricity procurement cost is guaranteed to be lower. Further, the CM model may offer less sensitive prices with respect to underlying changes such as production costs, demand levels or even network constraints. However, it appears that there exist time intervals where the SWM-TB model is rather poor at explaining the actual price, and this occurs when there are large downward or upward price spikes. A typical cause for the former could be unexpected influx of renewable power generation, while the large upward spikes could be due to strategic bidding, and we further investigate this in the next subsection. In the next subsection, we perform a comparison between SWM-TB and SWM-GT models, to better understand the properties of each model, relative to the target price, and to identify (in a probabilistic sense) if and when players were bidding strategically.

3.7.3.4 Social Welfare Maximisation: Truthful Bidding vs Game Theoretic

In this subsection we only look at results for the SWM Market clearing model, since this is more representative of the market, when compared to CM. We start with a high level comparison of the SWM-TB and SWM-GT models by summarising the relative mean error for both $\mathcal{T}_{train}$ and $\mathcal{T}_{test}$, in Table 3.6. By direct comparison of the relative mean error, we

	AT	BE	DE	FR	NL	Aggregate
SWM-TB ($\mathcal{T}_{train}$)	20.3%	14.2%	26.1%	14.5%	13.6%	17.9%
SWM-TB ($\mathcal{T}_{test}$)	28.8%	22.8%	30.5%	19.6%	18.5%	24.6%
SWM-GT ($\mathcal{T}_{train}$)	21.9%	18.5%	30.0%	18.2%	17.4%	21.4%
SWM-GT ($\mathcal{T}_{test}$)	26.7%	25.4%	34.2%	17.6%	17.6%	25.2%

Table 3.6: Comparison of relative mean errors for the Truthful Bids and Game Theoretic models, on train and test data sets.

observe that the Truthful Bids model outperforms the Game Theoretic one. However, the difference is rather small, and it is worth noting that while the cost scale parameters for the SWM-TB were fit via Gradient Descent, only a one step heuristic fit was performed for the parameters of the SWM-GT model. Further, the summary statistic presented here does not reveal any details with regards to the temporal structure, and producers may choose to bid strategically only at specific times. A potential reason for this is that the regulators require the producers to bid truthfully, in an attempt to minimise market power exercised by the supply side, but producers are concerned with their own profit, and thus participants may attempt to conceal exercising their market power by bidding strategically only at specific times.

A detailed view of the model and observed prices time series is shown in Figure 3.29, for a better intuition of the models' performance. We can see that the Game Theoretic model still accurately traces the target price, but while the Truthful Bids model has the tendency to under-predict, the Game Theoretic one is more likely to over-predict. We can qualitatively observe that the GT model is often very accurate at peak hours, when compared to the TB one. This is rather remarkable, given the extremely simple calibration of the GT model, and suggests that players may not only bid strategically, but also strategically choose the times at which they do so. One may argue against the possibility of strategic bidding, on the premise that no parameter fitting is required for our models, since they are of fundamental nature. However, the complexity of the players' cost structure makes it very difficult to obtain accurate representations without very granular data and analysis, or calibration. Further note that calibration of the SWM-TB model to the observed price data could in fact adversely incorporate and conceal gaming. To observe this, imagine a tacit agreement between all players to bid exactly twice their costs. In this case, the value of our cost scales would be double, but the model would perfectly represent the price series. Indeed, for our fit, we observe our cost scales to be well above one. This issue can be best solved by having highly granular and reliable cost data and an accurate cost model. In our case, given the limited information on cost structure, it is precisely the inconsistencies in the bidding patterns that help us reveal strategic behaviour.We can observe that there are isolated days where prices are much higher, while the demand pattern is essentially the same. This could be due to a mode (state) change: from truthful bidding to strategic bidding. Admittedly the

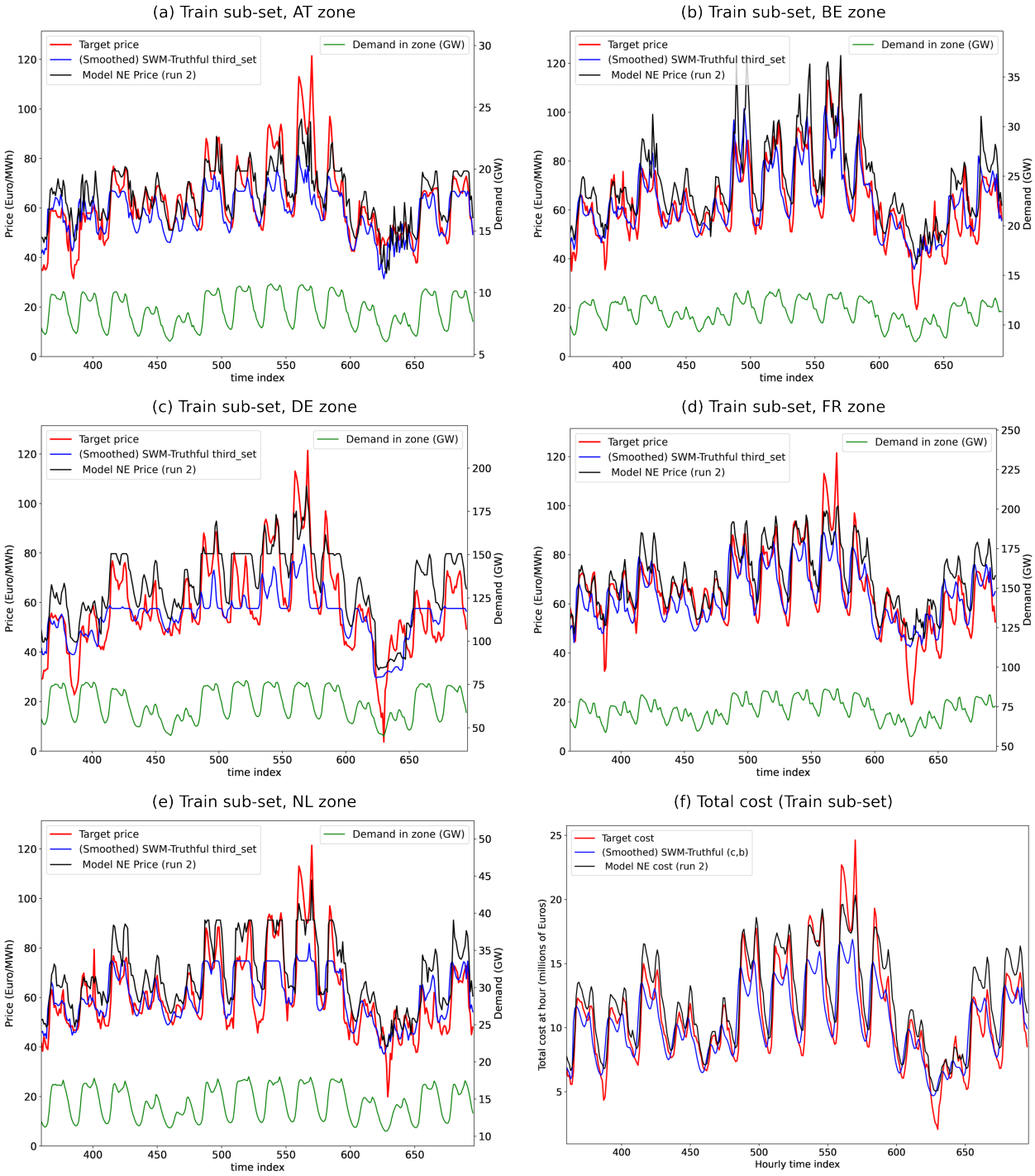


Figure 3.29: Price time series results (Training set): SWM - Truthful Bids (blue) and SWM - Game Theoretic (black) comparison against observed prices (red).

price spikes could occur due to fast changes in network constraints, while our reconstructed data may change more slowly, and there are other market features that our model does not consider.

Unfortunately it is very difficult, or perhaps even impossible to distinguish these two effects given the available data. However, since we only use the reconstructed constraints data, without forecasting into the future, and given the results in Chapter 2, it seems reasonable to assume that our constraints time series captures the main features of the real

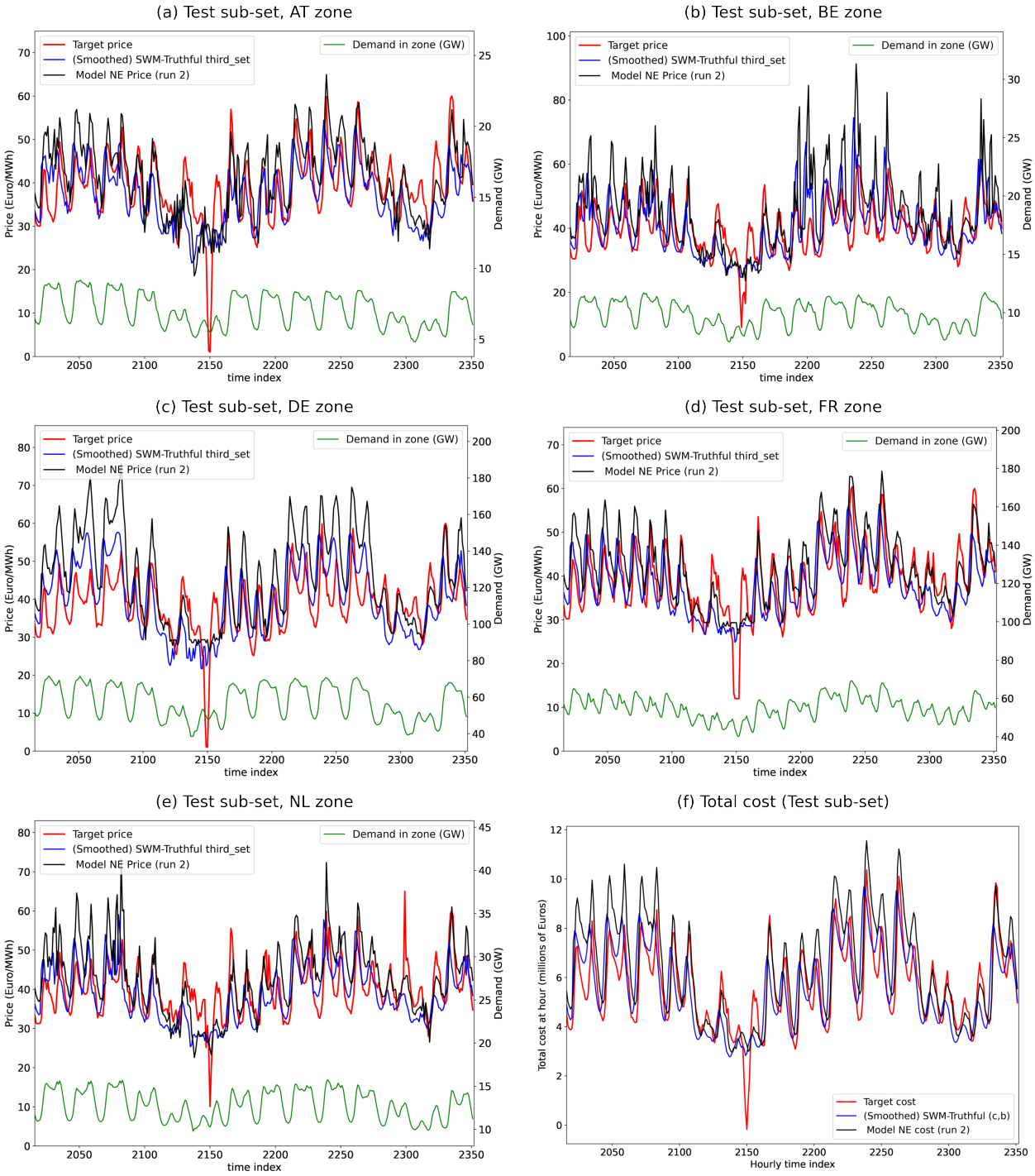


Figure 3.30: Price time series results (Test set): SWM - Truthful Bids (blue) and SWM - Game Theoretic (black) comparison against observed prices (red).

one. From Figure 3.30 we observe that both models perform very well on the test set, revealing the robustness of our fundamental models.

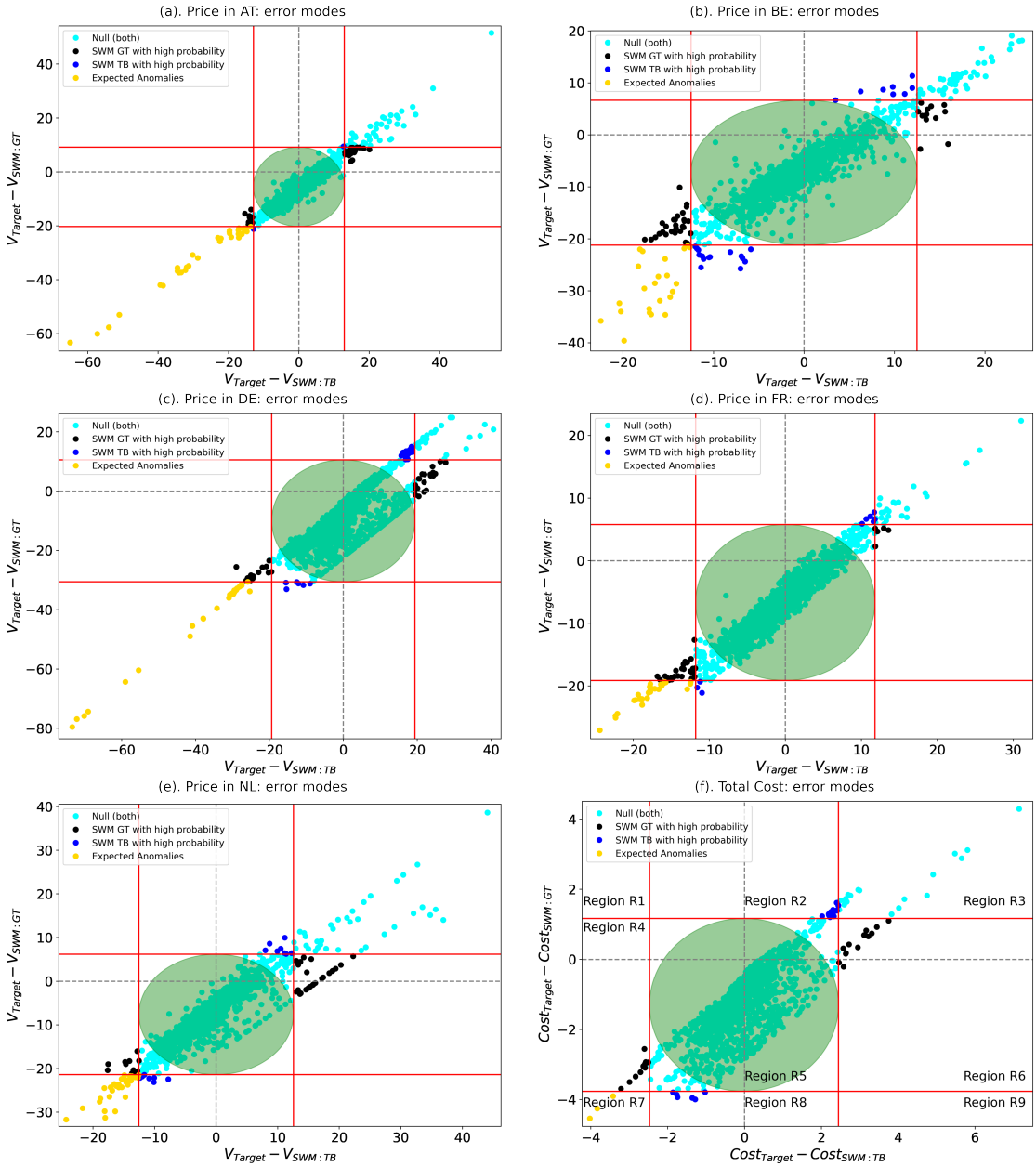


Figure 3.31: Classification of time points to their the most representative state. The red bars represent 97.5% CI for each axis respectively.

We next identify if and when players are gaming, assuming that our cost, constraints and demand inputs are representative of the actual values. We achieve this via simple hypothesis testing, and classifying different possible outcomes. Our analysis is performed based on price level, for each zone and per time point individually, and no time-dependent structure is considered. To this end we define two error time series, one for the TB and another for the GT models:

$$e_t^{TB} = P_t - v_t^{SWM-TB}; \;\; e_t^{GT} = P_t - v_t^{SWM-GT}, \tag{3.284}$$

where P_t is the vector of observed zonal prices at time t and v_t^{SWM-TB} and v_t^{SWM-GT} are

the vectors of zonal prices given by the SWM-TB and SWM-GT models.

For each zone z, each time point is assigned the coordinates $\left([e_t^{TB}]_z, [e_t^{GT}]_z\right)$, and hypothesis testing is performed for each of the two error components individually. The null hypotheses are that the error at time t comes from the error distribution of the TB (for $[e_t^{TB}]_z$) and GT (for $[e_t^{GT}]_z$) models respectively, which are approximated by Gaussians with parameters set as their empirical estimators. We reject the null hypothesis if the corresponding error (for TB or GT) lies outside a symmetric 97.5% confidence interval (CI) centered in the mean of the distribution. However, the null hypothesis can be rejected because $[e_t]_z$ is either *"very low"* or *"very high"*, and this gives us different information about the actual state of market. Thus, there are three regions of interest when performing hypothesis testing for each of the TB and GT models. Since we are interested in the Cartesian product of the e^{TB} and e^{GT} space, this means that there are 9 regions in total, and these are annotated in Figure 3.31 (f), for visualisation. If the error lies in the low end then the model over-predicts while a high error indicates under-predicting. The meaning of each region is then as follows:

1. If a time point lies in region R5 it means that neither the null hypothesis that the point comes from the TB or the null hypothesis that the point comes from the GT model can be rejected. In other words, we cannot confidently say if players were bidding truthfully or strategically. We call this state *Null* and denote it as $\mathcal{S}_0$.

2. If a time point lies in R4 or R6, then the null hypothesis that the error comes from TB was rejected, but the point still belongs to the 97.5% CI of the GT model, meaning that *with high probability* (w.h.p), the players were bidding strategically. We call this state *GT (w.h.p)* and denote it as $\mathcal{S}_{GT}$.

3. If a time point lies in R2 or R8, then the null hypothesis that the error comes from the GT model distribution is rejected, but not the one for TB, meaning that w.h.p the players were bidding truthfully. We call this state *TB (w.h.p)* and denote it as $\mathcal{S}_{TB}$.

4. If a time point lies in R3, both models under-predict with respect to the observed price. This suggests that both models are inappropriate in this case. Due to the large error we assign these points to $\mathcal{S}_0$.

5. If a time point lies in R7, then both models over-predict, meaning that the actual price is much lower. This case may occur when electricity prices become negative due to unexpected and high influx of renewable power [60], and thus we call these points *Expected Anomalies* and denote their set as $\mathcal{S}_{EA}$.

6. It is extremely unlikely for a point to lie in R1, as this means that the GT model severely under-predicts, while the TB model severely over-predicts. This requires the TB model giving a much higher price than the GT model. Due to multiple zones, this is not necessarily impossible but extremely unlikely. It is also fairly unlikely for a

point to lie in R9 where the GT model drastically over-predicts, while the TB model drastically under-predicts. We do not observe any of these points on our data set but classify these points as *Other Anomalies* and denote their set as $\mathcal{S}_{OA}$.

We call the method of assigning these states Two Dimensional State Detection (TD-SD). Note that the choice of the confidence threshold may impact results. However, this simple model still enables us to gather some insight into whether the players were bidding truthfully or strategically.

Further note that the analysis was performed on the price time series for each zone individually, and thus aggregating for a final single state at each time t over all z based on the results obtained for each of the 5 zones requires further definitions. One might argue that by performing the same hypothesis testing exercise on the total cost, the state for the aggregated zones can be obtained. While this is possible, it offers a rather poor aggregate if one is interested in detecting strategic bidding. The reason is that price decoupling happens fairly often and thus gaming may occur only in one or few regions. If gaming occurs only in a small region (say NL) and price decoupling occurs, the impact on price may be very large, but the impact on total cost may be low, and thus this change (with respect to TB) could be assimilated into the noise of the model. For this reason, we perform TD-SD independently for each zone, and define logical rules for aggregation. Let $\varsigma(t) \in \mathbb{R}^{N_z}$ be the vector of states assigned for each state, then we define the aggregate state $\hat{\varsigma}_t$ as follows:

1. If $\varsigma_z(t) \in \mathcal{S}_0 \ \forall z$, then the aggregate state is $\hat{\varsigma}_t \in \mathcal{S}_0$. In other words if for all zones, we cannot distinguish whether players are bidding truthfully or strategically, the same is true about the aggregated zones.

2. If $\varsigma_z(t) \in \mathcal{S}_0 \ \forall z$, $\exists z$ s.t. $\varsigma_z(t) \in \mathcal{S}_{TB}$ and $\nexists z$ s.t. $\varsigma_z(t) \in \mathcal{S}_{GT} \cup \mathcal{S}_{EA} \cup \mathcal{S}_{OA}$, then $\hat{\varsigma}_t \in \mathcal{S}_{TB}$. In other words, if for at least one zone we can say w.h.p that the state is TB, and for all other zones we can either say that the state is TB w.h.p or cannot distinguish between TB and GT, then the aggregate state is TB.

3. If $\exists z$ s.t. $\varsigma_z(t) \in \mathcal{S}_{GT}$ and $\nexists z$ s.t. $\varsigma_z(t) \in \mathcal{S}_{EA} \cup \mathcal{S}_{OA}$, then $\hat{\varsigma}_t \in \mathcal{S}_{GT}$. In other words, if we can say with high probability that in any zone the players are bidding strategically, and there are no anomalies, then players are bidding strategically for the aggregate region. Thus, for the aggregate results, state GT (w.h.p) can be seen as the statement that *"with high probability, players are bidding strategically in at least one zone"*.

4. If $\exists z$ s.t. $\varsigma_z(t) \in \mathcal{S}_{EA}$ and $\nexists z$ s.t. $\varsigma_z(t) \in \mathcal{S}_{OA}$, then $\hat{\varsigma}_t \in \mathcal{S}_{EA}$.

5. If $\exists z$ s.t. $\varsigma_z(t) \in \mathcal{S}_{OA}$, then $\hat{\varsigma}_t \in \mathcal{S}_{OA}$.

While the aggregation rules are partially a natural extension, there are decision rules that are defined somewhat arbitrarily. However, the aggregation of zonal results will enable us to summarise the main observations about the market as a whole, instead of describing each

country individually (and their interaction), which is much more complex. However, the zonal results can also be used if a more detailed analysis is required.

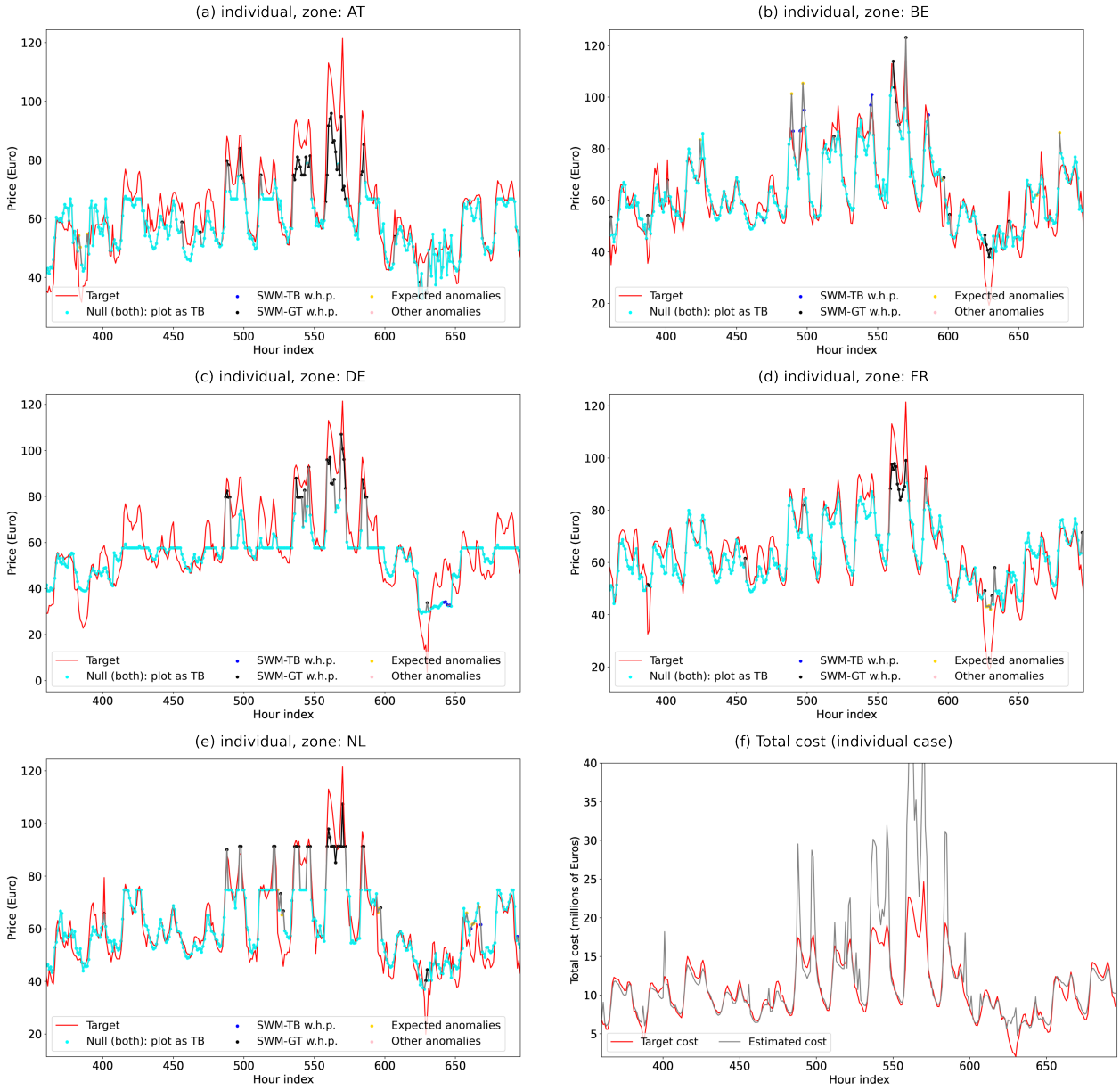


Figure 3.32: Comparison of price time series (individual TD-SD): State Detection results vs observed prices.

By using the results of TD-SD, we now plot the combined results of our two models, by accounting for the state obtained by TD-SD, against the target price series for better visualisation. At each time we plot either the TB value, if the state is not GT w.h.p, and plot the GT value otherwise. In other words, for the purpose of Figure 3.32 and Figure 3.33, we resolve the inability to distinguish between TB and GT, and *"anomalies"*, by using TB results as a baseline. From Figure 3.32 (a)-(e) we can observe that when accounting for the estimated states, we obtain a more accurate representation of the observed price series, with better ability to capture peaks. Note that Figure 3.32 (f) attempts to compute a cost estimated by simply adding up the individual costs of each zone, given

their own estimated states. However, these states need not coincide at a time t, making the computation of this cost inconsistent and thus somewhat unreliable, since zonal costs may come from different models and thus different market clearings, which clearly gives a sub-optimal quantity allocation and total cost. Thus we expect this type of cost estimate to often overshoot, and this can be observed in Figure 3.32 (f).

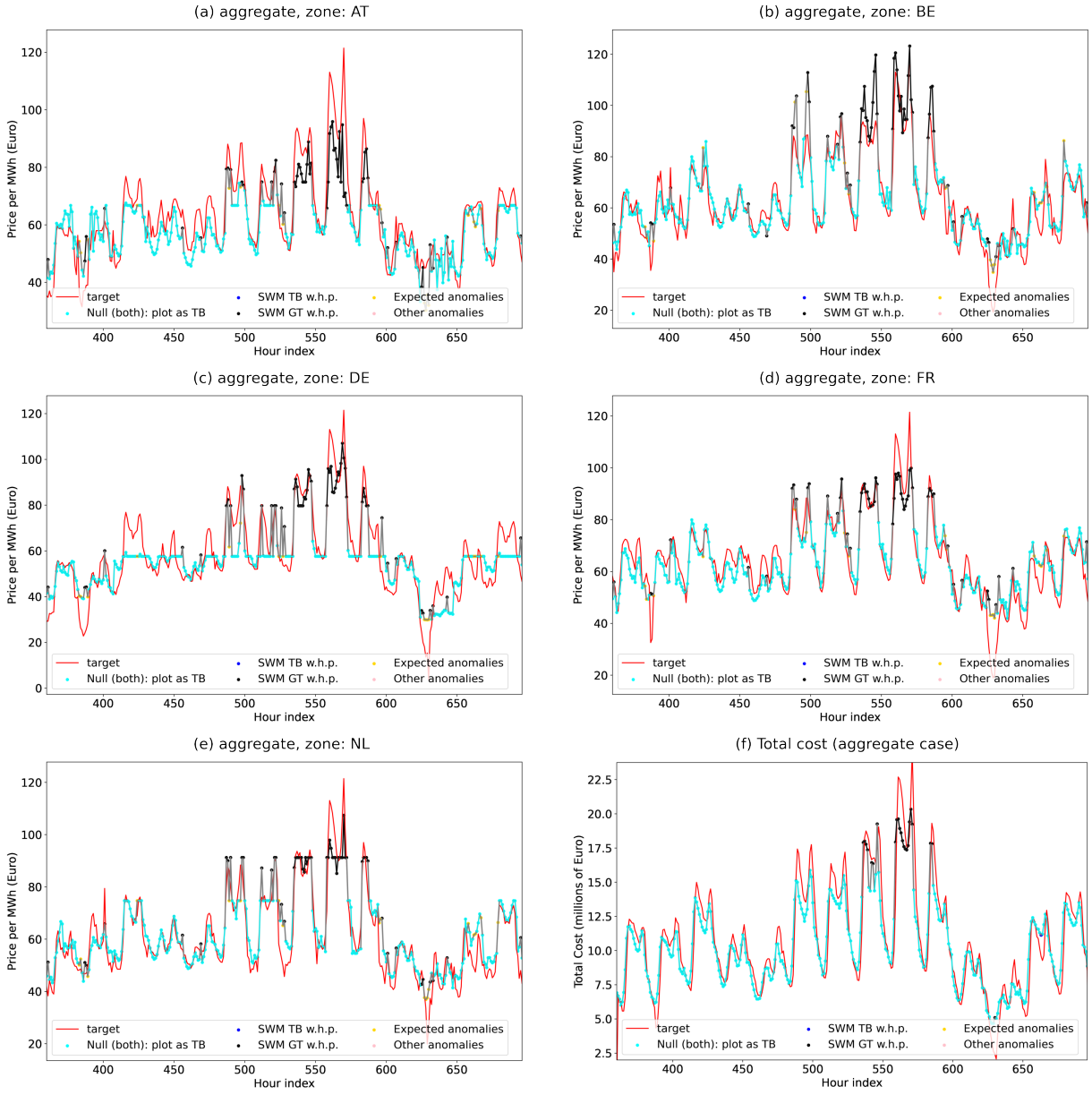


Figure 3.33: Comparison of price time series (aggregate TD-SD): State Detection results vs observed prices.

From Figure 3.33 we can see that the representation of cost in this case is much more accurate. We can also see that by looking at a particular zone, the assignment of state might not appear as optimal, due to the aggregation compromises incorporated in our logical rules. This issue can only be fully solved by considering all possible zonal combinations of players bidding truthfully or strategically, as opposed to assuming that players across all zones bid truthfully or strategically simultaneously. However, in our case there are $2^5 = 32$ possible

combinations and the computation of results for each series is very computationally intense. Nevertheless, our approach gives an indication of when players are bidding strategically, and we can observe that times tend to be consecutive, usually at peak hours, and under consecutive days. Strategic bidding around peak hours could be an approach employed by margin producers to mitigate the risk of being detected at least with respect to potential gain, since producers' market power is at its peak when demand is highest.

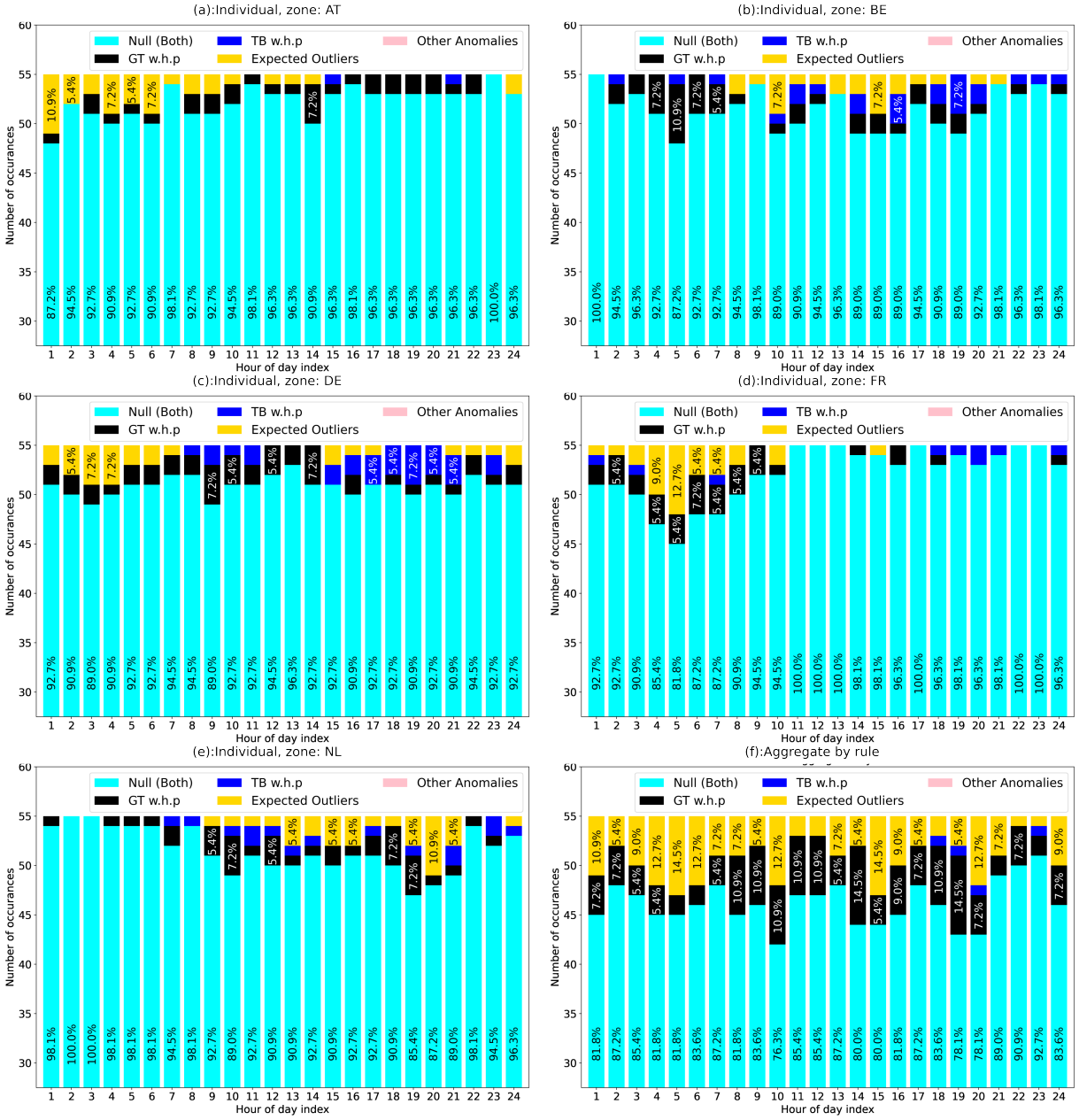


Figure 3.34: Results for the average day: proportion of each observed state.

Since it is very difficult to visualise the results for the whole length of the series, and ingest the main conclusions in this way, we review the state profile of an *average day*. To this end, we count the number of each type of states for each hour of the day, and plot the results in Figure 3.34. We observe that generally, for each zone we can say with high confidence much more often that the players are bidding strategically, than we can say they

are bidding truthfully. However, for a very large proportion of times we essentially cannot draw any conclusion. This is due to the fairly large variance of our model errors, which is dependent on model structure and inputs. This could be potentially improved if data of higher quality and granularity is available, as well as by including more market features in the model. However, this requires more reliable data sources, extensive added labour and increased computational cost, and for these reasons we confined ourselves to the current approach. Reducing the confidence requirement will increase the fraction of times we can classify, but this increases the chance of over-stating results. Thus, we adopt a conservative approach, requiring 97.5% confidence, and this still reveals interesting features.

Figure 3.34 reveals that strategic bidding can be observed in each zone for a significant fraction of times, and this generally tends to be more pronounced at intervals around peak hours: $8am - 1pm$ and $5pm - 9pm$. As discussed before, this could be due to a much more attractive risk-reward profile of strategic bidding alternative for the producers. We also observe that strategic bidding seems most pronounced in the Netherlands, and Belgium and least pronounced in France and Germany. This could be because the Netherlands and Belgium are fairly small trading zones with a fairly small number of players and therefore market power can be exercised much more easily. Heavy reliance on gas power plants and electricity imports also aggravate this issue. On the other hand France is a large trading zone and much cheap production in the form of nuclear power plants is available. Further these plants cannot easily withhold capacity and thus they do not have strong incentives to bid strategically. Out of the five, Germany is the largest trading zone, with the largest number of participants, and a large number of coal power plants ready to produce if price increase due to strategic bidding exceeds the cost of extra emissions. As a result, we can observe that for Germany we obtain the largest number of times for which we can say with high confidence that the producers were bidding truthfully.

It is interesting to see that the level of strategic bidding in Austria is also fairly elevated. While Austria is also a fairly small zone, the results could be somewhat over-stated due to valuation of Hydro storage power. This is difficult to price and our approach may be less conservative than the one employed by these plants' operations manager.

We also observe a fairly pronounced number of times where both SWM-TB and SWM-GT models under-predict (Expected Outliers). This occurs mostly in early morning hours, when demand is low and renewable energy production may be unexpectedly high due to high wind. This appears to be most pronounced in France, which is expected since nuclear power plants are not flexible to adjust, and prefer to sell at lower prices or even a loss.

The aggregate results presented in Figure 3.34 point to the following conclusion: while we cannot identify with certainty the bidding behaviour of players for a large number of times, strategic bidding (in at least one zone at each time) is fairly pronounced. In fact, the fraction of times we can conclude with high confidence that players in all zones were bidding truthfully is very small. While it is possible that all the unidentified time instances truly belong to the truthful bidding case, even in this situation, our results reveal that

the fraction of strategic bidding is rather high and cannot be neglected. This suggests that a market clearing mechanism more robust to strategic bidding may be required. The Cost Minimisation market clearing introduced by us offers such an alternative, for which we observed that price spikes are generally greatly reduced in frequency and magnitude, and the total electricity procurement cost is guaranteed to be lower, assuming the market clearing model is solved to optimality.

Chapter 4

Conclusion and Future work

In this chapter we summarise the main topics covered in this thesis and then discuss a few possible directions for future work.

4.1 Summary of Current Work

We started our discussion by reviewing the mechanics of spot electricity markets, and observed that the two main inputs for electricity spot price formation are the network constraints and bids and offers. Due to the idiosyncrasies of each electricity spot market, we chose the Central Western European (CWE) spot electricity market as a case study, since this also appears to be less understood by practitioners and with less academic research available. The work in Chapter 2 provides a literature review of the TSOs' approach to obtaining the network constraints, and we then develop an approach for obtaining these constraints using only publicly available data. Chapter 3 is then focused on bids an offers, and their inseparable relation with the market clearing mechanism. Under a game theoretic framework, bids and offers are a result of strategic bidding, balancing of supply and demand, and the cost or benefit structure of each market participant. We construct a game theoretic model and build efficient numerical algorithms to apply this to the real world case of CWE spot electricity market.

4.1.1 Main Points from the Literature Review

We first look at the key take-aways from the literature review of obtaining the network constraints for the CWE.

1. The network constraints (combination of PTDFs and RAMs) used by the market clearing mechanism are a linear set of constraints, constraining the zonal net production

levels for each zone. They are obtained by considering the maximum power flows that can be safely transmitted through each grid line.

2. These constraints are obtained by two levels of approximations: (i) the first one is using a DC model for the line power flows based on net nodal power injections, and (ii) the aggregation of nodal effects on transmission lines into zonal equivalent by considering a reference point (known as the base case) and an aggregation pattern (represented by the GSK). The second step introduces the larger error.

3. The base case and the GSK are effectively inputs provided by the grid operators for determining the (simplified) network constraints used in the market clearing. Since these inputs are chosen based on partial knowledge and expectations of the operator, and depend on a (slowly) changing grid state, the network constraints change over time.

4. The operators have some controls that can be used to re-distribute the flows through adjusting Phase Angles, but these are rather limited in practice.

5. These constraints are known as Flow Based Market Coupling (FBMC) network constraints.

From our literature review concerning the work in Chapter 3 we learned that:

1. Market clearing mechanisms for electricity markets are rather complex, and simultaneously satisfying a set of desirable criteria may be very challenging, or even provably impossible in some circumstances (see Myerson–Satterthwaite impossibility theorem).

2. As a result of this issue, combined with difficulty of storage and non-trivial transmission, spot electricity markets tend to be very idiosyncratic in nature, as different countries adopt different policies representing their preferences. For example, locational marginal pricing is generally preferred in American markets, while European markets aim to offer uniform prices for the whole Europe, and only allow for price decoupling at country level. Further differences can be observed in the way that physical constraints are enforced.

3. We have seen that the CWE uses a form of Social Welfare Maximisation objective with zonal pricing and FBMC network constraints.

4. The literature on Game Theoretic models that have been applied, or are even directly applicable to the CWE spot market is (at best) very scarce to our knowledge, due to the zonal pricing and FBMC network constraints peculiarities of this market.

4.1.2 Main Results

In this section we briefly discuss the main results of this thesis, by first providing an executive summary, followed by a more detailed discussion of the results in each chapter.

4.1.2.1 An Overview of the Main Results of the Thesis

1. We developed a new and detailed game-theoretic model for spot electricity markets considering the idiosyncrasies of network constraints and zonal pricing of European markets [78]. To the best of our knowledge, our model is the first to consider these idiosyncrasies, at least without making major simplifications in the game-theoretic realm.

2. This model requires the network constraints as an input, whose historical data is very sparse and incomplete. Therefore, in Chapter 2 we devise an optimisation model based on the fundamentals of the Flow Based Market Coupling (FBMC) approach to obtain the full set of historical constraints and perhaps more importantly, the underlying signals that govern the dynamics of these network constraints.

3. Chapter 3 is then focused on modelling the market clearing mechanism and incorporating this under a game-theoretic framework. Two market clearing mechanism are considered: a Social Welfare Maximisation (SWM) based optimisation model representing the current practice, and a Cost Minimisation (CM) model as an alternative introduced by us. We incorporate risk aversion and devise efficient numerical methods and implementations to compute the market clearing outcomes and (approximate) global equilibrium outcomes.

4. We demonstrated that our model variants produce realistic representations of the spot electricity price in the CWE, including spikes and off-peak regimes. We show that the CM market clearing model, when compared to the SWM, generally results in reduced prices, and always leads to reduced total cost. We also devise a simple method based on hypothesis testing to investigate whether players are bidding truthfully or strategically, and offer an indication that strategic bidding may be fairly pronounced.

4.1.2.2 Main results for each chapter of the thesis

Chapter 2 is focused on obtaining the full set of network constraints for each time instance.

1. We obtained the full electricity grid of the Central Western European trading region, and mapped the observed network constraints data (PTDFs and RAMs) to the obtained grid. The location, capacity constraints and production data for 436 power plants in CWE is also obtained and incorporated with the grid data. These tasks are not trivial since the consumption grid data is incomplete, power plant data is not

easily available, and mapping has to be done by node names since we are required to use different data sources.

2. Since the published network constraints data is very sparse, we devise a mathematical optimisation model based on the fundamentals (FBMC model) to obtain the full set of network constraints. This is done by first obtaining the much lower dimensional *underlying signals* known as the GSKs and Phase Angles, and this gives insight into operator behaviour that was not previously available. Our work offers, for the first time, a way to extract estimates of key operator behaviour (encoded in the GSKs and PAs), only from publicly available data, and by considering the electricity grid structure.

3. Due to large data size, and sparse structure, efficient numerical optimisation is required and thus we devise an alternating minimisation approach to solve for our optimisation model. This is achieved by exploiting marginal convexity in certain sub-spaces, and using stochastic optimisation for the most computationally intense parts. An efficient tensor implementation is used to further reduce computational time. Good representation of the actual constraints is obtained, in the rather strict sense of relative error based on euclidean norm, as opposed to domain-based metrics, which are ultimately of interest, and may be more forgiving.

4. Using the obtained GSKs, we perform numerical investigations that reveal a particular structure of the GSKs: they appear to come from a rather small subset of clusters, with added noise on top, which could suggest that operators choose from a set of typical response patterns and then adjust based on their knowledge and expertise, and this is consistent with the discussion in the work of Dierstein (2017) [21]. However, it is difficult to evaluate how much of the *added noise* is a result of TSO adjustment as opposed to data noise.

Chapter 3 focused on the outcome of the Day Ahead Auction market clearing (spot market), considering a game theoretic framework and two market clearing mechanisms. The contributions may be best understood by splitting them in three parts: (i) part one is concerned with simpler models with the goal of theoretical and practical understanding, (ii) part two is concerned with including as many realistic features as possible while focusing on obtaining computational tractability, and (iii) part three is concerned with the application of models devised in (ii) to the CWE market.
Chapter 3 (Part 1) can be summarised as follows.

1. The main simplifying assumption is that producers have very large capacities, and we consider the case of network constraints, inflexible demand and orders of linear marginal prices with respect to cleared quantities. For this case we introduce a Cost Minimisation (CM) optimisation model as a market clearing mechanism for the DAA,

which unlike the Social Welfare Maximisation, expresses the true cost of electricity procurement for inflexible demand.

2. Solving for the CM is more challenging that solving for the SWM, as price variables appear both in the objective and constraints, while for the SWM actual price variables are only computed after the optimal solution is obtained. Thus, we introduced the idea of ellipsoid network constraints and showed that the market clearing can be solved for efficiently in this case, requiring numerical optimisation of a Trust-Region like quadratic problem only in the low dimensional space corresponding to the number of trading zones (5 for the CWE in 2019-2020 period). All other variables can then be computed analytically. We extend this idea to polytope network constraints by solving iteratively over ellipsoids contained in the polytope.

3. Similar to the work of Hu and Ralph (2007) [85], we defined a game over the DAA auction, but we solved the corresponding numerical problem differently, by leveraging analytical results to define a system of non-linear equations describing the stationary Nash Points (a weaker version of NE). The system is solved as a non-linear least squares program via iterative methods (Gradient or Newton based). This approach is fast since it only requires solving a few 5D Trust region like sub-problems for each outer optimisation step when finding the stationary Nash points. However, this benefit comes at the cost of ignoring producers' capacity constraints which are important for price formation, and this issue is addressed in the next sections.

4. We discuss the issue of producers' market power, and from a theoretical perspective show that if players are not risk-averse, there exists a continuum of equilibria, and argue that prices may be arbitrarily large under inflexible demand. By representing risk aversion via a mean-variance framework, we show that risk aversion places a ceil on the ask prices, and thus on the market prices, as well as total cost. We show that this ceil reduces as the least risk averse player becomes increasingly risk adverse, and in the limit of infinite risk aversion, the producers will bid their true costs, even when trying to strategise for maximising their own benefit.

5. For the simple case of two zones and two players per zone, we show that if the least risk averse player is sufficiently risk averse, the stationary Nash Points (and thus the NE) become isolated. However, in practice we observe that these points may remain rather close to each other. Since these results are not very descriptive and not easily generalisable, it motivates us to introduce the non-parametric risk aversion presented in Section 3.5.4.

Chapter 3 (Part 2) is focused on adding capacity constraints and resolving the issues associated with the mean-variance risk aversion framework, resulting in a much more complex CM market clearing problem. Thus, a large portion of this section is concerned with

developing efficient numerical approaches to obtain the market clearing solution, as well as equilibrium solutions under the Game Theoretic framework. The contributions made here were as follows:

1. A general cost minimisation model including producers' capacity constraints is formulated and expressed in an equivalent bilinear form. We show how the iterative ellipsoid idea can still be applied to solve for this market clearing problem. However, the optimisation process has to be lifted to a much higher dimensional space due to the presence of capacity constraints at participant's level. This increases the computational cost and the risk of ill-conditioning but we introduce a way to re-condition the ellipsoids that drastically improves performance.

2. We also introduce and explore another three numerical approaches to solve for the market clearing, with different trade-offs between computational cost and convergence guarantees. The four methods introduced are:

   - a method based on iteratively solving simple LPs that is generally fast but has no convergence guarantees (ieq-LP-ma),
   - the extension of the iterative ellipsoids method adapted to capacity constraints and reconditioned (ie-CQP-wr), which offers (slightly stronger than) local convergence guarantees,
   - a branch and bound method in the space of zonal quantities called BBTree, that leverages the structure of the market clearing problem, and offers global convergence guarantees and a global optimality certificate, generally at increased computational cost,
   - by using strong (but partial) analytical results we devised a numerical method that iteratively solves polytope-constrained Convex Quadratic Programs over regions that depend on player's bid and capacities. This method offers global convergence guarantees on the finite size subdomain corresponding to the last solved CQP, which may be large. This convergence result is rather strong, but weaker than the purely global convergence guarantee of BBTree.

   We provide an evaluation of the four methods based on synthetic data, give some intuition with regards to their advantages and disadvantages, and discuss possible appropriate method choices based on different requirements and resources available. However, our study is limited in scope and should only be seen as an indication.

3. The partial analytical results corresponding to ib-CQP allowed us to obtain the analytical form of what we call *optimal zonal stack curves* for offers, which are a new concept and result to our knowledge. For the type of bids considered, these curves are piece-wise linear and the price is strictly increasing function of quantity, although upward (but not downward) price jumps are possible.

4. A novel type of risk aversion based on the idea of *worst case scenario* was introduced, and we refer to this as Robust Strategy Selection (RSS). This facilitates numerical computation of approximate global Nash Equilibria by reducing the strategy space to a convex, bounded and one-dimensional subspace for each player (in the case of linear marginal bids). This risk aversion model is non-parametric, reduces the dimensionality of the strategy variables and offers boundedness of the strategy set, ensuring that the zonal equilibrium prices are also bounded.

5. Using the fact that the subspace given by the RSS is a one dimensional interval for each player, we compute *approximate global* Nash Equilibria, by iteratively performing Gauss-Seidel or Jacobi updates to an initial strategy set (equilibrium guess), until a Nash Equilibrium point is found. This is similar to the work in [85], but the difference lies in the risk aversion used and the discretisation of the strategy space, which allows us for faster computation, and finding approximate global Nash Equilibria, as opposed to local NE or even simply stationary points. To compute the NE, time and computationally efficient algorithms are implemented using multiprocessing and multitasking, via cloud computing services provided by *Descartes Labs* [46].

In **Chapter 3 (Part 3)** we applied our methodology to the real world case of CWE Day Ahead Auction, and the contributions made here are as follows:

1. We introduced a version of the Social Welfare Maximisation (SWM) market clearing mechanism, consistent with our assumptions, that is representative of the actual market mechanism in the CWE, and this can be solved efficiently as a linearly constrained Convex Quadratic Program. Further, the Game-theoretic framework and the corresponding algorithms are directly applied.

2. Using the network constraints data obtained in Chapter 2, and by gathering producers data, we define players based on their fuel type, similar to the work in [53]. The producers' cost structure is parametrised in a rather simplistic way but accounts for fuel price changes over time. While our models are fundamental, and require no calibration in principle, if sufficiently granular and accurate data is available, due to time limitations, we only obtained the fuel costs and production capacities on a bottom-up approach, but proposed an optimisation approach to calibrate the cost scale for each zone based on the truthful bidding assumption. This fits only a very small number of parameters (1 or 2 per zone), and is only required to circumvent a more detailed bottom up approach and data gathering, but the latter could be done given sufficient available time.

3. We ran numerical simulations of our Cost Minimisation (CM) and Social Welfare Maximisation (SWM) market clearing models combined with the Truthful Bidding (TB) assumption and Game theoretic (GT) framework respectively, on the real world

data of CWE for the 2019-2020 period. We obtained results that represent the actual price time series well. To the best of our knowledge, detailed results obtained from the application of detailed Game theoretic models to real world spot electricity markets have not been obtained before, at least for the CWE market. These numerical results confirmed the computational tractability of our models and algorithms in real world applications, as well as their ability to represent the market dynamics.

4. Our numerical results show that our the SWM model generally replicates the actual prices well. However, we also show on the real data that when using the Cost Minimisation market clearing proposed by us instead of SWM, the market power of producers is reduced, as generally this results in decreased zonal prices and always decreases the total cost of electricity procurement. This offers a way for the regulators or operators to reduce producers market power if necessary.

5. We attempted to infer whether players are bidding truthfully or strategically in the CWE market, comparing the results given by the SWM-Truthful bidding model and SWM Game-Theoretic model against the real world price data. We devised a simple method based on hypothesis testing applied to our numerical results and the real world data, that identified if and when the players are bidding strategically. While we could not identify with high certainty the bidding behaviour of players for a large number of times, strategic bidding (in at least one zone at a time) appears to be fairly pronounced. In fact, the fraction of times for which we concluded with high confidence that the players in all zones are bidding truthfully is small compared to the number of times for which we concluded with high confidence that players are bidding strategically. Thus, we offered an indication, although not a proof, that strategic bidding may have take place in the CWE for the studied period.

4.2 Future Work

There are many possible future research directions based on this work, and we discuss natural continuations in the subsections below.

4.2.1 Forecasting of the GSKs and PAs

In our work in Chapter 2, we have formulated an optimisation model based on fundamental dynamics to recover the network constraints and the corresponding underlying signals (GSKs and PAs), based on publicly available data. However, to use these constraints as part of a decision making process, market participants may be interested in future values of the network constraints at specified times. This requires building a forecaster of the network constraints. In our opinion, it is much easier (and better) to forecast on the GSKs and PAs instead of on the final set of network constraints for the following reasons: (i) the GSKs and PAs are much lower dimensional than the PTDFs and RAMs, and (ii) GSKs and PAs are responses of the operators based on fundamental factors (such as for example weather), and this dependency might be easier to capture prior to being mapped (through a potentially changing map) to a higher dimensional space.

4.2.2 General Bids and General Cost Functions

So far we have only considered the case of linearly increasing marginal costs, and linearly increasing bids. This is somewhat limiting, but a simple and natural generalisation exists, although the computational cost might increase very significantly. The idea is that, for each player i, the quantities x_i and their bounds $[0, Q_i]$ can be replaced by a series of bids $(m_i^{(b)}, a_i^{(b)})$ with $b \in \mathcal{B}_i$, with corresponding accepted quantities $x_i^{(b)} \in [0, Q_i^{(b)}]$ ($Q_i^{(b)}$ may be taken as equal for simplicity) and under this case, any increasing offer (decreasing bid) function can be replicated by player i as $Q_i^{(b)} \to 0$ arbitrarily well, at least when setting $m_i^{(b)} = 0$, but this is not required if the desired function is still strictly increasing (decreasing). Further, the structure of (mc-BLP) does not change at all, although the number of $x_i^{(b)}$ has now greatly increased. Note that the number of decision variables of a player has now also increased, meaning that not only the MCM problem becomes more computationally intense, but also the search space for Nash Equilibria, meaning that the number NE, and computational cost of finding such NE could grow very rapidly with the number of bid discretisation points considered per player. Constraining the strategy space and/or more computationally efficient ways of finding the NEs may be required.

Since the cost structure does not directly appear into the (mc-BLP) problem, but only in the profit calculations, when using the approach described in Section 3.5, the cost structure (c_i, b_i) is only relevant for the argument used for the Robust strategy selection, giving the strategy subspace to search $\mathcal{B}_{LB}(i)$. Repeating the argument based on a different cost

structure is an option, or employing different risk aversion model, if the former approach fails. Note that while changing the cost structure does not require changing the approaches for computing the market clearing or the Nash Equilibria, the latter are affected by changing the cost structure and could in principle be very different.

4.2.3 Speeding Up the Market Clearing Solution Algorithms

So long as a full analytical solution for the Nash Equilibria is not available, the algorithms that find the market clearing solution are at the core of this methodology, and this is a fact irrespective of the type of bids or risk aversion assumption. Thus, the total computational cost required to obtain any kind of numerical results greatly depends on the market clearing solution algorithm. Although the marginal benefit of increasing computational speed may vary strongly with the types of bid and risk aversion models used, granular models applied to real data are likely to be computationally intense and depending on the application, computational speed may be key for trade execution in practice. Further, if the market clearing mechanism solution solution speed is improved sufficiently, one may be able to consider the ideas of generalising bid and offer models, as presented in subsection 4.2.2. Some ideas that could provide improved performance of numerical algorithms are as follows:

1. Resolve numerical issues with ie-CQP-wr that arise due to ill conditioning or singularity of the equality matrix $\mathbf{M}_e$, due to inequality constraints that are aligned or *"almost aligned"* based on the half-plane, in the initial $\mathbf{A}_I$. We only observe this to come from $\mathbf{M}_p$, and thus these can be resolved a-priori but they may also come from the combination of $\mathbf{M}_p$ with other constraints (for example capacity).

2. Using ib-CQP to equip BBTree may result in much faster pruning and potentially make BBTree much faster overall.

3. Occasionally, for ie-CQP-wr, a large chunk of time is spent finding the optimal solution on the boundary of the current ellipsoid. Consider improving the 1D solver for λ in (em-TR), for example consider bisection, regula falsi, etc.

4.2.4 Increasing Model Richness

While our model considers the main features relevant for price formation, it has a number of limitations. To increase the accuracy of the model, multiple time periods and inter-temporal time constraints could be considered, as well as complex orders of the fill-or-kill or block bid types. However, this would come at a very high computational cost and approximations or relaxations are likely necessary to allow for obtaining a numerical solution. Other possible model improvements could be to offer more attention to quantifying the cost of hydro power plants. Instead of charging cost based on a short term horizon as used in our model, the

hydro power plants normally determine a seasonal operation strategy based on a stochastic optimisation problem, that quantifies the opportunity cost of production, which is known as the water values [**?**]. This would require defining and solving an optimisation problem for at least the largest of the hydro water reservoir plants and the hydro pumped storage ones, and would be in itself a very challenging task.

Another possible improvement would be to consider power plant's production limit as given by the availability, instead of capacity. This would require obtaining availability data at power plant level and this could then be aggregated per type or commercial producer, or used for each power plant individually.

4.2.5 Considering both future and spot markets

Throughout this thesis we are concerned only with the spot market, but completely ignore futures and forward contracts trading (which we may refer to collectively as futures market for convenience). While the spot market is strongly influenced by momentary idiosyncrasies not generally considered or reflected in the futures market, the two markets are highly connected.

The futures market is influenced by the spot market to the extent that it has to price according to the expectancy of future spot prices, albeit by also considering peculiarities of electricity markets such as inability of storage, complexity of delivery, and many others. Thus the expectations of the spot prices greatly influence the futures market prices. However, the reverse is also true, albeit to a potentially smaller extent. Commercials and Speculators take positions in the futures market, and before delivery of electricity participants must inform the operator if financial or physical settlement takes place. However, the aggregation of all physical settlements may strongly influence the *"initial position"* of the spot market (which roughly speaking, we referred to as the base case), and this will influence the spot market network constraints, relative to this *initial position*. This does not impact only the base case, but also the GSKs and PAs, which are a reaction of operators based on the currently known and expected grid state. Further, complications can arise if based on the physical settlements in the futures market, the network becomes *pre-congested*, meaning that not all futures contracts can be delivered if no spot trading takes place. Due to the network constraints, the priority of the operators then becomes balancing of the quantities and not optimal objective function (which in our case is Social welfare, but could be total cost, prices etc). This has the consequence that a power plant considered *too expensive* in the futures market may increase/start production following the resolution of the spot market to ensure zonal balance, and this results in a higher spot price as compared to the futures price. The opposite will be true for the other end of the contract: the seller cannot find a (feasible) buyer at the corresponding forward price, but to ensure balance he must sell cheaper, reducing the spot price with respect to the corresponding forward price. This creates trading opportunities between futures market and spot market. By extending our

model to include the futures market, we can consider the behaviour of market participants when optimising for the profits as a whole, over a longer period of time (possibly with a discount rate), as well as the impact of forward positions on network constraints. Multiple time periods with trading decisions made by the participants can be considered for each time step, considering a future's market clearing mechanism as in [77], and a spot clearing mechanism as defined here. Inter-temporal constraints for producers can then be naturally introduced. The impact on forward positions on the network constraints can be estimated by assuming the operators take into account the forward positions into the construction of the D2CF scenario which determines the reference flows. This is clearly a very rich and complex model that requires a vast amount of work. In this regard, the DPhil work of Troha [77] is to a great extent complementary to this work.

4.2.6 Detection and forecasting of market state

We have proposed a simple way, based on hypothesis testing, to obtain statistical estimates of whether the players are bidding truthfully or strategically for each time period independently. While our method does provide some insight, it may be somewhat simplistic for the complex structure of the market, and non-convexities such as ramping constraints, minimum generation, fill-or-kill orders and block bids would ideally be added to have increased confidence when detecting the market state. However, this would result in an extremely challenging model to be solved. The task of identifiying the market state may then also be seen as a classification problem, where each time period has to be assigned to one of the multiple possible states (for example the ones defined by us in this work). Alternatively, it can be see as a Change Point Detection task, where change points indicate the transition from truthful to strategic bidding (or other states), or vice versa. Much work has been done on Change Point Detection (CPD) methods, with a very broad variety of methods being available, and a review of some of the most popular methods is presented in [10].

Bibliography

[1] Electricity market near-equilibrium under locational marginal pricing and minimum profit conditions. *European Journal of Operational Research*, 174(1):457–479, 2006.

[2] P. A. Vasina A. A. Vasin and T. Yu. Ruleva. On organization of markets of homogeneous goods. *Journal of Computer and Systems Sciences International, 2007, Vol. 46, No. 1, pp. 93–106*, 2006.

[3] S.R. Williams A. Rustinchini, M.A. Satterthwaite. Convergence to efficiency in a simple market with incomplete information. 1994.

[4] ACER. 3rd eri progress report. 2015, available at: www.acer.europa.eu.

[5] Ignacio Aravena and Anthony Papavasiliou. Renewable energy integration in zonal markets. *IEEE Transactions on Power Systems*, 32(2):1334–1349, 2017.

[6] Argus. available at: https://www.argusmedia.com/en/methodology/key-prices/api-2-coal.

[7] W.M. Edjroubi C.M. Atke. Scigrid open source transmission network model, user guide v0.2. 2015, available at: https://www.power.scigrid.de/pages/downloads.html.

[8] C. Byers and G. Hug. Modeling flow-based market coupling: Base case, redispatch, and unit commitment matter. 2020 17th International Conference on the European Energy Market (EEM), 2020, pp. 1-6, doi: 10.1109/EEM49802.2020.9221922.

[9] NEMO Committee. Euphemia public description single price coupling algorithm. 2019.

[10] D.J. Cook. A survey of methods for time series change point detection. *Knowledge and information systems; 51(2):339-67*, 2017.

[11] CWE Market Coupling. Jao publication handbook. 2017, avaliable at https://www.jao.eu/main.

[12] CWE Market Coupling. Jao utility tool. 2017, avaliable at http://utilitytool.jao.eu/Util.

[13] Ralph D. and Smeers Y. 2006 November. Epecs as models for electricity markets. In 2006 IEEE PES Power Systems Conference and Exposition (pp. 74-80). IEEE.

[14] de Maere d'Aertrycke G. Ehrenmann A. Ralph D. and Smeers Y. Risk trading in capacity equilibrium models (no. 1757). cambridge working paper in economics.

[15] D. Schönheit M. Kenis L. Lorenz D. Möst E. Delarue and K. Bruninx. Toward understanding flow-based market coupling: An open-access model. Advances in Applied Energy 2, 2021.

[16] Stephan Dempe and Alain Zemkoho, editors. *Bilevel Optimization*. Number 978-3-030-52119-6 in Springer Optimization and Its Applications. Springer, December 2020.

[17] K. Van den Bergh and E. Delarue. An improved method to calculate injection shift keys. 2016, Electric Power Systems Research Volume 134, Pages 197-204, doi: https://doi.org/10.1016/j.epsr.2016.01.020.

[18] K. Van den Bergh Boury E. Delarue. The flow-based market coupling in central western europe: Concepts and definitions. . 2016, Electricity Journal, 29(1), 24–29. https://doi.org/10.1016/j.tej.2015.12.004.

[19] K. Van den Bergh E. Delarue W. D'Haeseleer. Dc power flow in unit commitment models. 2014, Energy and Environment 240.

[20] Lirong Deng, Hongbin Sun, Baoju Li, Yong Sun, Tianshu Yang, and Xuan Zhang. Optimal operation of integrated heat and electricity systems: A tightening mccormick approach. *Engineering*, 7(8):1076–1086, 2021.

[21] C. Dierstein. Impact of generation shift key determination on flow based market coupling. 2017, 14th International Conference on the European Energy Market (EEM), 2017, pp. 1-7, doi: 10.1109/EEM.2017.7981901.

[22] D. Schönheit R. Weinhold C. Dierstein. The impact of different strategies for generation shift keys (gsks) on the flow-based market coupling domain: A model-based analysis of central western europe. Applied Energy, Vol 258, 2020, 114067, ISSN 0306-2619.

[23] Steven P. Dirkse and Michael C. Ferris. The path solver: A non-monotone stabilization scheme for mixed complementarity problems. *Optimization Methods and Software*, 5:123–156, 1995.

[24] R.O. Duda and P.E. Hart. Pattern classification and scene analysis. Wiley, New York, 1973.

[25] Davis Edwards. Energy trading and investing: Trading, risk management and structuring deals in the energy market. 2010, New York : McGraw-Hill.

[26] EEX. Daily spot gas prices at dutch ttf. available at: https://www.powernext.com/spot-market-data.

[27] Elia. Belgian grid data. 2020, available at: https://www.elia.be/en/grid-data.

[28] ENTSOE. Grid map. available at: https://www.entsoe.eu/data/map/.

[29] ENTSOE. Transparency data. available at: https://transparency.entsoe.eu/dashboard/show.

[30] M. Aguado et al. Flow-based market coupling in the central western european region - on the eve of implementation. 2012, CIGRE .

[31] P. Marannino M. Montagna S. Rossi I. Siviero F. Careri, C. Genesi. Bidding strategies in day-ahead energy markets: System marginal price vs. pay as bid. 2010.

[32] R.W. Ferrero, J.F. Rivera, and S.M. Shahidehpour. Application of games with incomplete information for pricing electricity in deregulated power pools. *IEEE Transactions on Power Systems*, 13(1):184–189, 1998.

[33] Steven A. Gabriel, Antonio J. Conejo, J. David Fuller, Benjamin F. Hobbs, and Carlos Ruiz. *Complementarity Modeling in Energy Markets*. Springer New York, NY, 2011.

[34] Donald Goldfarb and Ashok U. Idnani. A numerically stable dual method for solving strictly convex quadratic programs. *Mathematical Programming*, 27:1–33, 1983.

[35] Austrian Power Grid. Austrian grid data. 2019, available at: https://www.apg.at/en/Stromnetz/APG-Netz.

[36] Benjamin F. Hobbs, Carolyn B. Metzler, and Jong-Shi Pang. Strategic gaming analysis for electric power systems: An mpec approach. *IEEE Transactions on Power Systems*, 15(4), 2000.

[37] Sam Howison and Michael Coulon. Stochastic behaviour of the electricity bid stack: From fundamental drivers to power prices. *The Journal of Energy Markets, 2, 29-69*, 2009.

[38] Weber J.D. and Overbye T.J. 1999 July. A two-level optimization problem for analysis of market bidding strategies. . In 1999 IEEE Power Engineering Society Summer Meeting. Conference Proceedings (Cat. No. 99CH36364) (Vol. 2, pp. 682-687). IEEE.

[39] S. Kaminski, M. Dolanyi, K. Bruninx, and E. Delarue. Comparative analysis of risk-aversion and strategic investment behavior in generation expansion. *Electric Power Systems Research*, 210:108082, 2022.

[40] O. Karaca and M. Kamgarpour. Game theoretic analysis of electricity market auction mechanisms. pages 6211–6216, 2017.

[41] O. Karaca, P. G. Sessa, N. Walton, and M. Kamgarpour. Designing coalition-proof reverse auctions over continuous goods. *IEEE Transactions on Automatic Control*, 64(11):4803–4810, 2019.

[42] D. P. Kingma and J. Ba. Adam: A method for stochastic optimization. 2017.

[43] T. Kristiansen. The flow based market coupling arrangement in europe: Implications for traders. *Energy Strategy Reviews 27 (2020) 100444*, 2020.

[44] H. W. Kuhn and A. W. Tucker. Nonlinear programming. In *Proceedings of the Second Berkeley Symposium on Mathematical Statistics and Probability, 1950*, pages 481–492, Berkeley and Los Angeles, 1951. University of California Press.

[45] S. J. Reddi S. Kale S. Kumar. On the convergence of adam and beyond. 2018.

[46] Descartes Labs. https://descarteslabs.com/.

[47] Haifeng Liu, Leigh Tesfatsion, and A. A. Chowdhury. Locational marginal pricing basics for restructured wholesale power markets. In *2009 IEEE Power Energy Society General Meeting*, pages 1–8, 2009.

[48] J.M. Arroyo M. Carrion. A computationally efficient mixed-integer linear formulation for the thermal unit commitment problem. *IEEE TRANSACTIONS ON POWER SYSTEMS, VOL. 21, NO. 3*, 2006.

[49] J. MacQueen. Some methods for classification and analysis of multivariate observations. Proc. Fifth Berkeley Symp. on Math. Statist. and Prob., Vol. 1 (Univ. of Calif. Press, 1967), 281–297.

[50] M. Madrigal and V.H. Quintana. Degeneracy and duality gap on optimization-based electricity auctions. pages 332–337, 2000.

[51] G.J. Mailath and A. Postlewaite. Asymmetric information bargaining problems with many agents. *The Review of Economic Studies 57 (3): 351–367, doi:10.2307/2298018, ISSN 0034-6527*, 1990.

[52] Björn Matthes, Christopher Spieker, and Christian Rehtanz. Flow-based parameter determination in large-scale electric power transmission systems. pages 1–6, 2017.

[53] M.Troha and R. Hauser. The impact of startup costs and the grid operator on the power price equilibrium. 2014.

[54] Roger B Myerson and Mark A Satterthwaite. Efficient mechanisms for bilateral trading. *Journal of Economic Theory*, 1983.

[55] R.Garcia-Bertrand N. Alguacil, J.M. Arroyo. Optimization-based approach for price multiplicity in network-constrained electricity markets. *IEEE TRANSACTIONS ON POWER SYSTEMS, VOL. 28, NO. 4*, 2013.

[56] Karsten Neuhoff, Julian Barquin, Janusz W. Bialek, Rodney Boyd, Chris J. Dent, Francisco Echavarren, Thilo Grau, Christian von Hirschhausen, Benjamin F. Hobbs, Friedrich Kunz, Christian Nabe, Georgios Papaefthymiou, Christoph Weber, and Hannes Weigt. Renewable electric energy integration: Quantifying the value of design of markets for international transmission capacity. *Energy Economics*, 40:760–772, 2013.

[57] Tennet NL. Production and load data, 2019. Available at https://www.tennet.eu/electricity-market/data-dashboard/load/.

[58] Jorge Nocedal and Stephen J. Wright. *Numerical Optimization*. Springer, New York, NY, USA, 2e edition, 2006.

[59] M. Kamgarpour O. Karaca. Core-selecting mechanisms in electricity markets. 2018.

[60] M. Pahle, W.P. Schill, C. Gambardella, and O. Tietjen.

[61] Castro Pedro. A tighter piecewise mccormick relaxation for bilinear problems. (n.d.): n. pag. 3 June 2014. Web. 6 June 2015.

[62] M. Kamgarpour P.G. Sessa, N. Walton. Exploring the vickrey-clarke-groves mechanism for electricity markets. 2016.

[63] Philip Powell. Calculating determinants of block matrices. 2011.

[64] J.M Arroyo R. Fernandez-Blanco and N. Alguacil. Network-constrained day-ahead auction for consumer payment minimization. *IEEE TRANSACTIONS ON POWER SYSTEMS, VOL. 29, NO. 2*, 2014.

[65] J.M. Arroyo R. Fernandez-Blanco and N. Alguacil. On the solution of revenue- and network-constrained day-ahead market clearing under marginal pricing—part i: An exact bilevel programming approach. *IEEE TRANSACTIONS ON POWER SYSTEMS, VOL. 32, NO. 1*, 2017.

[66] James Renegar. A mathematical view of interior-point methods in convex optimization. SIAM, 2001.

[67] Charles R.Johnson. A gersgorin-type lower bound for the smallest singular value. Linear Algebra and its Applications, vol 112, 1989.

[68] V.C. Ramesh R.W. Ferrero, S.M. Shahidehpour. Transaction analysis in deregulated power systems using game theory. 1997.

[69] T. Felling C. Weber S. Voswinkel, B. Felten. Flow-based market coupling: What drives welfare in europe's electricity market design? 2019, online at: http://hdl.handle.net/10419/201591.

[70] L.Wyroll K. Kollenda C. Müller A. Schnettler. Impact of flow-based market coupling parameters on european electricity markets. 2018, 53rd International Universities Power Engineering Conference (UPEC).

[71] R. Besselink D. Dudoignon T. Ringelband P. H. Schavemaker J. Schwachheim and R. Sikora. Tsc's coordinated intraday capacity calculation concept. 12th International Conference on the European Energy Market (EEM), 2015, pp. 1-5, doi: 10.1109/EEM.2015.7216671.

[72] S. Schwenen. Market design and supply security in imperfect power markets. *Energy Economics*, 43:256–263, 2014.

[73] D. Schönheit. An improved statistical approach to generation shift keys: Lessons learned from an analysis of the austrian control zone. 2019 Z Energiewirtsch 43, 193–212, doi: 10.1007/s12398-019-00261-w.

[74] D. Schönheit and R. Sikora. A statistical approach to generation shift keys. 15th International Conference on the European Energy Market (EEM), 2018, doi: 10.1109/EEM.2018.8469900.

[75] SciGRID. The open source model of european energy networks. available at: https://www.scigrid.de/.

[76] A. Shahmohammadi, R. Sioshansi, A. J. Conejo, and S. Afsharnia. Market equilibria and interactions between strategic generation, wind, and storage. *Applied Energy*, 220:876–892, 2018.

[77] M. Troha. Fundamental models for the dynamics of electricity prices. *University of Oxford*, 2015.

[78] CWE TSOs. Documentation of the cwe fb mc solution. 2018, available at: https://www.jao.eu/support/resourcecenter/overview.

[79] B.F. Hobbs U. Helman and R.P. O'Neill. *Competitive Electricity Markets: The Design of US Wholesale Energy and Ancillary Service Auction Markets: Theory and Practice.* 2008.

[80] A. Vasin. Game-theoretic study of electricity market mechanisms. *2nd International Conference on Information Technology and Quantitative Management, ITQM 2014*, 2014.

[81] S. Voswinkel, B. Felten, T. Felling, and C. Weber. Flow-based market coupling: What drives welfare in europe's electricity market design? HEMF Working Paper 08/2019, Essen, 2019.

[82] J. Wang, M. Shahidehpour, Z. Li, and A. Botterud. Strategic generation capacity expansion planning with incomplete information. *IEEE Transactions on Power Systems*, 24(2):1002–1010, 2009.

[83] B. Felten P. Osinski T. Felling C. Weber. The flow-based market coupling domain - why we can't get it right. *Utilities Policy*, 2020.

[84] R. Wilson. Architecture of power markets. *Econometrica vol. 70, no. 4, pp. 1299–1340*, 2002.

[85] Hu X. and Ralph D. Using epecs to model bilevel games in restructured electricity markets with locational prices. *Operations research*, pages 55(5), pp.809–827., 2007.

[86] Hossein. et al Zeynal. Locational marginal price (lmp) assessment using hybrid active and reactive cost minimization.